Papers presented to the

CONFERENCE ON THE LUNAR HIGHLANDS CRUST

(NASA-CR-16243) CONFERENCE ON THE LUNAR HIGHLANDS CRUST (Lunar and Planetary Inst.) 219 p

N80-70705

Unclas
00/91 46105

Houston, Texas
14-16 November 1979

A Lunar and Planetary Institute
Topical Conference

NOV 1979
RECEIVED
NASA STI FACILITY
ACCESS DEPT.

UNIVERSITIES SPACE RESEARCH ASSOCIATION
LUNAR AND PLANETARY INSTITUTE
3303 NASA ROAD 1
HOUSTON, TEXAS 77058

PAPERS PRESENTED TO THE

CONFERENCE ON

THE LUNAR HIGHLANDS CRUST

SPONSORED BY THE LUNAR AND PLANETARY INSTITUTE

14 – 16 NOVEMBER 1979

Compiled by the
Lunar and Planetary Institute
3303 NASA Road One
Houston, Texas 77058

LPI Contribution 394

Material in this volume may be copied without restraint for library, abstract service, educational or personal research purposes; however, republication of any paper or portion thereof requires the written permission of the authors as well as appropriate acknowledgment of this publication.

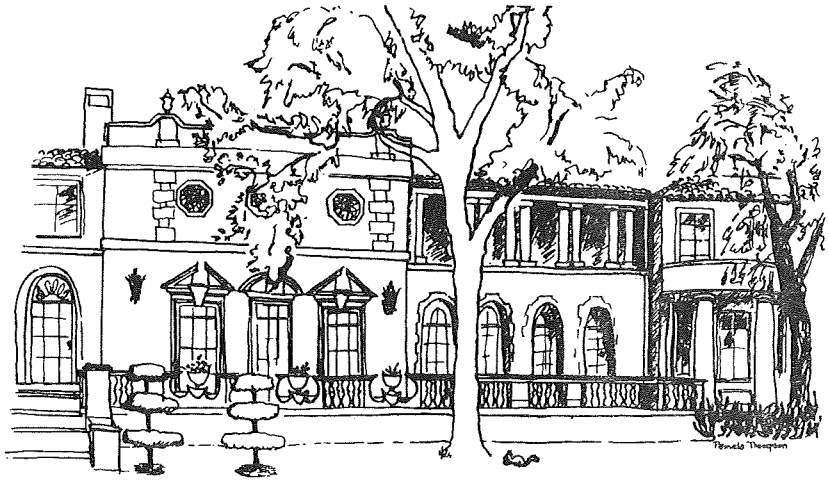

PREFACE

This volume contains papers which have been accepted for publication by the Program Committee of the Conference on the Lunar Highlands Crust. Papers were solicited which address one of the following major topics:

1. Petrology, chemistry, and chronology of lunar highland rocks
2. Regional characteristics of highland rocks
3. Physical processes of highland crust evolution: Geophysical evolution of the crust and lithosphere
4. Models for the formation of the lunar highlands crust
5. The lunar crust in a planetary context

The Program Committee consists of J. W. Head, III (*Brown University, Providence*), C. M. Hohenberg (*Washington University, St. Louis*), R. B. Merrill (*Lunar and Planetary Institute, Houston*), C. Meyer, Jr. (*NASA Johnson Space Center, Houston*), J. W. Minear (*NASA Johnson Space Center, Houston*), J. W. Papike, Co-convenor (*State University of New York, Stony Brook*), C. H. Simonds, Co-convenor (*Northrop Services, Houston*), P. W. Weiblen (*University of Minnesota, Minneapolis*).

Logistic and administrative support for this conference has been provided by P. P. Jones (*Administrative Assistant, Lunar and Planetary Institute*). This abstract volume has been prepared under the supervision of P. C. Robertson (*Technical Editor, Lunar and Planetary Institute*).

Papers are arranged alphabetically by the name of the first author. Indices by lunar sample number, subject, and author are provided.

The Lunar and Planetary Institute is operated by the Universities Space Research Association under contract No. NSR 09-051-001 with the National Aeronautics and Space Administration.

TABLE OF CONTENTS

PAGE

Chemical Diversity of the Lunar Light Plains from Orbital X-ray Data
C. G. Andre, T. A. Maxwell, F. El-Baz, and I. Adler 1

Pristine Primary Crustal Rocks or Secondary Plutonic Rocks?
A. B. Binder 3

Comparison and Synthesis of the Wood and Binder Models for the Formation of the Crust in a Convecting Magma System
A. B. Binder and M. A. Lange 6

Early Lunar History Recorded by Norite 78236
R. W. Carlson and G. W. Lugmair 9

Lateral Heterogeneity of the Lunar Eastern Limb
J. Conca 12

Role of Basin Ejecta in Highland Stratigraphy
R. A. De Hon 15

Petrology of Lunar Rock 66095: Implications for the Genesis of Highland Basalt and the Stratigraphy of the Apollo 16 Landing Site
J. R. Garrison, Jr. and L. A. Taylor 18

Distribution and Ages of Light-Colored Plains on the Moon
A. W. Gifford and F. El-Baz 21

Lunar Crustal Structure Beneath the Apollo Seismic Stations
N. R. Goins, A. M. Dainty, and M. N. Toksöz 24

Cratering Record: Processes and Effects
R. A. F. Grieve 27

Pressure – Temperature Estimates of Spinel Cataclasites: Comparison of Experimental Results in Complex and Simple Systems
T. L. Grove, A. E. Bence, and D. H. Lindsley 30

A Second Look at Variations of Iron Concentrations in the Lunar Highlands and Implications for Crustal Models
E. L. Haines and A. E. Metzger 33

Orientations of Central Peaks in Lunar Craters: Implications for Regional Structural Trends
W. L. Hale 36

Minor Elements in Plagioclase from Lunar Highland Rocks: New Data, Especially for Granulitic Impactites
E. C. Hansen, I. M. Steele, and J. V. Smith 39

Formative Conditions Controlling Structure of Planetary Highlands
W. K. Hartmann 42

On the Global Asymmetry of the Lunar Crust Thickness
J. B. Hartung 45,

Are Norite and KREEP Only Skin Deep? What are the Highlands Made of?
L. A. Haskin, R. L. Korotev, and M. M. Lindstrom 47

Multispectral Imaging of Lunar Crater Deposits
B. R. Hawke, D. MacLaskey, and T. B. McCord 50

Chemical Mixing Model Studies of Lunar Basin Ejecta Deposits
B. R. Hawke and P. D. Spudis 53

Geochemical Anomalies on the Lunar Eastern Limb and Farside
B. R. Hawke, P. D. Spudis, and P. E. Clark 56

Lateral Crustal Variations Determined from Geological Studies
J. Head 59

Lunar Highlands Volcanism: Geologic and Remote Sensing Data on Domes of Possible Extrusive Origin
J. W. Head and T. B. McCord 61

The Cordierite- to Spinel-Cataclasite Transition in the Moon, and its Bearing on the Structure of the Crust and Mantle
C. T. Herzberg and M. B. Baker 63

Physical–Chemical Constraints on Models of Planetary Crust Formation
C. T. Herzberg and W. S. Fyfe 66

Parentless Plutonium Fission Xenon in Troctolite 76535?
C. M. Hohenberg, B. Hudson, and F. A. Podosek 69

Lunar Magcons: Gross Correlation with Areas of Seismic Modification Associated with Major Basin Impacts
L. L. Hood 72

"Bunte Breccia" of the Ries Crater: Implications for Lateral and Vertical Redistribution of Large Scale Crater Ejecta
F. Hörz 75

On the Early Global Melting of the Terrestrial Planets
C. J. Hostetler and M. J. Drake 78

Regional Chemical Variations in the Lunar Crust
N. Hubbard 81

Laboratory Verification of the Lunar Orbital X-ray Fluorescence Experiment — Preliminary Results
N. Hubbard and B.-S. King 84

Thermal History of Fragment-Laden "Basalt" 77115
J. S. Huebner, C. R. Thornber, and R. F. Sanford 87

A Possible Role for Halogen-Rich Fluids in the Generation of KREEP Basalts
A. J. Irving 90

Petrology of the Major Rock Types of the Lunar Highlands
O. B. James 92

Highland Rocks — A View from Below
S. Jovanovic and G. W. Reed, Jr. 95

Statistical Criteria for the Presence of Pristine Rock Fragments in Lunar Impact Breccias
H.-D. Knöll and D. Stöffler 96

The Generation of Lunar Impact Melts: A Comparison of Theoretical and Observational Results
M. A. Lange and B. R. Hawke 99

Highland Chemistry: Preliminary Synthesis and Analysis of Major and Trace Element Relationships Using Statistical Methods
K. Livi, S. Brande, and A. E. Bence 102

Magma Oceanography Revisited: Formation of the Primitive Lunar Crustal Rocks
J. Longhi 105

The Apollo 15 Highland Regolith
D. S. McKay and A. Basu 108

Trace Elements in Plagioclase from the Lunar Highlands
C. Meyer, Jr. 111

Rusty Rock Consortium — Vapor: Petrographic Framework for Clasts of 66095
R. W. Meyer, J. R. Garrison, Jr., and L. A. Taylor 114

Pattern Recognition Studies on Highland Reference Suite Rocks and Related Lunar Samples
C. B. Moore, M. L. Parsons, B. Rock, and D. D. Pratt 117

Pristine Troctolites as Possible Source Rocks for Igneous Apollo 15 KREEP
M. D. Norman 119

Age and REE Abundances of Anorthositic Norite from 15455
L. Nyquist, H. Wiesmann, J. Wooden, B. Bansal, and C.-Y. Shih 122

Fractionation in the Stillwater Complex: An Analog for the Lunar Crust and Upper Mantle
L. D. Raedeke and I. S. McCallum 125

Physical Processes in the Formation of the Highland Shell
S. K. Runcorn 128

Lunar Highlands Chemistry: Exploration with Q-Mode Factor Analysis
G. Ryder, C. Fico, and R. Ehrlich 129

Volcanism Prior to the Termination of the Heavy Bombardment: Evidence, Characteristics, and Concepts
G. Ryder and P. Spudis 132

Petrography and Composition of Large Lunar Glass Objects
R. B. Schaal, K. H. Fryer, and F. Hörz 135

Are There Ancient Clasts in Lunar Highland Rocks?
O. A. Schaeffer, A. E. Bence, and G. Eichhorn 138

Evolution of Intermediate-Age Impact Basins on the Moon
P. H. Schultz 141

Lateral Mixing of the Crust: Evidence, Mechanisms, and Implications
P. H. Schultz and M. Mendenhall 143

Geological Content of the Skylab Lunar Multispectral Scanner Data
C. R. Seeger 145

Low Speed (8 km/sec) Impact-Accretional Heating and Early Fractionation of the Moon
C. H. Simonds 148

Interpretation of Non-Mare and Mare Samples in Terms of New Model for Sequential Episodic Differentiation of a Growing Moon
J. V. Smith and E. C. Hansen 151

Geophysical Evolution of the Lunar Crust and Lithosphere
S. C. Solomon 154

The Extent and Duration of Lunar KREEP Volcanism
P. D. Spudis 157

Trace Elements in Highland Plagioclase: Ion Probe Analyses of Li, Na, Mg, Ti, Sr and Ba
I. M. Steele and J. V. Smith 160

Problems of the Classification and Nomenclature of Lunar Highland Rocks — a Status Report
D. Stöffler and H.-D. Knöll 163

Lunar Highland Rocks with Evolved Compositions: Fractional Crystallization or Liquid Immiscibility?
G. J. Taylor, R. D. Warner, and K. Keil 166

The 67915 Consortium: Searching for Pieces of the Ancient Lunar Crust
G. J. Taylor, R. Warner, K. Keil, J. Geiss, K. Marti, E. Roedder, R. A. Schmitt, and P. Weiblen 169

Concepts of the Chemical Composition of the Lunar Highland Crust
S. R. Taylor 172

Mare-Terra Differences in Infrared/Radar Anomaly Occurrences: Implications about Crater Aging
T. W. Thompson, J. W. Cutts, R. W. Shorthill, and S. H. Zisk 175

Silicate Mineralogy of Highland Melt Rocks
D. T. Vaniman and J. J. Papike 178

The Lunar Magma Ocean Revisited
D. Walker 181

Major and Trace Element Systematics of Lunar Highland Samples
H. Wänke, G. Dreibus, and H. Palme 183

An Intrinsic Uncertainty in Determining the Chemical Composition of the Early Lunar Crust
J. L. Warner and C. H. Simonds 186

Petrology of 60035, a Polylithologic ANT Breccia
R. D. Warner, G. J. Taylor, and K. Keil 189

Certain Pristine Nonmare Rocks Formed as Cumulates from the Magma Ocean (But Many Others Did Not)
P. H. Warren 192

Comparing Facts about Pristine Nonmare Rocks with Theory about the Magma Ocean, to Constrain the Bulk Composition of the Moon
P. H. Warren and J. T. Wasson 195

Solar System Formation and Highland Cratering
G. W. Wetherill 198

Meteoritic Material in the Lunar Highlands: Clues to the Accretion History of the Moon
R. Wolf and E. Anders 200

Pristine Highland Rocks and Mare Basalts: Comparison of Siderophile and Volatile Elements
R. Wolf, A. Woodrow, and E. Anders 201

INDICES

Lunar Sample Index 203

Subject Index 205

Author Index 209

CHEMICAL DIVERSITY OF THE LUNAR LIGHT PLAINS FROM ORBITAL X-RAY DATA. Constance G. Andre,* Ted A. Maxwell,** Farouk El-Baz,** and Isidore Adler*. *University of Maryland, College Park, MD 20742. **National Air and Space Museum, Smithsonian Institution, Washington, DC 20560.

The return of highland impact breccias from the Apollo 16 landing site has prompted several revised theories for the origin of the light-colored smooth (Cayley) plains. Possible origins for this widely-distributed material include primary basin ejecta (1,2), fluidized primary basin ejecta (3), secondary ejecta of predominantly local material (4,5), volcanism (6), and several combinations of the above. Any single origin for smooth plains should account for: a) the wide range in age from pre-Nectarian to post-Orientale (7), b) the smooth surface with abundant secondary craters and crater-chains (8), c) the morphologic resemblance to mare material but with generally higher visible albedo (may also be lower than surrounding terra; 9), d) the local, patchy occurrence within older highland craters, e) the lunar-wide distribution outside the continuous ejecta facies of large basins (3), and f) the unimodal elevations of nearside plains units (10). On the basis of several conflicting characteristics, we feel that multiple origins for smooth plains in different regions are most likely. Using both high and low altitude X-ray fluorescence data, individual plains units on the near and east sides of the Moon are being studied in order to further constrain the possible modes of origin. In particular, Al/Si and Mg/Si data are being used to detect any chemical differences between plains deposits and surrounding soils and to measure the chemical uniformity among separate occurrences of plains.

Our findings show that plains materials in the Descartes, Palus Somni, Taurus Littrow and Langrenus areas have magnesium concentrations which contrast to those of adjacent highland soils. For instance, local chemical variations along six Apollo 16 groundtracks in the Descartes area indicate a 17% decrease in Mg/Si intensity ratios from adjacent terra to the smooth Cayley plains unit. However, in the Imbrian plains southeast of Langrenus, the Mg/Si values are 16% higher than the surrounding terra and the older plains units. Similarily, X-ray data for the small scattered occurrences of Imbrian plains in the Taurus Littrow and Palus Somni areas suggest higher magnesium concentrations compared to the surrounding terrain. The three plains deposits that have higher Mg/Si ratios also have lower albedos than both the adjacent highlands and other plains units. We believe that this association supports an endogenic origin in these cases. An interesting observation that may support this hypothesis is the distinctively high Mg/Si ratios at Macrobius A and B. These post-mare craters may have excavated a subsurface extension of the Mg-rich plains unit in Palus Somni. Those plains units that can be chemically distinguished from the adjacent highlands contradict a derivation from the local terrain, i.e. an accumulation of ejecta from small local impacts (11) or an <u>in situ</u> impact melt (12).

However, a local origin may be possible for the older, higher albedo plains unit east of Langrenus. Here, an Imbrian/Nectarian plains unit shows no observable difference in magnesium values from the surrounding highlands.

To test the hypothesis of a common distant source for plains units, the smooth plains at Descartes and the plains material in the Taurus Littrow highlands were compared. The dissimilarity between these compositions implies

unrelated sources. Therefore, based on orbital X-ray data, we believe that individual, geographically separate lunar light plains units may be characterized by both different chemical compositions and different modes of origin.

REFERENCES

(1) Chao, E.C.T., Hodges, C.A., Boyce, J.M., and Soderblom, L.A. (1975) U.S. G.S. Jour. Res., v. 3, p. 379-392.
(2) Moore, H.J., Hodges, C.A. and Scott, D.H. (1974) Proc. Lunar Sci. Conf., 5th, p. 71-100.
(3) Howard, K.A., Wilhelms, D.E. and Scott, D.H. (1974) Rev. Geophys. Space Phys., v. 12, p. 309-327.
(4) Oberbeck, V.R., Morrison, R.H., Horz, F., Quaide, W.L., and Gault, D.E. (1974) Proc. Lunar Sci. Conf., 5th, p. 111-136.
(5) Oberbeck, V.R., Horz, F., Morrison, R.H., Quaide, W.L., and Gault, D.E. (1975) The Moon, v. 12, p. 19-54.
(6) Hodges, C.A. (1973) U.S.G.S. Map I-739.
(7) Neukum, G. (1977) The Moon, v. 17. p. 383-393.
(8) Oberbeck, V.R., Quaide, W.L., Arvidson, R.E., and Aggarwal, H.R. (1977) Jour. Geophys. Res., v. 82, p. 1681-1698.
(9) Scott, D.H. and Pohn, H.A. (1972) U.S.G.S. Map I-799.
(10) Schultz, P.H., Spudis, P.D. and Sellers, D. (1979) Lunar and Planet. Sci. X, p. 1084-1086.
(11) Drake, M.J., Taylor, G.J. and Goles, G.G. (1974) Proc. Lunar Sci. Conf., 5th, p. 991-1008.
(12) Head, J.W. (1974) The Moon, v. 11, p. 327-356.

PRISTINE PRIMARY CRUSTAL ROCKS OR SECONDARY PLUTONIC ROCKS? A. B. Binder, Institut für Geophysik, Universität Kiel, 2300 Kiel, West Germany

Warren and Wasson (e.g., 1978, 1979a) have identified a suite of pristine crustal rocks which they consider to be relics of the primitive lunar crust. The criteria used to identify these rocks are: plutonic textures (coarse grain size, phase homogeneity, and cumulate character); low siderophiles ($< 2\times10^{-4}$x chondrite); low incompatibles ($< 5\times10^{-3}$x KREEP); large age ($> 4.2\times10^{9}$ yr); and low $^{87}Sr/^{86}Sr$ (0.6992). The rocks (rock clasts) which they consider to be pristine are mainly ferroan anorthosites and magnesian troctolites and dunites. They point out that the most abundant crustal rock types, i.e. anorthositic norites, are generally absent from their suite of pristine rocks. They have also convincingly argued (1978) against the model proposed by Delano and Ringwood (1978) that the pristine rocks were formed by secondary differentiation processes in impact melt pools. On the basis of these observations and arguments and some modelling considerations, Warren and Wasson (1979b) propose that the primitive crust of the moon consisted of cumulate ferroan anorthosites underlain by magnesian, mafic, layered intrusions of somewhat ill-defined origin.

There are several shortcomings to this model, the most prominent of which are: 1) the supposed pristine ferroan anorthosites have a very uniform An content (An_{95-97}). In contrast , the feldspars derived from the type of differentiating magma system described by Warren and Wasson (1979b) should have a wide range of An content (An_{80-97}). 2) An excessive amount (0.4 to 1.5 times the mass of the proposed ferroan anorthosite crust) of mafic-rich material would have had to be mixed with the original, anorthosite crust in order to account for the anorthositic norite composition of the current crust. 3) The supposed appreciable amounts of magnesium-rich mafics are proposed to have been situated between the iron-rich anorthosites of the crust and iron-rich mafics of the mare basalt magma source region. This requirement is inconsistant with any conceivable differentiation sequence for the moon as a whole or with the time scale for the melting of possible undifferentiated materials deep in the moon and their intrusion into the lower crust. This time scale is sufficiently long so that one can not account for the 4.5×10^{9} yr ages of some of the magnesian, mafic rocks. Because of these and other difficulties, we suggest that the Warren and Wasson primitive crustal model is incorrect and that the basic premise behind the model, i.e. that the so called pristine rocks are primary crustal rocks, is also incorrect.

We suggest that the rocks identified as pristine are <u>true</u> plutonic rocks formed by the differentiation of batholiths, stocks, etc. Such plutons could have originated as a result of

PRISTINE ROCKS

Binder, A. B.

the remelting and remobilization of the deeper parts of the primitive lunar crust which, on average, was anorthositic norite with Mg' of about 70 (e.g. Binder, 1976). As depicted in Fig. 1, model calculations show that 1) ferroan anorthosites (An_{96-97} and $35 \lesssim Mg' \lesssim 70$) could have formed in the upper parts of a differentiating body whose magma was derived by 1 to 20% partial remelting of such a primitive crust, and 2) magnesian dunites and magnesian troctolites (An_{90-98} and $70 \lesssim Mg' \lesssim 90$) could have formed in the lower parts of a differentiating body whose magma was derived by essentially total remelting of a portion of the primitive crust. Such true plutonic rocks would have all the characteristics needed to be identified by the Warren and Wasson criteria as being primary. We note further that lunar thermal models (e.g. Binder and Lange, 1979) show that the temperatures were high in the lower part of the crust for the first few hundred million years after it formed. This time scale is large in comparison to that for the development of batholith complexes in the terrestrial crust. Hence, it seems more than reasonable to expect that the primitive lunar crust underwent considerable endogenetic as well as exogenetic development in the first few hundred million years of lunar history - a time span which is comparable to the entire Phanerozoic Eon of the earth.

References:
Binder A. B. (1976), The Moon, 15, p. 275-314.
Binder A. B. and Lange M. A. (1979), J. Geophys. Res., in press.
Delano J. W. and Ringwood A. E. (1978), Proc. Lunar Sci. Conf. 9th, p. 111-160.
Warren P. H. and Wasson J. T. (1978), Proc. Lunar Planet. Sci. Conf. 9th, p. 185-217.
Warren P. H. and Wasson J. T. (1979a), Lunar Planet. Sci. X, p. 1301-1303.
Warren P. H. and Wasson J. T. (1979b), Proc. Lunar Planet. Sci. Conf. 10th, in press.

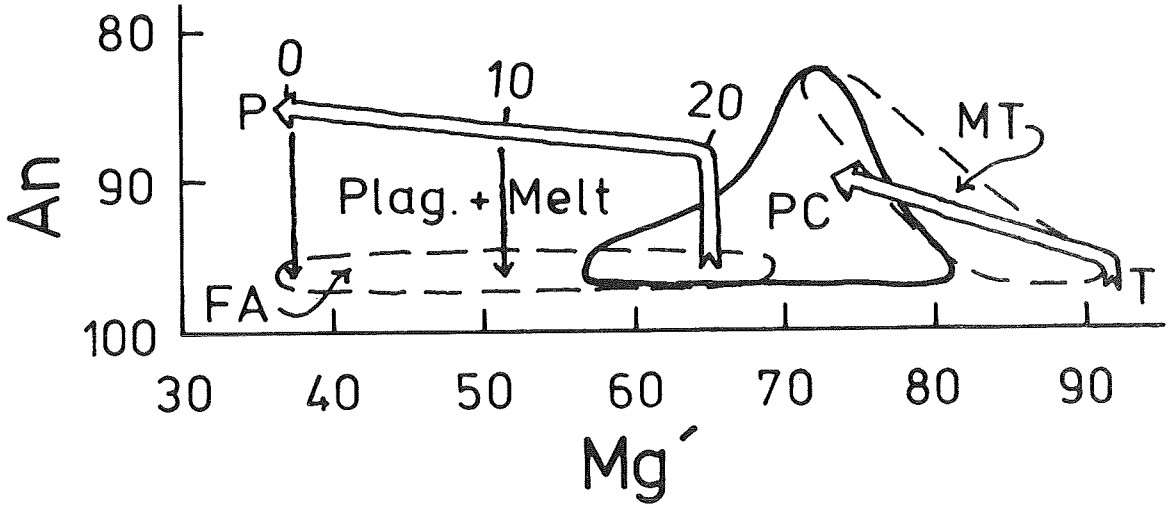

Fig. 1: Representative models for the formation of ferroan

anorthosites and magnesian troctolites and dunites from primitive crustal rocks. The fields where ferroan anorthosites, primitive (average) crustal rocks, and magnesian troctolites and dunites are found in this An vs Mg' diagram are labled FA, PC, and MT, respectively.

The broad arrow labled T is the equilibrium crystallization path for a totally melted portion of the primitive crust which had a noritic composition. Early differentiates from such a melt would be magnesian troctolites and dunites.

The broad arrow labled P is the equilibrium partial melting path (the percent of melting is given above the arrow) for a portion of the primitive crust which had an anorthositic composition. Ferroan anorthosites would form from such a melt by gravitational differentiation as early calcic plagioclase crystals and small amounts of trapped melt separated from the magma (as shown by the thin arrows).

COMPARISON AND SYNTHESIS OF THE WOOD AND BINDER MODELS FOR THE FORMATION OF THE CRUST IN A CONVECTING MAGMA SYSTEM.

A. B. Binder and M. A. Lange, Institut für Geophysik, Universität Kiel, 2300 Kiel, West Germany

The purpose of this paper is to present the results of a comparison and synthesis of the lunar crustal origin models developed by Wood (1975) and Binder (1975, 1976a). Both models are based on the basic concepts that (i) the primitive crust of the moon developed from a convecting magma and (ii) the composition of the current crust is representative of the suite of primitive crustal rocks. The latter premise has been recently challenged by Warren and Wasson (1978, 1979). They propose that the primitive crust is now represented only by a small number of so called pristine crustal rocks (mainly ferroan anorthosites and magnesian-troctolites and -dunites) whose compositions deviate significantly from those of the majority of the highland rocks. It is shown in an accompanying paper (Binder, this issue) that these "pristine rocks" are most probably of secondary, plutonic origin. Hence, we retain the concept that the chemical identity of the primitive crustal rocks is preserved in the current highland rocks despite severe mechanical and thermal modification during lunar history.

Review of Wood's model. Briefly, the essential points of Wood's model are: (i) The magma system from which the crust developed was well stirred by convection and probably impacts. (ii) Because of density differences, plagioclase crystals were concentrated at the top - and mafic crystals were concentrated towards the bottom of the system. (iii) When the point in the crystallization sequence was reached where the amount of residual fluid was $\sim$ 30%, the viscosity of the system increased dramatically and convection ceased. (iv) At this point, the proto-crustal column consisted of calcic feldspar crystals and a small amount of trapped, iron- and sodium-rich magma at the top and roughly equal amounts of calcic feldspar and magnesian mafic crystals together with a significant amount of trapped magma, with the above given composition, at the bottom. (v) After solidification of the column, the compositions of the rocks varied continuously from iron- and calcium-rich anorthosites at the top to magnesium- and sodium-rich norites at the bottom. Hence, the purpose of Wood's model to explain the reversed An-Mg' trend in the crust is achieved.

Review of Binder's model. The essential points of Binder's model are: (i) As the convecting and crystallizing magma system, from which the crust and upper mantle (mare basalt magma source region, Binder and Lange, 1978) formed, reached the plagioclase saturation point, calcic plagioclase crystals began to form near the surface and remained there due to their buoyancy. These crystals entrapped a small amount of iron- and sodium-rich melt and even smaller amounts of co-crystallizing mafic crystals. (ii) As crystallization proceeded, the majority of the plagioclase crystals were removed from the magma system by floatation - hence, the plagioclase formed essentially by disequilibrium crystallization. In contrast, the majority of the co-crystallizing mafic crystals sank and became mixed with the convecting

magma system below the crust - hence the mafics were formed basically by equilibrium crystallization. (iii) As this process continued, the ratio of crystals to melt increased in the entire magma system and hence in the material trapped by the plagioclase crystals. Simultaneously, because of the ever increasing ratio of crystals to liquid, the ability of the mafic crystals to seperate from the buoyant, calcic plagiocalse crystals decreased. Hence, the total amount of "entrapped" magnesian mafic crystals and iron- and sodium-melt increased. (iv) This disequilibrium / equilibrium crystallization ceased near the end of the sequence when the viscosity of the system reached a critical value. From that point on, equilibrium crystallization dominated and finally led to the development of the KREEP layer at the crust-mantle boundary. (v) At the end of the crustal formation process the early formed rocks at the top of the crust were generally iron- and calcium-rich, quartz-normative anorthosites. The later formed and hence deeper lying rocks were mafic, magnesium- and sodium-rich, and generally olivine normative.

Further, as a result of an analysis of the olivine to pyroxene ratios in the highland rocks, it was shown (Binder, 1976a) that the above described sequence must have taken place along the An-Ol cotectic and not at the Ol-Py-An peritectic. This cotectic crystallization is a consequence of the pressure induced shift of the Ol-Py cotectic (Binder, 1976a,b,c).

This model explains not only the reversed An-Mg' trend in the crustal rocks, but also - among others - the occurence of quartz normative anorthosites, the high ratio of olivine to pyroxene, and the occurence of troctolites and dunites (not their extremely magnesian varieties) in the crust.

Comparison: We have reviewed and expanded Wood's model in terms of the discussions given by Binder for his model (1976a) in order to compare both models. We find that Wood's model is basically capable to explain the variety of chemical characteristics of the highland crust. However, the major trends and crustal compositional boundaries as predicted by the Binder-model more readily fit the rock data. This is mainly due to the dynamical character of the Binder-model in contrast to Wood's static model. Wood's model also results in a continuous gradation from feldspathic crustal rocks to the peridotite of the upper mantle, i.e. there is no sharp chemical boundary between crust and upper mantle as is observed seismically. His model also precludes the formation of KREEP.

On the other hand, the critical role of the abrupt increase in the viscosity of the magma as its melt content decreases to $\sim$30%, as recognized by Wood, is not appreciated in the Binder model, i.e. Wood's physical model is more realistic than Binder's.

Synthesis: In synthesizing these relatively similar models, we have retained the dynamical character of the Binder-model and the static character of the Wood-model as follows. We suggest that there was a boundary-layer at the base of the growing crust in which crystallization occured. The crystal to melt ratio and hence the viscosity in this layer was higher than in the convecting magma below the forming crust for the majority of the sequence. We note here, that the computed density difference

between the plagiocalse crystals and the melt is less than a tenth of a g/cc. Thus, the crystals would have hardly been able to float towards the surface in an actively convecting system. We suggest that the boundary-layer protected these crystals from being drawn into the convecting magma. As the system evolved, the ever increasing viscosity within the boundary layer also reduced the ability of the heavier mafic minerals to sink out of this layer - as is required to explain the magnesian-mafic character of the later formed rocks. Until the critical viscosity within the convecting system was reached and the final stagnation occured, this system fed continually, chemically evolving magma into the boundary-layer.

The synthesized model is capable to explain the majority of the chemical characteristics of the primitive lunar crust as well as the physical aspects of its formation.

References:

Binder A. B. (1975), The Moon, 13, p. 431-473.
Binder A. B. (1976a), The Moon, 15, p. 275-314.
Binder A. B. (1976b), The Moon, 16, p. 115-150.
Binder A. B. (1976c), The Moon, 16, p. 159-173.
Binder A. B. and Lange M. A. (1978), Proc. Lunar Planet. Conf. 9th, p. 337-357.
Warren P. H. and Wasson J. T. (1978), Proc. Lunar Planet. Sci. Conf. 9th, p. 185-217.
Warren P. H. and Wasson J. T. (1979), Lunar Planet. Sci. X, p. 1301-1303.
Wood J. A. (1975), Proc. Lunar Sci. Conf. 6th, p. 1087-1102.

EARLY LUNAR HISTORY RECORDED BY NORITE 78236. R. W. Carlson and G. W. Lugmair, Chemistry Department and Scripps Institution of Oceanography, University of California, San Diego, La Jolla, California 92093

It is commonly believed that one significant feature of the early differentiation episode of the moon is the formation of a thick, plagioclase-rich crust above a global magma ocean. So far, remnants of this original crust provide the only materials for the direct study of the chronology and geochemical characteristics of the early lunar surface and interior. However, the intense meteorite bombardment of the lunar surface has altered much of the original igneous material through many phases of impact mixing, brecciation, remelting and shock metamorphism. One of the few highland samples which has retained features which might be expected for rocks forming in the early crust is the glass coated boulder found at the base of the Sculptured Hills. Samples returned from this boulder (78235,236,238) are noritic in composition with subequal amounts of plagioclase (Pl) and orthopyroxene (Opx) [1]. Grain sizes range up to 5 mm with some samples preserving a well defined cumulus texture [2]. In addition, REE analyses [3] and partial melting modelling [2] indicate that this norite could melt to produce liquids which have qualitatively similar relative REE patterns to that characteristic of KREEP.

This boulder has experienced at least one severe shock event which produced the brown glass coating surrounding and penetrating into the noritic interior. McCallum and Mathez [2] identify three chemical subgroups within the glass of 78235. These different glasses were interpreted as being due to the melting of bulk norite, and various degrees of mixing between "bulk rock" glass and liquid derived from the melting of individual plagioclase grains and intercumulus material. High concentrations of metal and troilite in the glass also indicate some degree of mixing with the impacting body.

No chronological information on this noritic boulder has been reported, with the exception of a Kr-Kr irradiation age of 292 m.y. for sample 78235 [4]. Therefore, based on the significance of this rock type to the formation of the early lunar crust and as a possible source material for KREEP basalt magmatism, we are investigating the internal Sm-Nd systematics of sample 78236.

Experimental Procedure. A 4.6g chip of 78236, with grain sizes of 2-3 mm, was disaggregated with a stainless steel needle. Plagioclase occurred as large distinct crystals which ranged in color from clear to milky white, to deep bluish grey. Some grains showed evidence of severe shock deformation including shock induced flow and melting along the rims of individual grains. Opx crystals were pale yellow brown in color with frosted surfaces due to extensive fracturing. Individual Opx grains could be disaggregated with the needle to produce a less than 50 μm grain size residue of crushed Opx fragments indicative of the high degree of shock induced fracturing experienced by this mineral.

Individual Pl and Opx crystal fragments of 0.5-1 mm grain size were separated by handpicking under a binocular microscope producing Pl separates of predominantly milky white grains, and three Opx separates. Opx separates Px-2 and Px-3 contained minor adhering and included brown spots and flakes, while Px-1 consisted only of clear to frosty grains with no obvious adhering material.

Dissolution, chemical separation and mass spectrometric procedures were similar to those described previously [5]. Measurement of unspiked Sm aliquots showed $^{149}Sm/^{150}Sm$ in 78236 to be 0.79% lower than the terrestrial normal, due to neutron capture on ^{149}Sm at the lunar surface. This large neutron effect is consistent with a long near-surface residence time as indicated by the 292 m.y. Kr-Kr exposure age of 78235 [4]. Measured Sm isotopic composition was used for Sm concentration determination.

Results and Discussion. Analytical results are presented in the Sm-Nd evolution diagram of Figure 1. As seen in Figure 1, the Sm-Nd data for

mineral separates of 78236 do not form a precise linear array. The best fit line through all the data points has a slope which corresponds to an age of 4.39AE. However, as seen in the insert to Figure 1, all data lie significantly off this line. Therefore, no strict time significance can be assigned to this age. It is obvious that at least one event of sufficient magnitude to partially reset the Sm-Nd system was experienced by this sample.

Variance in Sm-Nd analytical results for mineral separates could be due to either mixing of the original pristine minerals with some isotopically reset interstitial phase or by an incomplete reequilibration of the minerals during the last reheating episode. Of the three Pl separates measured, Pl-1 was optically distinguishable from Pl-2 and Pl-3 by a large amount of clear grains and fragments included with a lesser amount of milky translucent grains. Originally, these clear grains were believed to be less shocked plagioclases. However, the Sm-Nd results imply that this separate contains material which was severely affected by a late metamorphic event. As calculated from concentration data, it is evident that separate Pl-3, based on the lower Sm and Nd abundances of Pl-2, could have been contaminated by ~ 10% by weight of a phase with Sm-Nd similar to that reported for the interstitial glass of 78235 [3]. More detailed petrographic analysis of the separates are in progress. However, at this time, we believe that Pl-2 more closely represents the original cumulate plagioclase, while Pl-1 is dominated by plagioclase that was severely reworked during shock metamorphism and reheating. As discussed above, Opx separates Px-2 and Px-3 were optically indistinguishable. The concentrations of Nd and Sm measured for the Opx samples indicate that the variability in Sm/Nd cannot be due to mixing with other phases in the rock. Using the experimental distribution coefficients for Sm and Nd in Pl and Opx [6], a rough estimate shows that all Pl separates would be in equilibrium with a liquid with $^{147}Sm/^{144}Nd \sim 0.17$. This value is also calculated for the "whole rock" data from 78235 [3]. In contrast, only Px-1 could be in equilibrium with this liquid, while, for instance, a parental liquid with $^{147}Sm/^{144}Nd \lesssim 0.22$ would be required for Px-2. This might suggest that possibly only Px-1 and Pl-1 reequilibrated with one another during the last metamorphism.

Chronological constraints on the time of the last metamorphism may be derived from a tie-line connecting the most altered plagioclase (Pl-1) and pyroxene separates (Px-1). It is important to note that a tie-line connecting these points also passes through Px-3. These three data points define an age of 4.18 ± 0.04AE. It is not clear at present whether this age has any strict time significance. However, 4.17AE has been identified as a major metamorphic event by K-Ar and Pb ages for various A17 highland breccias and clasts [7, 8, 9].

Information on the crystallization age of 78236 can be derived from the separates which show the least evidence for reequilibration, Pl-2 and Px-2. A tie-line connecting these points defines an age of 4.49 ± 0.02AE. If either Px-2 or Pl-2 experienced partial reequilibration, then this age reflects a lower limit to the true time of crystallization. However, if this datum is indeed the true age, the slightly higher than Juvinas initial ($\varepsilon_{JUV}(T_o) = +1.5 \pm 0.06$) of this isochron might imply that the source materials of the norite had undergone prior evolution in a LREE depleted reservoir. An indication for this possibility might be given by the fact that the calculated equilibrium liquid for Px-2 has $^{147}Sm/^{144}Nd \lesssim 0.22$ (chondritic $^{147}Sm/^{144}Nd = 0.1936$). On the other hand, partial reequilibration of Pl-2 at a later time would be expected to increase its $^{143}Nd/^{144}Nd$, as was argued for the other Pl separates. This would imply that the age of 78236 is actually > 4.49AE with $\varepsilon_{JUV}(T_o)$ approaching zero.

EARLY LUNAR HISTORY RECORDED BY NORITE 78236.

R. W. Carlson

Although severely disturbed, the Sm-Nd data for 78236 may reflect two significant episodes in the history of this boulder and the lunar crust in general. Initial crystallization appears to have occurred at or prior to 4.49AE. A second event, possibly resulting in the excavation of this norite and severe metamorphism, caused incomplete reequilibration between plagioclase, orthopyroxene and LIL element-rich intercumulus phases. The Sm-Nd data indicate that this event occurred roughly 4.18AE ago, and, hence, may have been part of a large cataclysmic episode also recorded in other A17 highland samples.

Acknowledgment. This work was supported by NASA Grant NGL-05-009-150.

[1] Jackson E. D. et al. (1975) Bull. Geol. Soc. Amer. 86, p. 433-442. [2] McCallum I. S. and Mathez E. A. (1975) Proc. Lunar Sci. Conf. 6th, p. 395-414. [3] Winzer S. R. et al. (1975) Proc. Lunar Sci. Conf. 6th, p. 1219-1229. [4] Drozd R. J. et al. (1977), Proc. Lunar Sci. Conf. 8th, p. 3027-3043. [5] Lugmair G. W. et al. (1975) Proc. Lunar Sci. Conf. 6th, p. 1419-1429. [6] Weill D. F. and McKay G. A. (1975) Proc. Lunar Sci. Conf. 6th, p. 1143-1158. [7] Oberli F. et al. (1979) Lunar Planet. Sci. X, p. 940-942. [8] Jessberger E. K. et al. (1977) Proc. Lunar Sci. Conf. 8th, p. 2567-2580. [9] Staudacher Th. et al. (1979) Proc. Lunar and Planet. Sci. 10th, in press.

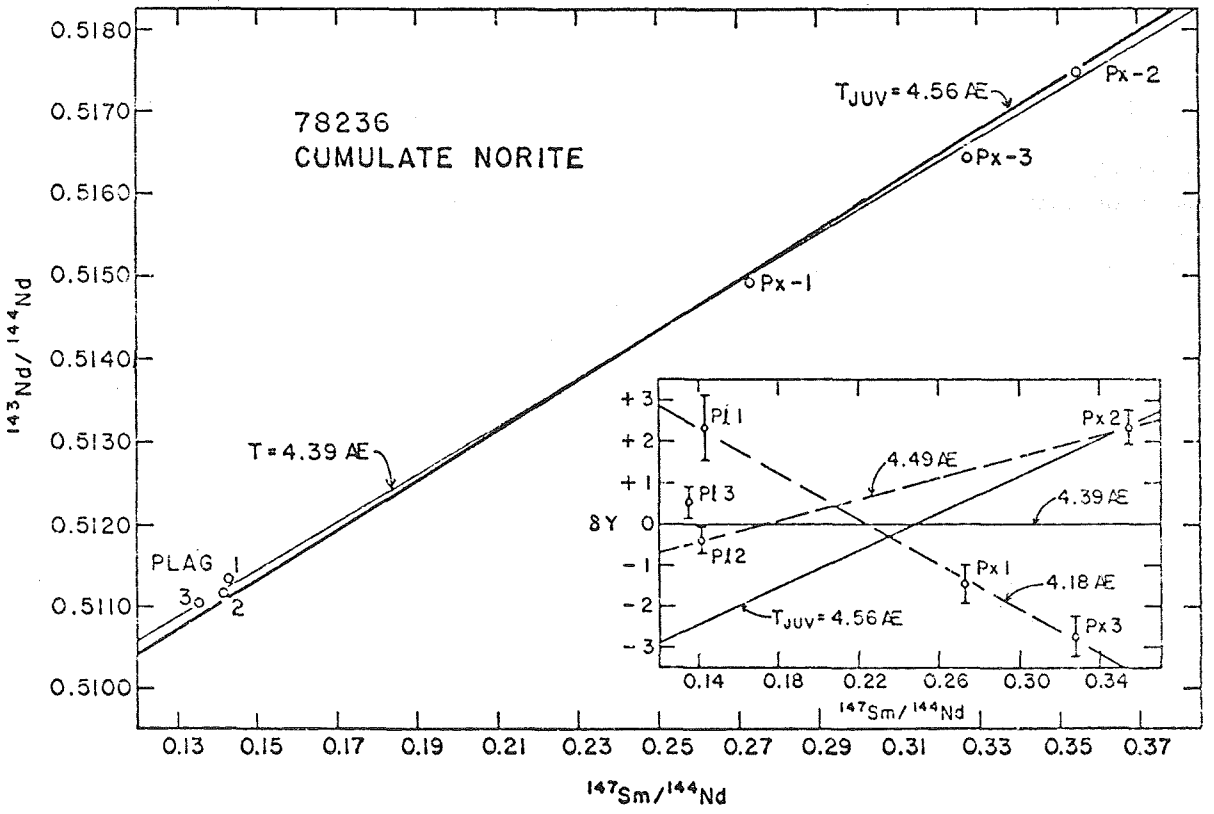

Figure 1: Sm-Nd evolution diagram for the cumulate norite 78236. As shown in the insert, the data obtained for six mineral separates do not form a precise linear array. Therefore, the age of 4.39AE corresponding to the best fit line through all the points does not have any time significance. However, a precise linear array is formed by three data points which possibly indicates the time of severe metamorphism 4.18AE ago. The time of original cumulate formation may have been at or prior to 4.49AE ago (see text for discussion). The isochron for Juvinas is given for reference. δY (in parts in 10^4) represents the deviation of $^{143}Nd/^{144}Nd$ of individual data points from an overall best fit line.

LATERAL HETEROGENEITY OF THE LUNAR EASTERN LIMB James Conca, California Institute of Technology, Pasadena, CA 91125.

Highlands East units mapped by Wilhelms and El-Baz (1) on the eastern limb of the moon (50°-105°E longitude) were investigated using improved orbital X-ray fluorescence data from Apollo 15 (2). Point by point orbital data plotted on a geologic map (1) and across Apollo 15 photographs of the eastern limb showed that geologic units of similar albedo and morphology, and mapped as identical units, have different surface chemistries depending on longitude and geographical relationship to Smythii Basin (Table I and Figure 1). The provinces east and west of 85°E longitude have distinctly different XRF and Gamma-ray characters. Although the Gamma-ray data were not compiled to represent seperate geologic units, the overall chemistry of the two provinces are quite dissimilar in the Gamma-ray data (Table II).

The highlands XRF data in Figure 1 fall into two groups, both centered near the norite-anorthosite line. Highlands west of 85°E are closer to the norite end and approximate an anorthositic gabbro composition. Highlands east of 85°E approach a gabbroic anorthosite composition. Highlands east of 85°E are higher in Al and lower in Mg than highlands west of 85°E and are lower in Th, K and Fe concentrations from the Gamma-ray data, as well as having a lower MgO/FeO ratio. Also the crustal thickness increases east over the region (3).

Generally, a more differentiated crust will be thicker, have a lower MgO/FeO ratio, higher Al and lower Fe concentrations (4), as is the case for highlands east of 85°E. However, if the lateral heterogeneity of the eastern limb was only the result of different differentiation histories from an originally homogeneous magma ocean then the K and Th concentrations of the more differentiated province would be increased. This is not the case for the highlands east of 85°E where K and Th are decreased relative to west of 85°E.

The XRF data also shows that the trend is not gradual over the 60° longitude studied but is confined to a 5°-10° range centered at 85°E where the XRF data is available. Also the change in K concentrations is abrupt at 90°E (5). This suggests that Smythii may be at the edge of a relatively sharp geochemical boundary between near and farside crusts in that region resulting from different petrogeneses; alternate differentiation histories and/or different initial materials.

(1) Wilhelms D.E. and El-Baz F. (1977) U.S.G.S. Map I-948.
(2) Hubbard et al. (1978) Mare Crisium: The View from Luna 24, p. 13-32.
(3) Bills B.G. and Ferrari A.J. (1976) Lunar Crustal Thickness. Proc. Lunar Sci. Conf. 7th. Frontpiece.
(4) Schonfeld E. (1977) Proc. Lunar Sci. Conf. 8th. p.1149-1162.
(5) Nishiizumi et al. (1976) Potassium Concentration. Proc. Lunar Sci. Conf. 7th. Frontpiece.
(6) Taylor S.R. (1975) Lunar Science: a post-Apollo view. Pergamon Press.
(7) Metzger et al. (1974) Proc. Lunar Sci. Conf. 5th. p. 1067-1078.

EASTERN LATERAL HETEROGENEITY

Conca, J.

TABLE I

HIGHLANDS EAST UNITS - Wt% Oxides XRF data

Unit+	Location	Al_2O_3 (± 1.0)	MgO (± 1.0)	Petrologic Type -	Al_2O_3	MgO
	West of 85°E Longitude					
pNbm	surrounding Crisium	25.0	9.0			
pNbr	west of Smythii	26.9	6.2			
	surrounding Crisium	26.9	8.6			
INfp	west of Smythii	25.5	7.3	Anorthositic* Gabbro	26.0	8.1
	south of Crisium	26.0	7.8			
NpNt	surrounding Crisium	27.1	7.7			
	southwest of Smythii	26.4	7.3			
	northwest of Smythii	29.0	8.3			
Ic_2	west of Smythii	26.0	5.6			
	East of 85°E Longitude					
pNbr	south of Smythii	28.6	4.8			
Ic_2	southeast of Smythii	29.6	4.0	Gabbroic* Anorthosite	31.4	3.4
NpNt	east of Smythii	30.4	4.0			

\+ as described by Wilhelms and El-Baz (1)
* values from Taylor (6)

TABLE II

HIGHLANDS EAST - Gamma-Ray data**

Location	Th (ppm)	K (ppm)	Fe (%)
West of 85°E Longitude			
55° - 83°E along A-16 track	1.3	980	8.6
60° - 82°E along A-15 track	1.4	1200	9.3
East of 85°E Longitude			
88° - 168°E along A-15 track	1.0	940	6.5
92° - 138°E along A-16 track	0.5	840	7.2

** values from Metzger et al. (7)

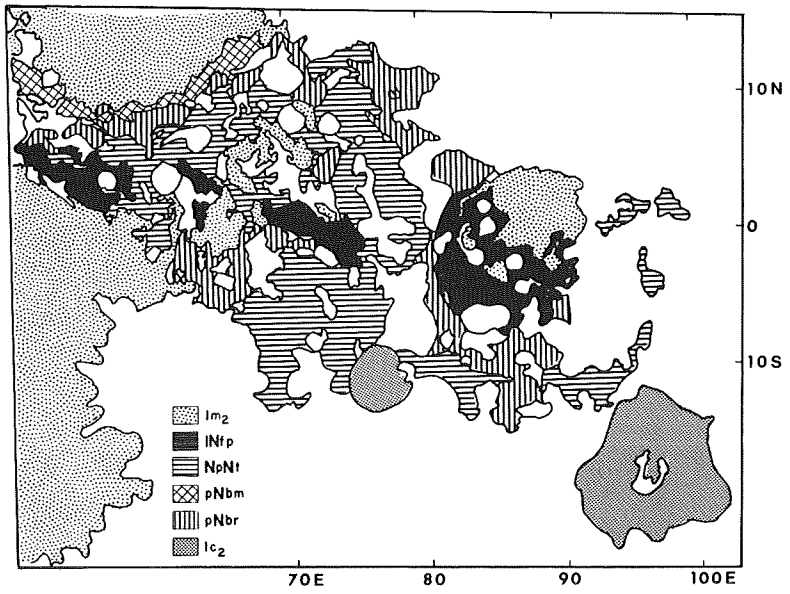

EASTERN LATERAL HETEROGENEITY

Conca, J.

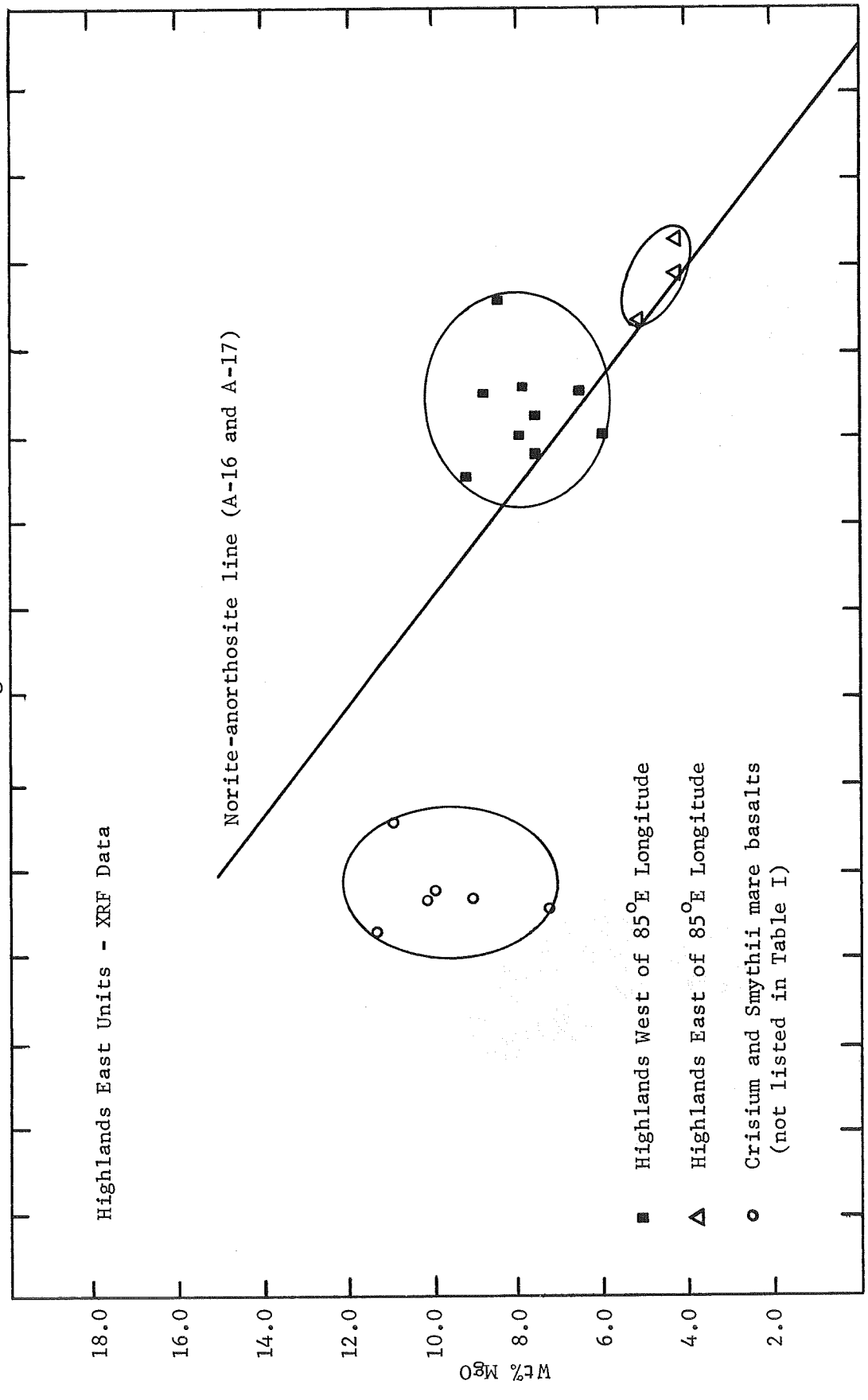

Figure 1

ROLE OF BASIN EJECTA IN HIGHLAND STRATIGRAPHY. R. A. De Hon, Department of Geosciences, Northeast Louisiana University, Monroe, LA 71209

Major impact basins and their associated ejecta serve as a framework for lunar farside stratigraphy. Observed superposition of basin materials and/or inferred relative ages based on the extent of degradation of basin rims allows construction of local stratigraphic columns (Table 1 and Fig. 1). Basin-related materials provide "marker horizons" by which other, less widespread, materials may be correlated(1). From the surviving remnant basins observed on the farside, it is apparent that the lunar surface was saturated with large basins during the first 0.5-1.0 b. y. of lunar history(1,2).

TABLE 1 CORRELATION CHART OF LUNAR FARSIDE BASINS

EAST	CENTRAL AND WEST		
		ORIENTALE	
MILNE	MENDELEEV		
	MOSCOVIENSE	HERTZSPRUNG	LEIBNITZ
		KOROLEV	
SMYTHII		APOLLO	INGENII
AUSTRALE	KELLER-HEAVISIDE		
AL KHWARIZMI-KING	FREUNDLICH-SHARONOV		
LOMONOSOV-FLEMING			
SOUTH POLE-AITKEN			

Modified from ref. 3, 4 and 5. Older basin assignments uncertain.

Basin formation excavates material from a growing impact cavity and redistributes the material as an ejecta blanket on the surface surrounding the basin. Based on the distribution of ejecta around large craters and around a small number of relatively young basins (Orientale, Imbrium, and Milne), the ejecta extends outward from the main basin rim crest to a distance of approximately one basin diameter. The surface of the ejecta blanket is composed of material derived from the greatest depth of excavation while materials of shallower origin occur in an inverse order within the ejecta blanket(6). By late Nectarian time, the lunar surface was completely blanketed by an imbricate pattern of basin ejecta (Fig. 1) derived from the deepest levels of impact excavation.

The combined thickness of brecciated materials of overlapping ejecta blankets may reach several kilometers thick, with an average thickness of around 2-4 km(7). Thus, the highland and pre-mare surfaces consist of a highly fragmented layer which comprises the lunar megaregolith(8). The megaregolith may or may not be geochemically homogeneous depending on the extent of impact mixing of the near surface layering. However, the megaregolith does consist of stratigraphically differentiated layers of overlapping ejecta blankets interbedded with other materials of impact and volcanic origins.

As in all crater rim deposits, the basin ejecta thins with increasing range, and the outer limits of the deposit consist of mixed basin ejecta and surface material churned by secondary cratering(9). Later impact cratering tends to destroy the characteristic surface patterns of the basin ejecta and to expose materials of the shallow pre-basin surface. A crudely time-dependent relationship exists for the lateral extent of recognizable basin

ROLE OF BASIN EJECTA IN HIGHLAND STRATIGRAPHY

De Hon, R. A.

ejecta and the age of the basin. Terrain beyond the limits of recognizable ejecta of old basins consists of an intermediate mixture of basin ejecta from depth and material of shallower sources re-exposed by later and small impacts. Presumably, there is a decreasing percentage of "deep component" within the degraded portion of the blanket at increasing distances from the basin rim crest.

The mechanism of basin formation governs, in part, the geochemical character of the lunar highlands. If the basins form by deep excavation by impact (depths near 1/5 to 1/10 of the basin diameter as observed in smaller craters), then basin ejecta on the surface represents material from 20 to 120 km deep. Each basin deposit would reflect a composition corresponding to materials at the depth of excavation; hence, basins of different sizes may be associated with ejecta blankets of different compositions. On the other hand, if basin excavation is limited by physical discontinuities at moderate depths (10), then all basins may display similar ejecta compositions derived from similar depths.

In conclusion, a megaregolith certainly must exist, but even a megaregolith will contain stratigraphically differentiated units. The youngest basins with well-preserved radial ejecta deposits provide the best targets for recognizing material derived from the greatest depths and for searching for compositional differences as a function of basin size. Moderately old basins (Nectarian in age) provide suitable targets for attempting to recognize a variable composition with increasing distance from the basin.

References: Howard K. A. et al (1974) Rev. Geophys. and Space Phys., 3, p. 309-327. (2) Baldwin R. B. (1969) Astron. J., 74, p. 570-571. (3) Scott D. H. et al. (1977) U.S.G.S. Misc. Inves. Map I-1034. (4) Wilhelms D. E. and El Baz F. (1977) U.S.G.S. Misc. Inves. Map I-948. (5) Stuart-Alexander D. E. (1976) U.S.G.S. Interagency Report 79. (6) Shoemaker E. M. (1962) Phys. and Astr. of the Moon, p. 283-359. (7) Short N. M. and Forman M. L. (1972) Modern Geology, 3, p. 69-91. (8) Hartmann W. K. (1973) Icarus, 18, p. 634-639. (9) Oberbeck V. R. and Morrison R. H. (1973) The Moon, 9, p. 415-455. (10) De Hon R. A. (1978) Lunar and Planet. Conf. 9th, p. 232-234.

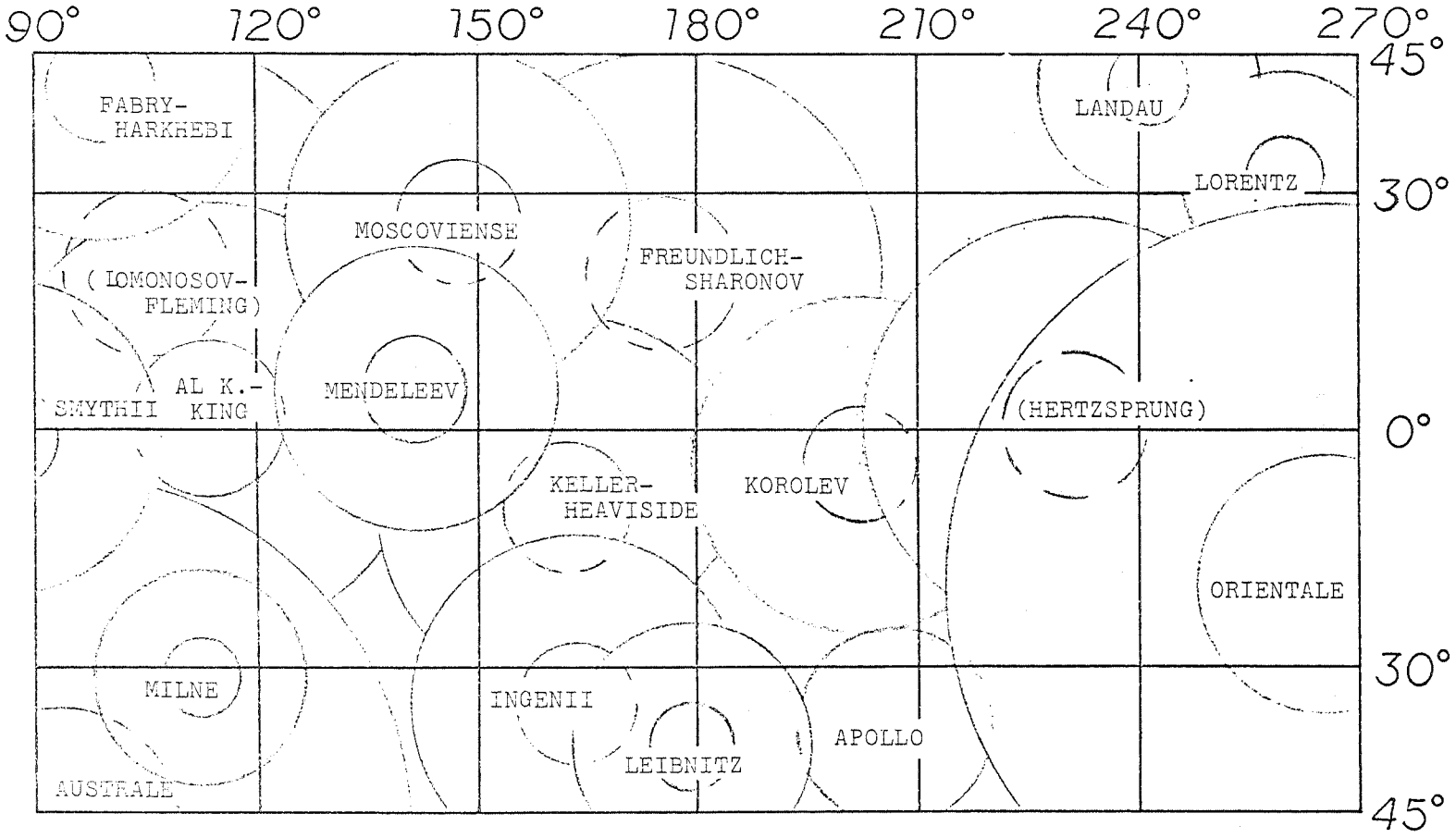

FIGURE 1. Location of lunar farside basins. Schematic representaion of the maximum extent of radial ejecta. Superposition relationships are constructed to match Table 1. South Pole-Aitken basin not shown.

PETROLOGY OF LUNAR ROCK 66095: IMPLICATIONS FOR THE GENESIS OF HIGHLAND BASALT AND THE STRATIGRAPHY OF THE APOLLO 16 LANDING SITE;
J. R. Garrison, Jr., and L. A. Taylor; Dept. of Geological Sciences, The University of Tennessee, Knoxville, Tennessee 37916

Lunar rock 66095 ("rusty rock") is a clast-rich impact-melt basalt in which clasts of anorthosite-troctolite, plagioclase, and basalt are set in a fine-grained matrix of plagioclase (An_{89-94}), olivine (Fo_{77}), and pigeonite (3.74-8.17 wt.% CaO). Basalt clasts consist of phenocrysts of plagioclase (An_{92-94}), olivine (Fo_{74-76}), and pigeonite in a very fine-grained mesostasis. Two of the examined basalt clasts contain small chondrules consisting of a fine-grained intergrowth of plagioclase and pigeonite. Rock 66095 contains numerous planar to slightly irregular fractures, commonly filled with shock-produced glass. There are also numerous blind veins filled with this same glass.

The components of 66095 were analyzed by broad beam microprobe techniques (DBA) with approximate corrections applied according to the methods of Albee, Quick, and Chodos (1). Analyses of seven areas of matrix material reveal highland basalt compositions. Nine analyses of glass are similar to the matrix analyses, although some of the low-Al_2O_3 glasses resemble low-K Fra Mauro basalt. Ten analyses of basalt clasts reveal a spectrum of compositions: four gabbroic anorthosites, five highland basalts, and one low-K Fra Mauro basalt. The two chondrules have gabbroic anorthosite compositions. The great diversity in mineralogy and chemistry between the various clasts, as well as the matrix, emphasizes that for most Apollo 16 samples the concept of whole-rock chemistry is meaningless.

A plot of Al_2O_3 versus FeO + MgO (Figure 1) shows the 66095 components relative to the compositions of gabbroic anorthosite, highland basalt (H), and Fra Mauro basalt rocks and glasses (2,3,4,5). The compositions of 66095 matrix and glass (representing shock melted matrix) appear to represent a mixing line between gabbroic anorthosite (and anorthosite) and Fra Mauro basalt. This suggests that the matrix of 66095 (and other highland basalts) were formed by impact melting of strata consisting of gabbroic anorthosite-anorthosite and Fra Mauro basalt. Notice that the compositions of the glasses appear to be displaced relative to those of the clasts and matrix. In fact, this is due to FeO enrichment in the glass, probably a consequence of the kinetics of shock melting.

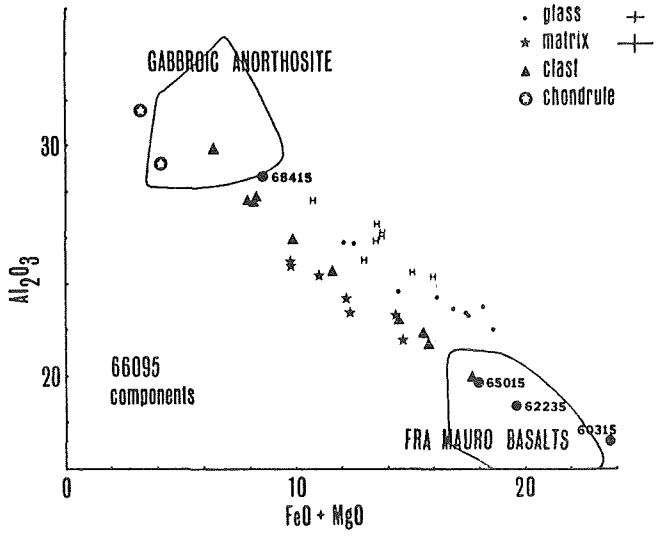

Figure 1.

PETROLOGY OF LUNAR ROCK 66095

Garrison, J. R., Jr.

In modeling highland rocks, it is a common practice to consider only "pristine" rocks as the end-members (6). However, this is certainly not feasible for a breccia such as 66095 which consists of clasts with 2nd, 3rd, or higher derivative remelts. In considering 66095, as well as similar breccias, we prefer a simple model in which a two layer stratigraphy is subjected to a basin-forming impact; large volumes of highland basalt melt containing clasts of the two strata (i.e. gabbroic anorthosite-anorthosite and Fra Mauro basalt) would be produced. 66095 contains clasts of gabbroic anorthosite and anorthosite (+ troctolite) which may represent one stratum, while the Fra Mauro clast represents the other stratum. If we remove the restriction that the end-members necessarily be "pristine" rocks, commonly used to model highland rocks, and consider only Apollo 16 rocks, both end-members are present in the igneous rock suite collected at the Apollo 16 site: 68415 represents the gabbroic anorthosite end-member and poikiloblastic rocks 62235, 60315, and 65015 represent the Fra Mauro component. The presence of highland basalt clasts (containing condrules) in 66095 indicates a more complex history involving more than one period of highland basalt formation, perhaps from nearby impacts.

Available trace element and isotopic data are consistent with a mixing model for the generation of highland basalts such as 66095. High abundances of U and Th in some of the Apollo 16 breccias (e.g. 66095) led Nunes et al. (7) to conclude that these rocks contain a large amount of KREEP-like material. 66095 has an abundance of incompatible elements intermediate between the two proposed end-members. 66095 has Ir (16.6 ppb) intermediate between gabbroic anorthosite 68415 (4.6 ppb) and Fra Mauro poikiloblastic rocks 60315 (35 ppb) and 62235 (20 ppb). 65015 has Ir (11.6 ppb) similar to 66095. Reported REE data for 66095 (8,9) also support a mixing model (Figure 2). 66095,36 has a pattern similar to low-K Fra Mauro basalt. 66095,37 has REE abundances much like gabbroic anorthosite-highland basalt. When compared to the representative end-members 68415 and 62235, both 66095,36 and 66095,48 show intermediate REE abundances.

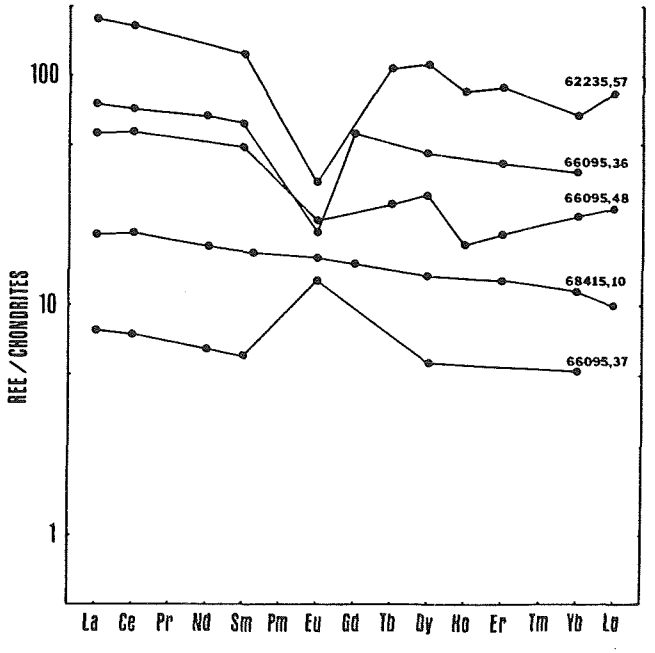

Figure 2.

PETROLOGY OF LUNAR ROCK 66095

Garrison, J. R., Jr.

The isotopic and geochronologic data of Nunes and Tatsumoto (10), Nunes et al. (7), and Nyquist et al. (11) combined with the above model allow a coherent geologic history for the Apollo 16 site to be reconstructed. A concordant U-Pb age for gabbroic anorthosite 68415 suggests that the lowermost crustal strata of gabbroic anorthosite-anorthosite formed at 4.47 b.y. ago. Since 66095 contains this crustal component, its 3-stage model Pb age of 4.47 b.y. is also consistent with this event. A Rb-Sr isochron age of 4.42 b.y. for the Fra Mauro rocks (i.e. 60315, 62235, and 65015) implies that the Fra Mauro basalts were younger and probably covered the older ANT crust. During the next 400 m.y., minor (or distant) impacts periodically added a minor amount of meteoritic material and a covering of Fra Mauro and highland basalt (with chondrules) debris. At 4.0 b.y. ago a major basin-forming impact (Imbrium event) occurred as evidenced by the 4.01 b.y. $^{207}Pb/^{206}Pb$ age of highland basalt 66095 and the 4.06 b.y. Rb-Sr isochron age for other Apollo 16 melt rocks. This impact event caused a complete redistribution of Pb. The Fra Mauro basalts were intensely metamorphosed and recrystallized as nearly all of their Pb was expelled, hence their high $^{206}Pb/^{204}Pb$ ratios (greater than 10,000) and U-Pb ages of 3.9-4.0 b.y. The highland basalts 66095 and 67015 and the Apollo 16 soils all contain excess radiogenic Pb, probably that lost from the Fra Mauro basalts. Nunes and Tatsumoto (10) found the uniform isotopic composition of the leachable Pb in 66095 to be consistent with Pb introduction at a discrete time.

It is possible that this volatilization and redistribution of Pb was accompanied by the redistribution of other volatile elements. The metaigneous Fra Mauro sample 65015 contains a factor of 2-10 lower Zn, Ag, Br, and Tl than Apollo 12 KREEP. Thus, it may be possible to explain the extreme enrichment of volatiles in highland basalts such as 66095 and 61016 as the result of their containing a large KREEP component and the addition of such volatiles redistributed from the volatile-rich Fra Mauro stratum during major impacts.

REFERENCES

(1) Albee, A. L. et al. (1977) (abstract) Lunar Science VIII, 7-9.
(2) Reid, A. et al. (1972) PLSC 3, 363-378.
(3) Dence, M. R. and Plant, A. G. (1972) PLSC 3, 379-399.
(4) Taylor, S. R. (1975), Lunar Science, Pergamon Press.
(5) Ryder, G. and Norman, M. (1978), JSC 14565.
(6) Ryder, G. (1979) Lunar Science X, 1046-1048.
(7) Nunes, P. et al. (1973) PLSC 4, 1797-1822.
(8) Brunfelt, A.O. et al. (1973) PLSC 4, 1209-1218.
(9) Hubbard, N. J. et al. (1974) PLSC 5, 1227-1246.
(10) Nunes, P. and Tatsumoto (1973) Science 182, 916-919.
(11) Nyquist, L. E. et al. (1973) PLSC 4, 1823-1846.

DISTRIBUTION AND AGES OF LIGHT-COLORED PLAINS ON THE MOON.

Ann W. Gifford and Farouk El-Baz, National Air and Space Museum, Smithsonian Institution, Washington, DC, 20560

Smooth, light-colored plains constitute a significant portion of the lunar surface. These plains are considered part of the lunar highlands based on the facts that: (1) their albedo is high, .150 on the average; (2) they show high Al/Si ratios in the results of X-ray fluorescence experiments (ref. 1); and (3) the Apollo 16 returned samples show that the plains in that site are impact breccias of anorthositic composition. The light-colored plains are widely distributed on the Moon within old basins, inside craters of varying sizes, and within inter-basin and inter-crater areas. Their most significant characteristic is a nearly flat surface; they are the least rugged of all lunar highland units.

Due largely to their smooth appearance, the origin of the lunar light-colored plains has been attributed to fluidized primary basin ejecta (ref. 2), ejecta from secondary basin impacts (ref. 3), and volcanism, at least in the case of the lunar "pitted plains" (refs. 4 and 5). The theory that light plains-forming materials may be ejecta from multi-ring basins or large craters is based on the fact that the Apollo 16 returned samples are nonvolcanic breccias. These interpretations have been applied to post-Apollo lunar geologic mapping. However, other interpretations should not be ruled out.

Three U.S. Geological Survey geologic maps cover the lunar limbs and farside (50°E to 50°W, 50°N to 50°S) at a scale of 1:5,000,000 (East Side, Central Far Side, and West Side; refs. 6, 7 and 8 respectively). These maps include plains units mapped as Nectarian, Imbrian-Nectarian, and Imbrian (Fig. 1). Several interesting patterns are apparent from this compilation based on the three maps.

The oldest plains units occupy large areas on the floors of the pre-Nectarian basins Al-Khwarizmi-King, Lomonosov-Fleming, Gagarin, and an unnamed basin centered at 18°N 175°E. Extensive plains units only slightly younger also occur in Mendeleev, Korolev, and Apollo. In order to support a secondary ejecta debris origin (ref. 9) for these oldest plains ejecta from several large Nectarian basins would have to be invoked to account for the areal extent. These plains are not necessarily older analogues of the Cayley (ref. 10) type plains. Figures 2 and 3 show the morphology of Nectarian and Imbrian-Nectarian plains units. The Lomonosov-Fleming basin in particular contains units which could be mixtures of volcanic material and ejecta debris (Fig. 3).

Imbrian age plains deposits are generally of smaller extent. Approximately 60% of these form crater floors. Over 30% of them are in a band concentric to the Orientale basin, a pattern which is apparent in figure 1. This is in contrast to the Nectarian plains which are mostly found within old basins rather than outside them in the position of ejecta. This suggests that although most Imbrian-age plains including Cayley type units form by the mechanism suggested by Oberbeck et al. (ref. 3), pre-mare volcanism should not be ruled out for the older plains on the basis of present photogeologic mapping. This is also suggested by variations in the overall chemistry of one plains area versus another as in the east side of the Moon (ref. 11).

REFERENCES

1. Adler, I. et al. (1973) Proc. 4th Lunar Sci. Conf., v. 3, 2783-2791.
2. Eggleton, R.E. and Schaber, G.G. (1972) Apollo 16 PSR: 29/7-16.
3. Oberbeck, V.R. et al. (1975) The Moon, v. 12, 19-54.
4. Wilhelms, D.E. and McCauley, J.F. (1971) USGS Map I-703.
5. Strom, Robert G. (1977) Phys. Earth Planet. Interiors, v. 15, 156-172.

DISTRIBUTION AND AGES OF PLAINS

Gifford, A. W. et al.

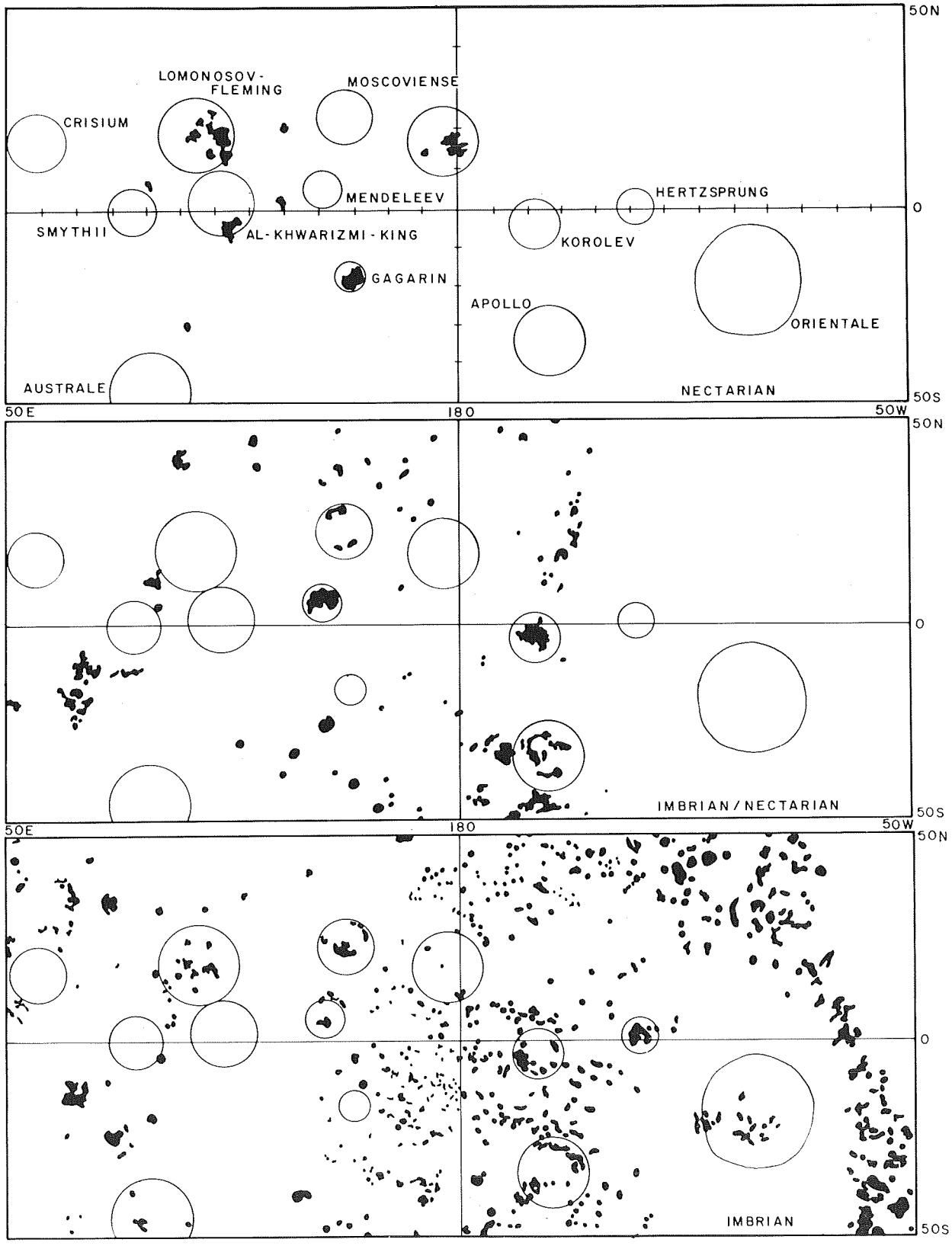

Fig. 1. Distribution maps of smooth, light-colored plains on the Moon based on U.S.G.S. geologic maps at 1:5 000 000 scale (ref. 6, 7, and 8).

DISTRIBUTION AND AGES OF PLAINS

Gifford, A. W. et al.

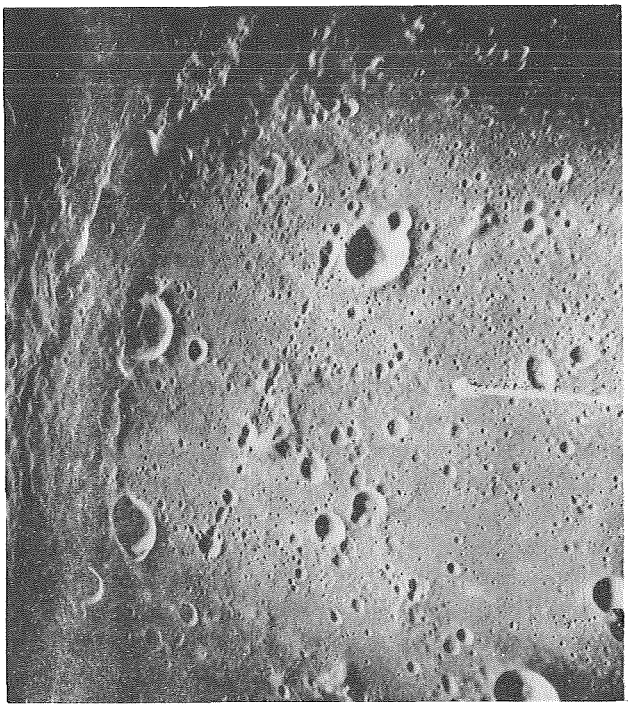

Fig. 2. The light -colored plains fill of the Mendeleev basin at 7 N, 140 E.

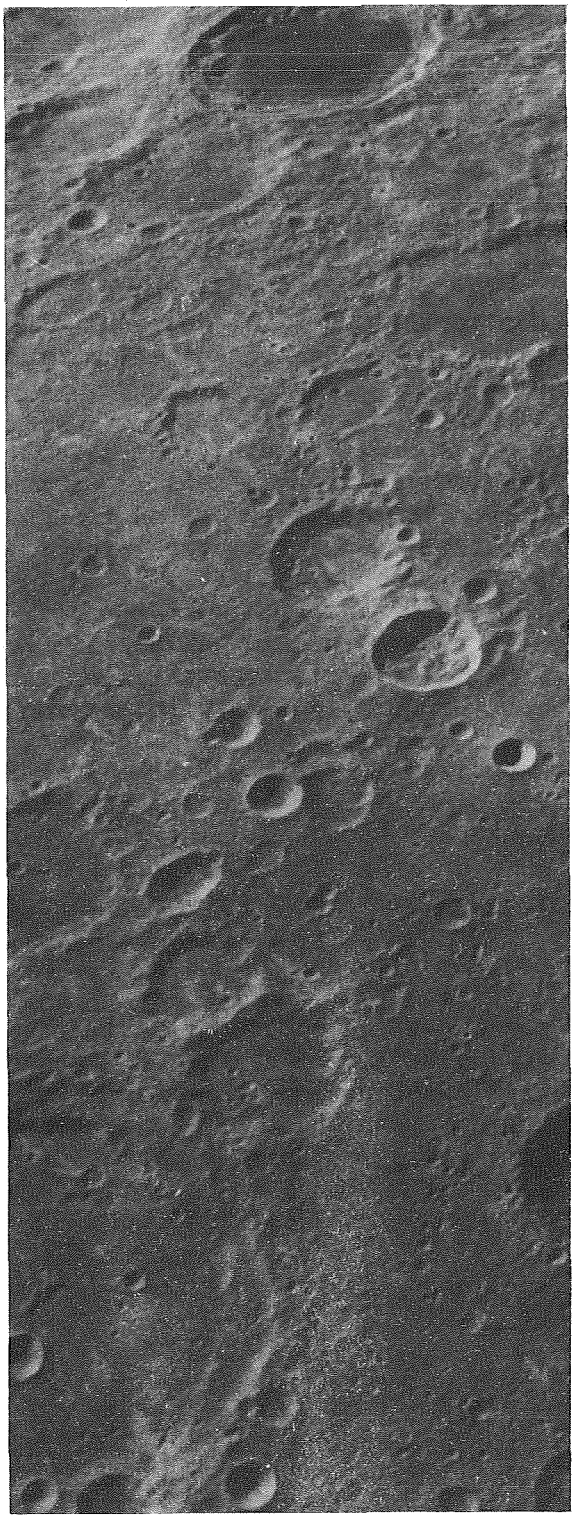

Fig. 3. Nectarian age plains at 20 N 113 E. The mare-filled crater Lomonosov is at the upper edge; the crater Fleming is at the lower left.

6. Wilhelms, D.E. and El-Baz, F. (1977) USGS Map I-948.
7. Stuart-Alexander, D.E. (1978) USGS Map I-1047.
8. Scott, D.H. et al. (1977) USGS Map I-1034.
9. Chao, E.C.T. et al. (1975) Jour. Res. USGS, 379-392.
10. Morris, E.C. and Wilhelms, D.E. (1967) USGS Map I-510.
11. El-Baz, F. and Wilhelms, D.E. (1975) Proc. 6th, 2721-2738.

LUNAR CRUSTAL STRUCTURE BENEATH THE APOLLO SEISMIC STATIONS. N.R. Goins, Mobil Research and Development Corporation, Dallas, TX 75221; A.M. Dainty, School of Geophysical Sciences, Georgia Institute of Technology, Atlanta, GA 30332; M. N. Toksöz, Dept. of Earth and Planetary Sciences, MIT, Cambridge, MA 02139

The seismic structure of the lunar crust has been determined primarily from the study of seismograms produced by impacting spacecraft sections onto the moon and observing the resulting ground motion at the four stations of the Apollo passive seismic network. Due to the sequential emplacement of the seismometers, most of this artificial impact data was recorded by the first two stations (12 and 14) and so the crustal model obtained from this data is only valid in the Oceanus Procellarum region near stations 12 and 14. The model is fairly well constrained and is discussed in (1), with earlier references cited therein.

In order to study the crustal structure at the other seismic station sites, we must turn to the seismic records produced by natural lunar events, such as meteorite impacts, shallow moonquakes, and deep moonquakes. A compilation of all such events that are large enough and sufficiently well observed to yield significant structural information is given in (2). As discussed therein, there are at least two major difficulties involved in using this data. The natural events occur at unknown locations and times, and since there are only four seismic stations a large fraction of the available data from each event must be used to simply locate the events in space and time. In addition, the intense scattering layer on the lunar surface destroys any coherent surface wave trains, makes even the direct P and S wave arrivals emergent, and spreads the direct arrival energy into long codas that effectively obscure later secondary body wave arrivals.

In an effort to overcome these difficulties, we apply a polarization filter to the three-component long-period seismograms so as to reduce the energy in the scattered coda and enhance the initial onset of secondary body waves, and use record sections to search for peg-leg multiples and converted waves resulting from crustal interfaces. The polarization filter is a time domain non-linear gain control applied point-by-point to the three-component long-period seismograms recorded at stations 12, 15 and 16. (The station 14 vertical-component seismometer did not operate properly.) The gain control is based on the shape of the particle motion ellipsoid in a running window along the trace; the initial unscattered onset of a body wave should have rectilinear particle motion while the energy in the obscuring scattered coda should arrive randomly with elliptical particle motion. This filter was originally proposed by Flinn (3) and first applied to lunar data by Dainty and others (4). Record section plots are constructed from these filtered records in an effort to eliminate "false-alarm" random rectilinear noise; only true arrivals should consistently line up on the record sections. Finally, theoretical travel time differences between the direct S wave arrivals and various possible peg-leg multiples (reflection at free surface and crustal interface) and converted waves (conversion at crustal interface) are computed for various structural models and plotted on the record sections in an effort to identify possible arrivals.

The results of this work are suggestive but not conclusive. The most convincing correlations indicate that there are two major crustal layers beneath the highland site of station 16; an upper crust from 0 to 20 km and a lower crust from 20 to 75 km depth. This is to be compared to the station 12-14 structure obtained from the artificial impact data of an upper crust from 0 to 20 km and a lower crust from 20 to 60 km. (The average velocity in each of the layers is assumed to be the same at both stations.) Thus the highland

LUNAR CRUSTAL STRUCTURE BENEATH APOLLO STATIONS

Goins, N.R., et al

crust appears to be about 15 km thicker overall. Weaker correlations suggest that the 20 km interface also exists at station 15, with some indications of boundaries at 60 and/or 90 km depth. Finally, there is some evidence that weak reflections can be seen at station 12 from the expected 20 and 60 km depths.

Before discussing the implications of these results, it is important to emphasize the uncertainties in the interpretations. The correlations discussed above represent general agreement of arrival times only. The predicted amplitudes of the suspected arrivals are in general far smaller than those observed on the records. There are several possible explanations for this discrepancy, such as focusing and tuning effects, and the non-linear nature of the polarization filter which will pass both signal and noise when the particle motion is rectilinear. Nevertheless, the time correlations themselves are only moderately consistent, and in light of the amplitude anomalies and the various assumptions concerning constant lateral velocities and arrival identifications, the above results must be considered tentative until confirmatory evidence can be found.

If the above results are valid, several conclusions can be drawn. First, the observed secondary waves represent the first direct seismic evidence that the lunar crust is in fact a moonwide phenomenon; this has been concluded previously on geochemical and geological grounds. For such reflections to occur, the crustal interfaces must be narrow compared to the seismic wavelengths of 6-8 km, say at most 2-3 km wide. Second, we note that the 15 km extra crustal thickness at the highland station 16 compared to stations 12-14 is enough to isostatically compensate the higher elevation (1.5 km relative to station 12), assuming crust and mantle densities of 3.0 g/cc and 3.3 g/cc, respectively. Thurber and Solomon (5) have shown that the above crustal thicknesses are compatible with the observed gravity data. Finally, we can make preliminary comments concerning the geological significance of the seismic results. The lower crustal layer appears to vary laterally in thickness and probably represents competent rock; the seismic velocities are compatible with a wide range of compositions. The most interesting aspect of the above results is the apparent existence of a 20 km upper crust at all stations including the highland site; this suggests that it cannot be mare basalt fill. In addition, the thickness (20 km) is greater than the maximum mare basalt thicknesses obtained from photogeologic studies (cf. reference 6). The 20 km interface itself could be caused by either a change in composition or a change in physical properties (e.g. fractured to competent rock; see reference 7); in either case its existence in a relatively widespread basis would have important implications for crustal formation properties and subsequent meteorite excavation.

(1) Toksoz M.N. et al. (1974) Rev. Geophys. Space Phys., 12, p. 539-567. (2) Goins N.R. et al. (1979) submitted to J. Geophys. Res. (3) Flinn E.A. (1965) Proc. IEEE, 53, p. 1874-1876. (4) Dainty A.M. et al. Proc. Lunar Sci. Conf. 7th, p. 3057-3075. (5) Thurber C.H. and Solomon S.C. (1978) (abstract) In Lunar Planet Sci. IX, p. 1169. (6) Howard K.A. et al. (1974) Rev. Geophys. Space Phys., 12, p. 309-328. (7) Simmons G. et al. (1973) Science, 182, p. 158-

LUNAR CRUSTAL STRUCTURE BENEATH APOLLO STATIONS

Goins, N.R., et al

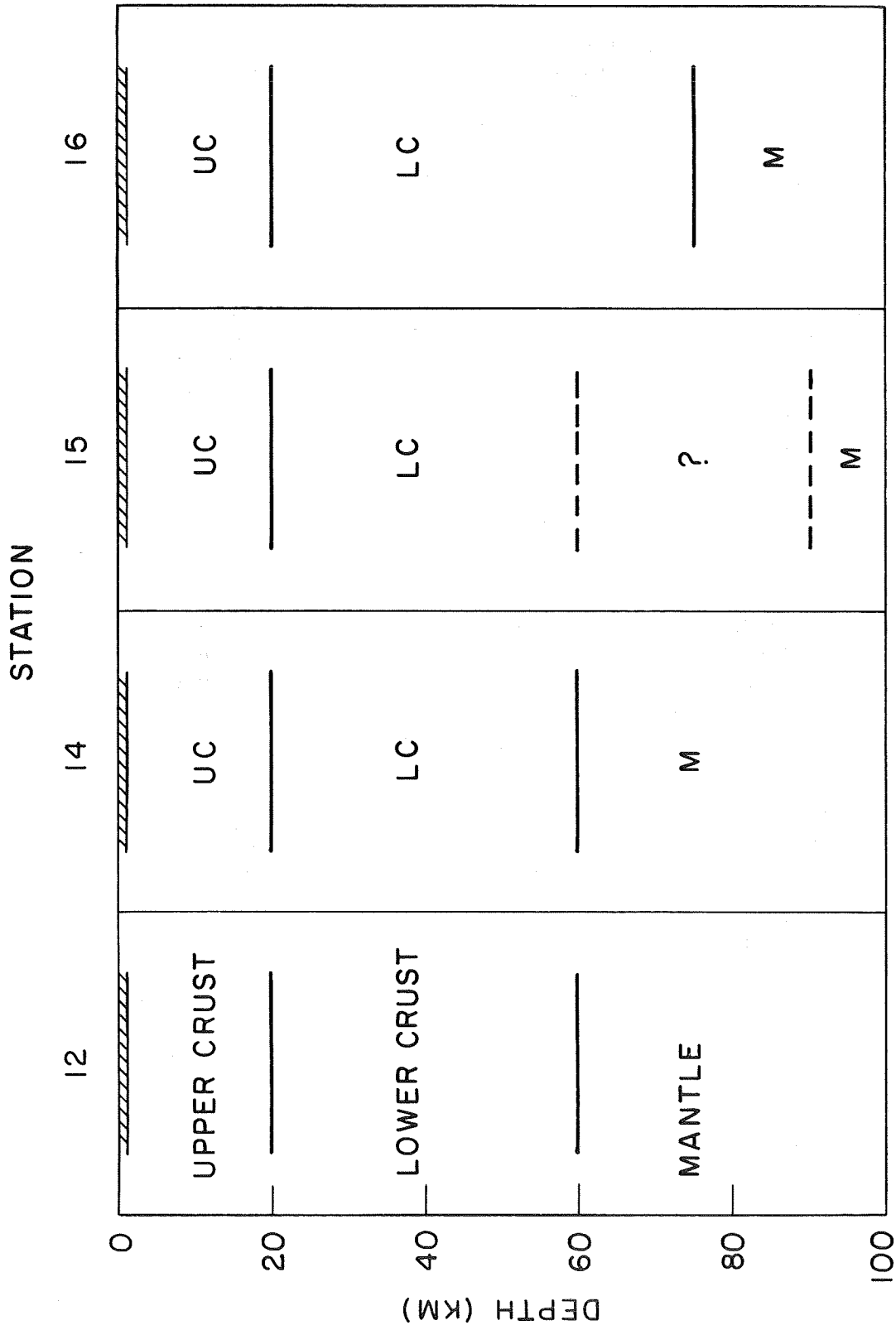

FIGURE 1: Proposed seismic structure of the lunar crust beneath the four stations of the Apollo seismic network.

CRATERING RECORD: PROCESSES AND EFFECTS. Richard A.F. Grieve, Earth Physics Branch, Department of Energy, Mines and Resources, Ottawa, Canada, K1A 0Y3.

The lunar surface retains an impressive record of hypervelocity cratering. The impact bombardment of the moon is responsible for features ranging from the second order topography and spatial dichotomy of the highlands and mare regions, through the physical and chemical character of the bulk of the returned highlands sample to the siderophile-enriched nature of the lunar regolith. The general appreciation of the profound effects impact bombardment had on early crustal and surface evolution of the moon, and the other terrestrial planets, has led to major efforts to understand the impact process (1). However, impact is basically a disruptive process. It imparts kinetic energy to the target, resulting in the excavation, physical mixing and redeposition of the original target materials, and it also deposits internal energy, producing characteristic structural disorder in crystals, and melting and vaporization of portions of the target. This physical and chemical disordering of the target, in combination with the potential for multiple impact events and the lack of strict geologic control, mean that considerable uncertainties remain with regard to the interpretation of the lunar highlands sample. Much of our understanding has drawn upon the terrestrial experience, where single impact events, either natural or experimental, in relatively well-controlled environments are avilable for detailed study.

The Cratering Record

There is no information on the pre-crustal impact history of the moon. It is relatively safe to assume that the flux was probably greater than that recorded on the oldest highlands crust and its effect was to retard crustal segregation by the physical mixing and the addition of near-surface heat to primary differentiation products (2). However, the relative inefficiency of impact homogenization with respect to internal evolution is evidenced by the completion of initial crustal differentiation by ~4.4 by (3). The observed record of the variation of crater density with age indicates that from an early high flux at ~4.4 by, of >30 times that recorded on the mare, the cratering rate decayed rapidly to within a factor of 2-3 of the mare rate by 3.9 by (4). However, a constant cratering rate was not achieved till ~3.0 by. The paucity of "crystallization" ages for highland samples older than ~3.9 $\pm$ 0.1 by has led to the suggestion that the moon underwent a "cataclysmic" bombardment at this time (5,6), leading to the formation of the major multi-ringed structures which later became the mare basins. Although challenged as requiring ad hoc models for the preservation of large impacting bodies over ~0.6 by (7), Wetherill (8) has shown that some large, ~10^{23} g, bodies may have survived for extended periods of time within the inner solar system.

The Highlands Sample

The bulk of the returned highlands sample are impact products, ~60% being breccias and ~30% impact melts (9). The dominance of impact mixing of pre-existing lithologies as a petrogenetic process poses considerable problems in the interpretation of the highlands sample. Recent extensive studies to determine pristine highlands rocks (low siderophile and incompatible elements, >4.2 by age, coarse grain size etc.) indicate that the primary highlands crust was dominated by anorthosite, troctolite and dunite (10, 11). However, the petrogenetic significance of such ubiquitous highland compositions as highland basalt and Low K Fra Mauro basalt (12, 13) is more doubtful. Both occur only

as impact products (11, 14) and as such may be regarded as mechanical mixtures, relationships to the plagioclase-olivine cotectic on the SiO_2-olv.-plag. pseudoternary notwithstanding (15).

Textural similarities between lunar samples and terrestrial impact deposits have been used to propose that the Fra Mauro formation may be a mixed, essentially clastic breccia, related to the Imbrium event (16, 17) and the Apollo 17 grey breccias melt-bearing ejecta from Serenitatis (18). However, important differences between impact breccias on the two planets have been recognized. For example, the common occurrence of thermally altered materials and the almost completely reset nature of the ages in the highlands sample is at variance with the terrestrial experience from single impact events and may reflect repetitive bombardment (19). Others, such as the much higher proportion of unshocked to shocked clasts in individual lunar suevitic breccias (18) may be attributed to the different physical conditions of cratering. In the lunar case, the lower surface gravity permits a greater volume of material to be excavated for a given energy, reducing the proportion of strongly shocked to less shocked ejecta by a factor of 3 over the terrestrial case. In addition, the absence of an atmosphere allows ejecta to land with undiminished ejection velocities, producing energetic secondary cratering, promoting the mixing of local material with primary ejecta and shocking the material for a second time.

In spite of these complications, individual melt clasts in Apollo 15 and 17 breccias have been identified with the Imbrium and Serenitatis impacts. They have been variously interpreted as a mixture of the entire 60 km thick highlands crustal column, compositionally equivalent to ~66% anorthosite, ~17% gabbro and ~17% troctolite (18), or as a sample of the crust, with a low K Fra Mauro composition, from depths of 20-35 km (20). Central to these interpretations is the recognition from terrestrial and experimental data that impact melts represent total melts of that part of the target shocked to pressures in excess of 60-100 GPa (21) and the melt matrix is an extremely well homogenized chemical mixture, even in targets with highly diverse original lithologies (22).

Depth of Excavation (Sampling)

If certain lithologies, such as clasts with specific shock levels (23, 24) can be identified as ejecta from individual basin-forming events, important information can be obtained on the stratigraphy of the crust, provided sampling depth can be estimated. This requires a coherent model for the excavation stage of large impact events. Unfortunately, there is considerable misunderstanding and disagreement on this topic. Depth estimates for Imbrium ejecta range from <30 km (25), ~100 km for material shocked to 10 GPa (24) and 148-328 km, again for a shock pressure 10 GPa (26). The disagreement centers on the application of strict proportional growth for the excavated cavity with increasing impact energy. Proportional growth argues that multi-ring basins, with apparent depth/diameter ratios of 1:50 or greater, are the highly modified final forms of original excavated cavities with dimensions in keeping with small simple bowl-shaped, apparent depth/diameter ratios ~1:5. Support for this comes from extensive studies at terrestrial craters; in particular those with stratigraphic control, which indicate that the amount of structural uplift in the center of central uplift and multi-ring structures increases with diameter and is numerically similar to the depth of the excavated cavity as extrapolated from simple craters (27). Although observations at terrestrial craters suggest large craters are less efficiently excavated than small craters (28), in agreement with the relative

variations in crater dimensions and shock wave attenuation with energy (29), there is no evidence for major variations in the relative dimensions of the excavated cavities over some ten orders of magnitude in energy. Nevertheless, the failure of particular restoration models (25) to predict deep excavated cavities for basin-sized events introduces considerable doubt to the significance of some highlands samples. However, these models may not approximate the modification process, which is still poorly understood (30), or alternatively it may be possible to reconcile them with proportion growth, provided bulking effects in the ejecta are considered (31).

The current lack of a consensus on some of the details of the effects of cratering on the highlands sample should not be viewed overly pessimistically. The increased awareness, since pre-Apollo times, of impact as a fundamental evolutionary process on early planetary crusts and the consequent level of effort and sophistication which has gone into studying the details of impact phenomena portends well for interpretations in the near-future.

References

(1) Impact and Explosion Cratering, Pergamon, 1977. (2) Solomon, S.C., PreC. Res. in press. (3) Jesserberger, E.K., LPS X, 625-627, 1979. (4) Chap. 8, BVSP, Houston, preprint, 1979. (5) Tera, F. and Wasserburg, G., PLSC 5th, 1571-1599, 1974. (6) Maurer, P. et al., GCA, 42, 1687-1720, 1978. (7) Hartmann, W.K., Icarus, 24, 181-187, 1975. (8) Wetherill, G.W., PLSC 8th, 1-16, 1977. (9) Simonds, C.H. et al., Am. Min., 61, 569-577, 1976. (10) Warren, P.H. and Wasson, J.F., PLPSC 9th, 185-217, 1978. (11) Bickel, C.E. and Warner, J.L., PLPSC 9th, 629-652, 1978. (12) Ridley, W.I. et al., PLSC 4th, 309-321, 1973. (13) Taylor, S.R. et al., GCA, 37, 2665-2683, 1973. (14) Reid, A.M. et al., PLSC 8th, 2321-2338, 1977. (15) Hess, P.C. et al., PLSC 8th, 2357-2373, 1977. (16) Dence, M.R. and Plant, A.G., PLSC 3rd, 379-399, 1972. (17) Chao, E.C.T., J. Res. U.S.G.S., 1, 1-18, 1973. (18) Dence, M.R. et al., PLSC 7th, 1821-1832, 1976. (19) Hörz, F. et al., PLSC 7th, 2931-2945, 1976. (20) Ryder, G. and Wood, J.A., PLSC 8th, 655-668, 1977. (21) Schaal, R.B. and Hörz, F., PLSC 8th, 1677-1730, 1977. (22) Grieve, R.A.F. and Floran, R.J., J.G.R., 83, 2761-2771, 1978. (23) Hawke, B.R. and Head, J.W., Imbrium Consort. Vol. 2, 91-96, 1977. (24) Dence, M.R., Imbrium Consort. Vol. 1, 147-155, 1976. (25) Head, J.W. et al., PLSC 6th, 2805-2829, 1975. (26) O'Keefe, J.D. and Ahrens, T.J., Phys. E.P. Inter., 16, 341-351, 1978. (27) Dence, M.R. and Grieve, R.A.F., LPS X, 292-294, 1979. (28) Grieve, R.A.F. et al., Impact and Explosion Cratering, 791-814, 1977. (29) Dabizha, A.I. and Ivanov, B.A., Meteoritika, 37, 160-167, 1978. (30) Grieve, R.A.F. and Robertson, P.B., Icarus, 38, 212-228, 1979. (31) Croft, S.K., LPS X, 248-250, 1979.

PRESSURE-TEMPERATURE ESTIMATES OF SPINEL CATACLASITES: COMPARISON OF EXPERIMENTAL RESULTS IN COMPLEX AND SIMPLE SYSTEMS: T. L. Grove, Dept. of Earth and Planetary Sciences, Mass. Inst. of Tech., Cambridge, MA 02139, A. E. Bence and D. H. Lindsley, Dept. of Earth and Space Sciences, State Univ. of New York, Stony Brook, N.Y. 11794

Introduction

A notable member of the sampled suite of the lunar highland crust is the high-Mg component (1), and the role played by this unique chemistry in the evolution of the highlands remains a matter of controversy. The high-Mg composition may arise (a) from mixing of a primitive chilled crustal and an anorthositic component, (b) as a residuum left from a partial melting event within the lunar crust (2,3) or (c) as a cumulate formed during fractionation processes (4). The spinel cataclasites (spin cat) are members of the high-Mg component and, although the samples are intensely brecciated, the constituent minerals forsteritic olivine-anorthite-aluminous orthopyroxene-pleonaste spinel (± cordierite) provide a record of lunar crustal T & P conditions and have been interpreted as samples from deep crustal levels (up to 60 km) (5,6,7).

We have carried out a set of experiments on a synthetic composition approximating that of spin cat 73263, 1, 11. The results of these experiments are used to estimate equilibration conditions which are then compared to the estimates of (6) based on thermochemical data and experimental data in the system MgO-Al_2O_3-SiO_2.

Experimental

The experiments on 73263 were designed to provide equilibrium data on the reaction:

$$Mg_2Si_2O_6 + MgAl_2O_4 \rightleftharpoons MgAl_2SiO_6 + Mg_2SiO_4$$

$$\text{en} + \text{pleonaste} \rightleftharpoons \text{Mg-Tsch} + \text{fo}$$

In the lunar system pyroxene, olivine and spinel may contain Fe, Al, Ti, Cr, Ca in addition to Mg, Si, Al and O. An experimental study that provided equilibrium data on all the exchange reactions involving Fe and Mg, as well as Ti, Al and Cr exchanges between spinel and pyroxene would be desirable, but extremely difficult. Instead, we assumed that the Fe-Mg exchange would attain equilibrium under our experimental conditions and we attempted to design experiments that reversed the content of Al in orthopyroxene. The experiments were performed in the range 1150° to 1280°C and 1 atm to 8 kbar, within the limits of stability for the assemblage orthopyroxene + spinel + olivine + plagioclase. The starting materials for the reversals were low-P, low-T and high-P, high-T syntheses made from an oxide mix, which provided the necessary range in orthopyroxene Al content. Run durations were 3 days (at 1280°C) to 14 days (at 1150°C). The experiments were carried out in Fe capsules, using evacuated sealed-silica tube and piston-cylinder techniques, and the run products were analyzed with an electron microprobe.

Results

Our experiments allow (a) an evaluation of the extrapolation of thermochemical and experimental data from simple systems to the interpretation of chemically complex lunar rocks and (b) a determination of the equilibration conditions of spin cat samples. Herzberg (6) estimated the P & T equilibration conditions for spinel cataclasites following the approach of (8,9,10). We followed the technique of Herzberg and calculated an equilibrium constant (K) and used the approximation of (11) to estimate activities. With the Ks derived from the spin cat experiments we have calculated ΔG° and compared

SPIN CAT EXPERIMENTS

GROVE et al.

$$K = \frac{a^{opx}_{Mg\text{-}Tsch} \cdot a^{oliv}_{fo}}{a^{opx}_{en} \cdot a^{sp}_{pleonaste}} = \frac{(X^{M1}_{Al})\ (X^{VI}_{Mg})^2}{(X^{M1}_{Mg})\ (X^{IV}_{Mg})\ (X^{VI}_{Al})^2}$$

these values to those derived by (9) and (10), where

$$\Delta G^{\circ}_{P,T} = \Delta H^{\circ}_{1,T} - T\Delta S^{\circ}_{T} + (P-1)\Delta V_{rxn} = -RT\ln K$$

$$\Delta G^{\circ}_{1,T} = -RT\ln K - (P-1)\Delta V_{rxn}$$

The values of $\Delta G^{\circ}_{1,T}$ are compared in Fig. 1 to those experimentally obtained by Fujii (10). An estimated ΔV_{rxn} derived from reversed spin cat experiments at 1 bar, 5 and 8 kbar was obtained (Fig. 2) and shows for the opx-spinel-olivine reaction very little pressure dependence of alumina solubility in orthopyroxene. This result supports the conclusion of others (8,9,10, etc.) that alumina content in pyroxene is temperature sensitive and pressure insensitive for this reaction. The experimental data corrected to 1 bar gives the following expression for ΔG :

$$\frac{\Delta G^{o}_{1,T}}{RT} = 19.89 \cdot \frac{10^3}{T,^{\circ}K} - 10.84 \quad (\Delta V_{rxn} = -.069 \text{ cal/bar})$$

The results of our 1150°C, 5 kbar experiment were not used in obtaining this expression, since the 1150°C experiment (Fig.1) appears not to have attained equilibrium after a period of 2 weeks.

As an example of the discrepancy between the spin cat and synthetic experiments, the value of ln K for our 1 bar, 1200°C experiments is -2.67 which yields a temperature of 810°C using the expression of Fujii (10). The result indicates that temperature estimates of spin cat assemblages (6) should be raised by 390°C, and reinforces the plea of (12) for reversed experimental studies and an integration of experimental results from natural and simple systems.

Conclusions

Several factors may contribute to the discrepancy between the pure and the spin cat system results. (a) The assumption of a simple multisite model in calculating K may introduce error. Of the phases involved (olivine, spinel and orthopyroxene) orthopyroxene is a likely candidate to show non-ideal behavior. A solution model that accounts for the effects of Fe, Ti and Cr in M1 (e.g. an activity coefficient as suggested in (7)), might reconcile differences between the two systems. (b) Some correction for a Ca-Tschermak's component may be necessary. (c) It is possible that the initial assumptions concerning the intracrystalline site distribution of Fe and Mg in orthopyroxene are in error. We conclude that geo- and seleno- thermometers and barometers derived from simple system experiments or thermochemical data must be tested by experiments on natural systems before they can be applied with confidence to the interpretation of natural assemblages.

References

(1) Taylor S. R. and Bence A. E. (1975) Proc. Lunar Sci. Conf. 6th, 1121-1141. (2) Bence A. E. and McGee J. (1976) Geol. Soc. Amer. Abstracts 8, 772. (3) Walker D. et al. (1973) EPSL 20, 325-336. (4) Prinz M. et al. (1973) Geochim. Cosmochim. Acta 37, 979-1006. (5) Bence A. E. et al. (1978) Lunar and Planet. Sci IX, 67-69. (6) Herzberg C. T. (1978) Proc. Lunar Planet. Sci. Conf. 9th, p. 319-336. (7) Herzberg C. T. (1979) Lunar and Planet. Sci, X, 537-539. (8) Wood B. J. (1975) Fortschr. Mineral. 52, 21-45. (9)

Obata M. (1976) Amer. Mineral. 61, 804-816. (10) Fujii T. (1976) CIWYB 75, 566-571. (11) Wood B. J. and Banno S. (1973) Contrib Mineral. Petrol. 42, 109-124. (12) Irving A. J. (1976) Amer. Mineral. 61, 638-642.

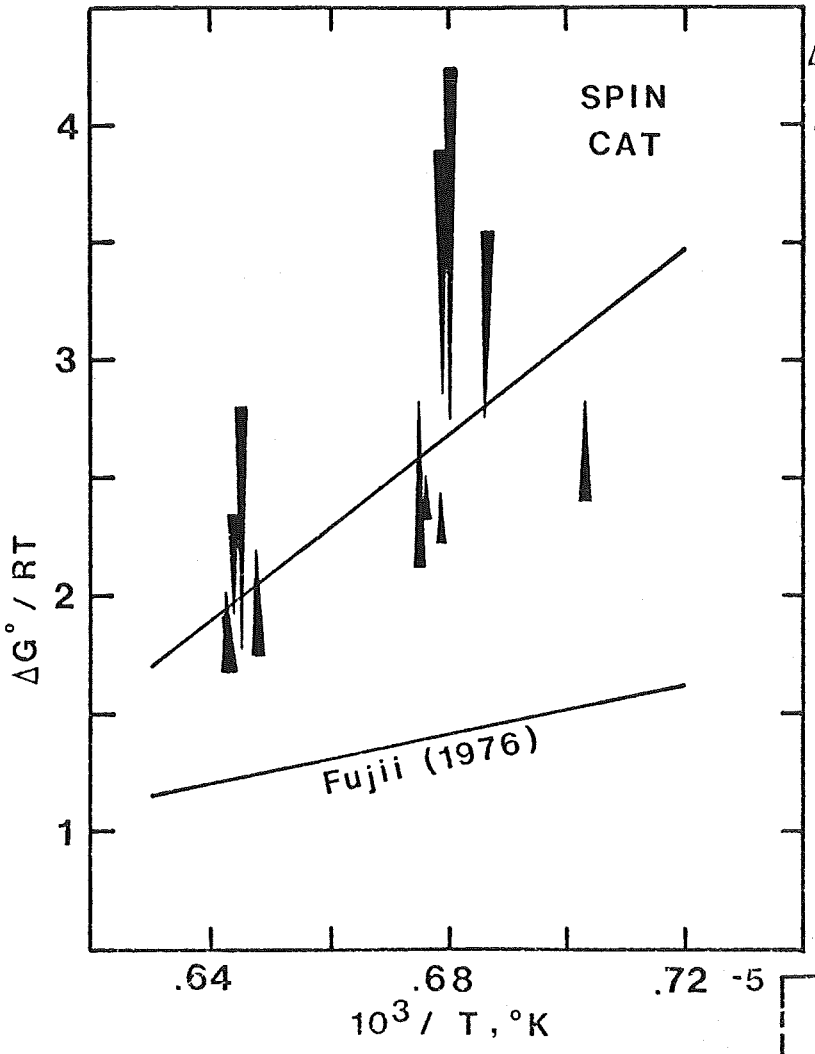

Fig. 1. The variation in $\Delta G^\circ/RT$ indicated by the arrows results from the Al^{VI} variability found in the pyroxenes from each experiment. The value used to calculate the curve is at the tip of each arrow and represents a maximum (for low P, low-T starting material) or minimum (high P, high-T starting material).

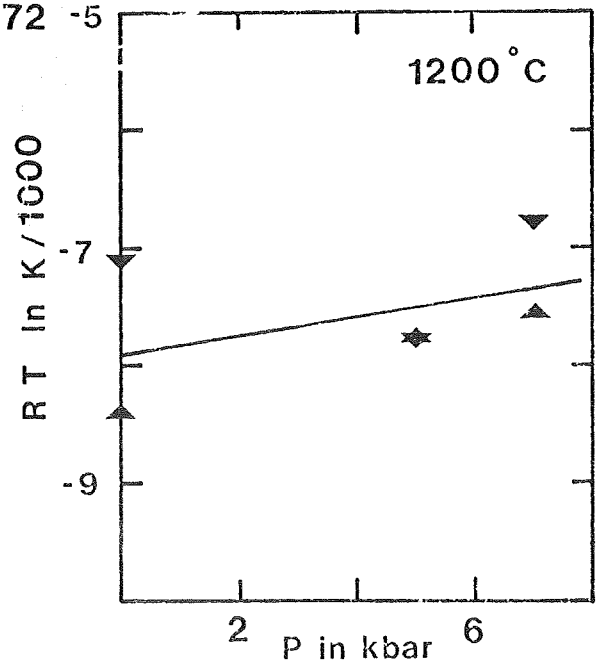

Fig. 2. These isothermal experiments at 1200°C were used to evaluate the pressure dependence of lnK in the orthopyroxene-spinel-olivine reaction.

A SECOND LOOK AT VARIATIONS OF IRON CONCENTRATIONS IN THE LUNAR HIGHLANDS AND IMPLICATIONS FOR CRUSTAL MODELS

E. L. Haines and A. E. Metzger, Jet Propulsion Laboratory, California Institute of Technology, Pasadena, California 91103

A set of Fe concentrations covering 32 lunar highland regions mapped by the Apollo 15 and 16 orbiting gamma-ray spectrometers has been derived by the energy band method. This method has been used previously in the analysis of Th [1], Ti [2] and Fe [3, 4]. In our first analysis of Fe [4] we employed the 6.37 MeV to 8.00 MeV energy band, and derived the regression curve by plotting count rates in this band against Fe derived by fitting the overall spectrum to a set of library functions [5]. While this band is sensitive to Fe, it also contains significant contributions from other elements for which corrections are necessary. Davis and Arnold [3] have found that the 6.99 MeV to 8.89 MeV energy band has smaller contributions for elements other than Fe, and therefore corrections are somewhat more reliable. In order to calibrate this band, Davis and Arnold [3] compared the count rates in defined lunar regions [1] with lunar soil Fe concentrations from nearby or contained Apollo and Luna landing sites, and fitted the Fe values to the corresponding count rates by linear regression [6]. The use of ground truth in place of modeled source values [7], together with the new energy band, has produced a more consistent set of Fe values. Our revised set has been prepared in the same manner.

Because the spectrometer was omnidirectional, the signals received contained gamma-rays from surrounding regions as well as from the region directly beneath. Neighboring chemical provinces with contrasting Fe concentrations, such as maria and highlands, dilute one another's signals and reduce the count rate contrast between them. A deconvolution method, derived from one applied to lunar Th concentrations [8], was used to extract the highland and mare count rate component for 12 regions whose neighbors were of markedly different chemistry. Deconvolved count rates from the 8 regions for which returned samples were available were compared with soil Fe concentrations by York regression [7]. The resulting regression line was used to generate Fe concentrations from regional count rates.

Thirty-two highland regional Fe concentrations were used to calculate highland crustal densities. Similar calculations have been reported earlier by Solomon [9] and Haines and Metzger [4]. Solomon's calculation used both x-ray and gamma-ray data, and was therefore restricted to the highlands on the fraction of the moon illuminated by the sun during the Apollo 15 and 16 missions. The calculations reported here, as those by Haines and Metzger [4] depend only or gamma-ray data and hence represent all the highlands along the Apollo 15 and 16 ground track. They differ from those of [4] by removal of the mare contribution from the observed highland regional rates, thereby reducing Fe values by up to 30%.

We assumed for our density calculations that the lunar highlands are dominated by three minerals: plagioclase (An96), orthopyroxene, and olivine. The En content of the orthopyroxene and Fo content of the olivine are constrained by the Fe and Mg regional concentrations. The weight ratio of pyroxene to olivine was assumed to be 3, consistent with highland melt rock modal abundances [10]. Plagioclase was taken by assumption to constitute the remainder after orthopyroxene and olivine were calculated from Mg and Fe. Mg was based on atomic Mg/Mg + Fe) $\cong$0.63 - 0.69 [10] rather than upon the values published by Bielefeld *et al* [6], which have not been spatially deconvolved.

A SECOND LOOK AT VARIATIONS OF IRON CONCENTRATIONS IN THE LUNAR HIGHLANDS AND IMPLICATIONS FOR CRUSTAL MODELS

E. L. Haines and A. E. Metzger

Bulk density was calculated from component mineral densities using the conservation of partial molar volumes. Calculated densities have little dependence on the assumed pyroxene/olivine ratio and are only moderately dependent on Mg. The sensitivity of the density to replacement of orthopyroxene by clinopyroxene, or of orthopyroxene and olivine by ilmenite, is smaller still. The largest density variations are due mainly to Fe variations, as expected. Densities are for non-porous rocks. We assume that surface densities thus calculated apply to the entire lunar crust within a given region [1].

Calculated regional densities are plotted against regional elevations in Fig. 1. The densities appear to fall into two families: I) $\rho \cong 2.90$ for elevations ≥ -1 km., and II) $\rho \cong 2.97$ for elevations ≤ 0km. Family I by itself forms a stochastic set, normally distributed about its mean density, 2.90. Family II comprises four farside basin regions, all in the Van de Graaff area, 6 nearside intermare regions, and 1 limb region. Family II also forms a stochastic set, but the two families combined do not. Although the density of Family II is lower than reported earlier [4] as a result of deconvolution, the separation of Family II from Family I is just as distinct.

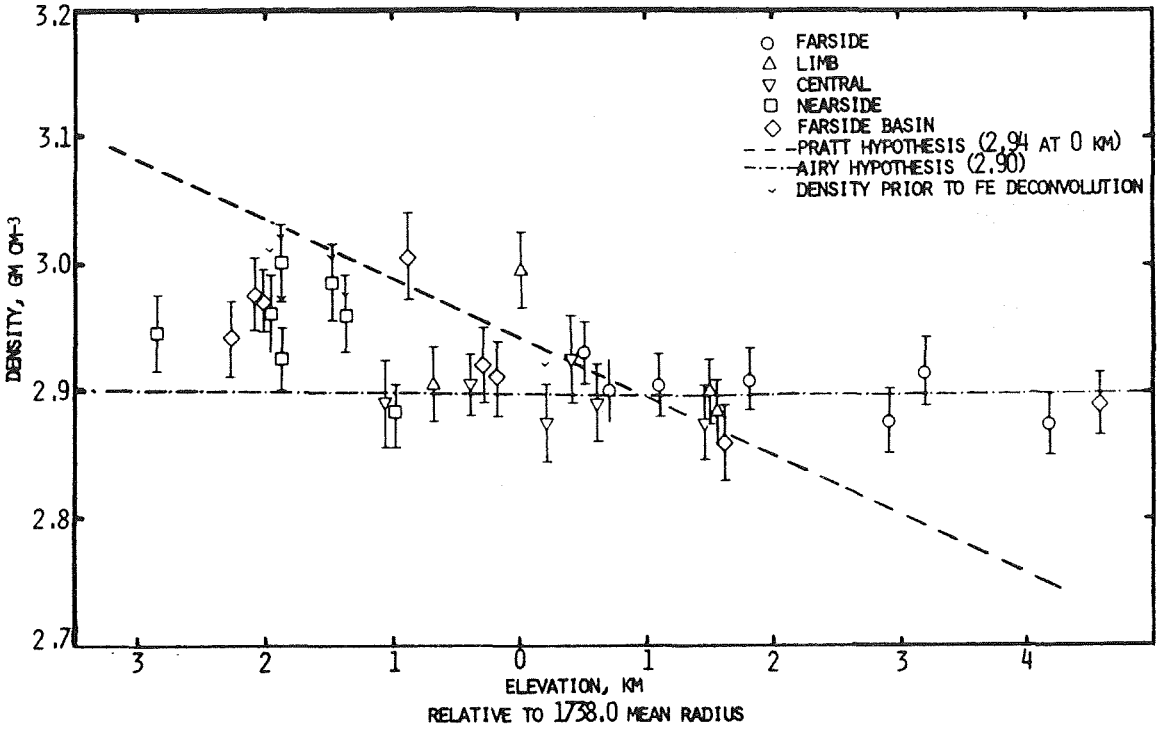

Figure 1. Density calculated from Mg and Fe concentrations, plotted against elevation relative to the mean lunar radius, for lunar highland regions. The dashed lines represent the trend the data would follow if the lunar elevations were the result of a fixed MOHO and density variations (Pratt hypothesis) or variable crustal thickness (Airy hypothesis).

Figure 1 suggests that most of the lunar highlands (Family I), those with higher elevations and farther from maria, have densities of 2.90 (with a 1σ spread of $\pm .02$) independent of their elevations, which span nearly 6 kilometers. We were led by our earlier work [4] to test the thesis that all lunar highlands possess the same density, and that the variations which produce Family II were artifacts of the instrument's extended view. Although the

average density of Family II was reduced from 3.00 to 2.97 (with a 1σ spread of $\pm$.03) by deconvolution of the count rates, Family II remains a distinct set. The regions of Family II are close to or surrounded by maria and/or possess low elevations. However, even within this group the densities do not vary inversely with elevation as required by the Pratt hypothesis of isostasy as appeared to be the case before deconvolution, but show no variation or a weak counter-variation. We suggest that crustal thickness, i.e. the Airy hypothesis of isostasy, is responsible for most of the variations in elevation, while density differences between the two families contribute to the separation of their elevations. The separation of these two families results from what appear to be significant differences in their crustal Fe concentrations. It is not possible to say from this information alone whether the Fe was introduced at the time of crustal genesis or later, perhaps during the flooding of the maria.

This work was supported under NASA contract NAS 7-100 at the Jet Propulsion Laboratory, California Institute of Technology.

References

1. Metzger, A. E. et al (1977) Proc. Lunar Sci. Conf. 8th, p. 949-999.
2. Metzger, A. E. and Parker, R. E. (1979) Earth & Planetary Science Letters, to be published.
3. Davis, P. A. & Arnold, J. R. (1979) Lunar and Planetary Science Abstracts X, p. 268-270.
4. Haines, E. L. and Metzger, A. E. (1979) Lunar and Planetary Science Abstracts X, p. 488-490.
5. Bielefeld, M. J., et al (1976) Proc. Lunar Sci. Conf. 7th., p. 2661-2676.
6. York, D. (1966) Can. J. Phys: Vol. 44, p. 1079-1086.
7. Reedy, R. C. (1978) Proc. Lunar and Planetary Sci. Conf. 9th, p. 2961-2984.
8. Haines, E. L., Etchegaray-Ramirez, M. I., and Metzger, A. E. (1978) Proc. Lunar Planet. Sci. Conf. 9th., p. 2985-3013.
9. Solomon, S. C. (1978) Proc. Lunar Planet, Sci. Conf. 9th., p. 3499-3511.
10. Vaniman, D. T. and Papike, J. J. (1979) The Lunar Highland Melt Rock Suite, preprint.

ORIENTATIONS OF CENTRAL PEAKS IN LUNAR CRATERS: IMPLICATIONS FOR REGIONAL STRUCTURAL TRENDS. Wendy Hale, Dept. of Geological Sciences, Brown University, Providence, RI 02912

Impact craters are the dominant landform on the lunar surface, with central peaks occurring in all craters with diameters larger than 35 km (1). Virtually all recent workers agree that these central peaks are related to the surrounding impact crater in origin. Previous studies of lunar central peak craters have determined that the central peaks can be described morphologically by their complexity (simple to complex) and geometry (symmetric, linear, or arcuate). Simple central peaks consist of a single peak or ridge, while complex ones consist of peak clusters. Symmetric central peaks are oriented concentric to the crater center, while linear or arcuate peaks consist of an elongated or curved ridge or cluster showing a preferential orientation other than the crater center (2). These studies have also suggested that linear central peaks, which comprise approximately 40% of all central peaks in fresh lunar craters, may result from some form of discrete structural control on peak formation or from an oblique impact angle for the projectile which formed the crater (2,3). They occur more frequently in craters developed on highland terrain than on mare material (2), lending support to the theory of a structurally controlled origin. Central peaks in general may form in response to the high stresses associated with shock and rarefaction waves concentrated at the sub-impact point during crater formation (4,5). Thus, any pre-existing regional structural trends could act as stress concentrators, controlling the final geometry of the central peak as well as the crater. Indeed, this is thought to be the reason for the polygonal outline of many fresh crater rims (6). If consistent sets of directions for structural weaknesses in the Moon's crust do exist, as has been postulated as the cause of the lunar grid, they may be portrayed as a consistent direction or set of directions of elongation of linear central peaks in lunar craters. Further, since a qualitative method of assigning ages to craters based on degrees of modification has been developed, it may be possible to detect changes in the regional stress pattern over geologic time by measuring changes in the preferred elongation directions over time. The purposes of this study were: 1) to examine a large number of craters with linear central peaks of all ages and sizes, to determine if any preferential orientation or orientations do exist and compare any orientations found with the previously established lunar grid, 2) to compare directions of elongation with the downrange direction of the impacting body as defined by asymetrically emplaced ejecta deposits and impact melt ponds in order to determine if obliquity of impact angle has an effect on elongation direction, and 3) to assess the degree of change in orientation of linear central peaks over geologic time.

The sample of craters used in this study includes 200 craters of all ages, including 74 from the nearside, 78 from the farside, 31 from the north polar region, and 17 from south polar regions. All craters were examined from Lunar Orbiter images. All orientations were measured relative to the lunar axis of rotation.

1) Preferred orientation of non-symmetric central peaks - Figure 1 shows plots of orientation directions obtained during this study. In general, a strong preferential orientation of elongation for linear central peaks exists at a selenocentric angle of 0° or N-S, with slightly weaker trends at $\pm$20°-30° east and west. On the nearside the trends are similar in significance, while on the farside and polar regions the N-S trend appears dominant. The nearside data is influenced by a trend in orientation towards the direction radial

ORIENTATIONS OF CENTRAL PEAKS IN LUNAR CRATERS

Hale, W.S.

to Mare Imbrium, which lies NW of the south central highlands where a significant percentage of the nearside craters are found. The superposition of a radial Imbrium pattern onto regional trends on the nearside results in a stronger NW trend for this region than is present in other areas. Only 7 craters (3% of the data set) have peaks with east-west orientations, two of which (Copernicus and Reinhold) are near the rim of the Imbrium basin. These two may be related to Imbrium concentric fractures. No evidence for a regional E-W trend is observed.

2) Elongation directions compared to downrange directions for oblique impacts - Previous workers have identified downrange directions for oblique impact angles in 33 lunar craters from asymmetrically emplaced melt pools and ejecta patterns (3). Of these, 17 have linear central peaks. A comparison of the downrange direction to the elongation direction shows coincidence in only 23% of the cases, or a total of four craters. This suggests that oblique impact angle is not directly related to the elongation direction of linear central peaks.

3) Changes in preferred orientation over time - In craters with linear central peaks of pre-Nectarian to Copernican age no change in elongation direction is observed. Indeed, where several craters of different ages with linear central peaks occur together, no appreciable change in orientation is observed over time. An example of this occurs north of Mare Crisium, where the craters Cleomedes (pre-Imbrian), Burkhardt (Imbrian), and Geminus (Eratosthenian) occur together and all three have elongation orientations of 30°. This suggests a similarity through time for any structural system exercising control on peak geometry.

Discussion and Conclusions - The Earth's moon is a tidally locked planet with one face turned always towards its primary. Studies of regional stress patterns induced by despinning to its present state may give clues to the Moon's early history and the petrogenesis of its surface. Previous studies of lunar regional stress systems as revealed by preferred orientations in surface features have determined the presence of a pervasive structural pattern on the Moon's nearside, termed the lunar grid (7,8). The grid is made up of intersecting lineaments which are comprised of definite linear faults, linear ridges and valleys, rilles, joints, crater chains and polygonal crater rims (7,8). These lineaments intersect and cross each other to form five distinct systems or families of structural trends, described by Fielder (7) as a SW-NE trending system (system A), a SE-NW trending system (B), a weak N-S system (C), a faint E-W system (D), and a joint system radial to Mare Imbrium (R1). Systems A and B are by far the strongest, and are mutually orthogonal with selenocentric position angles (measured clockwise from the lunar rotation axis) of 45° and 135° respectively. Strom (8) identified a closely similar system of trends with one major set trending at 45°-55° east and west of the rotation axis, a N-S system with a dominant trend parallel to the meridians and a less clearly defined system trending at 15°-20° from the rotation axis. No clear evidence of an E-W system was found in his study.

For 200 lunar craters with linear central peaks, three preferential elongation directions are identified in this study. These are 330°-340°, 0°, and 20°-30°. Comparing these preferred orientations to the lunar grid pattern it is found that the preferred elongation directions of the central peaks of craters are significantly different from the two dominant trends labeled by Fielder as A and B. These two trends are mutually orthogonal, with orientations at 45° and 315°, while the trends for linear central peaks meet at angles of 30° and 60°. However, the weaker trend

ORIENTATIONS OF CENTRAL PEAKS IN LUNAR CRATERS

Hale, W.S.

identified by Strom (8) as a NNE-SSW lineament system, oriented at angles of about 15°-20° from the Moon's axis of rotation corresponds within 10° to the observed orientation of the two weaker trends for linear central peaks. Weak N-S trends also identified by these workers coincide with the dominant orientation for linear peaks.

Of the two theories advanced for the origin of linear central peaks (structural control by the target or obliquity of impact angle) the first now appears more likely. Comparison of downrange directions for oblique impacts to peak elongation directions shows a coincidence of only 23%, indicating that oblique impact angle is not directly related to the formation of linear, central peaks. The preferential development of linear central peaks on highland terrain also supports this view. The presence of strong preferred orientations for peak elongation would therefore imply regional structural trends of similar orientations. It is thus suggested that a pattern of structural weaknesses similar to that identified as the lunar grid and having some orientations in common with it, exists over the entire lunar surface, and is portrayed in the elongation directions of linear central peaks in craters. Further, no change in prominence or direction of peak elongation is observed over a wide range of crater ages, indicating that this structural pattern may have originated early in lunar history and persisted throughout geologic time.

References: 1. Wood C.A. and L. Andersson (1978) PLSC9, 1267. 2. Hale W.S. and J.W. Head (1979) PLSC10, in press. 3. Hawke B.R. and J.W. Head (1977) Impact and Explosion Cratering, p. 815. 4. Head J.W. (1978) Lunar Sci. 9, p. 485. 5. Milton D. and D.J. Roddy (1972) IGC, Sess. 24, p. 119. 6. Baldwin R. (1963) The Measure of the Moon. 7. Fielder G. (1963) Quart. J. Geol. Soc. Lond., 65-94. 8. Strom R.G. (1964) Comm. Lunar Plan. Lab., 205.

FIGURE 1

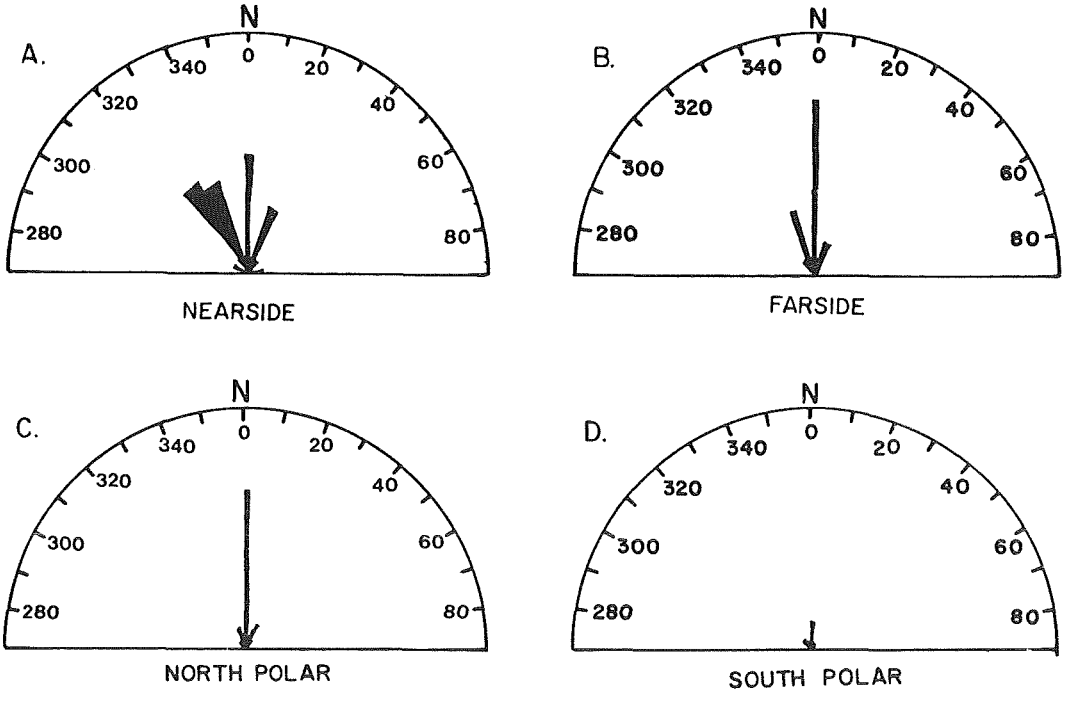

MINOR ELEMENTS IN PLAGIOCLASE FROM LUNAR HIGHLAND ROCKS: NEW DATA, ESPECIALLY FOR GRANULITIC IMPACTITES. E.C. Hansen, I.M. Steele and J.V. Smith, Dept. of Geophysical Sciences, University of Chicago, Chicago, Ill. 60637.

Since plagioclase is present in all lunar highland rocks, its chemistry is important for unravelling highland petrogenesis. We present electron probe analyses of Mg, Fe, K and Na for specimens additional to those in [1]. An accompanying abstract [2] reports ion probe analyses of several trace elements. Pristine lunar rocks fall into two distinct trends on a diagram of *mg* = atomic 100xMg/(Mg+Fe) vs. mol. Ab - anorthositic and Mg-rich plutonic [3,4]. Granulitic impactites are a group of non-pristine rocks with textures indicative of brecciation followed by metamorphism [5,6]; they have *mg*-Ab values which tend to fall in the gap between the anorthositic and Mg-rich plutonic trends. The new samples include Mg-rich plutonic rocks and granulitic impactites from [6].

Mg-rich plutonic group. The new samples (3 troctolites, 4 norites, 1 gabbro), together with previous ones [1], span the entire Mg-plutonic trend (Fig. 1), but tend to lie to the right of the Warner-Bickel line [4]. Plagioclase from Mg-rich plutonic rocks contains higher K than plagioclase from anorthositic rocks (Fig. 2), even when account is taken of the tendency for K to increase with Na. Whole-rock analyses show a similar pattern for bulk REE [7]. Two norites with 6.3% Ab have especially high K_2O in Fig. 2, and the other Mg-rich specimens show only a small increase of K with Na. Fig. 3 updates Fig. 2 from [1]: (note changes of symbols from Figs. 1 and 2). Most samples lie in a single band in this plot of *mg*(plagioclase) vs. *mg* (liquid) inferred from distribution coefficients for orthopyroxene-liquid [8] and olivine-liquid [9], but samples 67667,1 and 15689 deviate considerably. The new datum for 76535 (square at arrow-head) uses ion microprobe analyses [2]; the original electron microprobe analysis was probably wrong, and is being rechecked. There is a fairly good correlation between *mg*(plagioclase) and *mg*(olivine) for anorthositic and Mg-rich plutonic specimens (Fig. 4).

Granulitic impactites. Orbital data [10] and differences between sample populations from several Apollo sites indicate that the lunar highland crust is inhomogeneous. Because all pristine highlands samples came from only 3 sites it may be premature to conclude that no pristine rocks occur with *mg*-Ab values between those of anorthosites and Mg-rich plutonic rocks. In particular, granulitic impactites have been attributed to impact mixing of two pristine groups [6]. Eight of our new and 2 of our first samples (60619,12; 67746,1) are granulitic impactites, and the mineral chemistry provides a test of their origin. With the exception of peridotite 67667 (Fo 70-72), no pristine rocks are known with olivine compositions between Fo 65 and 80 [3,7], whereas most impactites contain olivines in this range. Mechanical mixing of anorthosites and Mg-rich plutonic rocks can be ruled out as a source of the impactites unless mixing was followed by chemical homogenization (note: orthopyroxene-bearing rocks do occur with *mg* between 65 and 80). All granulitic impactites but one contain plagioclase with mean Ab between 4 and 7, and K increases rapidly with Na (Fig. 2), quite unlike the trends for most of the anorthosites and Mg-rich plutonic specimens. Specimen 77115 has high Ab (~12). In addition to peridotite 67667, two clasts (from 15364 and 77135) contain well-preserved plutonic texture and olivine composition between Fo 65 and 80. All but two granulitic impactites (77115; 60275,1) lie in a cluster on the *mg*-Ab plot (Fig. 1). Although non-definitive, these data suggest that the main group of granulitic impactites should not necessarily be dismissed as mechanical mixtures, and might represent a

distinct primary rock type. If they do arise by metamorphic homogenization of mechanical mixtures, a troctolite containing a K-rich plagioclase and an olivine with Fo near 80 is needed as one end-member.

Discussion A puzzling aspect of lunar anorthosites is the coexistence of Fe-rich olivine and pyroxene with Ca-rich plagioclase and a low abundance of large-ion-lithophile elements. Attempts to resolve this paradox by mixing early-formed plagioclase with late-stage liquids [11] or mafic silicates [12] are inconsistent with our results which indicate that anorthositic plagioclase probably crystallized from an Fe-rich liquid. The Mg-rich plutonic rocks present an inverse paradox - the coexistence of a large percentage of plagioclase and high abundance of LIL elements with Mg-rich mafic silicates. An accompanying abstract [13] presents a new model for resolution of these paradoxes, together with a possible explanation of the genesis of mare basalts. Whatever the fate of this model, it is necessary to invoke crystallization of some lunar rocks from liquids with both primitive, feldspathic and fractionated components [14]. Together with the intriguing problem of the origin of the granulitic impactites, it is obvious that the lunar highlands require detailed study, especially by new sampling missions.

We thank I. Baltuska, R. Draus and O. Draughn for technical help, and NASA for grant 14-001-171.

1. E.C. Hansen et al. 1979 PLSC 10 in press. 2. I.M. Steele, J.V. Smith this vol. 3. P.H. Warren, J.T. Wasson 1977 PLSC 8 2215. 4. J.L. Warner, C.E. Bickel 1978 Am. Min. 63 1010. 5. J.L. Warner et al. 1977 PLSC 8 2051. 6. C.E. Bickel, J.L. Warner 1978 PLSC 9 629. 7. G. Ryder, M. Norman 1978 Catalog of Pristine Non-Mare Materials, Parts 1 & 2. 8. L.G. Medaris 1969 Am. J. Sci. 267 945. 9. J. Longhi et al. 1978 Geochim. Cosmochim. Acta 42 1545. 10. E. Schonfeld 1976 PLSC 7 1149. 11. J.A. Wood 1975 PLSC 6 1087. 12. R.F. Dymek et al. 1975 PLSC 6 301. 13. J.V. Smith, E.C. Hansen this vol. 14. S.R. Taylor, A.E. Bence 1975 PLSC 6 1121.

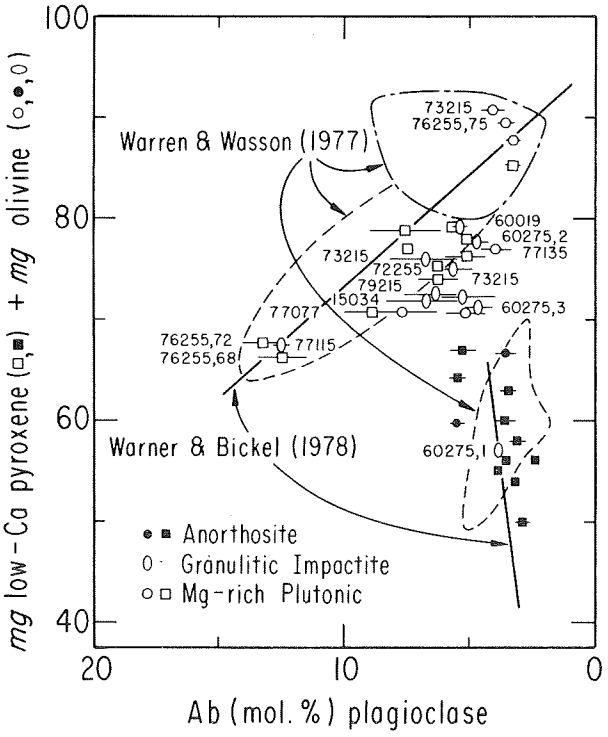

Fig. 1. Ab (plagioclase) vs. mg (olivine) and mg (low-Ca pyroxene). The olivine compositions for rocks listed in [1] are: 15346 Fo 71; 60619 Fo 72.4; 60665 Fo 66.7; 67637 Fo 59.7; 67667 Fo 71; 67746 Fo 75.3; 76535 Fo 87.3.

MINOR ELEMENTS IN PLAGIOCLASE FROM LUNAR HIGHLAND ROCKS:

Hansen, E.C. et al.

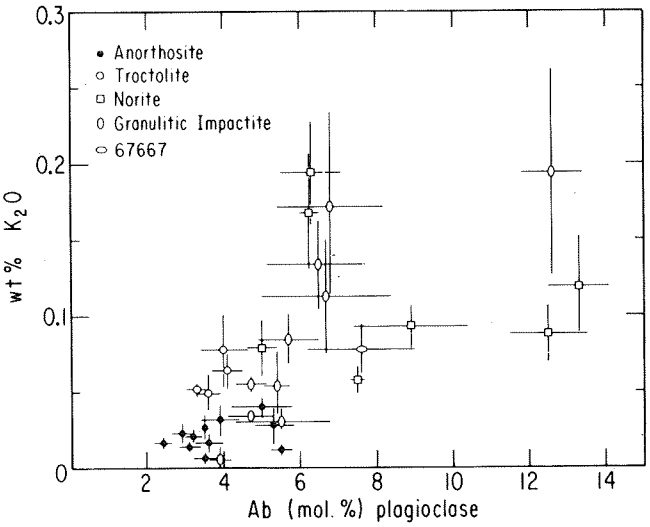

Fig. 2. Wt.% K_2O vs. mol.% Ab of plagioclase.

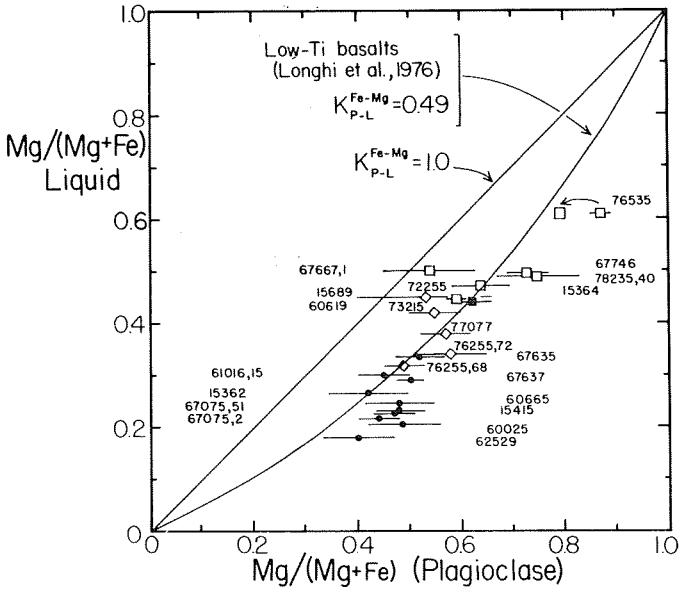

Fig. 3. mg (liquid) vs. mg (plagioclase). See text for probable movement of square for 76535.

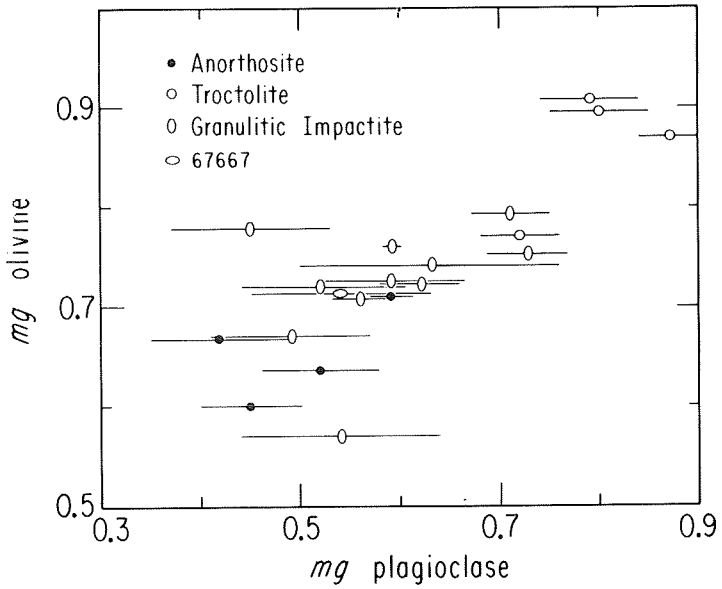

Fig. 4. mg (olivine) vs. mg (plagioclase).

FORMATIVE CONDITIONS CONTROLLING STRUCTURE OF PLANETARY HIGHLANDS. William K. Hartmann, Planetary Science Institute, Tucson, Arizona 85719.

Crater densities on highlands (or the most heavily cratered surfaces) of Moon, Mercury, Mars, Phobos, and Deimos reach remarkably similar values (Fig. 1), relative to the wide scatter of densities in other provinces. This coincidence may be telling us something about highland structure, and suggests some mechanism that defined an envelope of crater densities rarely exceeded on planetary landscapes. This process is likely to be a saturation or steady state mechanism, implying repeated pulverization of highlands, producing deep megaregoliths.

Reconstruction of early accretionary cratering (Fig. 2) can be done invoking (1) present-day observed flux rates; (2) observed decay of meteorite flux from 4 Gy ago to present, based on dated lunar samples; and (3) flux rate necessary to build Earth and Moon in time intervals compatible with meteorite formation intervals. The impact flux in the "missing" years from 4.5 to 4.0 Gy ago ranged about 10^3 to 10^7 times the present flux rate, had an average 20 to 45 my half-life, caused enormous rates of megaregolith production, and does not appear to require any anomalous "spike" of catastrophic cratering around 4.0 Gy ago.

Relative timing between magma ocean cooling, and decay rate of cratering was very important in controlling present day observed character of planetary highlands, since it controlled outcome of competition between preservation of intact igneous rock and conversion of igneous rocks into massive breccias.

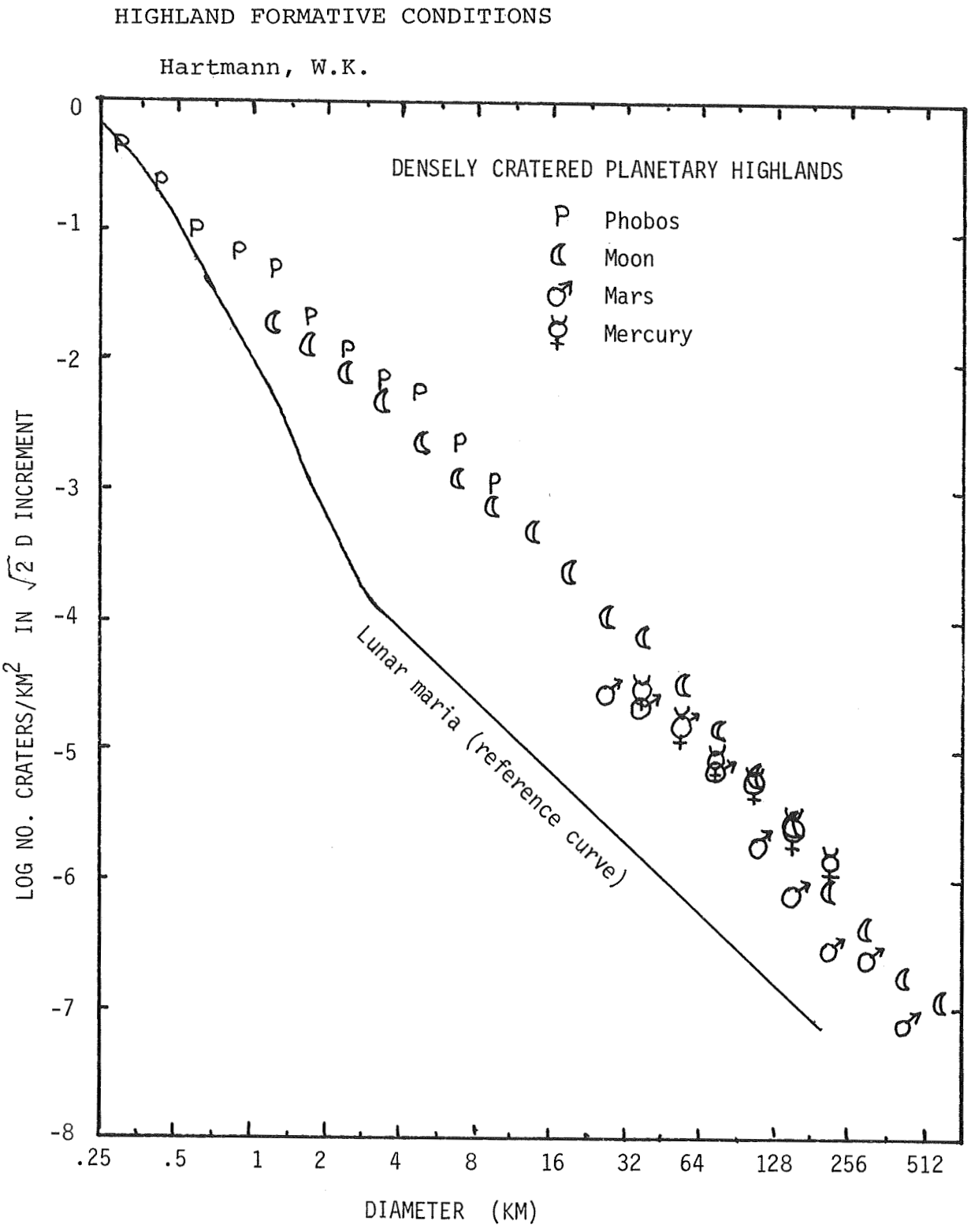

FIGURE 1. Crater densities on "highlands" provinces on several planets lie near values about 32 x those found among large craters in lunar maria. Clustering is tight relative to diversity of values in other provinces.

HIGHLAND FORMATIVE CONDITIONS

Hartmann, W.K.

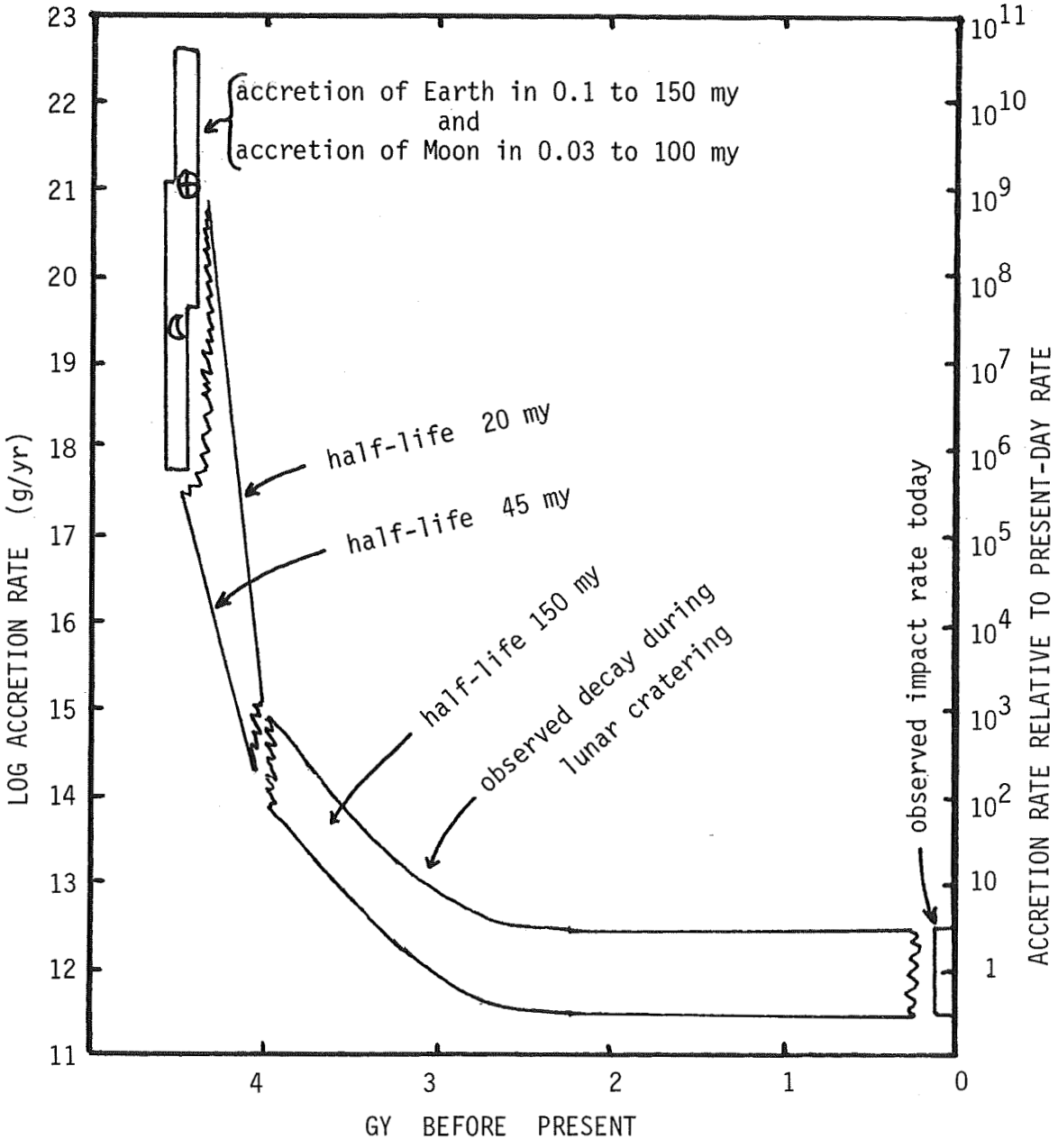

FIGURE 2. Schematic reconstruction of accretionary cratering without invoking a "spike" of catastrophic cratering 4 Gy ago. Present rate is observed (lower right) and projected back to 4 Gy ago using known impact rates determined from lunar dating. Additional datum is impact rate required to form Earth and Moon during their estimated formation intervals. Connection in "missing interval" from 4.5 to 4.0 Gy gives plausible planetesimal sweepup half-lives of the order 20 to 45 my.

ON THE GLOBAL ASYMMETRY OF THE LUNAR CRUST THICKNESS

Jack B. Hartung, Solar System Associates, Brewster Lane, Setauket, New York 11733

Lunar laser altimetry and spacecraft tracking data have confirmed that the center of mass of the Moon is offset, relative to the center of figure of the Moon, about 2 km roughly toward the Earth (1). Because the crust is dominated by anorthositic rocks, which are known to be less dense than either lunar basalts or the source material for lunar basalts, one interpretation of the observed center-of-mass offset is that the anorthositic crust is thinner on the Earth-facing side of the Moon (1). This view has been accepted by most planetary scientists to such an extent that the idea of a thinner lunar crust on the near side of the Moon appears in many lunar or planetary geology text books (2,3,4).

Acceptance of a Moon with an asymmetric distribution of crustal thickness has left us with a serious problem. What is the cause of such an asymmetry? This problem is perhaps a more difficult one than explaining the center-of-mass offset initially. Wood (5) suggested that thinning of the crust could have occurred as a result of a higher concentration of large impacts on the front compared to the back side of the Moon. Ransford and Sjogren (6) argued that a thinner crust could have developed on the Earth-facing side because the higher temperature of a molten Earth close to the Moon would have delayed crystallization on the front relative to the back side of the Moon. I have argued (7) that the center-of-mass offset may be explained without requiring that the Moon form or change in such a way that its crust becomes thicker on one side compared to the other.

It may be shown that the Earth's gravity acts on material at the Moon's surface asymmetrically. If an initially spherically symmetric Moon is assumed, that is, one with a uniform crustal thickness everywhere, then material at a distance, r, from the center of the Moon on its Earth-facing side is not pulled as strongly toward the center of the Moon as is material at a distance, r, from the center of the Moon on its back side (7). In other words, the tidal forces on the Moon due to the Earth's gravity are greater at the Earth-facing side of the Moon. For the present Earth-Moon distance this asymmetric effect is extremely small, corresponding to an elevation difference on the Moon of only a few tens of cm. However, the asymmetric effect varies inversely with the fourth power of the Earth-Moon distance; therefore, at an early time in the history of the Earth-Moon system. when the two objects were closer together, the asymmetric effect would have been much greater. For example, if the Moon were ever one-tenth of its present distance from the Earth, the asymmetric effect would correspond to an elevation difference of a few kilometers. Thus, if mare basalt magmas were being generated during this time, and if magma eruption occurred at gravitationally-favored sites, eruption on the Earth-facing side of the Moon would have been favored to the same extent that eruption at the bottom of a basin a few kilometers in depth was favored. This effect may explain why most lunar maria occur on the Moon's Earth-facing side.

To cause a center-of-mass offset assuming an initially spherically symmetric Moon required that an amount of mass be transported some distance. The process of mare basalt emplacement may have been the mechanism whereby mass was transported toward the Earth-facing side of the Moon. To account for a 2 km center-of-mass offset(1) it is necessary for a mass equivalent to

ON THE GLOBAL ASYMMETRY OF THE LUNAR CRUST THICKNESS

J. B. Hartung

that of all the maria combined (8) to move a distance equal to the diameter of the Moon. Over what horizontal distances did basalt magmas communicate? Lateral migration of magma of over tens of kilometers must have occurred. The separation of some mare-basalt-filled basins indicate lateral migration of hundreds of kilometers probably occurred. There appears to be no obvious reason why lateral migration of magma up to thousands of kilometers, large fractions of the Moon's circumference, could not have occurred. If this were the case, then the center-of-mass offset may have occurred in much the same way as mascons. The positive gravity anomalies associated with mascons and basalt-filled mare basins are directly analogous to the center-of-mass offset, which may be thought of as a gravity anomaly associated with the basalt covered Earth-facing side of the Moon. In short, the center-of-mass offset may be considered a global mascon.

To summarize, if one explains the offset of the center-of-mass of the Moon relative to its center of figure as a result of different crustal thicknesses, then one must explain how different crustal thicknesses originate. The center-of-mass offset may also be due to the asymmetric distribution of mare basalts over a previously spherically symmetric Moon caused by the Earth's gravity at a time when the Earth and Moon were much closer together. The latter mechanism is favored because it is more likely that the center-of-mass offset developed relatively later in the Moon's history, when its rigidity could more effectively sustain a disequilibrium configuration, rather than earlier, when the crust was being formed.

References

1. Kaula W.M., Schubert G., Lingenfelter R.E., Sjogren W.L., and Wollenhaupt W.R. (1972) Proc. Lunar Sci. Conf. 3rd, p. 2189-2204.

2. Short N.M. (1975) Planetary Geology. Prentice-Hall, Englewood Cliffs, New Jersey. 361 pp.

3. Taylor S.R. (1975) Lunar Science: A Post-Apollo View. Pergamon Press, New York. 372 pp.

4. Guest J.E. and Greeley R. (1977) Geology on the Moon. Wykeham Publications, London. 235 pp.

5. Wood J.A. (1973) The Moon 8, 73-103.

6. Ransford G. and Sjogren W. (1972) Nature 238, 260-262.

7. Hartung J.B. (1976) Proc. Lunar Sci. Conf. 7th, p. 3097-3112.

8. Head J.W. (1975) (abstract) Conference on the Origins of Mare Basalts and Their Implication for Lunar Evolution, 66-69. The Lunar Science Institute, Houston.

ARE NORITE AND KREEP ONLY SKIN DEEP? WHAT ARE THE HIGHLANDS MADE OF? L.A. Haskin, R.L. Korotev, and M.M. Lindstrom. Dept. of Earth & Planetary Sciences and McDonnell Center for Space Sciences, Washington University, St. Louis, MO 63130.

Highlands comprise most of Moon's surface. Based on remote sensing studies, highlands are compositionally variable (1-5). How well typical highland materials are represented among collected lunar samples is uncertain. The A-16 and L-20 missions landed closest to typical highlands; A-14,15, and 17 provided highland materials but from obviously atypical highland sites.

ENDOGENEOUS HIGHLAND ROCKS. Table 1 gives TiO_2, Al_2O_3, FeO, MgO, and Th concentrations of some highland materials. Fig. 1 shows REE distributions relative to chondrites for some highland rocks. The spread in concentrations of large ion, lithophile elements (LIL's, e.g., REE, Th) exceeds 4000 times. Yet, from massive anorthosite to the (petrographically uncharacterized) white clast of 14313 there is little change in relative REE abundances ($1.3<La/Yb<3.4$), except for Eu ($.23<Sm/Eu<13.3$). So little change except for the very systematic variation in Eu with REE concentration suggests a relatively simple genetic relationship among highland rocks. Except for nearly monomineralic dunite, LIL and Al_2O_3 concentrations are inversely correlated, reflecting mainly an increasing plagioclase contents with decreasing Th and REE. No such correlation between other major elements and LIL's is present.

Rocks with positive Eu anomalies in Fig. 1 have chemical and petrographic characteristics of cumulates; those with negative anomalies do not. All but perhaps the 14313 clast have low concentrations of siderophile elements (6,7). Most have counterparts with very similar compositions but higher concentrations of siderophiles, perhaps from meteoritic addition (8). One interpretation of this combined evidence is that Fig. 1 samples are the main endogenous highland rocks. If so, breccias and soils would correspond to mechanical mixtures of endogenous rocks. Data for breccias and soils, if added to Fig. 1, would crowd it in the range $5<La<200$ (chondrite normalized). REE patterns of nearly all those materials are parallel with similar trends of Eu anomalies.

The most heavily represented cumulate rocks among the lunar samples are anorthosites (9); REE concentrations among the massive anorthosites vary from La-0.36 (15415,65515) to 1.4 (62255) times the chondritic value. Data are too sparse to show variation with sampling site. The dichotomy in Fe/Mg (10) is not site dependent.

We use the term "KREEPL" for the chemical signature of the high LIL concentrations and relative abundances as found in KREEP (e.g., 11), without implications for bulk composition. Most KREEPLy samples are mafic. Concentrations vary with sampling site but there is substantial overlap. La concentrations for typical materials are 100 to 300 times the chondritic value; those of more silicic KREEPLy materials range up to 1580 times.

ORBITER CHEMICAL DATA. Concentrations of TiO_2, Al_2O_3, FeO, MgO and Th in typical near- and farside highland soils appear in Table 1. Frontside highland soils are richer in Th, slightly richer in FeO and MgO, and probably poorer in Al_2O_3 than farside highland soils. Both groups have more FeO, MgO, and TiO_2 and less Al_2O_3 than A-16 soils; the farside highlands also have less Th. Typical nearside soil is similar to L-20 soil but richer in TiO_2 and poorer in MgO. No soil sample closely matches typical farside highland soil.

Interpretations of seismic data (12) and heat flow (13) yield $\sim$75 km thickness for the crust ($\sim$12% of Moon's mass) and an average lunar Th concentration of 0.17 ppm (0.046 ppm Ux3.8), with significant Th still at depth.

ARE NORITE AND KREEP ONLY SKIN DEEP?

Haskin, L.A.

If half the Th were in the crust, the mean concentration there would be 0.6 ppm, intermediate between the values for typical front- and farside highlands. The Th concentration is not high enough to require that typical highland soil composition differ from average crustal composition.

PETROLOGICAL MODEL FOR ANORTHOSITE AND NORITE. A major process in formation of Moon's crust appears to be flotation of plagioclase (e.g., 14). Earliest lunar liquids probably had bulk compositions with olivine or orthopyroxene on the liquidus (e.g., 15); liquids crystallizing plagioclase would be expected first to evolve to noritic composition. Norite is the normative composition of most highland rocks having La between 10 to 300x the chondritic value (Fig. 1). Troctolite and dunite should not precipitate from noritic liquid; such rocks at A-17 would then require an alternative origin, perhaps in pods of liquid trapped in anorthosite blocks.

Blocks of plagioclase ($\rho \lesssim 2.8$) floating in residual liquid ($\rho \sim 3.?$) would nearly submerge. Two extremes for accumulated plagioclase seem possible, a slush of small blocks with much trapped interstital liquid (e.g., 16,17), or very large blocks nearly free of trapped liquid and almost covering Moon so noritic residual liquid near the lunar surface would be minimal (6). By the slush model, impacts would excavate a mixture of abundant noritic material (crystallized residual parent liquid) and massive anorthosite. The block model predicts excavation mainly of massive anorthosite; in that model most of the Th, FeO, MgO and TiO_2 found in typical highlands would be in a surface veneer, perhaps of solidified KREEPLy liquid.

At A-16 KREEPLy material is abundant and penetration of North Ray crater through atypical highlands (Cayley plains) into apparently more typical highlands exhumed considerable massive anorthosite. However, KREEP does not supply most of the FeO, MgO, and TiO_2 in the soil. Farside Th concentrations might also stem from spreading of KREEP but, as at A-16, MgO, FeO and TiO_2 concentrations are too high for a simple mixture of KREEP and anorthosite. Concentrations of those elements suggest that mafic material such as norite is abundant; this favors the slush model. Typical highlands may fall between the extremes, with considerable low-LIL norite exposed but large enough blocks of massive anorthosite that a small crater could excavate much of that material.

Simple arguments such as convergence of Eu values at ~20x chondrites between cumulate and non-cumulate rock types (Fig. 1) or general estimates of bulk highlands composition (18) suggest parent liquids for the highlands with La/Yb ~1.5 and La concentrations ~8 to 30x the chondritic value. Parent liquids for massive anorthosites, based on values of distribution coefficients for plagioclase, lie in that range. So do the parent for troctolite 76535 (19) and probably those for norite 78235 and dunite 72417, based on their interpretation as orthocumulates. Thus, the principal constituents of highlands all may derive from liquids with LIL concentrations at least several times those of chondrites and with fractionated relative abundances (20).

PETROGENESIS OF KREEPL. The origin of KREEPL remains enigmatic. KREEPL is surely a product of extensive igneous differentiation. Relative LIL concentrations in different KREEPs hardly differ (21). Attempts to model the genesis of KREEP by simple fractional crystallization of residual noritic liquid or by partial melting of its solidified counterpart have not been very successful. An origin of different KREEPs by dilution of a material more concentrated in LIL's (22) is attractive, but how is a liquid as concentrated in LIL's as the QMD (15405) or the white clast (14313) produced in the first place. Whatever its origin, KREEP is a major highlands material of the lunar frontside. Amounts of LIL's available to the highlands

ARE NORITE AND KREEP ONLY SKIN DEEP?

Haskin, L.A.

are sufficient to provide for a substantial shell of KREEP within the highlands (22).

SELF CONSISTENCY. The information discussed above does not appear to be self consistent. No mixture of Fig. 1 endogenous rocks yields A-16, L-20, or orbiter-based highland soil compositions. Soil TiO_2 concentrations suggest that soils are pure KREEP (Table 1) but Th concentrations limit KREEP to $\lesssim$ 10%. Soil FeO concentrations implicate norite as the main component, but MgO limits norite to $\lesssim$ 50%. An additional constituent similar to mare basalt or perhaps late stage accretional material would help, e.g. (23-25) but no such lithic component is abundant even among soil fragments (26). Why is this component missing from the list of endogenous rocks? Alternatively, might the norite-plagioclase model be essentially correct but highland soils not compositionally representative of bulk highlands?

Noritic liquids do not yield cumulate dunite or troctolite, but seem required to produce anorthosite. Dunite and troctolite could come from precursor liquids, but should be buried well beneath the anorthosite, not readily exhumed by impacts. Does their presence contradict the norite-plagioclase crustal model?

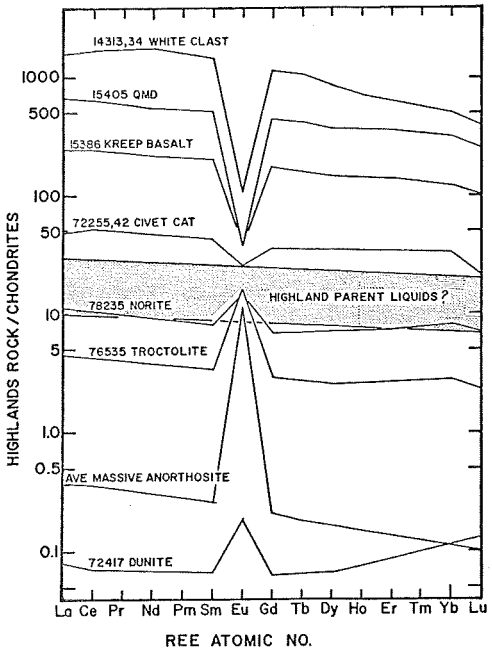

Figure 1. Chondrite normalized REE concentrations in several pristine highland rocks (except 14313). Date from: 14313,34 - a 12.5 mg sample from a larger, uncharacterized white clast (Haskin et. al. (1973) PLSC4, 1275); 15405 - Quartz monzodiorite (Nyquist et. al. (1977) LSVII, 738); 15386 - (Hubbard et. al. (1974) LSC5, 1227); 72255,42 - Norite clast (Blanchard et. al. (1975) Moon, 14, 359); 78235 - (Winzer et. al. (1975) PLSC5, 1219); 76235 - (Haskin et. al. (1974) PLSC5, 1213); Anorthosite - mean of several low - LIL pristine anorthosites; 72417 - (Laul and Schmitt (1975) PLSC6, 1231).

TABLE 1

%	Farside Highlands	Nearside Highlands	A-16 Soil	L-20 Soil	Anorthosite	Norite	KREEP
TiO_2	1.2±0.4	1.4±0.7	0.3-0.65	0.5	0.0	0.2	1.5
Al_2O_3	25 (est)	~22	26-29	23	36	15-20	15-20
FeO	6.5	8.5	4-5.7	8.1	0.3	5-10	7.5-11
MgO	4.7-6.9	8.0	5-6.2	10	0.0	12-15	7.5-10.5
Th (ppm)	~0.5	1.5	1-2.5	1.0	0.004	0.7-3	15-20

REFERENCES: (1) Bielefeld et. al. (1976) PLSC7, 2661. (2) Metzger et. al (1977) PLSC8, 949. (3) Bielefeld (1977) PLSC8, 1131. (4) Metzger and Parker (1979) EPSL, in press. (5) Davis P. A., Jr. (1979), in press. (6) Warren and Wasson (1977) PLSC8, 2215. (7) Warren and Wasson (1978) PLPSC9, 185. (8) Ganapathy et. al. (1970) PA11LSC, 1117. (9) Bickel and Warner (1976) PLPSC9, 629. (10) Dowty et. al. (1974) EPSC, 24, 15. (11) Meyer et. al. (1971) PLSC2, 393. (12) Kaula (1977) PLSC8, 321. (13) Langseth et. al. (1976) PLSC7, 3143. (14) Wood J. A. (1975) PLSC6, 1097. (15) Ringwood and Essene (1970) PA11LSC, 769. (16) Delano and Ringwood (1978) PLPSC9, 111. (17) Schonfeld (1975) PLSC6, 1375. (18) Taylor (1975) Lunar Science - A Post-Apollo View, Pergamon, NY. (19) Haskin et. al. (1974) PLSC5, 1213. (20) Hubbard and Minear (1976) PLSC7, 3421. (21) McKay et. al (1978) PLPSC9, 661. (22) Warren and Wasson (1979) Rev. Geophys. Space Phys., 17, 73. (23) Boynton et. al. (1976) PLSC7, 727. (24) Wänke et. al. (1978) PLPSC9, 83. (25) Wasson et. al. (1977) PLSC8, 2237. (26) Delano et. al. (1973) PLSC4, 537.

MULTISPECTRAL IMAGING OF LUNAR CRATER DEPOSITS. B. Ray Hawke, Donna MacLaskey, and Thomas B. McCord, Planetary Sciences Division, Hawaii Institute of Geophysics, Univ. of Hawaii, Honolulu, HI 96822

I. Introduction

Reflectance spectra obtained for lunar craters have been successfully used to address a number of major questions. While these spectra provide detailed chemical and mineralogic information for the area for which they are obtained, multispectral ratio images are necessary in order to define and characterize larger areas of crater ejecta as well as to map the areal extent of crater-associated spectral units. The purpose of this study was to obtain images of a number of fresh craters at eight to twenty wavelengths and utilize these images to investigate upper crustal stratigraphy and the impact cratering process. It is anticipated that a complete reduction and interpretation of all images thus far obtained will contribute to the solution of several important lunar questions including 1) the reality of "local mixing" in the distal portions of crater ejecta deposits, 2) the nature and origin of lunar rays, 3) the distribution shock melt around craters, and 4) pre-impact stratigraphy of the various target sites.

II. Method

The craters to be investigated were carefully selected using criteria which included size, relative age, target composition and stratigraphy, and accessibility for earth-based observation. Craters with different diameters were studied to determine the influence of crater size on the various problems under investigation. Although all of the craters chosen for study are relatively fresh, a range of ages is exhibited. Craters located in different types of terrain were chosen so as to allow an investigation of the influence of substrate and target configuration on the spectral characteristics of remotely sensed crater units. Digital vidicon images have been obtained for the following craters: 1) Tycho, 2) Copernicus, 3) Aristillus, 4) Lalande, 5) Kepler, 6) Proclus, 7) Aristarchus, 8) Theophilus, 9) Langrenus, and 10) Menelaus. Each crater was imaged at eight wavelengths which were chosen to aid in distinguishing lunar spectral units and to maximize compositional information. The wavelengths are as follows: 0.37, 0.40, 0.56, 0.73, 0.86, 0.93, 0.96, and 1.0 μm. These vidicon images were obtained in May and July, 1979, using the 88-inch telescope of the Mauna Kea Observatory.

Spectral ratio images were prepared by dividing registered and calibrated images obtained at two different wavelengths. In this study, all images were divided by the 0.56 μm image. The resulting multispectral ratio images were noise filtered, contrast enhanced, and mosaicked for study. The images are multispectral maps in which brightness changes represent differences in reflectance at one wavelength relative to that at another. The photometric precision of these images is on the order of 1% and they have a spatial resolution of less than 2 km. The reader is referred to McCord et al.[1, 2] for a more detailed discussion of the vidicon imaging system, data acquisition techniques, image calibration and analysis processes, and the significance of color differences displayed in the ratio images.

III. Results

The results presented here are for those craters for which data reduction is complete. Emphasis is placed on Tycho as a prime example of a very fresh, large highland crater.

Tycho Crater: The 0.56 μm image of the Tycho region generally shows albedo variations similar to those reported by other investigators (e.g. Van Deggel[3]). The crater interior exhibits a high albedo (0.159 - 0.169[4]) with the brightest material (0.159 - 0.180) occurring in the vicinity of

the central peaks and crater wall. Some slightly darker areas occur on small portions of the floor and wall. The crater rim crest is surrounded by two haloes. The inner, bright halo is narrow, discontinuous, and poorly developed south of the crater. The outer, dark halo (0.134-∿0.145) is more extensive and continuous. Although the dark halo extends in places to almost one crater diameter from rim crest, most of the halo and particularly the darker material, is concentrated closer to the crater. While the dark halo is most extensive to the SE, the greatest concentrations of the darkest material are east and west of Tycho. Outside the dark halo occur bright Tycho ejecta deposits and rays (0.150-0.180[4]). The dark halo is "dark" only relative to its bright surroundings and its albedo is typical of large portions of the mature lunar highlands.

The Tycho region appears remarkably uniform in the 0.40/0.56 μm image. The crater is outlined by a zone of higher 0.40/0.56 μm values (bluer area) which generally correlate with the brighter portion of the crater wall and rim crest. The central peak and a small portion of the floor are slightly bluer than their immediate surroundings. In general, the crater interior appears slightly bluer than the surrounding region.

The 0.73/0.56 μm image shows a very interesting pattern. Areas which exhibit a high albedo appear very dark (low values) in the 0.73/0.56 μm image. These areas include the central peak, major portions of the crater wall and floor, and much of the bright halo surrounding the rim crest. Low albedo regions which are concentrated in the dark halo but are also present on limited portions of the crater interior, appear somewhat brighter, indicating relatively higher 0.73/0.56 μm values.

Similar though more pronounced relationships are found in the 0.86/0.56 μm image. High albedo areas generally exhibit low 0.86/0.56 μm ratios while areas with lower albedos have higher 0.86/0.56 μm ratios.

Striking differences among the various Tycho deposits can be seen on the 0.95/0.56 μm image. The crater interior and bright halo are generally dark in this image, indicating a low 0.95/0.56 μm ratio. The lowest values are associated with the central peak and portions of the wall and rim crest. The dark halo exhibits relatively high 0.96/0.56 μm values.

The correlation of high 0.95/0.56 values with the dark halo offers an important clue to its nature and origin. Lunar 0.95/0.56 μm ratio images are generally thought to map soil maturity[1]. Fresh lunar soil appears dark (lower 0.96/0.56 μm values) in these images partly because of an electronic transition absorption band which appears in the reflectance spectra near 0.95 μm due to pyroxene. This pyroxene band becomes weaker as soils mature and become richer in glassy agglutinates. Based on both the high 0.95/0.56 μm and low albedo, the Tycho dark halo appear to be a region of relatively high maturity. This is supported by a comparison of reflectance spectra obtained for the crater peak, wall, and floor with the spectrum of a small area north of the crater which is largely within the dark halo[5]. The peak and flat floor are very immature whereas the area in the dark halo exhibits a maturity only slightly less than typical lunar highland regions[6]. This difference between dark halo and crater interior maturity levels is in some part a function of relief since fresh material is constantly being exposed on the steeper portions of the wall and peak. Still this factor cannot account for the difference in maturity between the flat floor and the dark halo. In addition, flat portions of the distal ejecta deposits have remained very bright.

Howard and Wilshire[7] presented evidence that the dark halo around Tycho was due to the presence of low albedo ponds and a thin, hard-rock veneer composed of impact melt generated during the Tycho impact event. They noted that the finely recrystallized and partly melted materials derived from

anorthositic highland rocks are much darker than their source rock and suggested that the dark halo was composed of such fine-grained recrystallized melt. While our results are basically consistent with this suggestion, we propose that the dark halo contains a significant component of impact-generated glass. Such a glass component is required to account for the high maturity exhibited by the dark halo.

Aristillus, Lalande, and Kepler craters: Other lunar craters have dark deposits similar to the dark halo around Tycho. Van Diggelen[3] presented photometric evidence for a dark halo around Kepler. Dark deposits also occur E, NE and N of Aristillus and NE and SE of Lalande. A comparison of the 0.95/0.56 μm images containing the above craters with the 0.56 μm images showed a fairly close correspondence between the lower albedo deposits and areas of high 0.95/0.56 μm values. This correlation suggests that the dark deposits around these craters may also contain a major component of impact melt glass.

Implications: The results of this study have several important implications. (1) Impact melt appears to be more widespread around fresh lunar crater than has previously been thought[7,8]. (2) The thin, exterior melt deposits are spectrally distinct and differ from the more massive interior melt deposits. (3) Multispectral imaging is a useful technique in identifying and mapping lunar crater deposits.

References:

1) McCord, T. et al. (1976) Icarus 29, 1. 2) McCord, T. et al. (1979) Icarus 37, 1. 3) Van Diggelen, J. (1969) The Moon 1, 67. 4) Pohn, H. and Wildey, R. (1970) U.S.G.S. Prof. Paper 599-E. 5) McCord, T. et al. (1972) The Moon 5, 52. 6) Charette, M. et al. (1974) JGR 79, 1605. 7) Howard, K. and Wilshire, H. (1975) Jour. Research U.S. Geol. Survey, 3, 237. 8) Hawke, B. and Head, J. (1977) Impact and Explosion Cratering, 815.

CHEMICAL MIXING MODEL STUDIES OF LUNAR BASIN EJECTA DEPOSITS.

B. Ray Hawke, Institute for Astronomy, University of Hawaii, Honolulu, HI 96822 and Paul D. Spudis, Department of Geology, Arizona State University, Tempe, AZ 85281

A major objective of lunar science is the determination of the lateral and vertical changes in the chemical composition of the lunar crust. Important clues can be provided by studies of material ejected by the lunar basins since these impacts have excavated crustal material from a variety of depths and deposited this ejecta in a systematic fashion. Valuable insight has come from investigations of Apollo and Luna samples derived from basins, notably Imbrium and Serenitatis. Still, there is a need to extrapolate the detailed chemical information for the individual landing sites to much larger areas of the lunar surface. This has been made possible largely through the use of the orbital geochemistry data returned by the Apollo 15 and 16 missions (1 - 4). Other remote sensing techniques, such as reflectance spectroscopy, have provided additional geochemical information (5,6). Geochemical data are currently available for portions of the terra surrounding several large multiring basins, interpreted as ejecta blankets of these impact structures. The purpose of this study was to perform mixing model calculations on the remotely sensed chemical compositions of the deposits surrounding the Crisium, Nectaris, and Orientale basins in order to establish which chemically-defined rock types are likely to be present and to make quantitative estimates of their relative abundances.

A least-squares mixing model program was used to translate the chemical composition of each region into the best mixture of given endmembers (7,8,9). Up to six elements (Mg, Th, Fe, K, Al, Ti) were used. The chemical data for the regions under study are those presented by Adler and Trombka (10), Bielefeld *et al.* (2,3,11), and Metzger *et al.* (4). Endmember selection was guided by lunar sample chemistry, regional geological considerations, and previous analyses of the orbital geochemistry data (4,12). Endmember compositions were selected from Taylor (13) and Ridley (14). These endmembers are not necessarily representative of the primary (monomict) components of the lunar crust, but rather represent chemically defined rock types shown to be abundant on the lunar *surface* by returned samples. Thus, rocks such as low-K Fra Mauro basalt (LKFMB) may be always polymict and present only on the lunar surface as basin and large crater melt ejecta. Therefore, caution must be excercised in attempts to interpret the mixing model data in terms of pre-impact crustal reconstruction, since pristine (primary) lunar rock types are still being defined (15, 16). The best solutions obtained for the various regions are presented in Table 1.

Crisium Basin Ejecta: Crisium predates Imbrium and Orientale and is younger than Fecunditatis, Nectaris, and possibly Serenitatis (17). If so, the circum-Crisium highlands might be expected to contain significant amounts of Crisium ejecta and variations in the composition of this highland region may reflect the pre-impact chemical variations in the crust of the Crisium target site. A recent study by Bielefeld *et al.* (11) correlated chemistry and albedo in the Crisium area and several data clusters were identified in the highlands S and SW of Crisium. Al and Mg data for these clusters were used along with regional chemical data to perform mixing model calculations (Table 1). Units C and D are the most extensive and generally ring Mare Crisium separating it from neighboring maria. The mixing model results show that both regions are dominated by anorthositic gabbro and contain lesser amounts of LKFMB. These components comprise the same relative proportions of the highland material present in both units. The units differ mainly in the amounts of mare basalt calculated to be present (~19% in D *vs.* ~3% in C). This difference can be understood in terms of the distribution of units in relation to the nearby mare surfaces. Unit D commonly separates C from nearby basalt deposits and probably represents a zone of small scale lateral mixing from the nearby mare deposits. The much smaller mare component in unit C is consistent with its occurrence at generally greater distances from the maria. Mixing model solutions for unit B, which is generally even more distant from mare surfaces, suggest that essentially no mare basalt is present. The unit can be modeled as a mixture of anorthositic gabbro and LKFMB present in approximately the same relative proportions as in the highland components of units C and D.

BASIN EJECTA DEPOSITS

Hawke and Spudis

Unit A is associated with a high albedo area centered in the Proclus crater region. The unit is chemically similar to unit C and the mixing model results suggests that unit A has slightly less mare basalt than unit C.

It is interesting to note that the mare basalt composition which yielded the best solutions for the above circum-Crisium units was average Apollo 12 basalt. The existence of mare material similar to the Apollo 12 basalts in the Mare Crisium-Mare Fecunditatis region is consistent with the results of recent studies of the distribution of mare basalt types based on spectral reflectance data (18,19).

In summary, the highlands around Crisium basin can be modeled as mixtures of anorthositic gabbro, LKFMB, and mare basalt. Little evidence is found for major changes in the composition of the highland components as a function of distance from the basin rim. If this highland component is taken to be largely Crisium ejecta, the lack of major changes in the relative proportions of the dominant rock types suggests that these materials may have been thoroughly mixed in the upper portion of the Crisium target site prior to basin formation. An earlier orbital mixing model study of Imbrium basin ejecta (Apennine Region) (20) suggested higher fractions of LKFMB as an ejecta component. Its lower abundance in the Crisium deposits add support to arguments that LKFMB is derived from deep crustal levels (21) since Crisium, being smaller than Imbrium, would excavate shallower crustal materials.

Nectaris Basin Ejecta: Although Nectaris is relatively older than several other major nearside basins (Imbrium, Crisium, and Serenitatis), its great distance from these structures and recent studies emphasizing the importance of local mixing (22) suggest that the composition of the surrounding highlands might be expected to reflect the nature of the Nectaris target site. Support is provided by the fact that numerous workers have related individual Apollo 16 samples to the Nectaris basin 23,24). In particular, it has recently been proposed that the KREEP-rich Apollo 16 samples were excavated from a deep crustal layer by the Nectaris impact event (23). If so, the distribution of LKFMB might be expected to vary in a systematic manner with respect to the basin. The results of preliminary mixing model calculations along the Apollo 16 groundtrack show that regions N and NE of the basin (1 - 4; 20.5°-42°E) contain a large highland component dominated by anorthositic gabbro. LKFMB comprises between 20% and 30% of the total highland material. No clear trend relative to basin structure can be recognized. Theophilus ejecta contains a large highland component which dominates the mare regions north of the crater. Major changes in composition occur in the Descartes region (14° - 20.5°E). Anorthositic material becomes more abundant, and mare basalt is present in only trace amounts. Further west (5° - 14°E) a medium-K Fra Mauro basalt (MKFMB) component yields better solutions in mixing calculations than LKFMB. The abundance of MKFMB increases to the west, away from Nectaris basin, and may be related to local KREEP-rich deposits in the Fra Mauro region, or alternately, to the Imbrium event (20).

In summary, the results obtained to date cannot be taken to support the hypothesis that Nectaris was the source of the KREEP-rich material in the Apollo 16 region. However, no pristine KREEP samples at Apollo 16 have been found; KREEP is present only as a component in polymict rocks. Thus, the possibility that Apollo 16 KREEP is derived from the large LKFMB component seen from orbit cannot be ruled out; in this instance, the MKFMB seen to the west would be related to post-Nectaris geologic events and Nectaris ejecta is either thin, non-existant, or more anorthositic in composition.

Orientale Basin Ejecta: Mixing model calculations were performed on the composition of a portion of the ejecta blanket north of the Orientale basin. The area is near the inferred rim of the transient crater cavity and thus should contain material excavated from the lower levels of the cavity. This area can best be modeled as a mixture of about 60% anorthositic gabbro and 40% gabbroic anorthosite. However, "gabbroic anorthosite" in returned lunar samples is always polymict (e.g. Taylor (13) gives 68415, an impact melt, as an example of gabbroic anorthosite). Since this rock type is not well defined chemically, particularly with regard to Th content, no conclusions can

be drawn regarding the apparent absence of LKFMB in Orientale basin ejecta, and this region is currently undergoing continued analysis.

Summary: Results of mixing model calculations for highland regions surrounding the Crisium, Nectaris, and Orientale basins suggest the presence of anorthositic gabbro and low-K Fra Mauro basalt as primary constituents of lunar basin ejecta. Due to the peculiarities of the Apollo orbital coverage, chemical data are available only for portions of these basin ejecta blankets. In addition, the definition of the suite of primary rock types in the lunar crust is still a matter of controversy. Therefore, the conclusion that systematic variation in the proportions of highland rock types with respect to basin distance and position is not well defined, must be considered tentative until more complete orbital and sample information is available.

REFERENCES

1. Andre C. *et al.* (1977) Science 197, 986. 2. Bielefeld M. *et al.* (1976) PLSC 7, 2661. 3. Bielefeld M. (1977) PLSC 8, 1131. 4. Metzger A. *et al.* (1977) PLSC 8, 949. 5. Pieters C. and McCord T. (1976) PLSC 7, 2677. 6. Charette M. *et al.* (1977) PLSC 8, 1049. 7. Bryan W. *et al.* (1969) Science 163, 926. 8. Wright T. and Doherty P. (1970) GSA Bull 81, 1995. 9. Hawke, B. and Ehman W. (1976) Lun Sci VII, 351. 10. Adler I. and Trombka J. (1977) Phys Chem Earth 10, 17. 11. Bielefeld M. *et al.* (1978) *Mare Crisium: View from Luna 24,* 33. 12. Schonfeld E. (1977) PLSC 8, 1149. 13. Taylor S.R. (1975) *Lunar Science,* Pergammon Press. 14. Ridley I. (1976) Ann Rev Earth Planet Sci 4, 15. 15. Warren P. and Wasson J. (1977) PLSC 8, 2215. 16. Ryder G. (1979) PLPSC 10, (in press). 17. Wilhelms D. (1976) PLSC 7, 2883. 18. Head J. *et al.* (1978) *Mare Crisium: View from Luna 24,* 43. 19. Pieters C. (1978) PLPSC 9, 2825. 20. Hawke B. and Head J. (1978) PLPSC 9, 3285. 21. Ryder G. and Wood J. (1977) PLSC 8, 655. 22. Oberbeck V. (1975) Rev Geophys Space Phys 13, 337. 23. Maurer P. *et al.* (1978) GCA 42, 1687. 24. Head J. (1974) Moon 11, 77.

TABLE 1. Results of mixing model calculations for selected regions around Crisium (Apollo 15 groundtrack), Nectaris (Apollo 16 groundtrack) and Orientale (Apollo 15 and 16 groundtracks; gamma-ray data) basins. Crisium A, B, C, and D refer to units defined by Bielefeld *et al.* (11).

Region	Longitude	Anorthosite	Gabbroic Anorthosite	Anorthositic Gabbro	Low-K Fra Mauro Basalt	Med-K Fra Mauro Basalt	A 12 Mare Basalt	A 11 Mare Basalt
Crisium Basin								
A	---	---	---	75.5	22.7	---	1.8	---
B	---	---	---	78.8	21.2	---	---	---
C	---	---	---	75.1	22.3	---	2.6	---
D	---	---	---	61.4	19.9	---	18.7	---
Nectaris Basin								
1. HL West of M. Fecunditatis	37.5°-42°E	---	---	62.4	23.0	---	---	---
2. Isidorus and Capella	30°-37.5°E	---	---	74.7	25.3	---	---	---
3. Mare Nectaris S. of Torricelli	26°-30°E	---	---	50.7	21.8	---	27.5	---
4. Portion of Theophilus Ejecta	20.5°-26°E	---	---	65.5	16.1	---	---	18.4
5. Descartes	14°-20.5°E	21.2	---	47.4	27.7	---	---	3.7
6. HL West of Descartes	5°-14°E	9.2	---	63.6	---	14.7	---	12.5
Orientale Basin								
Orientale rings and ejecta	76°-110°W	---	40.1	59.9	---	---	---	---

GEOCHEMICAL ANOMALIES ON THE LUNAR EASTERN LIMB AND FARSIDE, B. Ray Hawke, Planetary Sciences Division, Hawaii Inst. of Geophysics, Univ. of Hawaii, Honolulu, HI 96822, P. D. Spudis, Dept. of Geology, Arizona State Univ., Tempe, AZ 85281, P. E. Clark, Chemistry Dept., Univ. of Maryland, Coll. Park, MD

I. Introduction

The orbital geochemistry data have shown that some lunar regions have unusual abundances of certain elements relative to surrounding or adjacent areas or have a surface chemistry unlike that which would be anticipated from the examination of local geologic relationships. Investigation of the formation of these geochemical anomalies can provide important clues to understanding impact and volcanic processes operative during the early phases of lunar evolution. For example, such studies have proven useful in outlining the history of KREEP volcanic activity in the western maria[1,2,3,4]. The purpose of this study was to investigate the geology and geochemistry of selected anomalous highland regions on the eastern limb and farside and attempt to understand the processes responsible for their formation.

II. Causes of Geochemical Anomalies

There has been an increasing tendency in recent years to relate geochemical anomalies and many variations in lunar surface chemistry to lateral heterogeneities produced by the chemical differentiation of the global magma ocean. While this explanation is probably valid for large-scale variations, it must be recognized that other processes are capable of producing geochemical anomalies in the lunar highlands. These include the following:

A. Basin-forming impacts - Large objects impacting near the end of crustal formation may have produced localized melting and lateral chemical heterogeneities. More recent large impacts excavated crustal material from a variety of depths and systematic changes in the composition of basin ejecta deposits may represent changes in the vertical composition of the lunar crust at the target site. The composition of the associated body of impact melt may represent a homogenized section of the upper crust[5] or may have differentiated to form a variety of rock types[6].

B. Highland volcanism - Volcanic activity has also been an important process in determining the composition of the lunar surface. Although this is most obvious in the case of mare volcanism, premare or highland volcanism may have been very important. Very early (>4.0-4.1 b.y.) highland volcanic deposits were probably destroyed during the terminal bombardment of lunar surface but may have left geochemical and mineralogic signatures. The heavily impact reworked KREEP-rich breccias collected at the Apollo 14 site are probably the products of such an episode of early highland volcanism[3]. More recent episodes of highland volcanism may have produced deposits which are both compositionally and morphologically distinct. A prime example of these younger deposits is the Apennine Bench Formation[2,3].

C. Mare volcanism - Mare volcanic deposits emplaced considerably before the end of the terminal bombardment would have been thoroughly reworked and mixed with highland material (see Ryder and Taylor[7]). While little morphologic evidence of these very early basalts would remain, they would still influence the remotely sensed surface composition of the area in which they were extruded. Later mare basalts, extruded close to the end of the terminal bombardment, may have been buried by thin layers of highland debris. These ancient mare basalts are represented on the lunar surface by certain light plains with dark-haloed craters (see Schultz and Spudis[8]). These later basaltic deposits, though present in the subsurface, would still exert an influence on regional chemistry by mixing with the highland material during the emplacement of the debris unit and by vertical mixing of the mare basalt

with overlying material.

Pyroclastic deposits in regions of explosive volcanic activity are capable of producing areas of mare-like chemistry in the lunar highlands. A prime example is the Sulpicius Gallus Fm. in the Haemus Mts. at the southwest edge of Mare Serenitatis (Schonfeld and Bielefeld[9]). Since pyroclastic activity seems to be concentrated in the vicinity of basin rims, care must be exercised in inferring surface compositions in these areas[10,11,12]. Complications arise if the pyroclastics are difficult to detect as would be the case if the deposits were either very old or thin and had been substantially mixed with subjacent material or if the pyroclastics had a higher albedo than that which generally characterizes such deposits.

III. Geologic and Geochemical Studies of Specific East Limb and Farside Anomalies

A. Region near Langemak - Hubbard et al.[13] pointed out the rather striking variations in Mg/Si and Al/Si intensity ratios which occur in the vicinity of Langemak crater. The lowest average Al/Si ratios (∿1.0) and the highest average Mg/Si ratios (∿0.8) are found around 115°E. In addition, Clark et al.[14] noted that an adjacent highland area immediately northeast of Pasteur crater was defined by the unusual combination of high Fe and high Al/Si values, an exception to the general inverse correlation of orbital Fe and Al/Si values. No apparent radioactivity anomaly has been identified in this general region[15]. Important clues to understanding the source of the geochemical anomalies have come from the work of Schultz and Spudis[8], who correlated high Mg/Si intensity ratios with dark-haloed craters in the region. The existence of these dark-haloed craters with associated geochemical anomalies strongly suggest the presence of a buried ancient basalt layer. The existence of other dark-haloed craters in the region demonstrates that this unit is not limited to the immediate vicinity of Langemak and may, in fact, underlie some or most of the Imbrian and Nectarian light plains units in the region. The correspondence of an area of geochemical anomalies with an area of probable ancient mare volcanic activity suggests that early volcanism may be an important process in the production of regional chemical anomalies elsewhere on the lunar surface.

B. Mare Marginis region - The results of Th deconvolution modeling studies by Haines et al.[1] allowed the identification of a region north of Mare Smythii with Th concentrations well above highland levels. This region is dominated by Mare Marginis, and the mare-flooded crater Neper but also contains highland units inlcuding light plains deposits in Babcock crater and just east of Marginis. While Haines et al. reported a Th concentration of 3.4 ppm for this region as a whole, they noted that when the model was modified by decoupling the Mare Marginis-Neper and highland portions, the resulting fit was equally as good; the resulting highland Th concentration was 2.3 ppm and the mare concentration was 5.4 ppm. The high Th concentrations are clearly associated with the mare material and hence there appears to be a mare basalt unit on the eastern limb with a Th concentration of at least 3.4 ppm and perhaps as high as 5.4 ppm; both values are considerably in excess of those associated with the Apollo mare samples. The high Th content of the Mare Marginis basalts suggests that they are intermediate in composition between mare and KREEP basalts and may be similar to the Apollo 17 KREEPy basalt described by Ryder et al.[16]. Estimates of Apollo 17 KREEPy basalt Th concentrations based on reported K_2O values[16] range from ∿4 to 6 ppm and are comparable to those for the Mare Marginis-Neper region. In addition, the MgO values reported by Andre et al.[12] for Neper (∿8-9%) are similar to the average composition of Apollo 17 KREEPy basalt (∿8%).

Geochemical Anomalies
Hawke, B.R., et al.

C. Balmer crater region - Another area with anomalously high Th concentrations (~4.0 ppm) was identified by Haines et al.[1] just north of Balmer crater (68°E, 15°S). This Th high corresponds to an area of Imbrian-age light plains which contain a cluster of dark-haloed craters[8] which suggest the presence of a buried basaltic unit. While this anomaly may be related to a genuine episode of highland volcanism[1], it is also possible that the covered basalt is the source of the high Th material. The area is surrounded (within 250 km) by five major impact structures of Imbrian or younger age which could have contributed to the thin cover of highland material. The subjacent basaltic material would have been mixed with crater material during ejecta emplacement and by subsequent vertical mixing. If this explanation is correct, the basaltic unit must have had Th concentrations approaching those found in KREEP.

D. Terrain north of Taruntuis - An expanse of low-lying terrain north of Taruntuis crater has been mapped as Imbrian-aged plains and smooth terra material[17]. The area is included in Unit E as defined in the Crisium region of Bielefeld et al.[18] on the basis of the natural clustering Al/Si concentration ratios ($E \tilde{=} 0.48$), Mg/Sl concentration/ratios ($E \tilde{=} 0.50$), and albedo values. Elsewhere, unit E generally corresponds to mare material (Mare Spumans, Mare Undarum, etc.) or a narrow mare-dominated mixed unit along mare-highland contacts. Hence, mare material might be expected to be associated with the deposits north of Taruntuis. Deposit morphology is consistent with an extrusive origin (embays rugged highlands terrain and exhibits a mare-type ridge; 8°N, 48.5°E). In Whitaker's .61-.37 μm color difference photograph, the deposits appear slightly less "red" than the adjacent highlands to the north. The evidence suggests that the plains and smooth terra units north of Taruntuis are volcanic units with possible mare affinities. The geochemical data are consistent with a mixture of roughly 50% mare material (unit H^{18}) and 50% highlands material (unit B^{18}). If highland contamination has been minimal, a less mare-like initial composition would be required and non-mare volcanism would be suggested.

E. Van de Graaff region - Several major geochemical anomalies have been located in the Van de Graaff region. The region contains relatively high Th, K, and Fe concentrations and low Ti content[19,20]. A basic question is whether the chemical anomalies are related (1) to material excavated by the various basins in the region[20,21], (2) to exotic material transported from some distant source[22], or (3) to a local episode of volcanism. A major objection to the last of these has been the limited areal extent of mare-like basalts[22]. A partial explanation may involve thinly covered basaltic units. The region is antipodal to Imbrium basin and any pre-Imbrian volcanic deposits could easily have been covered by the extensive mass-wasting caused by seismic waves associated with Imbrium[23]. Dark-haloed craters have been identified in the region[8] and suggest the presence of buried basalt units.

References: 1) Haines, E. et al. (1978) PLPSC 9, 2985. 2) Spudis, P. (1978) PLPSC 9, 3379. 3) Hawke, B. and Head, J. (1978), PLPSC 9, 3285. 4) Metzger, A. et al. (1979) PLPSC 10, in press. 5) Ryder, G. and Wood, J. (1977) PLSC 8, 655. 6) Head, J. (1974) The Moon 11, 327. 7) Ryder, G. and Taylor, G. (1976) PLSC 7, 1741. 8) Schultz, P. and Spudis, P. (1979) PLPSC 10, in press. 9) Schonfeld, E. and Bielefeld, M. (1978) PLPSC 9, 3037. 10) Hawke, B. et al. (1979) PLPSC 10, in press. 11) Head, J. (1974) PLSC 5, 207. 12) Andre, C. et al. (1979) PLPSC 10, in press. 13) Hubbard, N. et al. (1978) Mare Crisium: The View from Luna 24, 13. 14) Clark, P. et al. (1978) PLPSC 9, 3015. 15) Frontispiece (1977) PLSC 8. 16) Ryder, G. et al. (1977) EPSL 35, 1. 17) Wilhelms, D. (1972) USGS Map 1-722. 18) Bielefeld, M. et al. (1978) Mare Crisium: The View from Luna 24, 33. 19) Bielefeld, M. et al. (1976) PLSC 7, 2661. 20) Davis, P. (1979) submitted to JGR. 21) Schonfeld, E. (1977) PLSC 8, 1149. 22) Stuart-Alexander, D. (1978) USGS Map I-1047. 23) Schultz, P. and Gault, D. (1975) The Moon 12, 159.

LATERAL CRUSTAL VARIATIONS DETERMINED FROM GEOLOGICAL STUDIES.

James W. Head, Dept. of Geological Sciences, Brown Univ., Providence, RI 02912

Variations in the chemistry and structure of planetary crusts can result from several factors including 1) primary variations associated with processes of crustal formation, and 2) secondary variations related to post-crustal formation processes such as impact cratering and volcanism. Primary crustal variations on the Earth's Moon are very likely related to the period of melting of the outer several hundred kilometers of the Moon and the associated processes of segregation and flotation.[1] Primary and secondary factors may have combined in the case of the lunar crust since the energy source for melting may have come from impacts, and impacts are likely to have heavily modified the embryonic crust,[2] often penetrating and stirring the cooling materials.

Geological variations on the surfaces of planets other than the Earth have been determined primarily from mapping and interpretation of surface morphology.[3] This approach is extremely limited for the period of formation and early evolution of the lunar crust because of the high rate of impact cratering during that time. Not only is the surface continually renewed morphologically by impact upon impact, but the resulting surficial blanket of debris (megaregolith)[4] exceeds in thickness the dimensions of many of the features (volcanic constructs, flow fronts, etc.) that provide evidence for crustal diversity and history. Thus, studies based on morphology alone are not likely to cast significant light on actual crustal variation in the first few hundred million years of lunar history. However, studies ot the morphology of younger features, such as craters and basins, has provided a basis for understanding the processes that were important during these early years. Two exceptions exist to this general view. First, variations in regional topography (the most general form of morphology) may reveal something about the general composition of the crust and regional variations, based on isostatic considerations.[5] Secondly, the combination of morphology and remote geochemistry has proven to be an important approach for determining lateral crustal variations during the later evolution of the Moon (emplacement of the mare basalts).[6] This approach is presently being applied to the crusts of the Moon and Mars and may provide significant steps in unravelling primary crustal variations in the future. However, at the present, the main contribution of geologic studies comes from an understanding of processes related to secondary crustal variations, such as impact cratering and volcanism.

Impact Processes

Impact craters range from the tiniest blemish to basins over a thousand km in diameter. It is useful to consider separately the effects of craters and basins. Craters (≲200 km diameter) are most abundant and collectively produce regional deposits (regoliths). The larger basins are much less abundant but each creates impressive regional lateral and vertical variations in composition and structure.

Craters - The pioneering work of Oberbeck[7] and co-workers has shown that impacts in general are not efficient in lateral mixing of material by ejecta transport. The mass of ejecta decreases as a function of range, while its velocity increases. This results in the contiguous excavated material lying primarily within a crater radius of the rim crest, while material ejected to greater ranges impacts with such a high velocity that it reexcavates many multiples of its own mass in local material, destroying its coherence in the process. Although lateral mixing takes place, single events do not produce significant lateral mixing on a global, crustal scale. Vertical mixing is a significant aspect of impact cratering since ejecta is a vertical sample of

crust affected by the projectile impact. The zone of brecciation associated with a single event clearly exceeds the depth of material that actually moves within the cavity. Thus, the uppermost part of the target leaves the cavity as ejecta, deeper material may be partly ejected (but return as fallback), and even deeper material may be compressed and/or brecciated. Monte Carlo model considerations[8] strongly suggest that over half the surface has been cratered to depths of only a few (2-3) kilometers. Thus, vertical mixing by craters occurs predominantly in the upper part of the crust. Although not an extensive process, the vertical mixing produces a megaregolith several kilometers thick[4,8] which obscures detailed geologic structure and texture.

Basins - The exact nature of the basin-forming process is not uniformly agreed upon.[9] These uncertainties make a detailed understanding of the depth of sampling and extent of vertical mixing difficult. Although estimates of the depth of sampling for Imbrium have been as large as several hundred km, many workers believe (on the basis of sample, remote geochemical, and photogeologic evidence) that sampling was largely confined to crustal depths. However, this is a significant question for further study. Lateral variations resulting from basin events are of two types: 1) basin exterior, where the ejecta is relatively continuous and dominated by primary ejecta within a radius from the basin rim. Basin events have affected each of the Apollo and Luna non-mare landing sites to varying degrees;[10] 2) Interior deposits include vast quantities of impact melt produced by the basin event. Most such deposits have been covered by maria, but the relatively unflooded Orientale basin shows extensive melt deposits[9] totalling about 200,000 km^3. For lateral crustal variations, then, basin impact events can be regionally important since basin radii may exceed 500 km.

Volcanic Processes

The flat and relatively smooth nature of many highlands plains led numerous workers to interpret them as deposits of highland volcanism. The Apollo 16 mission showed these plains in the Descartes region to be dominated by impact breccias. Thus, several impact-related processes appear to mimic plains of volcanic origin, such as the lower albedo maria. There is some photogeologic evidence for high albedo plains of volcanic origin,[11] but supporting evidence from remote geochemical measurements will be required to help distinguish these from impact deposits. Volcanic constructs are also mimicked by impact deposits[12] but there are several examples of constructional features which are both morphologically and spectrally distinct from surrounding highlands.[13,14] The Gruithuisen and Mairan domes[14] provide strong evidence for non-mare volcanism of a type that may have been more abundant in earlier crustal history, but largely obliterated by the impact record. Finally, dark-halo craters of impact origin on light plains support the hypothesis that mare volcanism began prior to the end of the major phase of bombardment of the lunar crust.[15]

References: [1]S. Solomon and J. Longhi (1977) PLSC8, 583; [2]F. Herbert et al. (1978) PLPSC9, 249; [3]D. E. Wilhelms (1972) USGS Interagency Report: Astrogeology 55; [4]W. K. Hartmann (1973) Icarus 18, 634; [5]S. Solomon (1978) PLPSC 9, 3499; [6]J. W. Head et al. (1978) Icarus 33, 145, J. W. Head et al. (1978) Mare Crisium, 323; [7]V. R. Oberbeck (1975) RGSP 13, 337; [8]F. Hörz et al (1976) PLSC7, 2931; [9]J. W. Head (1974) Moon 11, 327, H. Moore et al. (1974) PLSC5, 71; [10]J. W. Head and M. Settle (1976) Imbrium Consortium 1, 5; [11]B. R. Hawke and J. W. Head (1978) PLSC9, 3285, P. Spudis (1978) PLSC9, 3379; [12]J. W. Head (1972) NASA SP-315,29-16, C. A. Hodges (1972) NASA SP-315,29-20; [13]M. C. Malin (1974) EPSL 21, 331; [14]J. W. Head and T. B. McCord (1978) Science 199, 1433; [15]P. Schultz and P. Spudis (1978) Lunar Plan. Sci. IX, 1033.

LUNAR HIGHLANDS VOLCANISM: GEOLOGIC AND REMOTE SENSING DATA ON DOMES OF POSSIBLE EXTRUSIVE ORIGIN. James W. Head, Dept. of Geological Sciences, Brown Univ., Providence, RI 02912; and Thomas B. McCord, Institute for Astronomy, Univ. of Hawaii, Honolulu, HA 96822.

Three major classes of features have historically been cited as representing possible sites of lunar highland (non-mare) volcanic activity,[1] including craters and crater chains (such as Davy), smooth plains (such as the Cayley Formation),[2] and domes and cones (such as the Descartes Formation).[3] Prior to Apollo 16, there was a strong feeling in the photogeologic community that many occurrences of smooth plains, domes, and cones were of extrusive volcanic origin. Indeed, the Apollo 16 mission was targeted to the Descartes region to sample areas of such plains and domes.[4] The samples from these two terrain types proved to be breccias of impact origin,[5] casting doubt on the interpretation of any such morphologic features on the Moon as possibly representing extrusive volcanism. Several subsequent studies have combined morphologic and remote geochemical observations to suggest that there are indeed some examples of lunar highland (non-mare) volcanic features.[6,7,8] The purpose of this paper is to describe the geologic setting and spectral reflectance characteristics of three examples of such features in the Oceanus Procellarum region of the Moon. We will show that these features have distinctive morphologies, are of non-mare composition (yet distinct from surrounding highlands), are relatively young parts of the highlands crust, and may represent a type of feature more common in earlier crustal history, but obscured by the high impact flux.

Geologic Setting - The major positive structures are located in three areas near the edge of Oceanus Procellarum. The Gruithuisen domes[8,9] include Gruithuisen γ (319°20',36°30'N) which is superposed on the edge of an upland plateau and is partly embayed by adjacent mare deposits. Its shape is roughly circular, measuring 18 by 24 km at its base, and the dome is capped by a broad, flat crest about 1200 m in elevation. Several domes occur on the summit, the largest of which is over a kilometer in diameter. The slopes or flanks are locally characterized by a distinctive ridged and furrowed texture oriented downslope. These slope units are interpreted as flow units emanating from the vicinity of a NW trending linear and continuing down the flanks and out onto adjacent terrain. Gruithuisen δ (320°30',36°10'N) is also superposed on the edge of an upland plateau and its slope and summit units are identical to those on Gruithuisen γ. This dome, however, is distinctly rectangular in plan view (33 x 13.5 km) with the long axis oriented NW, parallel to the lineament on the summit of Gruithuisen γ. Estimates of the dome summit elevation range from 1470-1660 m. The rectangular shape may be caused by the coalescence of two separate eruption centers, as suggested by the presence of two distinct summit areas. A third, smaller dome (6 x 9 km), is located to the NW of Gruithuisen γ and is uniformly called "Northwest" dome (310°55',37°10'N). It rises ∿1100 m above the surrounding terrain. The Mairan domes are located about 225 km NW of the Gruithuisen domes. Mairan T (311°50',41°50'N) is surrounded and apparently embayed by mare, is about 6.7 km at its base, and about 930 m in height. It is distinctly different from the other domes in that its summit is characterized by a series of coalescing craters together forming a summit depression about 3-4 km in diameter, rather than a summit plateau. The concentration, location, and coalescence of the craters suggest an internal, non-impact origin. The morphology of Mairan T is close to that of a cone, but it may represent a dome whose summit has collapsed. "Central" dome (312°25', 41°20'N) is superposed on a prong of highland material, embayed by mare, has a

DOMES OF POSSIBLE EXTRUSIVE ORIGIN

Head, James W. and McCord, T. B.

broad summit, and is low relative to its diameter (12.1 x 10.7 km, 570 m high). "Southern" dome (312°30', 40°30'N) is 4.7 x 3.4 km and about 460 m in elevation. Hansteen α is located in southwest Oceanus Procellarum (309°,12°S) just north of the crater Billy. The feature is triangular in plan view (informally called "Arrowhead") with each side of the traingle being about 28 km. It is surrounded and apparently embayed by mare material and is apparently not influenced by ejecta from Hansteen and Billy craters, both of Imbrian age.[2] This suggests an Imbrian age for the dome. The top of Hansteen α is not as flat as the major Gruithuisen domes but the surface texture is rough and similar to the flow-like deposits at Gruithuisen. In addition, there are several linear pits (about 1 x 3 km) oriented parallel to the edges of the structure.

Composition - The Gruithuisen domes are prominent in color-difference images obtained at 0.40/0.56 μm but not in those obtained at 0.95/0.56 μm. An inspection of the relative reflectance spectrum for these lunar surface features and Hansteen α reveals the strong ultraviolet absorption responsible for the red color. Other reflectance spectra demonstrate the existence of additional regions of lunar surface material of high albedo which have similar spectral reflectance properties.[8] These characteristic red spot spectra differ from the usual spectra of mature upland regions in this spectral range only in the strong ultraviolet absorption. No known mare area spectra are similar to the red spot spectra. Thus, the Gruithuisen and Hansteen α domes are spectrally distinct from the surrounding highland and mare material but are quite similar in a distinctive way to other areas of high albedo on the western lunar nearside known as red spots.

Age - The domical structures in the three regions appear on the basis of geological relationships and crater counts[6,9] to be of Imbrian age, synchronous with the emplacement of many mare basalts.

Conclusion - The Gruithuisen, Mairan, and Hansteen α domes appear morphologically and texturally distinct from the surrounding mare materials and show no obvious affinities with background highland topography. The morphology and surface texture suggest a volcanic origin for the domes, distinct from mare basalt eruption styles, and comparable to styles typical of more acidic terrestrial compositions. The age suggests synchronous eruption of these materials and mare basalts. Although these features could represent crustal material melted by the ascending mare baslats, they may also represent the only preserved vestige of an earlier stage of highland volcanism, the earlier structures having been obliterated by the high impact flux characteristic of the first 600 m.y. of lunar history. The spectra indicate that the dome areas are covered with mature (agglutinate-rich) soils with a lower content of iron and titanium than mare soils, and perhaps lower than most highland soils. However, the specific compositional property causing the ultraviolet absorption in the red spot spectra is unknown. Correlations of red spots and KREEP basalts have been suggested.[6] However, preliminary analyses of laboratory spectra have not yet established any correlation with specific types of highland basalts. We are presently comparing the spectra of these deposits with a range of lunar samples in an attempt to determine more closely their compositional affinities.

References - [1]J. W. Head (1978) RGSP 14, 265; [2]D. Wilhelms and J. McCauley (1971) USGS Map I-703; [3]D. Milton and C. Hodges (1972) USGS Map I-748; [4]N. Hinners (1972) NASA SP-315, 1-1; [5]LSPET (1972) NASA SP-315, 7-1; [6]M. Malin (1974) EPSL 21, 331; [7]C. Wood and J. Head (1975) Origins of Mare Basalts, 189; [8]J. Head and T. McCord (1978) Science 199, 1433; [9]J. Head et al. (1978) LPS IX, 488.

THE CORDIERITE- TO SPINEL-CATACLASITE TRANSITION IN THE MOON, AND ITS BEARING ON THE STRUCTURE OF THE CRUST AND MANTLE. C. T. Herzberg[1] and M. B. Baker[2], Lunar and Planetary Institute[1], 3303 NASA Road 1, Houston, TX 77058, Harvard-Smithsonian Center for Astrophysics[2], 60 Garden Street, Cambridge, MA 02138.

In previous papers (1,2) it was noted that the lunar spinel cataclasite whole rock compositions could crystallize to either olivine + plagioclase + Al-orthopyroxene + spinel (spinel cataclasite) or olivine + plagioclase + Al-orthopyroxene + cordierite (cordierite cataclasite) depending on the temperature and pressure of equilibration in the lunar crust. The end-member univariant reaction which describes this cordierite- to spinel-cataclasite reaction is:

$$5Mg_2SiO_4 + Mg_2Al_4Si_5O_{18} = 5Mg_2Si_2O_6 + 2MgAl_2O_4 \quad (1)$$

The T-P location of reaction (1) was calculated from thermochemical data (1), and the result was extended to lunar spinel cataclasites in 15445, 73263, and 72435. These calculations showed that such cordierite-free clasts equilibrated somewhere in the lower half of the crust prior to excavation by the Imbrium and Serenitatis impact events.

Reversal experiments on reaction (1) in the system $MgO-Al_2O_3-SiO_2$ have since been completed in order to assess the accuracy of the thermodynamic data. The results are shown in Fig. 1. The experiments were run at 1150-1300°C in order to overcome the usual kinetic problems. The slope (dT/dP) is strongly negative, in contrast to that calculated from the thermodynamic data. Extrapolation of the experimental brackets using the Gibbs free energy relation yields:

$$P = \frac{RT}{-1.43}\left[\frac{-401.6}{T} - 1.839 - \ln(1 - X_{Al}^{M1})_{opx}^{5}\right] \quad (2)$$

where T is in °K, -1.43 is the standard volume change, and (X_{Al}^{M1}) is the mole fraction of Al in the M1 site of orthopyroxene along reaction (1). Also shown is the location of reaction (1) in the system $MgO-Al_2O_3-SiO_2-H_2O$ calculated from the thermodynamic hydration model of Newton and Wood (4) with equation (2) as the dry reference state. The calculation is able to predict the experimental results of Seifert (5) and Fawcett and Yoder (6) to within $\pm$ 0.2 kbar. Thus, the experimental work from 3 different laboratories on the T-P location of reaction (1) in the wet and dry systems corroborate to within $\pm$ 0.2 kbar over a 2 kbar and 780-1300°C range.

The results in Fig. 1 are particularly encouraging because the errors in P estimates generated from uncertainties in the temperature at which spinel cataclasites equilibrated will be minimal. Also, extension of the experimental data in the simple synthetic system to spinel cataclasites in 15445, 73263, and 72435 via the method described previously (1) should be accurate because of the dilute amounts of other components (ie., Fe and Cr) in the phases. Recall that these spinel cataclasites are the most primitive clasts yet reported, with olivine compositions averaging Fo_{92} in 15445 (1 and this work).

Using the selenothermometers from (7,8,9) together with these experimental results and our new microprobe data on 15445,177 and 72435,30, the conditions of equilibration of the lunar spinel cataclasites are:

CLAST	T(°C)	DEPTH (km)
15445,177	700-900 (1020)*	≥ 26 (12)*
73263,1,11**	750-1000	≥ 20
72435,30	680-1200	≥ 12

**microprobe data from (10)

THE CORDIERITE- TO SPINEL-CATACLASITE TRANSITION

Herzberg, C.T.

The T-P conditions indicated as * are calculated from the most chrome-rich spinels in the clasts. These are improbable, and are due to the assumption of ideality in the activity of $MgAl_2O_4$ in spinel. Due to reciprocal lattice effects (11), the required activity coefficients will reduce the temperatures and *increase* the pressures. Errors generated from the assumption of ideality in these calculations will be small, but will invariably result in *under*-estimations of the above pressures (see 1).

The spinel cataclasites are materials which resided at depth in the lunar crust. To our knowledge, their low pressure cordierite-bearing equivalents are not present in the lunar sample collection, with the notable exception of 72435,8 (12 and this work). Other clasts of differing parageneses may also have been deep-seated (2) but the evidence is not as compelling. It is possible that only the largest impact projectiles, such as those which produced the Imbrium and Serenitatis basins, had the energy to penetrate and excavate lower crustal materials; spinel cataclasites have been reported only from the Apollo 15 and 17 missions. Even so, our microprobe data on 72435,8,30, and 31, which show they are polymict breccias, can be interpreted to indicate that the primary equilibrium high Al orthopyroxenes may have suffered partial and, in some cases, complete reequilibration to surficial compositions. These are pyroxenes with typically higher Ti/Al, lower Al_2O_3 and significantly higher CaO contents; such values are common in poikilitic and granulite clasts. Thus, transport of these deep-seated rocks to the surface and exposure to impact melt may have destroyed much of the primary mineralogy (eg., coronas around pleonaste spinels (13)) and the mineral chemistry of many spinel cataclasites. We think this retrograde metamorphism produced considerably more cordierite than has been reported.

Spinel cataclasites are not only mineralogically unique to the lunar sample collection (ie., coexisting high Al orthopyroxene and spinel), but they also have some of the highest Mg/(Mg+Fe) ratios reported for highland clasts (0.90-0.92 molar). Thus, the evidence is strong in favour of a layered lunar crust (1,3) in which the parameters Mg/(Mg+Fe) and modal spinel increase with depth from the surface to the crust-mantle interface. It should be noted that Mg/(Mg+Fe) must then *decrease* from the crust-mantle boundary to the depths of the lunar mantle in order to provide a source for mare basalts (1).

If it is safe to assume that this layering is an artifact of processes which operated during the crystallization of the lunar magma ocean, an understanding of what these processes were should place important constraints on models of magma oceanography. Two explanations are currently under consideration. The first is that the layering is the product of inefficient gravitational removal of olivine and spinel precipitates during crystallization of the magma ocean due to entrainment by plagioclase floatation from below(1). This requires whole moon compositions which crystallized spinel after olivine (14,15,1), rather than plagioclase or pyroxene after olivine. One would then expect spinel cumulate layers to be present in the lunar mantle. A *preliminary* analysis of an enhanced seismic data base yields velocity-depth profiles which show a high velocity bulge at about 800 km depth (H. Jarosh, personal communication), which would lend some support to this expectation. However, because these compositions which precipitate spinel have Ca/Al ratios which are less than chondritic, Longhi and Boudreau (15) have appealed to the formation of lower crustal spinel layers via the interaction of convecting primitive magmas with the underside of anorthite-rich rockbergs. Such primitive magmas may have evolved from Taylor-Bence whole moon compositions with chondritic Ca/Al ratios. It appears that the solution to the problem may lie in determining the rate at which the lunar crust grew. Presumably, there is a dynamical trade-off in space and time between plagioclase floatation and suspension in a

THE CORDIERITE- TO SPINEL-CATACLASITE TRANSITION

Herzberg, C.T.

vigorously convecting magma ocean envisioned by Herbert et al. (16).

(1) Herzberg C. T. (1978) Proc. Lunar Planet. Sci. Conf. 9th, p. 319-336. (2) Herzberg C. T. (1979) In Lunar and Planetary Science X, p. 537-539. Lunar and Planetary Institute, Houston. (3) Ryder G. and Wood J. A. (1977) Proc. Lunar Sci. Conf. 8th, p. 655-668. (4) Newton R. C. and Wood B. J. (1979) Contrib. Mineral. Petrol. 68, p. 391-405. (5) Seifert F. (1974) J. Geol. 82, p. 173-204. (6) Fawcett J. J. and Yoder H. S., Jr. (1966) Amer. Mineral. 54, p. 1645-1653. (7) Sack R. O. (1979) Contrib. Mineral. Petrol., in press. (8) Evans B. W. and Frost B. R. (1975) Geochim. Cosmochim. Acta 39, p. 959-972. (9) Danckwerth P. A. and Newton R. C. (1978) Contrib. Mineral. Petrol. 66, p. 189-201. (10) Bence A. E. et al. (1974) Proc. Lunar Sci. Conf. 5th, p. 785-827. (11) Wood B. J. and Nicholls J. (1978) Contrib. Mineral. Petrol. 66, p. 389-400. (12) Dymek R. F. et al. (1976) Proc. Lunar Sci. Conf. 7th, p. 2335-2378. (13) McGee J. J. et al. (1978) Proc. Lunar Planet. Sci. Conf. 9th, p. 743-772. (14) Longhi J. (1978) Proc. Lunar Planet. Sci. Conf. 9th, p. 285-306. (15) Longhi J. and Boudreau A. E. (1979) Proc. Lunar Planet. Sci. Conf. 10th, in press. (16) Herbert F. et al. (1978) Proc. Lunar Planet. Sci. Conf. 9th, p. 249-262.

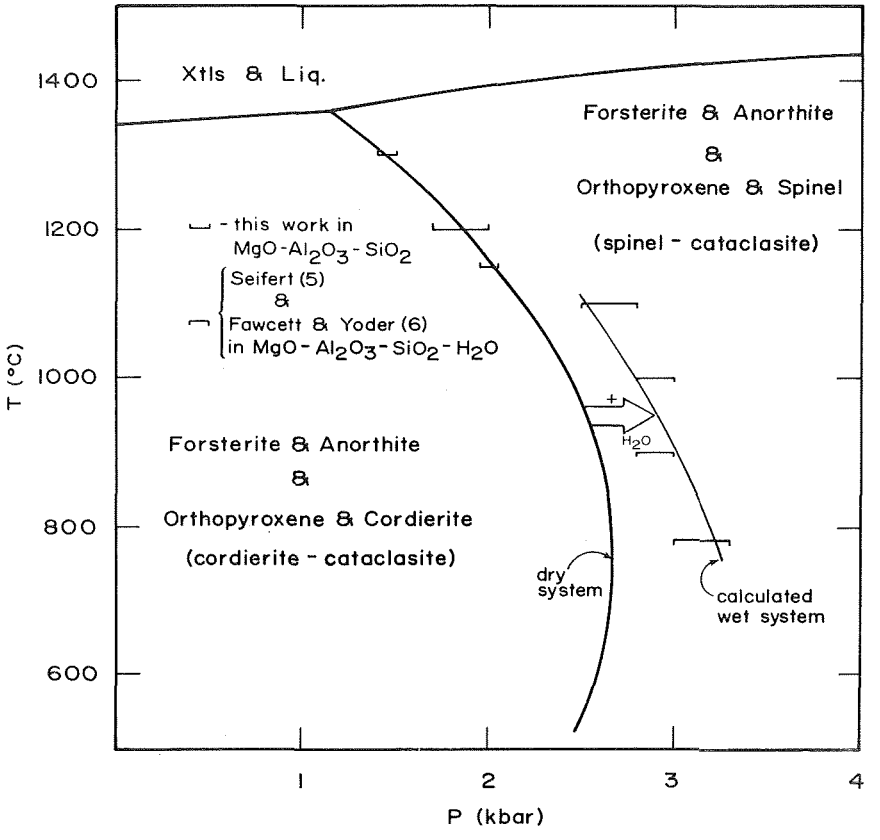

FIGURE 1: The cordierite- to spinel-cataclasite transition in the system $MgO-Al_2O_3-SiO_2$ (H_2O). The components FeO and Cr_2O_3 contract the cordierite field due to preferential partitioning into spinel (1). The pressure estimates for 15445, 73263, and 72435 consider these effects by application of solid solution thermodynamics to the above end-member system.

PHYSICAL-CHEMICAL CONSTRAINTS ON MODELS OF PLANETARY CRUST FORMATION. C. T. Herzberg[1] and W. S. Fyfe[2], Lunar and Planetary Institute[1], 3303 NASA Road 1, Houston, TX 77058, Department of Geology[2], University of Western Ontario, London, Ontario, Canada N6A 5B7.

There are fundamental similarities and differences between the lunar highland crust and the Precambrian crust of the earth in terms of their mineralogy and chemistry. These presumably reflect similar and disparate physical-chemical process of planetary crust formation.

In very general terms, the upper crust of the moon is composed mainly of noritic anorthosite with appreciable amounts of anorthosite sensu stricto (ie., > 90% plagioclase), and is the product of a differentiation event of an anhydrous (but with CO-CO_2 gas?) magma ocean (1) which took place at the birth of the solar system. The highland crust materials are largely breccias formed by intense meteorite bombardment of the primordial crust. This bombardment terminated about 3.8 b.y. ago, which is about the age of the oldest rocks on earth. The original textures and mineral parageneses are thus obscured to a large extent, although mineralogically there appear to be some notable exceptions (2). Bearing in mind this incomplete record of the earliest history of the moon's crust, it is probably safe to assume that the gross bulk chemical composition of the upper lunar crust has remained essentially unchanged (ie., at least in terms of the major elements) from the time of its formation.

The Archean rocks of the earth are at least an order of magnitude more variable mineralogically, due mainly to the effects of H_2O, CO_2, and alkalis in the igneous, metamorphic, and sedimentary cycle. The most common of these ancient rocks are tonalite/granodiorite gneisses (grey gneisses) of calcalkaline affinity and basic metavolcanics (references in 3). *Massif anorthosites are extremely rare in the Archean, but become relatively abundant later in the Proterozoic.* The precursors of the 3.8 b.y. grey gneisses appear to have been mainly igneous rather than sedimentary (4). It is reasonable, therefore, to presume a thin and globally encircling pre 3.8 b.y. primordial crust of grey gneiss composition which formed from the differentiation of the earth's magma ocean (5,6). The grey gneiss composition is compelling because of well established theoretical, experimental and petrologic observations on the effects of high H_2O activities in basic magmas which undergo fractionation. As with the lunar crust, the primordial textures, mineral parageneses, and radiometric clocks were reset about 3.8 b.y. ago, but the gross whole rock chemistry in terms of the major elements probably remained unchanged.

A common element of the earth and moon is that the densest materials are located in their interiors, and the least dense at their outermost shells. Of the solid silicate materials which crystallized from the magma oceans of the earth and moon, plagioclase has the lowest density. Fig. 1 shows the liquidus densities of plagioclase compared to the densities of anhydrous basic magmas from which it can crystallize at atmospheric pressure. Three parameters dominate the densities of such magmas: FeO content (this compilation), H_2O solubility (7,8), and pressure (9,10).

Where the density difference between a magma and plagioclase is marginal (ie., $\Delta\rho = \rho magma - \rho plagioclase$; eg. + 0.04 gm/cm^3) the fate of the plagioclase can be largely determined by the fluid dynamics of a flowing crystal mush current (11,12). Although a $+\Delta\rho$ does not ensure that plagioclase will float

PLANETARY CRUST FORMATION

Herzberg, C.T.

to form massive anorthosite accumulations, the reverse is not true. That is, the formation of volumetrically significant amounts of anorthosite sensu stricto (lunar and terrestrial) requires that either $\Delta\rho$ be positive, or the magmas from which plagioclase crystallized was unusually aluminous, thereby permitting an extended crystallization interval of plagioclase only. The generation of such magmas in the crust or mantle of the earth has continued to be problematic, requiring special circumstances (eg. high partial pressures of H_2O) which violate the observations of the rocks (eg. primary anhydrous mineral assemblages). Fig. 1 shows that a clean separation of plagioclase from other crystallizing mafic phases as well as the crystallizing magma itself is possible. Indeed, plagioclase floatation is a simple mechanism because it is likely to occur in a whole range of "common" basaltic melt compositions and, in particular, those which are iron rich and fractionate at depth. Note that the lunar anorthositic crust was fractionated from a number of possible whole moon compositions, all of which (including and especially their FeO enriched residual liquids) are denser than anorthosite by 0.06 to 0.20 gm/cm^3. By analogy, and from the above density constraints, we infer and note the following:

1. Early Archean anorthosites are rare because differentiation of the earth's magma ocean was, at least in part, calcalkaline in nature with high activities of H_2O. Therefore it is likely that $\Delta\rho$ was marginally negative or positive, and accumulation of large volumes of anorthosite was inhibited. Because of the likelihood of an inhomogeneous distribution of H_2O and CO_2 in the earth's magma ocean, or because of H_2O and CO_2 outgassing (13), simultaneous fractionation of dry basic magmas may have occurred. Due to a thin primordial crust, fractionation of plagioclase was at high levels in the mantle, and $\Delta\rho$ marginally positive.

2. Large volumes of massif-type anorthosite in high level layered intrusions such as Skaergaard and Stillwater do not occur because $\Delta\rho$ was marginally negative or positive due to low pressures (Fig. 1). That is, the same magmas, if allowed to fractionate at depth would result in massive anorthosite accumulations as suggested in 3 below.

3. Proterozoic anorthosites are not uncommon because of fractionation of anhydrous tholeiitic magmas from the mantle at the crust-mantle interface ($\sim$ 30 km). $\Delta\rho$ was large and positive. Dense ferromagnesian minerals settled to the mantle. The high pressures is consistent with the common association of Proterozoic massif anorthosites with high pressure metamorphic assemblages (14,15). The common incompatibility of olivine and plagioclase in these anorthosites via the production of spinel and/or garnet at high temperatures is a typical high-pressure reaction (14,15). Although it remains to be established, such metamorphic reactions are inferred to have taken place by isobaric, or near isobaric cooling at depth (15). This rationale suggests that where present day active oceanic ridge systems become overlain by a thick continental crust, massif anorthosites may be in the making.

4. Finally, of the three states of matter (ie., solids, liquids, and gases) the tenets of physical chemistry, as well as everyday experience, illustrate clearly which are the most or least compressible. Experimental results on the change of magma density with pressure (9) is yet another

PLANETARY CRUST FORMATION

Herzberg, C.T.

example. In particular, silicate liquids are considerably more compressible than silicate solids by about an order of magnitude. An appreciation of its significance regarding silicate systems of geological importance is long overdue. This is especially the case with respect to the differentiation of large planetary objects such as the earth. Because alumina and iron partition preferentially into magmas which crystallize olivine, it is highly possible that olivine may have the same (or lower) density as ultramafic liquids at depths above the olivine-spinel transition (10). Similarly, large density variations may have occurred for liquids which crystallized the high pressure polymorphs of olivine over a range of pressures in the mantle. Although the earth's magma ocean may have extended throughout its mantle, *differentiation to produce the primordial crust of the earth may have involved only its outermost layers.* (1) Wood J. A. et al. (1970) Proc. Apollo 11 Lunar Sci. Conf., p. 965-988. (2) Herzberg C. T. (1978) Proc. Lunar Planet. Sci. Conf. 9th, p. 319-336. (3) Windley B. F. (1976) The Early History of the Earth, Wiley. (4) Tarney J. (1976) In The Early History of the Earth, Wiley, p. 405-417. (5) Fyfe W. S. (1973) Philos. Trans. R. Soc. London 273, Ser. A, p. 457-461. (6) Hargraves R. B. (1976) Science 193, p. 363-371. (7) Bottinga Y. and Weill D. F. (1970) Am. J. Sci. 269, p. 169-182. (8) Campbell I.H. et al. (1978) Contrib. Mineral. Petrol. 67, p. 369-377. (8) Fujii T. and Kushiro I. (1977) Carnegie Inst. Wash. Yearbk. 76, p. 419-424. (10) Stolper E. et al. in preparation. (11) Walker D. et al. (1975) Proc. Lunar Sci. Conf. 6th, p. 1103-1120. (12) Irvine T. N. (1979) Am. J. Sci. 279A, in press. (13) Collerson K. D. and Fryer B. J. (1978) Contrib. Mineral. Petrol. 67, p. 151-167. (14) Herzberg C. T. (1978) Geochim. Cosmochim. Acta 42, p. 945-957. (15) Martignole J. and Schrijver (1971) Can. J. Earth Sci. 8, p. 698-704.

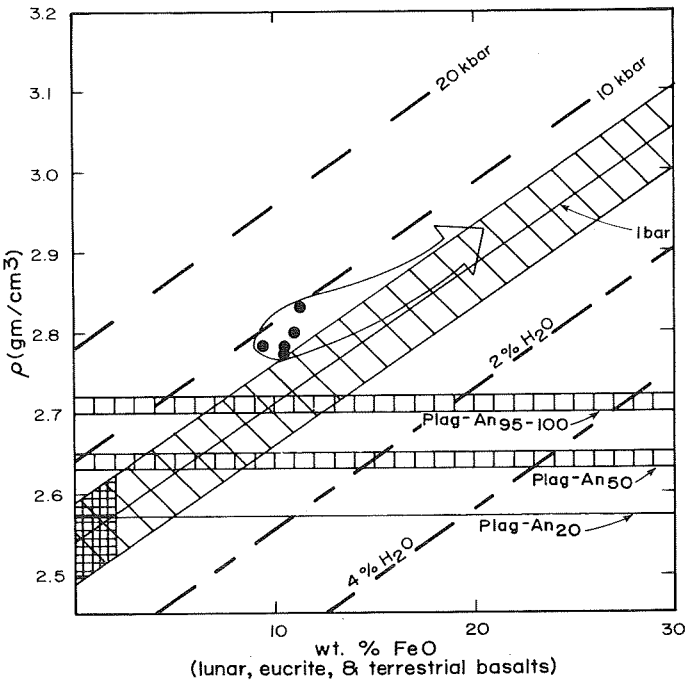

Figure 1. Densities of basalts and plagioclase at liquidus temperatures. Densities of andesitic compositions are ≤ those for basalts at any given FeO content. Circles in arrowed area are for a range of proposed whole moon compositions at 1 bar. Arrow points to density increases of evolved compositions. Vertical and horizontal hatched area are estimates for magmas of grey gneiss composition (dry, 1 bar). Note that magma density is controlled mainly by its FeO and H_2O contents, and pressure.

PARENTLESS PLUTONIUM FISSION XENON IN TROCTOLITE 76535?

C. M. Hohenberg, B. Hudson, and F. A. Podosek, McDonnell Center for the Space Sciences, Washington University, St. Louis, MO 63130

Amounts of plutonium fission xenon in excess of that which could be produced by in situ decay have been observed in the majority of the gas rich breccias from the Apollo 14 and 16 sites (1, 2). The fission contribution is always enriched in the low temperature fractions, indicating that it is more weakly bound than solar wind xenon; recent results on size separates from 14301 indicate that it is preferentially sited along grain surfaces (3). We report here data from 76535 that show remarkable similarity with the Apollo 14 and 16 breccias in the low temperature release of plutonium fission xenon. 76535 is, however, neither a breccia nor is it rich in solar wind gases and, in contrast with some of the gas rich breccias, does not contain quantities of fission xenon that are incompatible, in principle,with in situ decay. Low temperature release of a large fraction of the fission xenon, large variations of the effect among the samples analyzed, and the absence of association with volume-correlated components suggest that the effect cannot be explained simply by the in situ decay of an undisturbed system.

Xenon data for three samples of 76535 are reported in Table 1. The amounts and the spectra are quite different among these samples; the reasons for the difference must first be addressed. There is good evidence that mechanical crushing can introduce substantial contamination from terrestrial atmospheric xenon (11) and the contamination, so introduced, cannot be separated from xenon indigenous to the sample. The LaJolla sample was crushed to less than 90μ and the data indeed suggest the presence of an atmospheric component. Partitioning the observed $^{126}Xe/^{130}Xe$ for this sample between the atmospheric ratio and the ratio observed in either of the other two samples suggests that about 79% of the ^{130}Xe in 76535,64 may in fact be atmospheric contamination. Subtracting the corresponding atmospheric contributions from all isotopic results in the corrected (lunar) xenon spectrum shown in parentheses in Table 1. Note that this spectrum, both in amount and composition, closely resembles that obtained for 76535,75. We will henceforth limit our discussion to 76535,15 and ,75. In spite of the difference in the quantity of ^{136}Xe among these samples, the quantity of spallation produced ^{126}Xe is essentially identical in each sample and is compatible with the 211 m.y. exposure age of 76535.

Figure 1 shows a three isotope correlation plot for xenon released in stepwise heating of 76535,75, for a single stage melt of 76535,15 and for stepwise heating of 14301,57 and ,110 (numbers on the points represent the temperatures of the extraction filament in hundreds of degrees celsius; actual sample temperature may be several hundred degrees lower). Three components are present in this plot: a trapped component of solar wind composition, represented by surface correlated xenon in mare soil (SUCOR, 13), spallation xenon to the upper left, and fission xenon to the right. The 1600 through 2000°C points approximate pure spallation xenon at those temperatures and mixtures of such spallation and trapped xenon would plot along a line connecting SUCOR with this cluster of points. Additions of fission xenon causes departure to the right of the line in proportion to the relative amount of fission-produced ^{136}Xe.

Enhancement of the fission contribution in the low temperature fractions of 14301 can be seen in figure 1 (open circles) as a small protrusion above the "air" point. Although 14301 exhibits the largest fission effect at low temperature of all the gas rich breccias, it is clearly dwarfed by the fission enhancements in the low temperature fractions of 76535, which are the largest

xenon fission effects seen in any lunar sample studied to date (for instance, 84% of the ^{136}Xe in the 800°C fraction is due to fission). In spite of the differences in magnitude the release pattern of the low temperature fission effects is quite similar to that of the gas rich breccias except that it is not accompanied by appreciable solar wind xenon.

Fission yield spectra can be obtained from the low temperature data by suitable component analysis. The 800°C and other low temperature fractions are largely fission at the heavy xenon isotopes; the high temperature fractions, typified by the 1800°C point, are largely spallogenic. If sufficient quantities of solar wind xenon are added to the more spallogenic fractions to match spectra at the fission-shielded isotopes with the more fissiogenic fractions, the two compositions will differ only by the presence of more fission xenon in the spectrum; good aggrement with the known ^{244}Pu fission yield spectrum is obtained for both 76535,75 and 76535,15 (using whole rock 76535,75 as the spallation-rich component).

Radiometric ages for 76535 range from ^{39}Ar-^{40}Ar and Sm-Nd ages of 4.3 b.y. (7, 9) to an apparent Rb-Sr age of 4.6 b.y. (12) with some evidence of isotopic disturbance of these systems. The uranium content has been measured in two different samples of 76535 with values of 56 and 54 ppb (5, 8) providing about 1.7 x 10^{-13}ccSTP/g of ^{136}Xe from the spontaneous fission of ^{238}U. The observed quantities of fission-produced ^{136}Xe are 7.2 x 10^{-12}ccSTP/g for 76535,15 and 0.9 x 10^{-12}ccSTP/g for 76535,75, so, as inferred from the spectra , these samples are dominated by plutonium fission. If one were to attribute the fission xenon to in situ decay of plutonium, xenon closure times of about 4.4 b.y. and 4.2 b.y. for 76535,15 and 76535,75 are suggested assuming an initial Pu-U ratio of 0.016 at 4.55 b.y. While this does not appear to be inconsistent with the radiometric data there is evidence that the fission effects, at least at the lower temperatures,are not due to in situ decay and are most likely attributed to xenon redistribution, either on a local or global scale. Considering the whole rock data for 76535,15 and 76535,75, it is also difficult to imagine conditions under which two samples of the same rock (separated by only 1 or 2 cm) could differ in xenon retention times by 200 m.y. or differ in initial plutonium content by a factor of eight (especially when there is no evidence for a variable uranium content).

There is now substantial evidence that plutonium is geochemically coherent with the rare earth elements (4, 6). Association with the rare earth elements is fortunate in this type of analysis since ^{126}Xe from the spallation of rare earth targets becomes a natural tracer for xenon released from sites containing rare earth elements. If we have coherence and in situ decay of plutonium we should therefore observe a constant ratio between fission-produced ^{136}Xe and ^{126}Xe from rare earth spallation. Such correlation has been demonstrated in Angra dos Reis (9, 6) with a ratio of $^{136}Xe_f$ to $^{126}Xe_{REE}$ of about 8. Adjusting for the difference in cosmic ray produced ^{126}Xe, one would predict a ratio of about 2 for an object 4.55 billion years old with an exposure history similar to that of 76535. Note that (Table 2) the whole rock data of 76535,15 yields a ratio of 4.5, suggesting that it would predate ADOR by about 100 m.y. if the fission effects were indeed found to be coherent with the rare earths. In Table 2 we also show the total amounts of ^{126}Xe from spallation, the estimated contributions from the rare earths, and the quantities of fission-produced ^{136}Xe for each temperature fraction of 76535,75. Column 4 of the table shows that the ratios of rare earth spallation to fission xenon are not even approximately constant in the stepwise heating data (even allowing for possible variations in target abundance ratios). The low temperature fractions are dominated by fission effects, not accompanied by appreciable spallation xenon; the high temperature fractions are totally

Plutonium Fission Xenon in 76535

Hohenberg C. M. et al.

dominated by spallation. More than 25% of the fission xenon and less than 2% of the spallation xenon is released in the low temperature fractions. We conclude that fission in 76535 does not correlate with rare earth spallation or any volume-correlated component. As was the case for the gas rich breccias, the low temperature release of fission xenon in 76535 seems to require low activitation energies which suggest that it is probably similarly sited along intergranular boundaries.

	x 10^{-13}ccSTP/g [126]	[136]	124	126	128	129	130	131	134	136
76535,75	64.3	14.2	35.63 8	64.47 11	101.54 14	141.18 17	78.31 10	342.42 40	20.71 7	14.20 5
76535,15	65.9	83.0	24.76 16	44.50 35	69.61 23	95.14 38	51.53 26	234.92 77	55.53 20	56.11 23
76535,64[9] (< 90μ)	65.8	603.8	2.10 4	3.49 6	11.78 14	101.0 3	18.20 9	91.42 27	37.82 9	32.03 9
(-air)	(60)	(14)	(34)	(62)	(98)	(150)	(75)	(321)	(20)	(14)

Table 1. Isotopic Compositions of Xenon from 76535 (^{132}Xe ≡ 100). Values that appear in parentheses represent the data from 76535,64 for which xenon of atmospheric composition have been removed (78.8% of the observed ^{130}Xe).

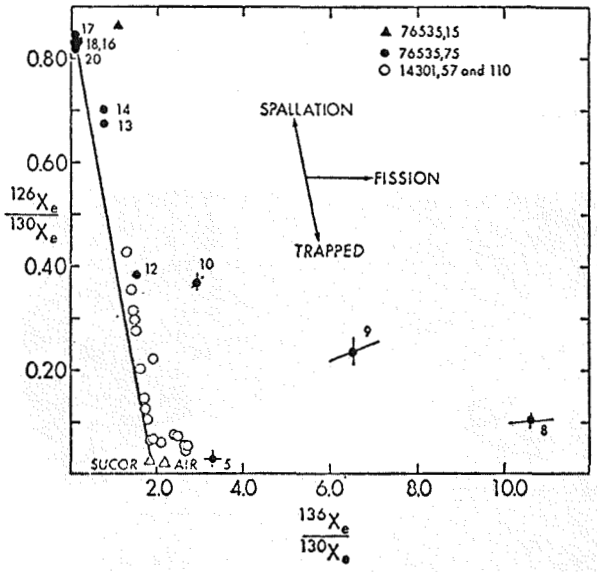

76535,75	(x 10^{-15} cc STP/g) $^{126}Xe_{sp}$	$^{126}Xe_{REE}$	$^{136}Xe_f$	$\frac{^{136}Xe_f}{^{126}Xe_{REE}}$
500	0.006	0.0015	2.1	1400
800	0.74	0.19	81.	426
900	0.84	0.22	20.	91
1000	3.0	0.77	15.6	20
1100	9.2	2.4	23.6	9.8
1200	16.4	4.2	22.9	5.5
1300	34.6	8.9	21 ± 2	2.4 ± .3
1400	66.7	17.1	44 ± 4	2.5 ± .3
1500	2965	762	464 ± 160	0.6 ± .2
1700	1271	326	113 ± 69	0.3 ± .2
1800	1931	496	104 ± 104	0.2 ± .2
2000	110	28	9 ± 6	0.3 ± .2
Total Rock	6408	1646	921 ± 344	0.6 ± .2
76535,15	6330	1614	7200	4.46

Table 2. $^{126}Xe_{REE}$ is the amount of ^{126}Xe from spallation of REE, estimated using whole rock abundances (33ppm Ba and 11.7ppm La (5)) and a production rate of 5 for REE (norm. to La) relative to Ba (6).

(1) Behrman C. J. et al. (1973) Earth Planet. Sci. Lett. 17, 446. (2) Bernatowicz T. J. et al. (1978) Proc. Lunar Planet. Sci. Conf. 9th, p. 1571. (3) Bernatowicz T. J. et al. (1979) Proc. Lunar Planet. Sci. Conf. 10th (in press). (4) Boynton W. V. (1978) Earth Planet. Sci. Lett. 40, 63. (5) Haskin L. A. et al. (1974) Proc. Lunar Planet. Sci. Conf. 5th, p. 1213. (6) Hudson B. et al. (1979) Geochim. Cosmochim. Acta (submitted). (7) Husain L. and Schaeffer O. A. (1975) Geophys. Res. Lett. 2, 29. (8) Keith J. et al. (1974) Proc. Lunar Planet. Sci. Conf. 5th, p. 2121. (9) Lugmair G. W. et al. (1976) Proc. Lunar Planet. Sci. Conf. 7th, p. 2009. (10) Lugmair G. W. and Marti K. (1977) Earth Planet. Sci. Lett. 35, 273. (11) Neimeyer S. and Leich D. A. (1976) Proc. Lunar Planet. Sci. Conf. 7th, p. 587. (12) Papanastassiou D. A. and Wasserburg G. J. (1976) Proc. Lunar Planet. Sci. Conf. 7th, p. 2035. (13) Podosek F. A. et al. (1971) Earth Planet. Sci. Lett. 10, 194.

LUNAR MAGCONS: GROSS CORRELATION WITH AREAS OF SEISMIC MODIFICATION ASSOCIATED WITH MAJOR BASIN IMPACTS. L. L. Hood, Lunar and Planetary Laboratory, University of Arizona, Tucson, AZ 85721.

Schultz and Gault have argued that seismic effects from major basin impacts have played an important role in modifying the morphology of highland crustal terrains on the moon and Mercury (1). In particular, grooved and hilly terrains at the antipodes of the two youngest large lunar basins, Imbrium and Orientale, and at the antipode of the Caloris basin on Mercury were ascribed to this mechanism. In this paper, we discuss orbital geophysical and photogeologic evidence implying that compositional as well as morphological alteration has occurred in seismically modified highland regions located antipodal to the four youngest large lunar impact basins.

Indications of strong compositional anomalies in the Van de Graaff region (nearly antipodal to Imbrium; see Fig. 1) have come from analyses of orbital gamma ray, electron-reflectance, and magnetometer data [see the summary by Stuart-Alexander (2)]. The source(s) of the radioactivity anomaly have not been identified due in part to the inherent low resolution ($\sim 10^{\circ}$) of the measurements. Several patches of maria (which are normally more radioactive than the highlands) are present but the anomaly is primarily over highland terrain. Likewise, the sources of the magnetic anomalies in the Van de Graaff region have not yet been identified. Model-fitting techniques have been used to more accurately locate the surface positions of the major sources (3) but no correlation with major geologic units was found. The source locations are scattered randomly across the terrae (no coverage across the mare patches was available) and the visible surface units at these locations are diverse in origin and age although the grooved and hilly terrain is generally characteristic of the entire region.

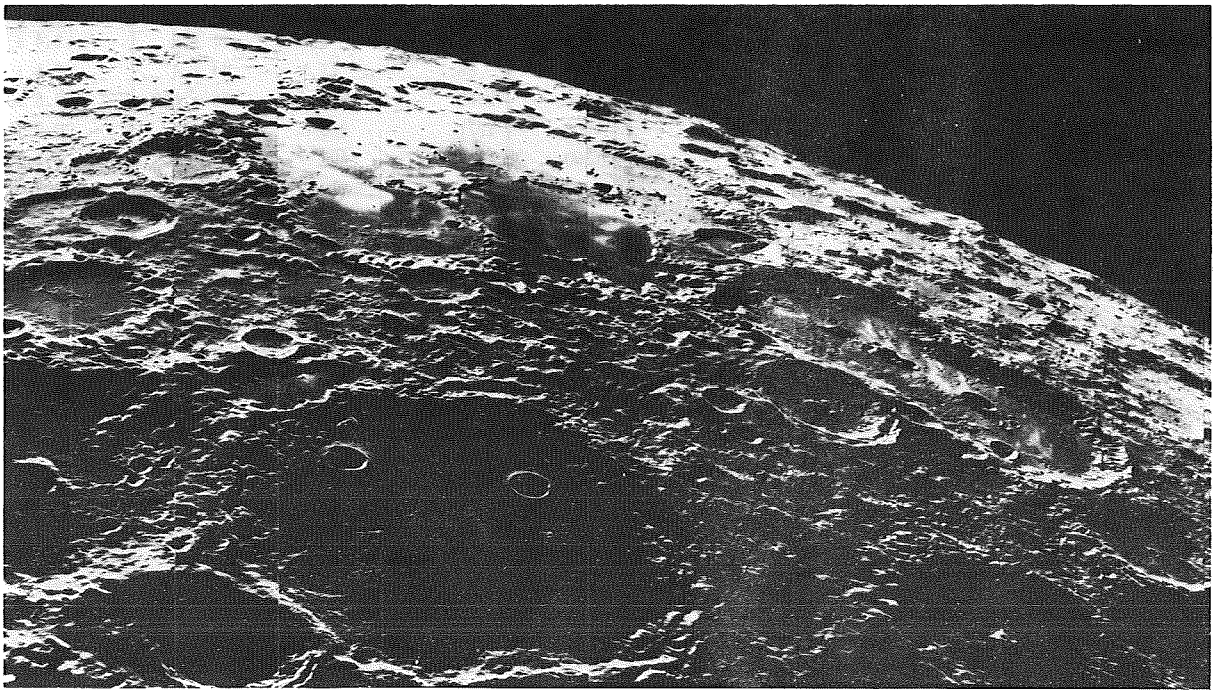

Fig. 1 Section of a Lunar Orbiter V photograph showing the region antipodal to the Imbrium basin. Mare Ingenii is at top center; the double crater Van de Graaff is at right center. Note the unusual terrain and the light-colored swirls of the Reiner Gamma Formation.

LUNAR MAGCONS: GROSS CORRELATION WITH AREAS OF SEISMIC MODIFICATION

Hood, L.L.

Further insight into the identity of the magnetic field anomaly sources (and possibly the radioactivity sources as well) in the Van de Graaff region has come from more recent mapping of vector magnetometer measurements over the nearside maria (4). A single strong anomaly [amplitude >20γ ($1\gamma=10^{-5}G=10^{-9}nT$) at ∿20 km altitude] was detected coincident with an unusual light-colored marking on western Oceanus Procellarum known as Reiner Gamma (5) (Fig. 2). It has been speculated that Reiner Gamma is composed of unusually magnetic deposits of secondary crater ejecta associated with the large nearby 3.2±0.2 b.y. old crater Cavalerius (6). This interpretation is consistent with studies of returned samples which have shown that the strongest magnetization levels are present in certain classes of impact-generated breccias (7).

Light-colored, swirl-like surface features similar to Reiner Gamma exist in quantity throughout the Mare Ingenii-Van de Graaff crater region (Fig. 1). These features were first noticed by El-Baz (8) and were subsequently classified geologically as members of the "Reiner Gamma Formation" [see the summary by Schultz (9)]. As seen in Fig. 1, the Ingenii-Van de Graaff swirls are most easily discernible against a background of relatively dark mare basalt. The same markings, if present in the terrae, are partly obscured by the complexity and higher albedo of the underlying terrain. In view of the correlation of Fig. 2, which was obtained under optimal conditions, it is probable that Reiner Gamma-like deposits near Van de Graaff are closely associated, if not identical with the magnetic field sources of the region.

Additional swirl-like albedo features, also classified as members of the Reiner Gamma Formation, occur in a prominent belt across and north of Mare Marginis, roughly antipodal to the Orientale Basin (8,9) (Fig. 3). Although the electron-reflectance map is characterized by extremely low resolution, it may be significant that the two remaining prominent maxima are in the Apollo/Oppenheimer region (antipodal to Serenitatis) and in a diffuse area near the crater Gerasimovic (antipodal to Crisium)(R.P. Lin, pers. comm., 1979).

In summary, there is a tendency for the largest concentrations of lunar magnetic anomalies to occur in areas antipodal to the major lunar basins, marked by seismically modified terrain and Reiner Gamma-like surface features. The likely presence of compositional (specifically free

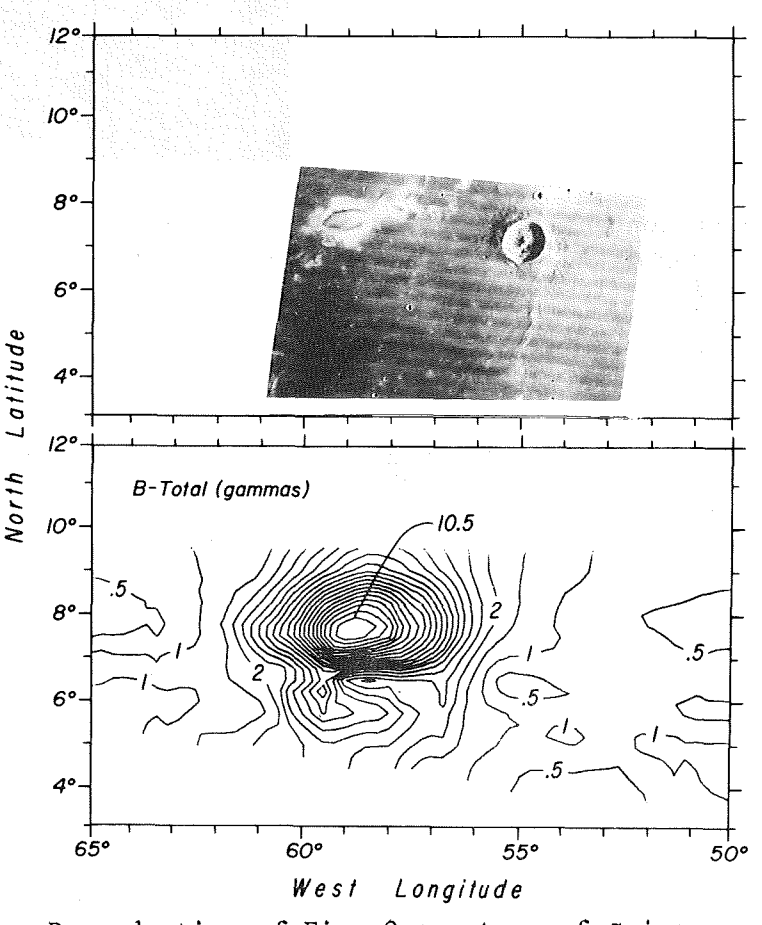

Fig. 2 Correlation of a large magnetic field maximum detected by the Apollo 16 subsatellite magnetometer with an unusual light-colored marking on western Oceanus Procellarum known as Reiner Gamma (5).

Reproduction of Fig. 2 courtesy of *Science*

LUNAR MAGCONS: GROSS CORRELATION WITH AREAS OF SEISMIC MODIFICATION

Hood, L.L.

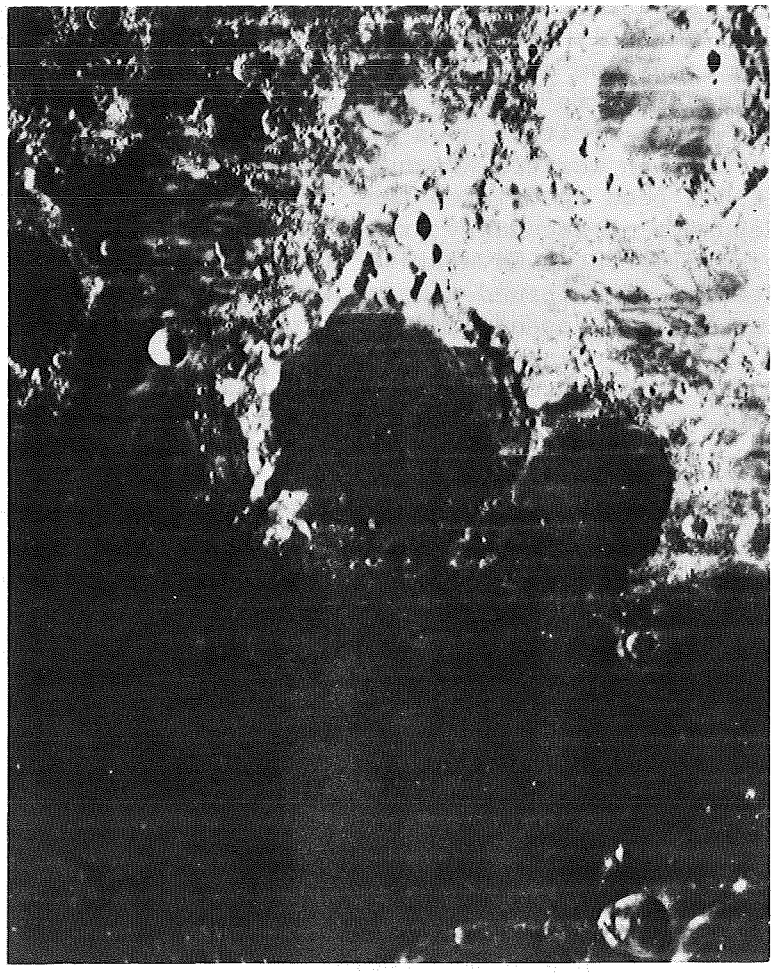

Fig. 3 Section of Lunar Orbiter IV frame 17 showing part of the region antipodal to the Orientale basin. The flooded crater at center is Goddard. Light-colored swirls of the Reiner Gamma Formation are visible across the top of the photograph (8).

iron content) alteration in these areas implied by the magnetic anomaly data is supported by the existence of a radioactivity anomaly in the Van de Graaff region. The sources of the magnetic anomalies may be unusually magnetic deposits of secondary crater ejecta generated by subsequent impacts on the seismically modified crustal terrain. (1) Schultz P.H. and Gault D.E. (1975) The Moon 12, p. 159-177. (2) Stuart-Alexander D.E. (1978) U.S. Geol. Survey Map I-1047. (3) Hood L.L., Russell, C.T., Coleman P.J., Jr. (1978) Proc. Lunar Planet. Sci. Conf. 9th, p. 3057-3078. (4) Hood L.L. (1978) EOS Trans. Amer. Geophys. Union 59(12), p. 1122. (5) Hood L.L., Coleman P.J., Jr., Wilhelms D.E. (1979) Science 204, p. 53-57. (6) Hood L.L., Coleman P.J., Jr., Wilhelms D.E. (1979) Proc. Lunar Planet. Sci. Conf. 10th, in press. (7) Strangway D.W. et al. (1973) Nature 246, p. 112-114. (8) El-Baz F. (1972) Apollo 16 Prelim. Sci. Rep., p. 29:93-29:97. (9) Schultz P.H. (1976) Moon Morphology (Univ. of Texas Press, Austin), p. 420-423. (10) Frontispiece (1977) Proc. Lunar Sci. Conf. 8th, Vol. 1.

"BUNTE BRECCIA" OF THE RIES CRATER: IMPLICATIONS FOR THE LATERAL AND VERTICAL REDISTRIBUTION OF LARGE SCALE CRATER EJECTA: F. Hörz, NASA Johnson Space Center, Houston, TX 77058, R. Ostertag, Univ. of Münster, Germany and D. A. Rainey, LEC, Houston, TX 77058

The continuous deposits of the 26 km diameter Ries Crater were investigated via a shallow drilling program: a field report (1), clast population studies (2), the distribution of shock metamorphic grades (3), and detailed description of a single core (4) were reported earlier. We now report on grain size analyses and heavy mineral contents of all core materials (≈520 running m of 4" diameter cores taken at 9 different locations) in an attempt to supplement the macroscopic descriptions (1, 2) with a detailed description of the matrix (4). Material of <1 cm grain size was defined as "matrix" (1); 300 samples of ≈300 g each, representing macroscopically different matrix types, were sieved into 7 different grain size fractions; heavy minerals (>2.85 g/cc) were separated from the 125-250 μm fraction and heavy mineral population data are based on typically ≈300-400 grains. Lithologic-stratigraphic assignments and sizes of ≈18,000 clasts >1 cm (= "macroscopic" observations, 2) as well as "microscopic" data (≈300 sieve analyses and 300 heavy mineral populations) were computer formatted for ease of data reduction. All parameters were then plotted for individual cores as a function of core depth or other suitable formats. Due to space limitations, however, only average results can be illustrated in this report.

Because of the well documented pre-impact stratigraphy and general geologic setting (e.g., 1, 5), it is possible to assign specific stratigraphic sources to most clast- and matrix-materials and thus to distinguish between excavated crater materials and those from the "local" environs. Major results of the lithologic-stratigraphic characterization are illustrated in Fig. 1. Assuming a maximum depth of H = 2.0 km for excavation and a transient cavity radius r ≈5 km (5, 6), the following results emerge: all materials derived from depths ≳.3H (≳600 m) comprise generally less than .1% of the total continuous deposits over a radial range of ≈2 to 7 r, measured from the rim of the transient cavity; materials from ≳.2H (≳400 m) comprise typically .5 to 1% and those ≳.1H (≳200 m) make-up some .1-5%. Materials originating from the upper 10% of the entire stratigraphic section are typically present in the 10-20% weight range. Tertiary clasts derived from outside the transient cavity (= "local") comprise some 15-50% of the entire deposit. No systematic trends in vertical profile regarding the distribution of these clast-materials were observed: "local" or "crater" materials may be evenly distributed and/or concentrated at random depths; an inverted stratigraphy of "local" materials only was observed in core 2 (4).

The matrix is composed predominantly of "local" Tertiary components as revealed by heavy mineral studies and grain size data as well as macroscopic field criteria; however it is extremely difficult to determine the mixing ratio of Tertiary fresh water sediments (OMM) and marine deposits (OSM) based even on the most diagnostic indicator, i.e., the garnet/epidote ratio (G/E) as illustrated in Fig. 2: "Pure" Tertiary data were obtained from monomict OMM and OSM megaclasts typically >1 m in dimensions. G/E for OMM is typically <2, however G/E for OSM is highly variable, depending on the depositional environment. Nevertheless the data indicate that in most cases the matrix is indeed a mixture of the two Tertiary units, the best example being core 2. However in every core one may find specific matrix sections that are almost entirely composed of either OSM or OMM materials. These data lend additional support to the prior conclusions (1) that individual matrix sections are indeed reflecting distinct, localized source regions and individual brecciation-, mixing- and transportation histories. The entire deposit may be envisioned as an

"BUNTE BRECCIA" OF THE RIES CRATER

F. Hörz et al.

irregular mixture of two different megaclast types, typically a few m. in dimension (although smaller and larger ones (>10 m) may also occur): (a) monolithic clasts derived from the crater and local sources (these clasts may either be undeformed, moderately deformed, or completely brecciated: i.e., monomict breccias) and (2) polymict breccias of highly variable clast populations and matrix compositions, the latter, however, almost exclusively (>90%) derived from local sources.

Figure 3 illustrates detailed grain-size distributions averaged for each individual core. Monolithic megaclasts (>128 cm) comprise ≈30% of the deposit between ≈2 and 5 r, although clasts >5 m are known from field studies (7) to occur commonly out to ≈8 r. The 1-128 cm fraction makes up some 20-30%. The <1 cm fraction (= "matrix") tends to increase with radial distance. The somewhat irregular patterns of grain-size distribution are interpreted as localized (= random) phenomena and - together with other field evidence - there is no compelling reason to ascribe the "coarse" cores 2, 11 and 6 to effects of cratering mechanics and/or mechanisms of ejecta deposition (e.g., 8). The Bunte Breccia is "poorly" sorted, especially if individual grain-size analyses are plotted as a function of core depth; no evidence for aerodynamic sorting was observed in the "Bunte Breccia" which comprises ≈90% of all Ries deposits.

These observations are consistent with ballistic ejection of primary crater ejecta triggering a secondary cratering regime that results in a ground hugging debris surge of combined primary and secondary ejecta (9, 10, 1). Indeed the main feature of this hypothesis, i.e., the admixture of local components into the continuous crater deposits is amply verified: according to Fig. 1 approximately 60-85% of the entire deposit are locally derived. The evidence reported by (11) in support of a purely nonballistic transport mechanism is entirely consistent with the above "secondary" debris surge. Furthermore these core studies also indicate, unfortunately, our limitated understanding of cratering mechanics especially in relating sample provenance to target stratigraphy; it appears that secondary cratering and the ensuing debris surge during large scale impacts thoroughly mask and distort the systematics conventionally expected from an "orderly" ejection sequence.

References:

(1) Hörz, F. et al. (1977) Impact and Explosion Cratering," Pergamon Press, p. 425-448.
(2) Hörz, F. and Oberbeck, V. R. (1978) 9th L.P.C., Abstracts, p. 543-545.
(3) Banholzer, G. and Hörz, F. (1979) 10th L.P.C., Abstracts, p. 63-65.
(4) Ostertag, R. and Stöffler (1978) 8th L.P.C., Abstracts, p. 844-846.
(5) Pohl, J. et al. (1977) "Impact and Explosion Cratering," Pergamon Press, p. 343-404.
(6) Hörz, F. and Ostertag, R. (1979) 10th L.P.C., Abstracts, p. 570-572.
(7) Gall, H. et al. (1975) Geologische Rundschau, 64, p. 915-947.
(8) Schultz, P. and Gault, D. E. (1979) Jour. Geophys. Res. 79 (in print)
(9) Oberbeck, V. R. (1975) Rev. Geophys. Space Phys. 13, 337-362.
(10) Morrison, R. H. and Oberbeck, V. R. (1978) Proc. L.P.C. 9th, p. 3763-3785.
(11) Chao, E.C.T. and Minkin, J. A. (1977) "Impact and Explosion Cratering," Pergamon Press, p. 405-424.

"BUNTE BRECCIA" OF THE RIES CRATER

F. Hörz et al.

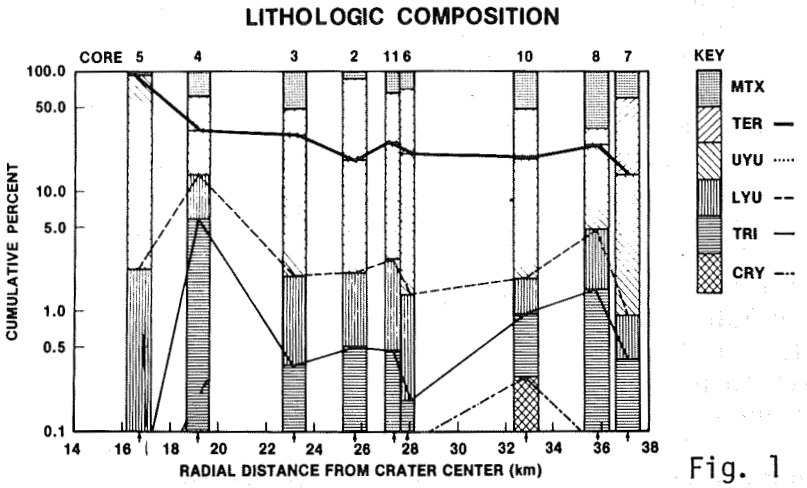

Fig. 1

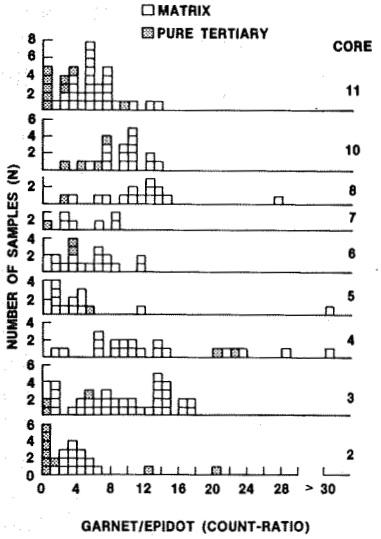

Fig. 2

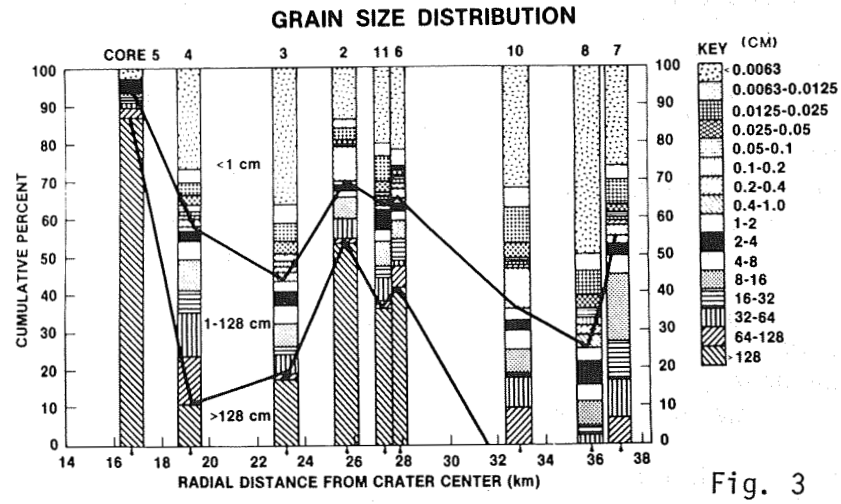

Fig. 3

Fig. 1: Average lithological composition of 9 Bunte Breccia drill cores (MTX = matrix; <1 cm, predominantly of "local" origin); TER = Tertiary (= local); UYU = upper Jurassic, LYU = lower and middle Jurassic; TRI = Triassic; CRY = crystalline basement); heavy, solid line separates breccia components of "local" versus crater derived sources.

Fig. 2: Garnet/Epidot ratios of breccia matrix and pure Tertiary megaclasts.

Fig. 3: Detailed grain size distributions of "Bunte Breccia" cores. Note irregularities due to localized conditions as well as a weak trend towards generally more fine-grained deposits with increasing range.

ON THE EARLY GLOBAL MELTING OF THE TERRESTRIAL PLANETS. Charles J. Hostetler and Michael J. Drake, Department of Planetary Sciences and Lunar and Planetary Laboratory, University of Arizona, Tucson, AZ 85721.

In order to decipher the crustal records of the terrestrial planets we must investigate their early thermal histories. The first order question, which we address in this work, is the possibility of magma oceans, analogous to the lunar magma ocean, on other terrestrial planets. We introduce a heating model linked to a chronology of the early solar system in order to examine the relative heating of the terrestrial planets.

We consider seven factors which possibly affected the early heating of the terrestrial planets: 1) Solar luminosity of 10^3 to 10^4 times that of the present during a Hyashi phase of the sun, 2) electromagnetic induction during a T-Tauri phase of the sun, 3) adiabatic compression of nebular gases onto the surfaces of accreting planets, 4) accretion, 5) short-lived radioactivities, 6) tidal stresses, and 7) loss of heat acquired by the first six mechanisms (the thermal "output function"). The parameters influencing these seven factors are listed in Table 1, and their approximate relative values for the terrestrial planets are listed in Table 2. We have cast the seven factors in terms of thermal input (or output) per unit mass.

We now consider these heating mechanisms in a chronological context. From theoretical studies of the formation of solar mass stars, the time during which enhanced solar luminosity may have been operative is believed to be short, probably not longer than 10^4 years after star formation. The major heat producing short-lived radionuclide, Al^{26}, also must have operated early as its half life is about 7×10^5 years. The complete chronology is shown in Figure 1; space does not permit further elaboration. Note that adiabatic compression of nebular gases and electromagnetic induction cannot operate simultaneously because a thick atmosphere or an ionosphere will short out the currents generated by induction.

From Figure 1 it becomes apparent that there are seven different time windows during which a terrestrial planet may attain its final mass. Given that adiabatic compression and electromagnetic induction cannot operate simultaneously, the number of possible combinations of heating mechanisms is eleven. The primed model numbers in Figure 1 indicate models in which inductions operates, the unprimed model numbers indicate models in which adiabatic compression operates. We have provided for varying the relative importance of each heating mechanism as we lack a priori knowledge of their relative contributions.

It is useful to choose a planet which we believe went through a global melting event as a comparison standard. In the models presented here, we have chosen the Moon, making the assumption that it accreted in a heliocentric orbit of radius 1 A.U. Our uncertainty concerning the origin of the Moon is accounted for by also considering additional possible modes of origin. We consider lunar bodies which formed independently of the Earth in heliocentric orbits of 2.0 and 0.4 A.U. and were subsequently captured by the Earth. We treat the fission hypothesis by scaling the Earth to the Moon, i.e., the Earth must have melted in order to boil off its outer layer. We cannot treat the multiple or disintegrative capture hypothesis by this method, our only information being that a large number of small bodies differentiated relatively early.

Table 3 contains the results for those models in which not all of the terrestrial planets melted, along with the assumed relative importance of each heating mechanism. Note that in models 4, 3, 3', 2, and 1 all bodies received at least as much heat per unit mass as did the lunar comparison

GLOBAL MELTING OF TERRESTRIAL PLANETS

Hostetler, C.J. and Drake, M.J.

standard and, we conclude, would have experienced magma ocean events. These models occur relatively early in our schematic chronology. The survival of undifferentiated material as represented by the chondrites could be viewed as evidence against a large contribution of heat from solar luminosity or short-lived radioactivities, assuming that the chondrites did not form substantially later than the Moon. We note also that the Earth and Venus received as much thermal input as the lunar comparison standard in all models except 7, 6, and 6'. More definitive conclusions may be drawn if a better estimate of the time at which each planetary object reached its present radius is obtained, or if the relative importance of each heating mechanism can be better constrained.

Supported by NASA grant NSG 7576.

Table 1

Thermal mechanisms and their principal controlling parameters

	Mechanism	Parameters	Comments
1.	output function	$1/R^2$	1/R due to surface/volume effect, 1/R to retention of atmosphere
2.	solar luminosity	$1/r^2R$	1/R due to surface/volume effect, $1/r^2$ inverse square law
3.	Al^{26}	1	assumption
4.	adiabatic compression	ρ	1/R surface/volume, R_ρ due to escape velocity
5.	tidal stress		1/81 for earth, 1 for moon, all others 0
6.	accretion	R^4	accretional cross-section
7.	induction		important only for small bodies

R = radius of body
r = heliocentric radius of orbit
ρ = density

Table 2

Numerical values of thermal mechanisms for the terrestrial planets

Mechanism	Mercury	Venus	Earth	M1*	M2*	M3*	Mars
1	0.5	0.08	0.07	1.0	1.0	1.0	0.26
2	4.7	0.55	0.27	1.0	6.3	0.25	0.22
3	1.0	1.0	1.0	1.0	1.0	1.0	1.0
4	1.3	1.3	1.3	1.0	1.0	1.0	1.1
5	0	0	0.01	1.0	1.0	1.0	0
6	2.8	42.0	49.0	1.0	1.0	1.0	7.4
7	0	0	0	1.0	2.0	0.25	0

*M1 = moon at 1 A.U.
M2 = moon at 2 A.U.
M3 = moon at 0.4 A.U.
see text

GLOBAL MELTING OF TERRESTRIAL PLANETS

Hostetler, C.J. and Drake, M.J.

Table 3

Results of thermal calculations for the terrestrial planets

Model Number	Mercury	Venus	Earth	Moon1	Moon2	Moon3	Mars	Relative Importance of Heating Mechanism 4	5	6	7
7	*	*	*	Y	Y	Y	*	-	1	-	-
6 a	Y	Y	Y	Y	Y	Y	Y	1	10	-	-
b	*	*	*	Y	Y	Y	*	10	1	-	-
c	?	?	?	Y	Y	Y	?	1	1	-	-
6'a	*	*	*	Y	Y	*	*	-	1	-	10
b	*	*	*	Y	Y	Y	*	-	10	-	1
c	*	*	*	Y	?	?	*	-	1	-	1
5 a	Y	Y	Y	Y	Y	?	Y	-	1	1	1
b	*	Y	Y	Y	Y	Y	?	-	10	1	1
c	?	Y	Y	Y	Y	*	?	-	1	1	10
d	Y	Y	Y	Y	Y	Y	Y	-	1	10	1
e	*	Y	Y	Y	Y	?	*	-	10	1	10
f	Y	Y	Y	Y	Y	Y	Y	-	10	10	1
g	Y	Y	Y	Y	Y	?	Y	-	1	10	10
5'a	Y	Y	Y	Y	Y	Y	Y	1	1	1	-
b	*	Y	Y	Y	Y	Y	?	1	10	1	-
c	Y	Y	Y	Y	Y	Y	Y	10	1	1	-
d	Y	Y	Y	Y	Y	Y	Y	1	1	10	-
e	?	Y	Y	Y	Y	Y	?	10	10	1	-
f	Y	Y	Y	Y	Y	Y	Y	1	10	10	-
g	Y	Y	Y	Y	Y	Y	Y	10	1	10	-
4'a	?	Y	Y	Y	Y	*	*	-	-	1	10
b	Y	Y	Y	Y	Y	Y	Y	-	-	10	1
c	Y	Y	Y	Y	Y	*	Y	-	-	1	1

Y = received as much or greater thermal energy as comparison body.
? = received from 0.6 to 1.0 times as much thermal energy as comparison body.
* = received less than 0.6 times as much thermal energy as comparison body.
- = mechanism did not operate in this model.

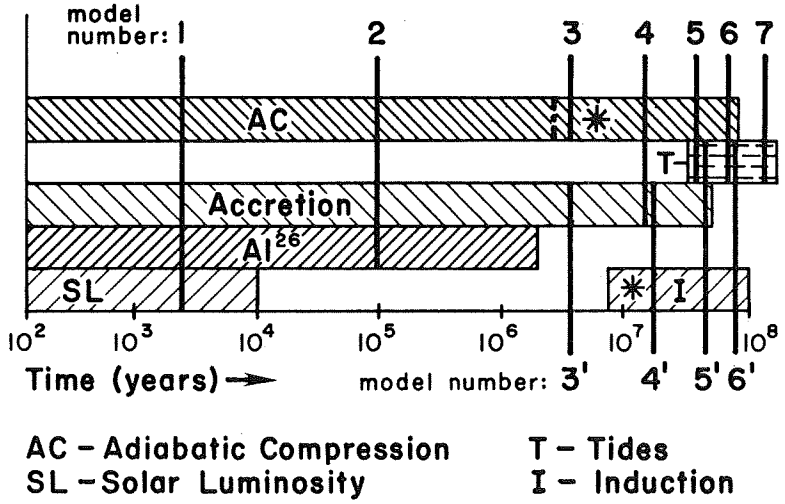

*both mechanisms cannot operate simultaneously - see text.

Fig. 1. Chronology for early thermal history of the terrestrial planets. Model numbers indicate discrete time windows during which the terrestrial planets may have attained their present sizes. The heating mechanisms intersected by a model line are operative in that model.

REGIONAL CHEMICAL VARIATIONS IN THE LUNAR CRUST: Norman Hubbard, NASA Johnson Space Center, Houston, TX 77058

It seems highly probable that the early planetary differentiation that produced the anorthositic and related terra materials of the lunar highlands and non-mare areas profoundly influenced the conditions under which subsequent basaltic volcanism developed. From this viewpoint, regional chemical studies of mare volcanism can be used to delineate some of the major chemical features produced at depth by early lunar differentiation, thereby broading our sketchy view of this early event. Two major variables for basaltic volcanism, strength of the heat source and bulk chemical composition of the source region were very probably fixed by early differentiation. Information about these two variables can be obtained using chemical data from the orbital x-ray and gamma ray experiments. Only the chemical data from these experiments have the specificity and areal coverage suitable for such studies. Equally important, these data can be directly combined with lunar sample chemical data, once errors in the orbital data are understood. Some information has already been published about regional chemical variations. The terra areas east of Smythii have lower Mg/Si ratios, for similar Al/Si ratios, than the terra areas west of Smythii, which suggests (1) that Smythii is located at the approximate eastern boundary between frontside and farside petrogenetic provinces. The central highlands have much higher Th concentrations than do other terra areas (2, 3), indicating that they are not a typical highland area. Metzger et al. (3) show that for other terra areas there is a good correlation between Th concentration and surface elevation and conclude that this correlation is a direct consequence of the early differentiation. Hubbard (1) demonstrates that mare surfaces are not seriously contaminated by impact transported terra materials and concludes that for maria the increase in Al_2O_3 concentrations and decrease in Th concentrations toward the east for the maria in the Imbrium-Smythii area (Fig. 1) must reflect parameters of magma generation and that these data are evidence for regional chemical gradients in the source regions of the mare basalts that flooded the surfaces of these maria. However, most of our best studied samples of mare lavas (common Apollo mare basalts in Fig.1) deviate from this well developed relationship and it is not known if these compositions are as abundant as those sampled by the orbital experiments. Additional evidence is found when FeO and Al_2O_3 data are compared for maria and mare basalts (Fig. 2). The most revealing feature of this graph is the way the tie lines between mare basalt types at a single site parallel the overall Al_2O_3 vs. FeO variation and the lines showing the effect of removing 10% of terra material from the orbital data points for Mare Crisium and Mare Serenitatis. The observation that mare basalts with similar Al_2O_3 concentrations have widely different Th concentrations but, that the FeO concentrations are much more related to the Al_2O_3 values, is probably due to the fact that the distribution of incompatible trace elements is heavily controlled by different factors than is the distribution of major elements. The Al_2O_3 vs. Th and FeO vs. Al_2O_3 correlations can be viewed as mixing between an anorthositic composition and a mare composition, such as that of the Apollo 11 high K mare basalts. Because this cannot be caused by mixing on the lunar surface (1), it must have been produced during magma generation. The immediate implication is that there existed a regional scale lateral variation in plagioclase and trace element concentrations in the source regions of mare magmas. These and additional remote sensing and lunar sample data have been combined (1) to support the scenario shown in Fig. 3. The essence of this scenario is that the equatorial belt of the moon has a major lateral chemical heterogeneity and that the most important aspect of this heterogeneity is the concentration of heat producing elements (K, U, Th) in the lunar frontside.

REGIONAL CHEMICAL VARIATIONS IN THE LUNAR CRUST

Norman Hubbard

As recognized by Soderblom et al. (4), increased concentrations of heat producing elements will increase the time available for igneous differentiation (this assumes that there is an adequate supply of material that can yield

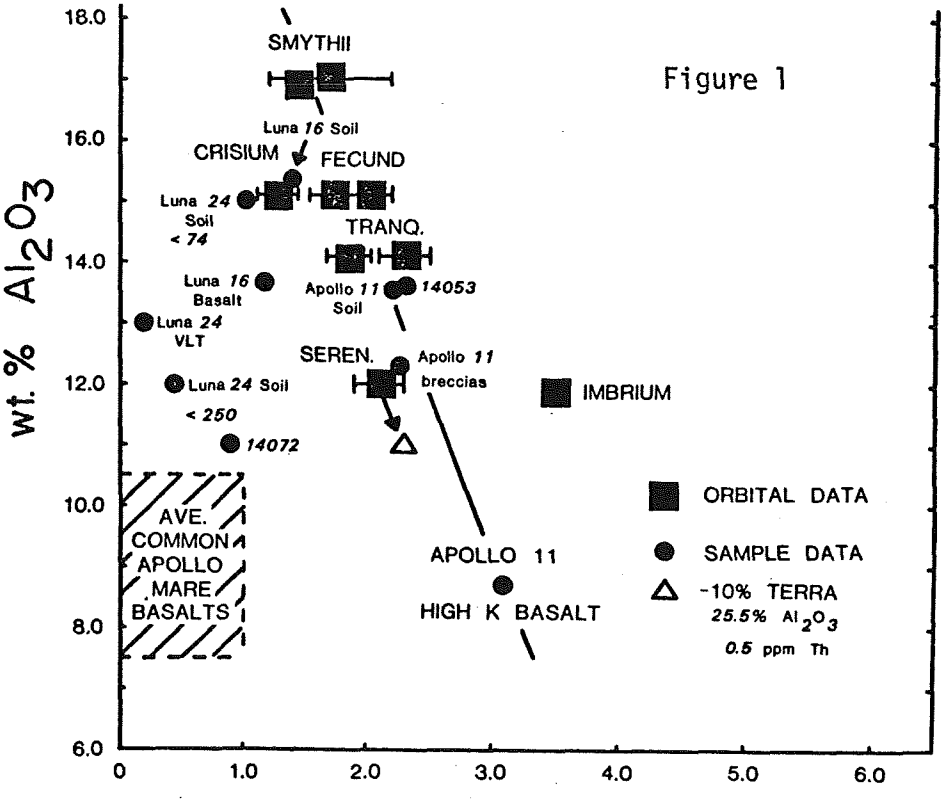

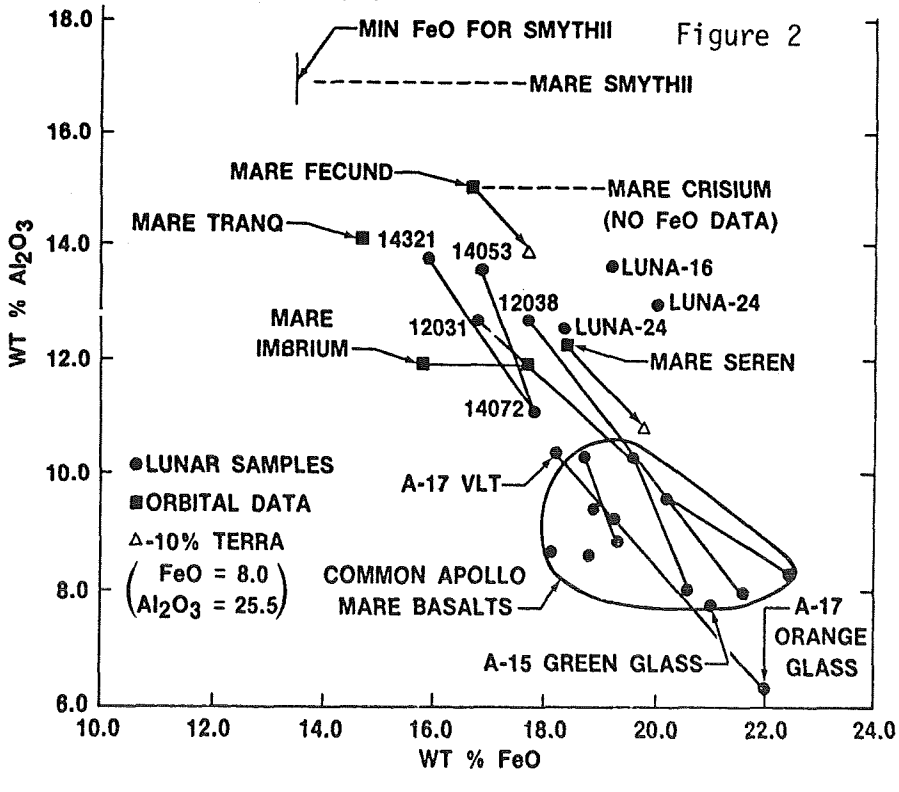

Norman Hubbard

magma). The effect of this was calculated by Hubbard and Minear (5), who show that U(K, Th) concentrations well below those inferred from combining thermal equilibrium models with lunar heat flow data appear to be adequate to support basaltic volcanism on the moon and that initial U concentrations less than about 10 ppb appear to be inadequate. This major lateral heterogeneity in heat producing elements must have been directly related to, perhaps caused by or present during the early differentiation and therefore can be expected to have influenced the differentiation of the later terra compositions as well as mare compositions. Because the moon appears to have differentiated in a monotonically cooling environment (5, and numerous others), the distinction between a stage of differentiation that produced terra compositions and one that produced mare compositions is arbitrary. From this scenario it can also be anticipated that many of the terra samples collected by Apollo are the products of a longer lived and more rigerous differentiation than that which occurred on the lunar farside.

References:
(1) Hubbard N. (1979) Proc. Lunar Planet. Sci. Conf. 10th, in press.
(2) Hubbard N. and Woloszyn D. (1977) Phy. Earth Planet. Inter., 15, p. 287-302.
(3) Metzger A. E., Haines E. L., Parker R. E., and Radocinski (1977) Proc. Lunar Sci. Conf. 8th, p. 949-999.
(4) Soderblom L. A., Arnold J. R., Boyce J. M., and Lin R. P. (1977) Proc. Lunar Sci. Conf. 8th, p. 1191-1199.
(5) Hubbard N. J. and Minear J. W. (1976) Proc. Lunar Sci. Conf. 7th, 3421-3435.

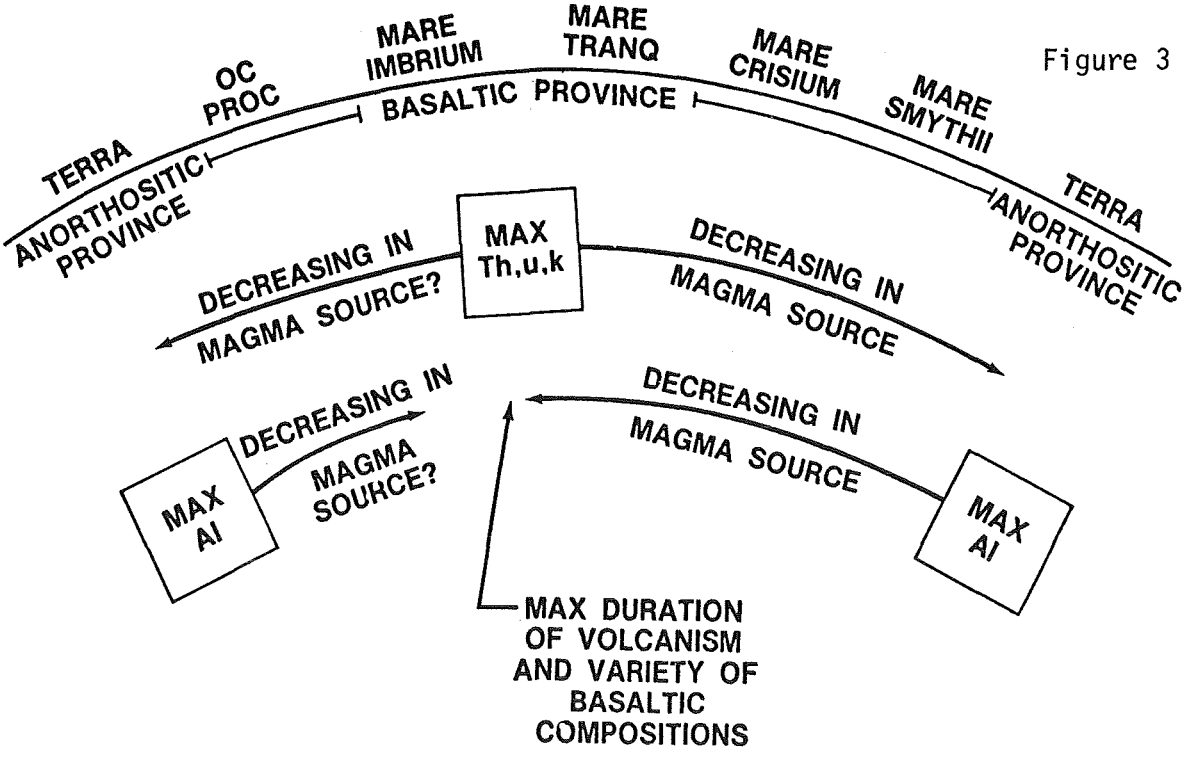

Figure 3

LABORATORY VERIFICATION OF THE LUNAR ORBITAL X-RAY FLUORESCENCE EXPERIMENT--PRELIMINARY RESULTS: Norman Hubbard, NASA Johnson Space Center, Houston, TX 77058 and Bi-Shia King, USGS, Menlo Park, CA 94025

The major recent uncertainty in using orbital x-ray fluorescence data for geochemical studies has been the errors associated with the conversion of Al/Si and Mg/Si intensity ratios at Al_2O_3 and MgO concentrations (1). Attempts to use lunar sample data to calibrate the orbital data have been made (2, 3, 1) but are very unsatisfying because of the assumptions and extrapolations required. Theoretical calculations are no more satisfying because modeling the physical condition of the lunar surface and its effect on the intensity ratios measured is difficult. The original conversion of intensity ratios to concentration ratios was made using theoretical calculations (4) but, little information is given such that the calculations can be reviewed in the light of current lunar knowledge. Specifically, no information is given about the effects of variations in particle size or other physical effects or the expected degree of linearity over the wide range of chemical compositions known from Apollo 11 through 16 for typical lunar soils. As a partial remedy to this situation, we have completed the preliminary analyses of an experiment that assesses the degree of linearity between Al/Si and Mg/Si intensity ratios and Al_2O_3/SiO_2 and MgO/SiO_2 concentration ratios for a wide range of chemical compositions. Variations in particle size and other physical parameters of lunar soils are investigated by the use of soils having a wide range of maturities. These loose soil samples were placed in a commercial x-ray fluorescence spectrometer (KEVEX 0700) and irradiated sequentially under vacuum with the K-series x-rays of Ti, Ca and S and the continuum radiation from a Rh tube operated at 3.0 KV. These x-ray energies were choosen to simulate the solar x-ray flux over a wide range of solar activities because they have penetration depths similar to those of solar x-rays. Penetration depth is the presumed parameter of major importance if lunar soil grains have a thin surface coating that is an important influence on the x-ray fluorescence of Si, Al and Mg. The samples rested on a thin organic film (<4 microns) that allowed high transmission of Si, Al and Mg x-rays. Between runs the samples were shaken in their sample cups to expose new material to the x-ray beam. A few samples were run in duplicate.

The preliminary data are shown in Fig. 1, 2 and 3. X-rays from S have a penetration depth similar to that for the effective excitation energy of solar x-rays during periods of "quiet" sun, such as was common during Apollo 15 and 16. Fig. 1 shows that for excitation by S x-rays a well defined relationship exists between the intensity and concentration ratios (5) for lunar soils and that the soils of basaltic and anorthositic composition are colinear. Terrestrial rocks and lunar sample 74220 form a different line: 74220 is not a typical lunar soil. Increasing the energy of the incident x-radiation to Ti simulates a more "active" sun and results in a colinear plot for lunar soils and terrestrial rocks (not shown). Fig. 2 shows an error analysis of the data in Fig. 1 and the effects of variations in soil maturity on the data. For the error analysis in Fig. 2 the intercept in Fig. 1 is shifted to 0.0 by subtracting the intercept on the intensity ratio axis from the measured intensity ratios. The concentration ratio has been ratioed to the shifted intensity ratio and plotted against the best available measure of soil maturity (I_s/FeO, 6). A 2 sigma error bar of $\pm$ 4.0% is shown for multiple measurements on one sample. For all samples except 74220, which plots at about 2.7 on the vertical axis, the scatter on the concentration/intensity ratios has a 2 sigma of $\pm$ 9.4%. Because areas sampled by the orbital XRF are very largely mature soils, we computed the scatter for samples that have I_s/FeO greater than 40, which gives a 2 sigma of $\pm$ 6.6%.

LABORATORY VERIFICATION--PRELIMINARY RESULTS

Norman Hubbard and Bi-Shia King

Results for Mg are shown in Fig. 3, where it is seen that data for all lunar soils form a single line and that data for terrestrial rocks form a quite different line. Data for terrestrial rocks do not become colinear with the lunar soils over the range of incident wavelengths investigated: only the intersection of the two lines shifts. An error analysis like that shown in Fig. 2 gives 14.5% 2 sigma for the scatter of these data and no relationship to soil maturity is seen.

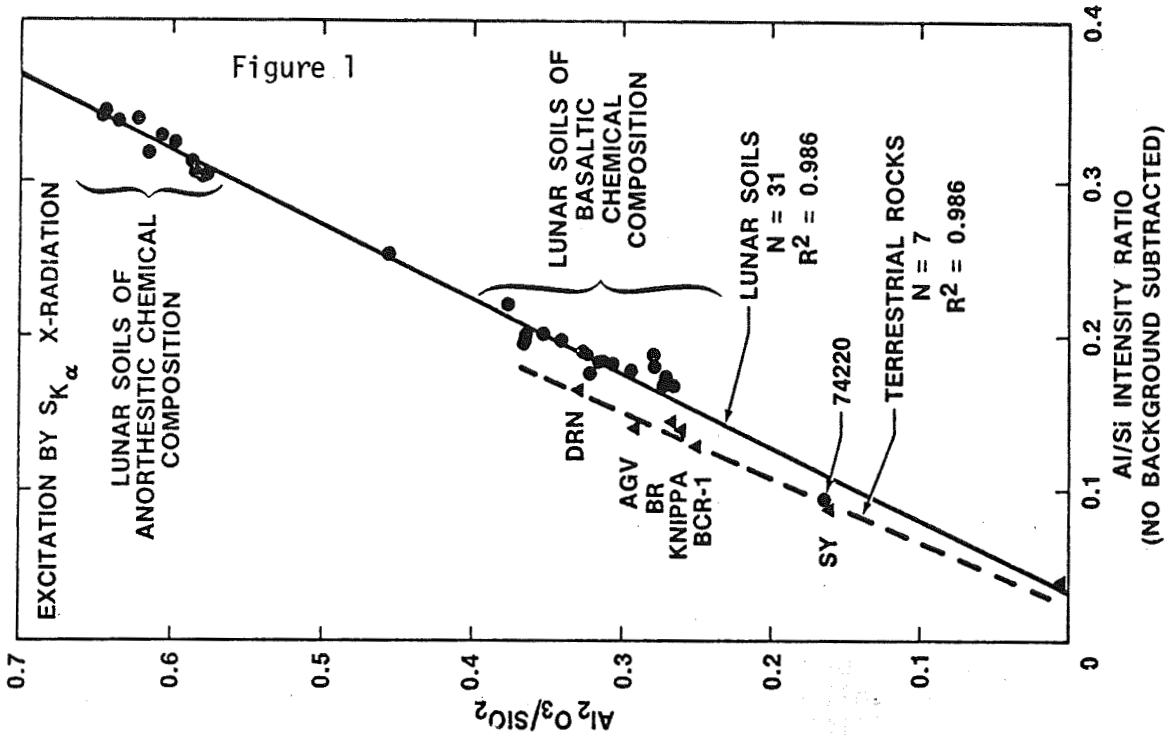

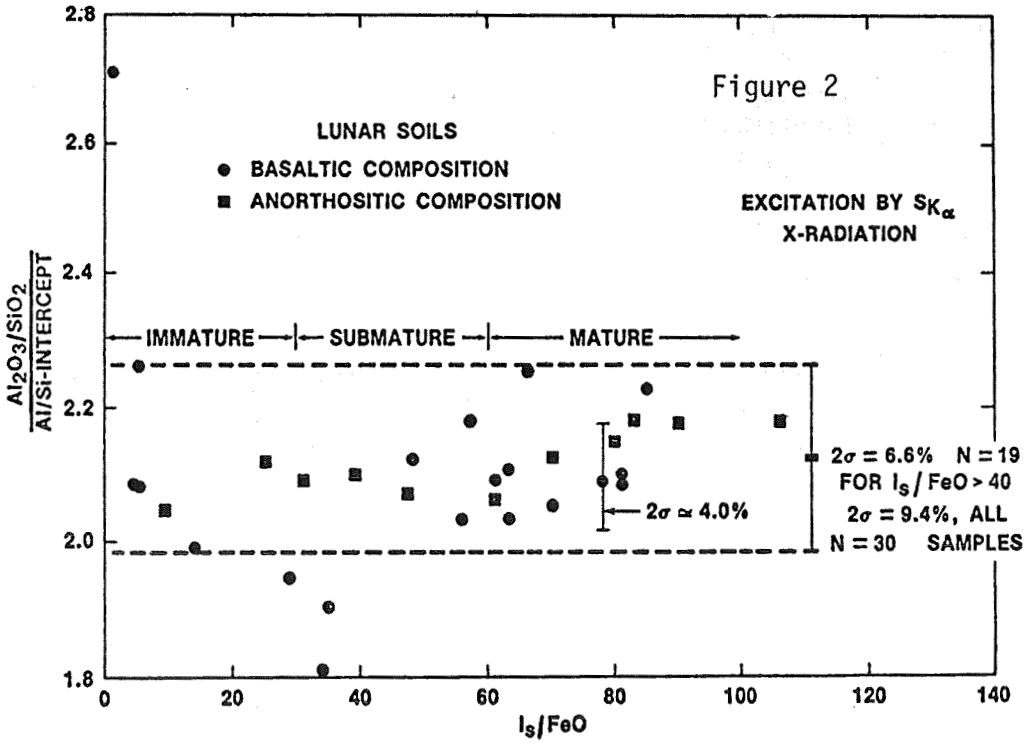

LABORATORY VERIFICATION--PRELIMINARY RESULTS

Norman Hubbard and Bi-Shia King

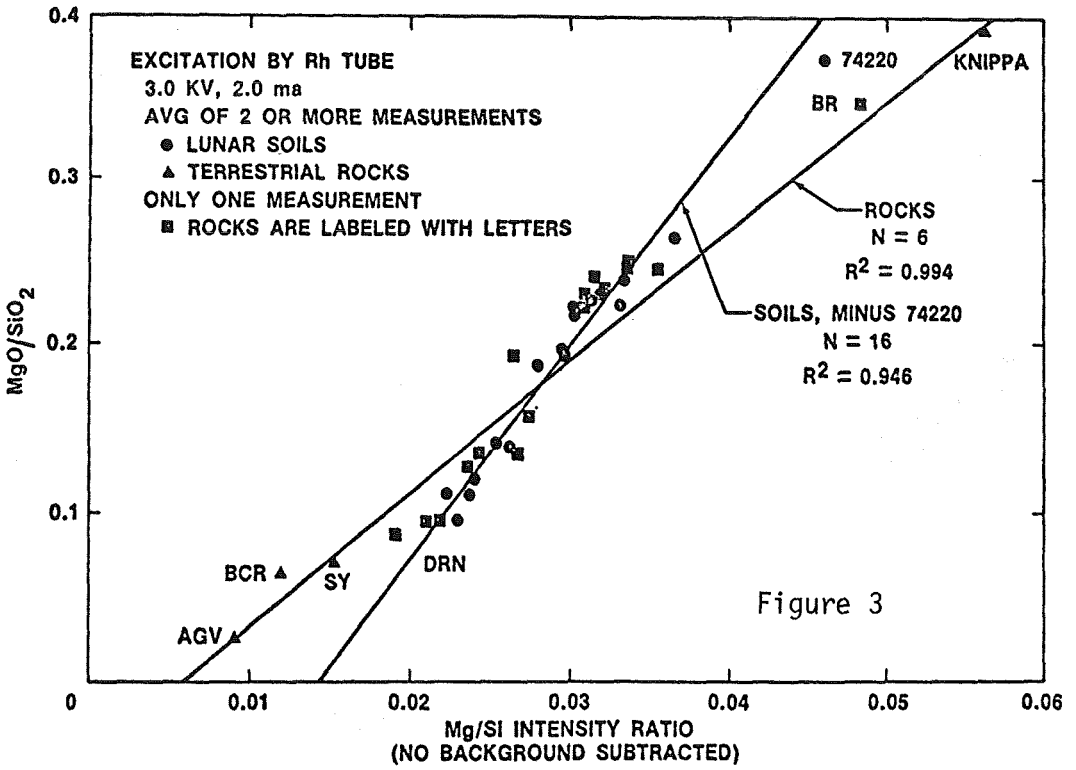

Figure 3

The difference between the lines for lunar soils vs. terrestrial rocks may be due to differences in effective particle size, to the presence of a coating on the lunar soil grains or to the vitreous nature of lunar soil grains. These possibilities are being investigated.

MAJOR CONCLUSIONS: (a) Over the entire known range of chemical compositions of typical lunar soils there is either a single relationship of concentration ratio to intensity ratio or a number of closely spaced relationships. (b) Soil maturity is not an important variable for the lunar orbital x-ray fluorescence experiment. (c) There are physical differences between the finely ground terrestrial rocks used in this experiment and lunar soils that seriously effect the relationship of x-ray intensity to elemental concentrations even when data for elements of adjacent atomic number are ratioed.

References:
(1) Hubbard N. (1979) Proc. Lunar Planet. Sci. Conf. 10th, in press.
(2) Maxwell T. A., Strain D. L. and El-Baz F. (1977) Proc. Lunar Sci. Conf. 8th, p. 933-944.
(3) Bielefeld M. J. (1977) Proc. Lunar Sci. Conf. 8th, p. 1131-1147.
(4) Adler I., Trombka J., Gerard J., Lowman P., Schmadebeck R., Blodget H., Eller E., Yin L. and Lamothe R. (1972) Science 175, p. 436-440.
(5) Heiken G. (1974) A Catalog of Lunar Soils - Draft. Johnson Space Center informal publication.
(6) Morris R. V. (1977) Proc. Lunar Sci. Conf. 8th, p. 3719-3747.

THERMAL HISTORY OF FRAGMENT-LADEN "BASALT" 77115.

J.S. Huebner, C.R. Thornber, and R.F. Sanford, U.S. Geological Survey, 959 National Center, Reston, Virginia 22092.

Lunar highlands sample 77115, the "blue-gray breccia" incorporated in the Apollo 17 station 7 boulder, is a fragment-laden feldspathic pigeonite basalt (1,2). The majority of samples from the highlands region southeast of Mare Serenitatis are similar to 77115 in texture, lithology, and chemistry and are likewise interpreted as having been fragment-laden melts (7). Knowledge of the cooling history of this rock type is critical to understanding the generation of the lunar highlands crust, particularly the durations of individual events.

Three different kinds of observations constrain the thermal history deduced for lunar sample 77115. First, dynamic crystallization experiments set a maximum temperature for the beginning of crystallization and constrain the rates of cooling during early and late magmatic crystallization. Second, the persistence of xenocrysts that could not have been in equilibrium with the melt indicates that the melt could not have remained long at near liquidus temperatures. Third, diffusively zoned olivine xenocrysts indicate cooling for a limited duration at temperatures close to the solidus. (Lengthy annealing at these temperatures would have eliminated the zoning.) All experiments used an analogue of the 77115 matrix with the composition reported by (2).

The equilibrium phase relations of the 77115 matrix composition were determined in iron capsules, in vacuo, with melting experiments (utilizing sintered starting material) and crystallization experiments (using glass starting material). Equilibrium runs (Fig. a) are a standard against which the dynamic crystallization experiments can be compared. At equilibrium the bulk composition intersects the liquidus at 1258°$\pm$5°C and the solidus at 1055°$\pm$25°C.

The differences in texture and mineralogy resulting from the various dynamic crystallization runs constrain the early cooling history of the lunar sample. All runs in which the starting material was completely melted, then cooled (curves #9, 11, 12, and 13 in Fig. b) resulted in coarse radial growths of plagioclase. Microsubophitic texture, similar to but finer than that of the 77115 matrix, was attained only in those runs which crystallized from temperatures at which crystals and liquid were present (curves #15, 16, 17, and 71). In these runs, the finely disseminated crystalline residua of partially melted starting material served as nucleii for crystallization. Run #18, initially cooled rapidly from 1225°C, a temperature at which abundant olivine and plagioclase is present, then held at 1040°C for 80 hours, produced a coarser microsubophitic intergrowth of plagioclase, olivine, and minor pyroxene which closely resembles the igneous texture of the lunar 77115 matrix, but has a different modal mineralogy. Pigeonite, the major mafic phase observed in the lunar sample, was absent in all runs cooled through the $\sim$1190°-1110°C interval (where olivine reacts with liquid to form pigeonite) at a rate greater than 25°C per hour. Pigeonite is present as a minor phase in runs #17, 18, and 37 which were cooled at 17°, 10°, and 7° per hour through this interval. Presumably lunar rock 77115 cooled more slowly than 7°C per hour during the last stages where melt was present in order for matrix olivine to react almost entirely with residual melt and to crystallize a large proportion of pigeonite.

The cooling history of 77115 is also restricted by the observed general absence of xenocryst resorption by melt (matrix). Many xenocrysts could not have been in equilibrium with the melt which once surrounded them. For example, the survival of orthopyroxene xenocrysts ($Wo_{2.5-4.9}En_{68-76}Fs_{21-31}$) which could never have been in equilibrium with the melt at low pressure, rules out the possibility that the melt crystallized slowly. Analogue xenocrysts placed in

the 77115 matrix and cooled along curve #18 partially to completely reacted during cooling, supporting the suggestion that if the melt cooled through the interval in which the xenocrysts were not stable, it cooled more rapidly than curve #18 (~10°C per hour). Similar agruments can be made regarding olivine xenocrysts at temperatures in excess of 1243°C.

The formation of compositionally zoned "rims" in the margins of olivine xenocrysts by Mg-Fe diffusion in 77115 is an integrated function of time and temperature. Previous investigators had no knowledge of the temperature and rate at which crystallization began (5,8). They assumed isothermal diffusion and, because olivine diffusion in 77115 xenocrysts reflects approach to equilibrium with matrix crystals, not melt (Huebner in (2)), they arbitrarily chose 1050°C as the temperature for the process. However, they recognized that a family of curves, such as is shown in Fig. c, would yield the observed olivine diffusion. We modelled the olivine zoning using a computer program modified from that described by (3).

We experimentally modelled the formation of compositionally zoned rims by dynamically crystallizing 77115 matrix about olivine plates (analogue xenocrysts) of Fo_{92} composition. Olivine plates cooled along curve #18 (fig. b) display compositional profiles similar to those observed in the lunar sample. Of particular importance is the composition of the outermost rim (Fo_{79}), which approaches that of olivine in the analogue matrix, Fo_{67}, and the lunar matrix, Fo_{68}. When cooling is initiated at a higher temperature, as in #37, the "xenocryst" rims (Fo_{81}) again approach the composition of the matrix olivine (Fo_{75}), but both are more magnesian than the lunar matrix. We suspect that these different results are due to differences in the evolved composition of the melt during the diffusion process. In #37, which cooled relatively slowly through the olivine crystallization interval, much of the Fe-Mg exchange diffusion must have occurred between olivine and a relatively magnesian [large Mg/(Mg+Fe)] liquid. In contrast, significant olivine diffusion in run #18 must have occurred after crystallization was more advanced, and therefore with a less magnesian liquid (or with crystalline matrix). In order to achieve the much closer correspondence observed between olivine xenocryst rims and matrix olivine in 77115, greater equilibration is required, such as would be achieved by slower cooling at moderate temperatures (e.g., 1000°C).

The evidence presented above severely constrains the permissible cooling history of 77115. The constraints of fast cooling (>10° per hour over the range 1230°-1180°C) followed by slower cooling (<7° per hour below 1190°C) can be met simply by a cooling curve that asymptotically approaches a final temperature of 900°-1050°C (figure c). We suggest that the melt sheet represented by 77115 was intruded into, or ejected onto, material that was still hot. (This material may have been a slightly older, hot sheet similar to 77115). The rapid initial cooling is most easily met by a sample that was originally located close to the contact or margin of the adjacent material. (Extremely fast crystallization, that could be produced by the initial thermal equilibration of cold clasts and melt, results in too fine a texture (curve #71 of fig. c)).

The fact that the olivine xenocrysts did not reach equilibrium (with the matrix) or become homogeneous, constrains the length of time that the lunar sample followed the cooling curve. The olivine rims observed in 77115 would have formed in 2200-15000 hours (fig. c), at which time the cooling process must have been perturbed, perhaps due to excavation by a subsequent impact or cooling due to surface radiation from an overlying sheet. If incompletely diffused olivines are a common feature of the fragment-laden melts [(6) notes zoned olivines in 73215], one could conclude that the inferred history of 77115 is representative of conditions in the Mare Serenitatis region 3.9 Aeons ago.

THERMAL HISTORY

Huebner, J.S., et al.

Additional evidence may support the cooling history that we propose. The xenocrysts of pigeonite and calcic orthopyroxene in the lunar 77115 are optically homogeneous. Were they to have cooled slowly to 800°C, the pigeonite should have inverted and the orthopyroxene should have exsolved augite, as observed in the related noritic breccia 77215 (4). These features should now be examined by electron microscopic methods to confirm the petrographic observations.

References (1) Chao, E.C.T., J.A. Minkin, and C.L. Thompson (1974) Earth Planet. Sci. Letters, 23, 413-428. (2) Chao, E.C.T., J.A. Minkin, C.L. Thompson and J.S. Huebner (1975 Proc. Lunar Sci. Conf. 6th, 493-515. (3) Goldstein, J.I., and A.E.Moren (1978) Met. Trans. A, 9, 1515-1525. Program kindly provided by A. Romig. (4) Huebner, J.S., M. Ross, and N. Hickling (1975) Proc. Lunar Sci. Conf. 6th, 529-546. (5) Huebner, J.S. (1976) Lunar Sci. VII, 396-398. (6) James, O.B. (1976) Proc. Lunar Sci. Conf. 7th, 2145-2178. (7) James, O.B. (1978) Proc. Lunar Sci. Conf. 9th, 789-819. (8) Sanford, R.F. and J.S. Huebner (1979) Lunar Sci. X, 1052-1054.

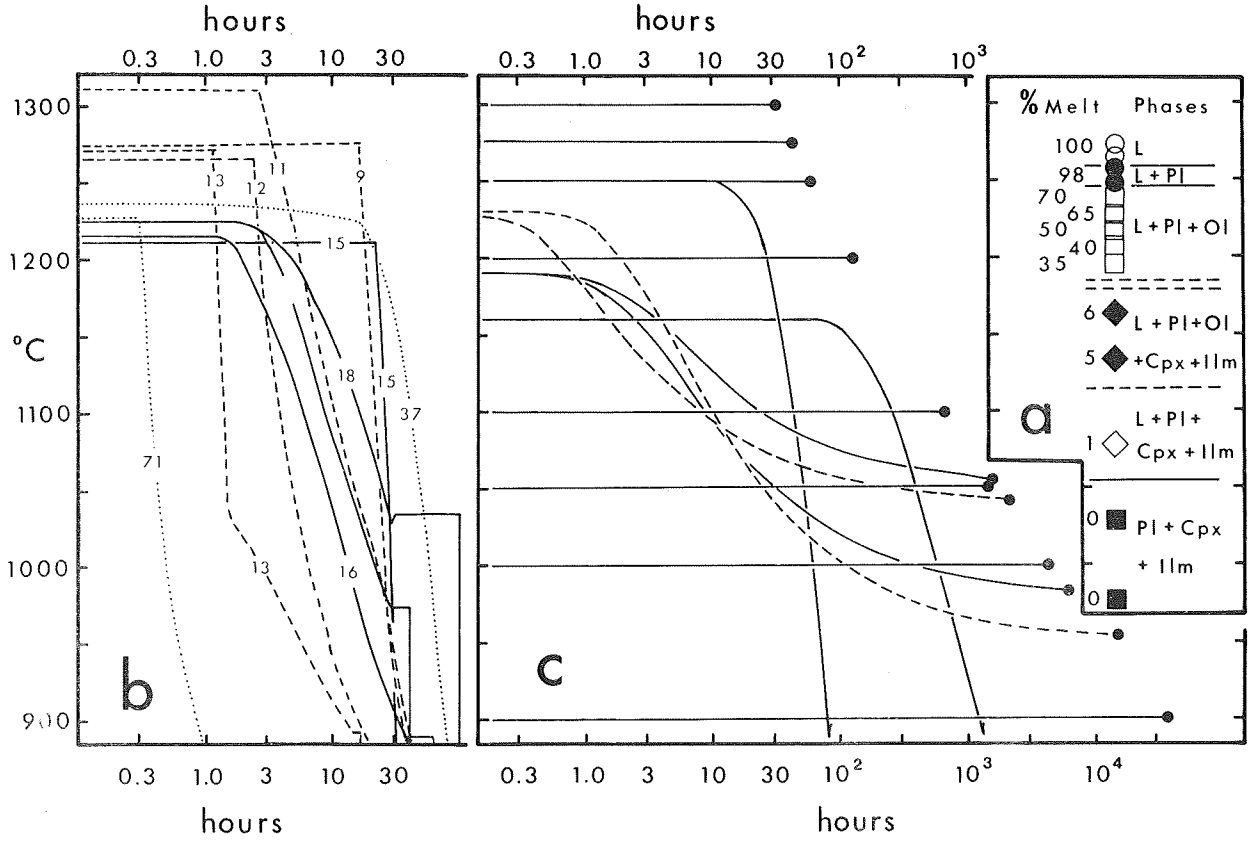

Figure. Results of investigation. The temperature scale is the same throughout. a) Equilibrium experiments, conducted isothermally. b) Dynamic crystallization experiments; initial temperature was achieved within the first 0.01 hour (not shown). c) Family of model curves; at its termination (dot), each curve would have yielded the olivine diffusion profile observed in the lunar sample. The preferred curves for the cooling of 77115 are dashed.

A POSSIBLE ROLE FOR HALOGEN-RICH FLUIDS IN THE GENERATION OF KREEP BASALTS. Anthony J. Irving, Dept. of Geological Sciences, University of Washington, Seattle WA 98195

Various lines of petrologic and morphologic evidence (1,2,3,4) leave little doubt that KREEP basalts of the type found abundantly at the Apollo 15 site are volcanic rocks extruded just prior to (and perhaps simultaneously with) mare basalt flooding of the Imbrium Basin. The origin of these lavas is a major unresolved problem in lunar petrogenesis. The main two types of hypotheses are that KREEP basalts represent (1) partial melts of lunar crustal rocks (eg. 5,6,7,1) or (2) residual melts derived directly from early lunar differentiation (eg. 8,9,10). Many variants of these hypotheses have been proposed, and all have their strong, weak and ad hoc aspects. Major difficulties for the residual melt hypotheses which have not been adequately addressed are how to reconcile the relatively high Mg/Fe ratios and high Cr contents of KREEP basalts with high degrees of crystallization of the lunar magma ocean. Partial melting models also have some weaknesses, but for the purposes of this paper a partial melting model is assumed.

Both petrologic and isotopic studies (eg. 6,1,11,12) suggest that troctolitic rocks composed dominantly of olivine and plagioclase (but possibly with minor pyroxene) are the most likely source materials. A feature of lunar troctolites and norites (such as 76535, 78235,78238) is the presence of accessory phosphates and Zr-bearing phases (13,14,15). These same phases are, of course, also characteristic of Apollo 15 KREEP basalts (16,17,7) and other KREEP-rich impact melt rocks (18,19). The phosphate minerals in all these rocks apparently consist of approximately equal amounts of apatite and whitlockite. The whitlockites contain essentially no volatile components, but the apatites contain an average of 4 wt.% halogens, made up of 2.8 to 4.0 wt.% F and 1.2 to 0.04 wt.% Cl (13,14,18,19). No measurements of bulk halogen contents of Apollo 15 KREEP basalts have been made, but Jovanovic and Reed (20) report 81 ppm F and 4.2 ppm Cl in 14310 (bulk P_2O_5 content 0.37 wt.%). Assuming equal amounts of apatite and whitlockite and similar P_2O_5 contents in the mesostasis glasses of 14310 and a typical Apollo 15 KREEP basalt (bulk P_2O_5 content 0.70 wt.%), the latter might contain $\sim$150 ppm F and $\sim$8 ppm Cl (all residing in apatite, which would not be stabilized unless such large anionic species existed in the KREEP basalt melts).

What role, if any, do these halogens play in the genesis of KREEP basalts? Is it possible that discrete halogen-rich fluids existed in the lunar interior? Here it is tempting to draw analogies with processes recently proposed for the generation of terrestrial highly alkalic basalts, wherein migratory H_2O-rich and CO_2-rich fluids (containing also minor amounts of halogens) have been postulated to locally metasomatize the terrestrial upper mantle and ultimately trigger partial melting (21,22). A feature of these models is that larger degrees of melting than generally supposed are predicted because of pre-enrichment of the source regions by the LIL species dissolved in the fluid(s). If halogen-rich fluids existed in the lunar interior they too might be expected to scavenge all the LIL trace elements characteristic of KREEP basalts.

Unfortunately, there are few experimental data on melting behavior in silicate-halogen systems, and even fewer data on the nature of fluid phase solutes. However, the studies by Wyllie and Tuttle (23,24) on the effects of HF, HCl and other species, in addition to H_2O, on the melting temperatures of albite and granite demonstrate the dramatic influence of the halogens in particular. These authors found that the lowering of melting temperatures of

albite compared to its melting temperature in the presence of H_2O alone was 200°C for HF and 100°C for HCl. Furthermore, they found that Na-rich material was abundantly dissolved in the vapor phase in both sets of experiments. If similar depression of solidus temperatures is appropriate for deep lunar crustal troctolites invaded by halogen-rich fluids, then the difficulties mentioned by Minear and Fletcher (25) of finding a heat source to generate KREEP basalt partial melts as late as 3.9 AE may be alleviated. If LIL elements are indeed preferentially soluble in halogen-rich fluids, then it is possible that the elusive KREEP component may be contained in a fluid phase residue formed very late in the primary lunar differentiation.

The ideas presented here are speculative, yet tantalizing; they may leave more questions unanswered than not. They are offered in the spirit of planetary adventure.

References: (1) Irving A.J. (1977) Proc. Lunar Sci. Conf. 8th, p. 2433-2448. (2) Hawke B.R. and Head J.W. (1978) Proc. Lunar Planet. Sci. Conf. 9th, p. 3285-3309. (3) Spudis P.D. (1978) Proc. Lunar Planet. Sci. Conf. 9th, p. 3379-3394. (4) Head J.W. and McCord T.B. (1978) Science 199, 1433-1436. (5) Walker D. et al. (1973) Earth Planet. Sci. Lett. 20, 325-336. (6) McKay G.A. and Weill D.F. (1976) Proc. Lunar Sci. Conf. 7th, p. 2427-2447. (7) Dowty E. et al. (1976) Proc. Lunar Sci. Conf. 7th, p. 1833-1844. (8) Steele I.M. and Smith J.V. (1973) Proc. Lunar Sci. Conf. 4th, p. 519-536. (9) Lipin B.R. (1978) Amer. Mineral. 63, 350-364. (10) Warren P.H. and Wasson J.T. (1979) Rev. Geophys. Space Phys. 17, 73-88. (11) Lugmair G.W. and Carlson R.W. (1978) Proc. Lunar Planet. Sci. Conf. 9th, p. 689-704. (12) Carlson R.W. and Lugmair G.W. (1979) Lunar Planet. Sci. X, p. 178-179. (13) Dymek R.F. et al. (1975) Proc. Lunar Sci. Conf. 6th, p. 301-341. (14) McCallum I.S. and Mathez E.A. (1975) Proc. Lunar Sci. Conf. 6th, p. 395-414. (15) Irving A.J. et al. (1974) Amer. Mineral. 59, 1062-1068. (16) Steele I.M. et al. (1972) The Apollo 15 Lunar Samples, p. 158-160. (17) Meyer C. (1977) Phys. Chem. Earth 10, 239-260. (18) Gancarz A.J. et al. (1972) Earth Planet. Sci. Lett. 12, 1-18. (19) Albee A.L. et al. (1973) Proc. Lunar Sci. Conf. 4th, p. 569-595. (20) Jovanovic S. and Reed G.W. (1976) Proc. Lunar Sci. Conf. 7th, p. 3447-3459. (21) Menzies M. and Murthy V.R. (1978) EOS 59, 1215. (22) Boettcher A.L. et al. (1979) The Mantle Sample: Inclusions in Kimberlites and Other Volcanics, p. 178-182, Amer. Geophys. Union. (23) Wyllie P.J. and Tuttle O.F. (1961) Am. J. Sci. 259, 128-143. (24) Wyllie P.J. and Tuttle O.F. (1964) Am. J. Sci. 262, 930-939. (25) Minear J.W. and Fletcher C.R. (1978) Proc. Lunar Planet. Sci. Conf. 9th, p. 263-283.

PETROLOGY OF THE MAJOR ROCK TYPES OF THE LUNAR HIGHLANDS:

Odette B. James, U.S. Geological Survey, Reston, VA 22092

Introduction. The purposes of this paper are 1) to summarize what is known about several significant highlands rock types, and 2) to speculate upon their origins and interrelations to help formulate directions for future research. Only data from large rock samples are considered. Each discussion of specific rock types emphasizes data from one site only, because it is critical to understand the interrelations of spatially associated samples before making generalizations concerning moonwide processes.

Highlands rock groups. Whole-rock analyses of highlands samples plotted on an olivine-anorthite-silica pseudoternary diagram [1] form several distinct groups (Fig. 1). Rocks within individual groups tend to have similar textures: A, granulated plutonic anorthosites (ferroan anorthosites [2]); B, plutonic norites; C, plutonic troctolites (plus dunite and spinel troctolite); D, fragment-laden impact melts (low-K and medium-K Fra Mauro compositions); E, fragment-laden melts and endogenous (KREEP) basalts; and F, (the ANT trend [3]), granulitic impactites [4]. In addition, all the groups contain the compositions of bulk breccias and clast-free impact-melt rocks; such rocks will not be discussed in this abstract.

Plutonic (ferroan) anorthosites from Apollo 16. Most are unrecrystallized cataclastic rocks. Prior to crushing, most were coarse grained, with plagioclase crystals as much as one cm across forming a coarse granular mosaic (e.g., 60015, 60025, 60215, 62255). Only a few percent mafic minerals are present; other phases are few in number and are present only in trace amounts [5-6]. A few samples differ texturally and modally from the coarse granular samples. These were also once coarse granular rocks, but they were granulated and recrystallized prior to the final cataclasis, and they tend to contain more abundant and more compositionally varied mafic minerals than the coarse granular rocks (e.g., 67075, 62236, 62237 [7-9]).

Plagioclase compositions are very calcic with a restricted range, An_{92-99} for the whole suite [5-9]. Mafic minerals are iron-rich, and have a large compositional range over the entire suite [5-9]: olivine, $\sim Fo_{40-62}$; low-Ca pyroxene, $\sim En_{60-70}$; inverted pigeonite (lamellar intergrowths of augite and low-Ca pyroxene), $\sim En_{40-55}$; and augite, $Wo_{40-45}En_{30-43}Fs_{12-30}$.

Genesis and interrelations of these rocks are still unresolved. An origin as igneous plagioclase cumulates is suggested by the nearly monomineralic compositions and positive Eu anomalies. If the rocks are cumulates, the overall mineralogic variations suggest a "magma ocean" origin, with the plagioclase being a floated phase. (The very calcic compositions and homogeneity of the plagioclase suggest it is an early precipitate from a large volume of magma; the compositional diversity of mafic minerals can be explained if they separated from the melt at various stages of crystallization -- i.e., some would be inclusions in plagioclase, others would be rafted by floating crystals, and others would be crystallized from trapped interstitial liquid.) Two inconsistencies of this hypothesis remain to be resolved: 1) in some rocks olivine seems too coarse and too abundant to have been rafted by floating plagioclase [8]; 2) mafic minerals crystallized from trapped liquid should have associated Na-enriched plagioclase, but none has been observed.

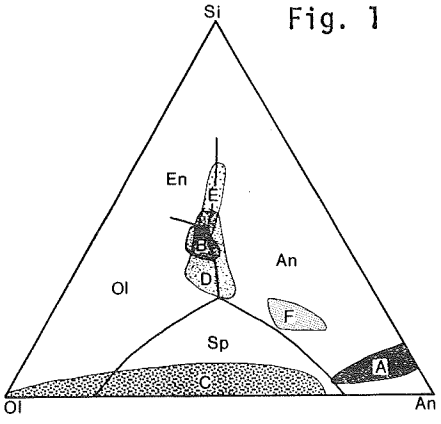

Fig. 1

Depth of origin has not been resolved. Key information is: 1) the distance over which mineral compositions were equilibrated [10], and 2) the

scale of exsolution separation of pyroxenes. These data give estimates of cooling history, which can yield estimates of depth of origin. With respect to 1): If 67075 and 62237 are monomict, then the wide range of Fe/Fe+Mg in their mafic minerals suggests that they had little subsolidus reequilibration, and either formed in the upper part of the crust where rapid cooling could have taken place, or they were excavated soon after they formed. With respect to 2): Exsolution features are comparable to those in Stillwater Complex pyroxenes [7]; if cooling histories were comparable, comparable depths are indicated.

Age of the rocks is also unresolved. In most samples, the K-Ar system has been reset, and Rb-Sr internal isochrons cannot be determined. Initial $^{87}Sr/^{86}Sr$ is primitive, however, suggesting that the rocks are relics of the earliest crust [11,12]. No Sm-Nd data are available.

Plutonic norites from Apollo 17. 78235 [8,13,14] and 77215 [15] are representatives of a group of closely related Apollo 17 norites. These rocks have igneous textures, and 78235 is an orthopyroxene-plagioclase cumulate with grain size $\leq$ 6 mm [16]. Trace phases are abundant and varied, and some are rich in K, Nb and Zr. The group as a whole shows strongly correlated variations of Mg/Mg+Fe in pyroxene (0.80 to 0.66) and Ca/Ca+Na in plagioclase (0.95 to 0.88), suggesting that all were derived from a single differentiated complex. For 77215, [15] estimate a depth of $\sim$10 km. For 78235, [16] estimate a depth like that of terrestrial layered mafic complexes, 5-30 km. Age is not resolved, but the evidence seems to favor $\geq$4.4 b.y. [17].

Plutonic troctolites, dunite, spinel troctolite. Troctolite 76535 [8, 18], a representative sample of this group, is an olivine (Fo_{86-88})-plagioclase (An_{95-97}) cumulate. The rock had prolonged high-temperature subsolidus reequilibration, estimated at $\sim$1000°C at 10-30 km for $>10^8$ y [10,18]. Interpretation of the age data is still uncertain, but the best interpretation now available is that the rock crystallized $\sim$4.61 b.y. ago and remained hot until $\sim$4.26 b.y. ago, at which time it cooled to a temperature below that necessary for isotopic reequilibration or was excavated by an impact [19,20].

Dunite 72415 has mineralogy similar to 76535, but its history was much more complex [8,21]. It is an olivine cumulate (original grain size $\leq$1 cm), which was later shocked, partly melted, recrystallized, and granulated again. The similar mineralogies suggest similar depths for the dunite and 76535; thus, the dunite is not a mantle rock. A Rb-Sr internal isochron yields an age like that of the troctolite, 4.55 b.y. [11].

Most spinel-bearing rocks occur as small clasts in Apollo 15, 16 and 17 breccias. The major minerals are Mg-Al spinel, magnesian olivine (Fo > 84), and calcic plagioclase (An > 96); several samples also contain aluminous enstatite [22]. Examples are clasts from breccias 67435 [23] and 15445 [22,24]. Most of these rocks were once coarse grained, but have been extensively granulated. Depth is estimated at >30-40 km for the enstatite-bearing samples [25]. No age data are available.

KREEP basalts (Apollo 15 and 17). Examples are 15382 [26] and clasts from breccia 72275 [27]. Textures and mineralogies support an endogenous origin [26-29] and indicate rapid crystallization at the surface. Major minerals are relatively sodic plagioclase (An mostly <88) and relatively Fe-rich low-Ca pyroxene (En mostly <70); abundant K-rich mesostasis is present. Isotopic evidence suggests that the source for these rocks formed early, before $\sim$4.25 b.y., and was extensively remelted at 3.9-4.0 b.y. to form the basalt magmas [19,30-31].

Interrelations of plutonic rocks and possible relation to KREEP. The compositions of the major minerals in the plutonic rocks (An in plagioclase vs. Mg/Mg+Fe in mafic minerals) indicate that these rocks fall into two distinct

suites [32,33]. One consists of the ferroan anorthosites and is typified by calcic plagioclase associated with iron-rich mafic minerals. As outlined above, most data are consistent with these rocks being from a layer of floated cumulus plagioclase formed in a primordial "magma ocean". The second suite consists of the spinel-bearing rocks, dunite, troctolites and norites; I will refer to these rocks as the "magnesian" suite, because for a given plagioclase composition they have more Mg-rich mafics than the anorthosites. Mineralogic variations are attributable to normal igneous differentiation: magnesian olivine and calcic plagioclase occur in the most primitive members of the suite, and iron-rich pyroxene and sodic plagioclase occur in the most evolved members. Many of these rocks have relict igneous textures, and plagioclase appears to have been a settled phase [16]. Inferred depths of origin, as well as the mineralogic variations, suggest that the rocks come from large layered plutons, with spinel-bearing rocks deepest, troctolites at intermediate levels, and norites uppermost. The presence of the olivine-rich rocks within the crust and the evidence that plagioclase sank cannot be easily reconciled with origin in a "magma ocean". Thus, these rocks are probably not complementary cumulates to the ferroan anorthosites, but instead crystallized from distinct magma(s). Age data suggest that the rocks of both suites crystallized > 4.4 b.y. ago.

Rare-earth-element data for the magnesian-suite rocks suggest a relationship to KREEP rocks [13,20,34,35]. Compositions of plagioclase and pyroxene in KREEP basalts [26,27], a felsite [36], and a quartz monzodiorite [37] fall on the extension of the trend line defined by a plot of An in plagioclase vs. Mg/Mg+Fe in mafic minerals for rocks of the magnesian suite, further supporting a genetic relationship to KREEP. Melting in the magnesian-suite plutons at 3.9-4.0 b.y. may have been the process that formed the KREEP basalt magmas [14].

Granulitic impactites [4,33]. Examples are 77017 [38], 79215 [39,40], and 78155 [41]. These rocks represent aggregates of fragments that were heated to near-solidus temperatures (~1100-1200°C), recrystallized, reequilibrated, and/or partly melted [33,36]. They are probably from the uppermost few km of the crust. Both bulk compositions and average mineral compositions are intermediate between the ferroan anorthosite and magnesian-suite trends [33]. The parental aggregates of fragments were polymict breccias, probably made up of clasts from both ferroan anorthosite and magnesian suite rocks. Thus, the bulk compositions are probably mixtures and not the product of primary igneous differentiation.

The time of metamorphism is unresolved. Ages were reset at 3.9-4.0 b.y. or reflect earlier events at 4.15-4.3 b.y. [42-43]. It is not known if the old ages represent the time of metamorphism or the ages of the premetamorphic parent rocks, or if they have been partly reset at 3.9-4.0 b.y.

References: [1] PLSC 3, 797. [2] EPSL 24, 15. [3] GCA 37, 979. [4] PLSC 8, 2051. [5] PLSC 6, 263. [6] PLSC 4, 1033. [7] EPSL 26, 36. [8] PLSC 6, 301. [9] PLPSC 9, 185. [10] LS-VI, 774. [11] PLSC 6, 1467. [12] PLSC 4, 1823. [13] PLSC 6, 1219. [14] PLSC 6, 395. [15] PLSC 7, 2287. [16] BGSA 86, 433. [17] PLSC 7, 2309. [18] GCA 38, 1329. [19] PLSC 7, 2035. [20] PLSC 7, 2009. [21] PLSC 7, 1845. [22] J. Geol. 81, 621. [23] Science 179, 74. [24] PLSC 8, 1895. [25] PLPSC 9, 319. [26] PLSC 7, 1833. [27] Moon 14, 327. [28] PLSC 6, 363. [29] PLSC 8, 2433. [30] PLSC 6, 1445. [31] PLPSC 9, 689. [32] PLSC 8, 2215. [33] PLPSC 9, 629. [34] PLSC 5, 1213. [35] Blanchard & Budahn, PLPSC 10, in press. [36] PLSC 8, 2459. [37] EPSL 29, 255. [38] PLSC 5, 287. [39] PLSC 7, 1793. [40] PLPSC 9, 743. [41] PLSC 8, 2007. [42] PLSC 6, 1509. [43] PLSC 9, 841.

HIGHLAND ROCKS - A VIEW FROM BELOW. S. Jovanovic and G. W. Reed, Jr., Chemistry Division, Argonne National Laboratory, Argonne, IL 60439

An approach to understanding the origin and the evolution of anorthositic highland rocks is to see what, if any, genetic relationship they have to mafic rocks derived from great depths. We will review and elaborate on a large volume of data and interpretations that we reported in many Lunar Science Conference and journal papers. A number of incompatible element ratios are the same in the two groups of samples suggesting a common source, namely a differentiating magma ocean. Complementary relationships among other elements such as those for Eu in the REE patterns may or may not indicate a common source. The chemistry of the system would require such correlations regardless of whether there was a single source. We have previously interpreted Cl and P_2O_5 in all types of samples as elements that identify related differentiates. These results require several separately differentiating magmas. Some support for multiple magma seas was found in Rb-Sr data for basalts. The incompatible trace elements Cl, P_2O_5, Rb, Ba, K, and La (?) suggest relationships between highland and basaltic rocks. There are too few data from the highland reference suite and from some of the rock classifications of Wilshire et al. (1973) for a definitive test of the correlations noted. In addition more separated highland breccia components must be measured to test the trace element interrelations within the highland rocks and between these rocks and basalts.

Extensive data on volatile and non-volatile trace elements in 66095 have been acquired. For most elements the concentrations are so high as to require a lunar source yet the relative concentrations of a number of pairs of trace elements in 66095 are the same as in many Ap 16 and other highland breccias with much smaller, $\leq$ 1/5, concentrations. The implication is that in all these samples trace elements such as Cl, P_2O_5, Ru, Os, Zn, and ^{204}Pb had a common lunar source.

Another perspective on highland rocks will be presented based on the unreported stepwise heating patterns for Hg and Br. Melt rocks and basalts might be expected to have similar patterns since the [Hg] in high $\geq$450°C and low $\leq$450°C temperature sites reflects the temperature of equilibration. Rapidly cooled melts of either type contain relatively more Hg in high temperature sites. Metamorphism will cause reequilibration of Hg between sites. These data will contribute to the complex thermal-brecciation history of highland rocks.

Wilshire H.G., Stuart-Alexander D.E., and Jackson E.D. (1973) J. Geophys. Res., p. 2379-2392.

STATISTICAL CRITERIA FOR THE PRESENCE OF PRISTINE ROCK FRAGMENTS IN LUNAR IMPACT BRECCIAS. H.-D. Knöll and D. Stöffler, Institute of Mineralogy, University of Münster, 4400 Münster, Germany

Since the paper of (1) several chemical criteria have been developed for identifying pristine lunar rocks (2,3,4,5,6). Theoretically every lunar impact breccia, which commonly has undergone several impact events, contains pristine rock fragments. This paper presents a method to calculate the probability of bearing pristine rocks for any breccia.

If we assume that the mineral fragment population in an impact breccia is in accordance with the modal composition of the lithic fragment population of this breccia there must be a possibility to derive the nature of the lithic clasts from the nature of the mineral clasts. This method is based on the statistical provenance analysis which has been previously performed on some Fra Mauro breccias (7). Meanwhile it has been refined and the computer program PIOS (8) has been developed for performing the statistical provenance analysis for the mineral clasts in breccias. This analysis requires a solid data base, which contains all known mineral compositions of the possible source rocks in their real frequency distribution in the source rock. The method assigns mineral fragments to rock types using basic statistical considerations. The PIOS program calculates also the regression and correlation coefficients for both the source rocks and the assigned mineral fragments. In addition it computes the t-test of the mean values. This t-test gives a number for the degree of congruence of the compositional distribution of the mineral clasts with that of the reference rock.

The following shall demonstrate the procedure of obtaining a probability for the presence of clasts of a specific rock type (e. g. a pristine rock) in a breccia:

1. collect all available compositional data of the main minerals of the possible igneous source rocks of the breccia. For the present status of the program at maximum four source rocks can be considered.
2. measure the compositions of the corresponding minerals which are embedded as clasts in the breccia.
3. work out for every considered mineral two independent compositional criteria for distinguishing the rock types by mineral composition. Usually a multiple regression analysis is helpful.
4. the PIOS program assigns the mineral clasts in the breccia to none, one, or more rock types. These assignments are weighted by probability factors for

calculating the clast population of the breccia. All selected mineral clasts are also taken for the t-test.

The last step in this procedure may be demonstrated by this example: We have shown previously (7) that the mineral fragment population of the Fra Mauro breccias varies from breccia to breccia (Fig.1). The proportion of the source rock also varies from mineral to mineral of one particular breccia. This latter variation is partly due to the variable proportions of the minerals in their source rocks. The t-test of the mean values (Fig. 2 + 3) shows that the congruence of the compositional distribution of the assigned mineral fragments (plagioclase: x = An, y=FeO; pyroxene: x = CaO, y = TIO_2; olivine: x = Fo; y = CaO) with that of the source rock minerals in most cases is best for the nonmare basalt suite (KREEP- and high-alumina basalts). Since, in addition, the frequency of mineral fragments assigned to nonmare basalts is rather high in the Fra Mauro breccias (7), there is a high probability that nonmare basalt rock fragments are rather frequent in Fra Mauro breccias.

A first microscopical examination of the lithic fragments in these breccias confirmes this assumption. (1) Warren P.H. and Wasson J.T.(1977) Proc. Lunar Sci. Conf. 8th, p. 2215-2235. (2) Wänke H. et al.(1978) Proc. Lunar Sci. Conf. 9th, p. 83-110. (3) Delano J.W. and Ringwood A.E.(1978) Proc. Lunar Sci. Conf. 9th, p. 111-159. (4) Anders E.(1978) Proc. Lunar Sci. Conf. 9th, p. 161-184. (5) Herzberg C.T.(1979) Lunar and Planet. Science X, p. 537-539. (6) Ryder G.(1979) Lunar and Planet. Sci. X, p. 1046-1048. (7) Stöffler D. and Knöll H.-D.(1977) Proc. Lunar Sci. Conf. 8th, p. 1849-1867. (8) Knöll H.-D.(1978) Fortschr. Min., 56, Beih. 1, p. 64.

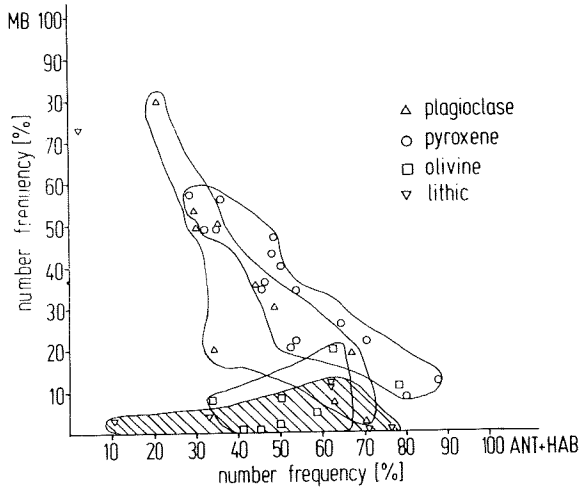

Fig. 1: Clast population of Fra Mauro breccias 14006, 14055, 14063, 14066, 14306, 14311, 14312, 14319, 14320, and 14321.

ROCK FRAGMENTS IN LUNAR IMPACT BRECCIAS

Knöll, H.-D.

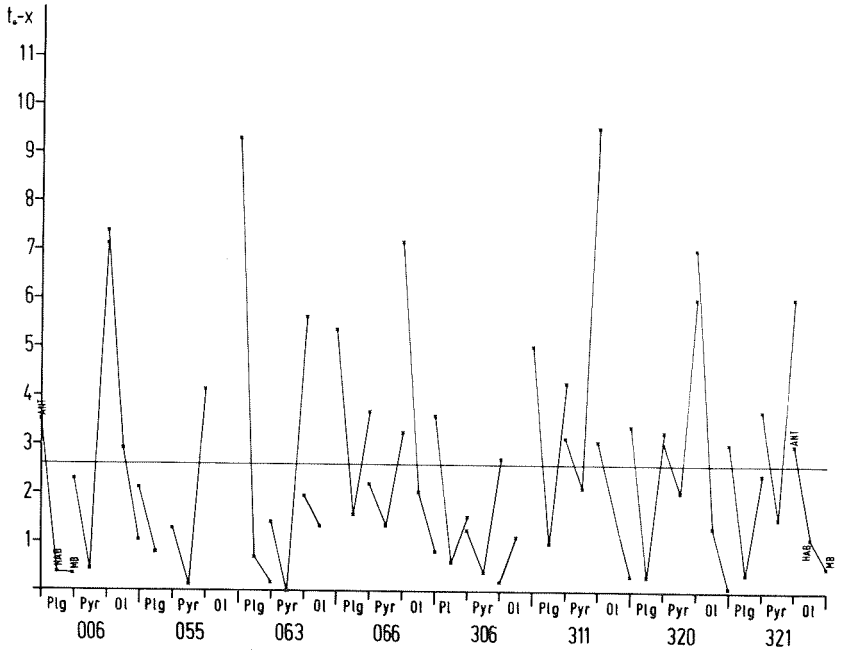

Fig. 2: t-test of the x-value distribution of plagioclase (Plg), pyroxene (Pyr), and olivine (Ol) with the ANT-, KREEP- and high-alumina-basalt (HAB), and mare basalt (MB) rock suites. Numbers refer to Apollo 14 samples.

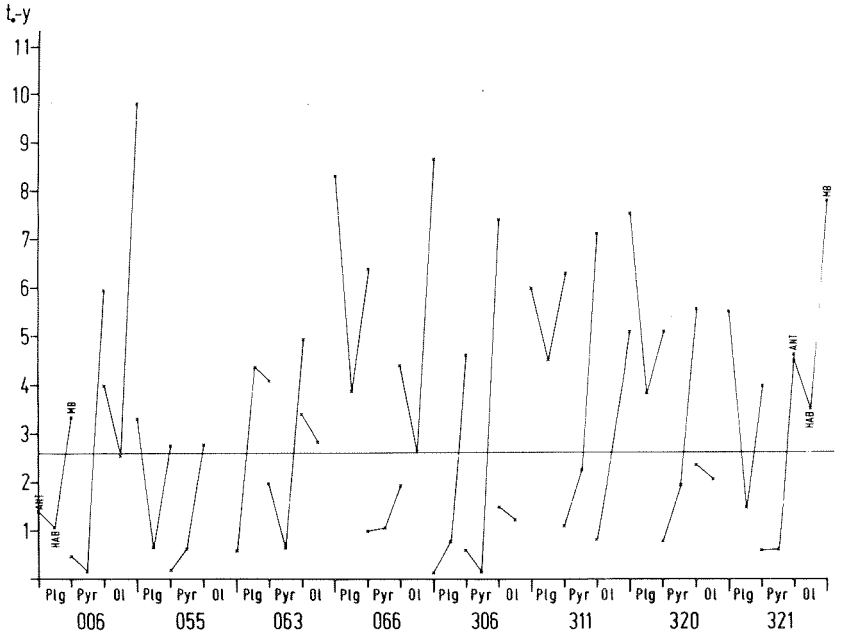

Fig. 3: t-test of the y-value distribution. For further explanation see Fig. 2.

THE GENERATION OF LUNAR IMPACT MELTS: A COMPARISON OF THEORETICAL AND OBSERVATIONAL RESULTS.

Manfred A. Lange, Institut f. Geophysik, Neue Universität, 2300 Kiel, W.-Germany and B. Ray Hawke, Institute f. Astronomy, University of Hawaii, Honululu, HI 96822

Impact melting was one of the major selenological forces throughout the history of the moon. First indications for this fact came from early photogeological studies by (1) and (2) which revealed the occurence of lavalike deposits in the vicinity of large lunar craters. Recent studies by (3) and (4) have provided strong evidence that these deposits are of impact origin. Further support comes from the large amount of impact melt rocks in the Apollo sample collection.

Experimental and theoretical model studies (e.g. (5) and (6)), together with in-situ studies of terrestial impact melt deposits have been used to develop theoretical methods for the understanding of impact melting and the mode of melt emplacement. These methods can -with minor modifications- be applied to lunar craters. Since in-situ observations of lunar melt deposits are not available, the detailed photography and remote sensing data of the Apollo missions are used to test the validity of theoretical predictions for the amount of impact melt (as derived from terrestrial considerations) under lunar conditions.

Theoretical predictions of impact melt volumes: Based on theoretical energy partitioning studies of (7) and empirical relations between crater diameter and kinetic energy of the meteoroid, as derived by (8), and (9), Lange & Ahrens (10) have shown that the melt volume associated with impact craters can be predicted by:

$$V_m(km^3) = k' D^C(km) \qquad (1).$$

The values for k' are 1.8×10^{-4} km^3/km^C and 3.8×10^{-4} km^3/km^C for lunar and terrestrial craters, respectively. The exponent C is approximately equal to 3 for craters in which the target strength dominates the final size and equal to 4 for larger, gravitationally controlled diameter values. We have assumed the value C=3.4, first proposed by (11), which includes both effects. Melt volumes as a function of crater diameter D, according to eq. (1) for terrestrial and lunar craters are given in Fig. 1 as solid and dashed lines, respectively.

Also shown are well constrained estimates for the melt volumes of selected terrestrial impact craters given by (12) and (13). As can be seen, the agreement between theoretical and observed values is reasonably good and hence, supports the theoretical prediction. However, with the exception of Brent and Manicougan, all other observed melt volumes are smaller (11) or slightly smaller (12) as the theoretical predictions. This can partly be explained by the fact that the observed values are considered to be minimum values and hence, should fall below the theoretical values. The higher melt volume observed at Brent Crater however, suggest that it is probably insufficient to use only one relation between melt volume and crater diameter for both, simple, bowl shaped and complex craters.

LUNAR IMPACT MELT

Lange, M. A. et al.

Melt volumes associated with lunar craters: Melt deposits were identified using the criteria established by (3) and (4). Quantitative measurements of melt volumes were made for craters for which high-quality topographic and photographic data are available. The areas covered by melt deposits were measured and thickness estimates were made using measured flow thickness, hummock heights, and local slope analyses. Extensive use was made of the new Lunar Topographic Orthophotomaps. Only ponds, flows, and the thicker portions of melt veneers were included in the volume determinations. No allowances were made for very thin, irregular veneers, melt drainage into subjacent breccias, widely dispersed molten material, or the possible clast content of some deposits. The melt volume estimate for Tycho (240 km^3) is that suggested by (2). The value for Copernicus (560 km^3) represents the amount which Howard and Wilshire found to be visible in and around the crater. The observational results are compared with those from theoretical calculations in Figure 1.

Discussion: The observed melt volume estimates or estimate ranges for small lunar craters ($D < 2$-3 km) are in relatively good agreement with those predicted from theoretical considerations. Simple craters of this size differ little in form from the transient cavities that existed at the end of the excavation stage of the cratering event. The melt ponded on crater floors represents shock melt which originally lined the transient cavities and collected in the bottoms of the craters at the end of the impact events.

Hawke and Head (14) recently reported that the amounts of interior melt are quite variable in fresh craters from 7-15 km in diameter and range from unobserved or present in only trace amounts to quite abundant. Wall modification has been more extensive at fresh craters of this size than at smaller craters and at least some of the variability in interior melt abundances may be attributed to differing efficiencies of melt burial or incorporation by mass wasted clastic debris.

While most fresh primary impact craters between 15 and 30 km in diameter do contain at least some melt, the amounts are extremely variable. Fresh craters in this size range which exhibit no interior melt are generally characterized by the presence of extensively scalloped walls and/or swirl textured floors which are indicative of pervasive wall failure. Analysis of the interior morphologies of these craters suggests that the interior melt was completely buried by scallop material. The variable quantities of interior melt associated with craters between 15 and 30 km in diameter can be explained by differences in the degree and style of wall failure.

At larger, terraced-wall craters ($D \gtrsim 30$ km), wall failure has been more extensive and deep-seated and wall material does not appear to have buried major quantities of interior melt. Still, Figure 1 shows that the observed melt volumes at craters of this size are consistently less than those predicted from theoretical considerations. If both the theoretical calculations and the observed melt volume estimates are generally correct, then major quantities of melt must be accounted for. The possible locations of this melt include the following:

LUNAR IMPACT MELT

Lange, M. A. et al.

(i) Some melt was undoubtedly ejected at high velocities early in the cratering event and was widely dispersed far from the parent craters.
(ii) Melt may have mixed with a portion of the bulk ejecta during the excavation stage of the cratering event.
(iii) Large amounts of melt may be present as a thin but extensive veneer surrounding major impact structures.

References: (1) Strom R.G. and Fielder G. (1968) Nature 217, 611-615. (2) Shoemaker E.M. et al. (1968) Techn. Rep. 32-1264, 9-76. (3) Howard K. and Wilshire M. (1976) J. Research U. S. Geol. Survey 3, 237-251. (4) Hawke B.R. and Head J.W. (1977) in Impact and Explosion cratering, Roddy D.F. et al., eds., 815-841. (5) Gault D.E. et al. (1968) in Shock Metamorphism of Natural Materials, ed. by B.M. French and N.M. Short, 87-99, Mono, Baltimore. (6) O'Keefe J.D. and Ahrens T.J. (1975) Proc. Lunar Sci. Conf. 6th, 2831-2844. (7) O'Keefe D.J. and Ahrens T.J. (1977) Proc. Lunar Sci. Conf. 8th, 3357-3374. (8) O'Keefe J.D. and Ahrens T.J. (1978) Phys. Earth Plan. Int. 16, 341-351. (9) Oberbeck V.R. et al. (1975) The Moon 12, 19-54. (10) Lange M.A. and Ahrens T.J. (1979) Proc. Lunar Planet. Sci. Conf. 10th, in press. (11) Vaile R.B. (1961) J. Geophys. Res. 66, 3413-3438. (12) Grieve R.A.F. et al. (1977) in Impact and Explosion Cratering, Roddy D.F. et al., eds. 247-275, Pergamon, N. Y. (13) Phinney W.C. and Simonds C.H. (1977) in Impact and Explosion Cratering, Roddy D.F. et al., eds., 771-790, Pergamon, N.Y. (14) Hawke B.R. and Head J.W. (1979) LPS X, 510. (15) Hawke B.R. (1979) unpublished data.

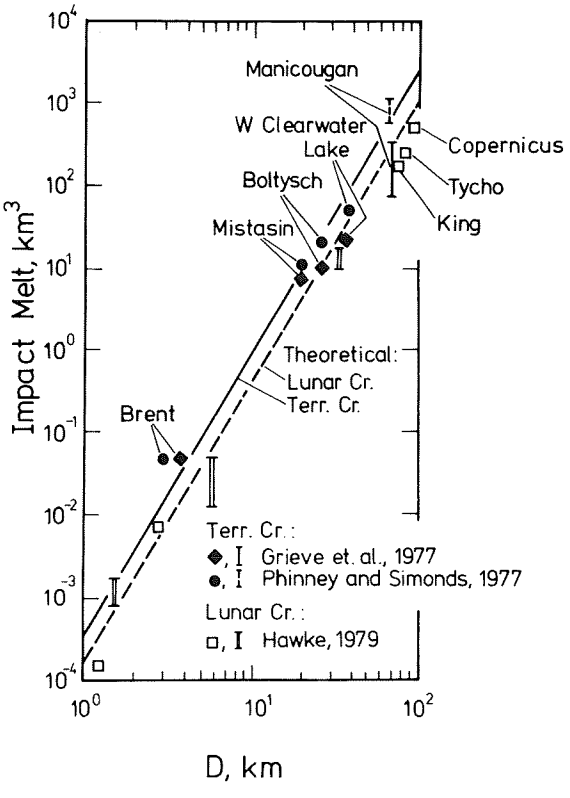

Figure 1: Theoretically predicted impact melt volumes for terrestrial (solid) and lunar (dashed) craters. Also shown are observed melt volumes for terrestrial (12 and 13) and lunar impact craters (15).

HIGHLAND CHEMISTRY: PRELIMINARY SYNTHESIS AND ANALYSIS OF MAJOR AND TRACE ELEMENT RELATIONSHIPS USING STATISTICAL METHODS. K. Livi, S. Brande, and A. E. Bence, Department of Earth and Space Sciences, SUNY, Stony Brook, N. Y. 11794

The chemistry of the highland crust places important constraints on calculations of whole moon bulk composition and on models for the formation of the moon and subsequent evolution. Estimates of the average highland composition are based upon the orbital XRF and γ-ray measurements and upon elemental correlations as determined from the rocks and soil samples, e.g., (1). Both the remote sensing and ground-based studies reveal large scale surficial heterogeneties indicating that complete homogenization of the highlands did not take place during the period of intense meteorite bombardment that ended at about 4.0 AE. Thus, identification of an "average" highland composition is virtually impossible. Attempts to obtain additional information on the relative abundances of highland compositional units and the identification of "primitive" lithologies involve frequency estimates of the major element compositions of glasses in the soils, e.g., (2), (3), (4). Trace element correlations were not made in these studies. Thus, correlations of the preferred glass compositions with the crystalline rock types is incomplete.

As part of a review of the chemistry and mineralogy of the lunar highlands, we have archived published major and trace element analyses and selected isotope ratios, radiometric ages, and analytical techniques for the highland soils, glasses, and crystalline rocks. Approximately 4000 analyses involving 84 variables from the Apollo 14, 15, 16, 17 and Luna 20 missions were stored. A series of software programs process the data in three stages, which involve numeric sorting and statistical analysis. One option, squeeze, involves making a composite analysis out of several separate analyses; each of which has only a few of the variables of interest. This operation is useful when different laboratories have analyzed the same rock for different groups of elements. All of the variables may or may not be considered to belong to the same rock depending upon its homogeneity. The programs permit the recovery of selected variables for plotting purposes.

The statistical investigation comprises calculation of basic statistical quantities for each site and the search for structure within and among sampling sites. Multivariate techniques are employed.

To assess both within-sample scatter and among-sample heterogeneity, we have used a generalized cluster analysis technique. Operating on sets of individual analyses, clustering programs calculate interanalysis distance in the full variable space, and then sequentially join analyses by the criterion of minimum distance. Based on overall similarity, analyses which are closest together will be aggregated together. The advantage of clustering by overall similarity is that analyses may be measured for any number of variables, such as all the trace elements, and the results are seen as a tree diagram in two dimensions. We have confirmed by this technique the similar grouping by rock type of a suite of Apollo 16 highland basalt analyses similar to that seen in the Apollo 16 drill core glasses (4).

Discriminant function analysis is used to characterize and emphasize differences among samples. Analysis of the highland samples from Apollo 14, 15, 16, and 17 reveals that sites 14, 16, and 17 are discriminated largely on the basis of CaO and MgO which are negatively correlated with FeO (Fig. 1). Apollo 15, which has the poorest statistical representation, is discriminated from the others by CaO and Al_2O_3 which also are negatively correlated. It is interesting to note group overlap and how frequently samples fall within their predicted group. Overall, almost 75% of the samples fall within their

predicted groups. Successful predictions for only 63% of the Apollo 15 and 17 samples were obtained. This reflects the greater chemical heterogeneity of the Apollo 17 highland rocks and poor statistics for Apollo 15.

Bivariate plots are useful in documenting mixing lines and visualizing inter- and intra-site trends. For example, TiO_2 vs Mg# (Mg/Mg + Fe^{2+}), Al_2O_3 vs Mg#, CaO/Al_2O_3 vs Mg# and Ba vs K (Figs. 2 - 5), illustrate some major inter- and intra-site compositional differences. The high Mg# samples occur only at the 16 and 17 sites and all the Apollo 14 samples have more evolved (higher TiO_2, Ba, K and lower Mg#) compositions than the others. The Mg-rich and anorthositic trends identified by many investigators and thought to represent primitive highland compositional units are well defined on these diagrams.

These results are preliminary. We are continuing our synthesis by correlation trace element abundances and isotopic ratios with the major elements.

References

(1) Taylor S. R. and Jakeš P. (1974) Proc. Lunar Sci. Conf. 5th, p. 1287-1305.

(2) Reid A. M. et al. (1972) Proc. Lunar Sci. Conf 3rd, p. 363-378.

(3) Ridley W. I. et al. (1973) Proc. Lunar Sci. Conf. 4th, p. 309-321.

(4) Naney M. T. et al. (1976) In Lunar Science VII, p. 607-609. Lunar and Planetary Institute, Houston, Texas.

Table 1

ACTUAL GROUP	NO. OF CASES	PREDICTED GROUP MEMBERSHIP GP. 1	GP. 2	GP. 3	GP. 4
Group 1 (A14)	54.	45. 83.3%	4. 7.4%	0. .0%	5. 9.3%
Group 2 (A15)	19.	0. .0%	12. 63.2%	5. 26.3%	2. 10.5%
Group 3 (A16)	166.	1. .6%	0. .0%	133. 80.1%	32. 19.3%
Group 4 (A17)	105.	7. 6.7%	15. 14.3%	16. 15.2%	67. 63.8%

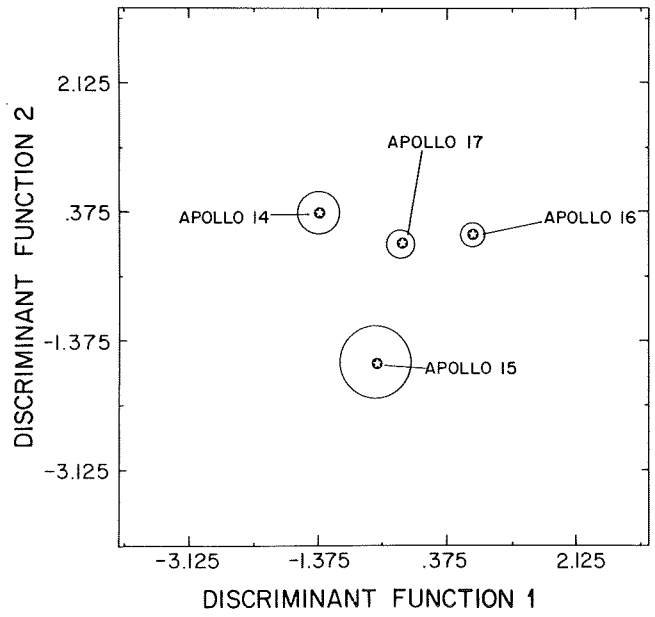

Fig. 1. 90% confidence circle to sample means.

HIGHLAND CHEMISTRY

Livi, K., et al.

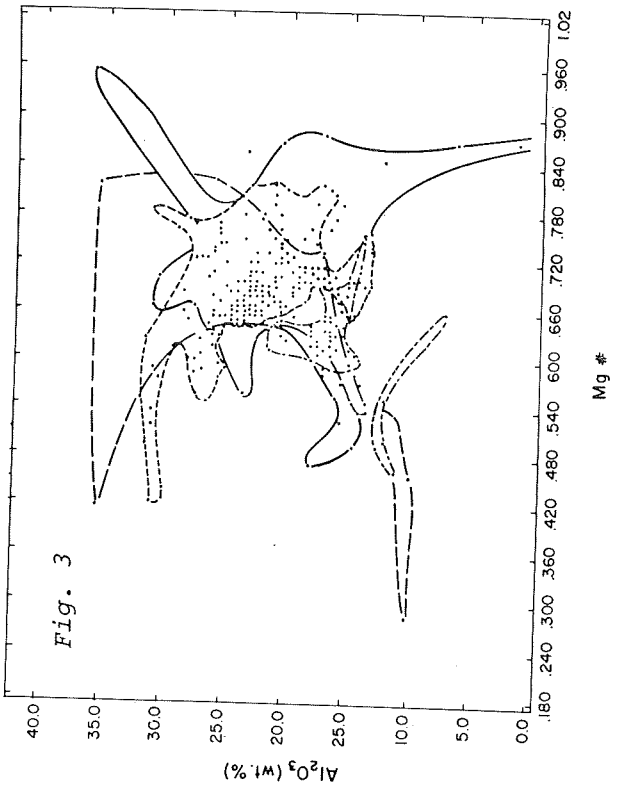

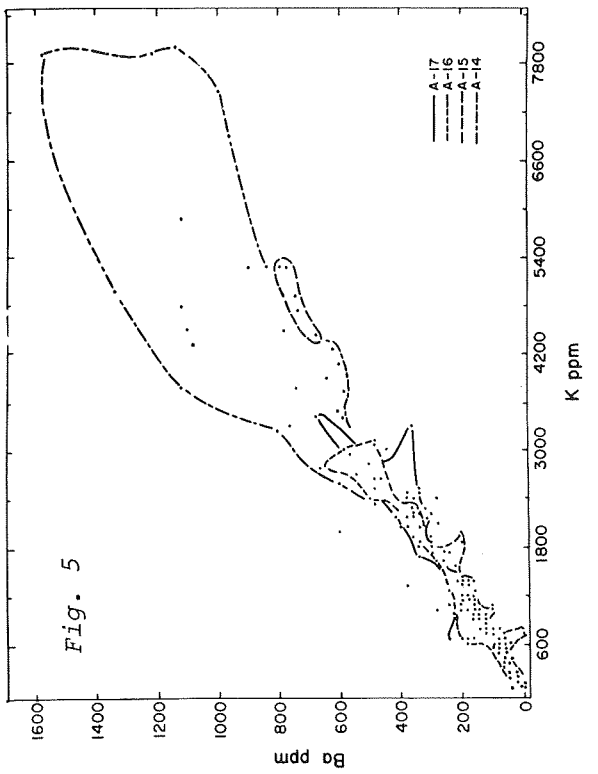

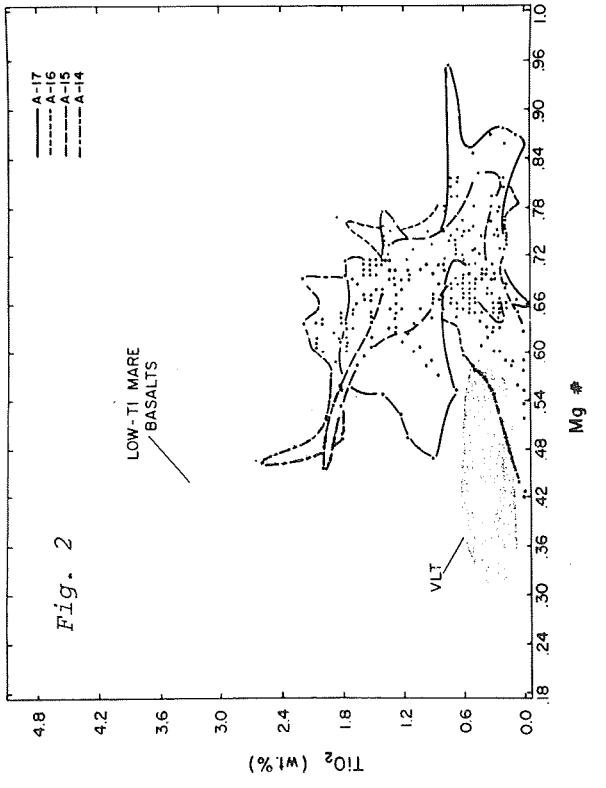

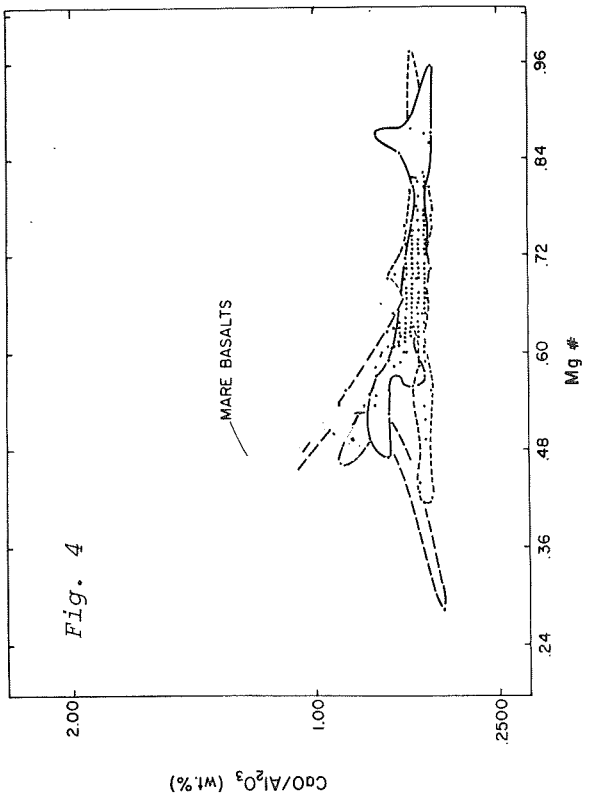

MAGMA OCEANOGRAPHY REVISITED: FORMATION OF THE PRIMITIVE LUNAR CRUSTAL ROCKS. John Longhi, Dept. of Geology, Univ. of Oregon, Eugene,OR 97403

Many investigators, e.g., (1), have proposed that the outer few hundred kilometers of the moon were molten at or soon after accretion, and that solidification of this "magma ocean" produced a gross differentiation of the outer portion of the moon into a plagioclase-rich crust, 60-100 km thick, and an underlying plagioclase-depleted mantle that ultimately is the source region of the mare basalts. Understanding the nature of the differentiation and crust forming processes is the key to understanding not only the subsequent evolution of the moon, but also is a first step in determining the early history of the other terrestrial planets.

The best clues as to the nature of the early lunar differentiation are presumably found in the suite of primitive crustal rocks, which a) are free of meteorite contamination, b) retain textural evidence of a cumulus igneous origin, and c) have isotopic evidence of an age > 4.3 Gyr. These primitive crustal rocks (2) are members of a larger grouping of "pristine" crustal samples (no meteorite contamination) that include KREEP basalts as young as 3.95 Gyr (3). The suite of primitive crustal rocks contains several paradoxical petrological and chemical features which rule out a simple course of crystallization for the most likely parent, a chondritic magma ocean:

1) The primitive rocks fall into two general groups, ferroan anorthosites and Mg-rich cumulates, which are separated from each other by a distinct hiatus on a plot of Mg/(Mg+Fe) in olivine or low-Ca pyroxene versus Ca/(Ca+Na+K) in plagioclase (2). The extent of the hiatus is such that members of the two groups could not have crystallized from the same magma.

2) Within the suite of Mg-rich cumulates, decreasing Mg/(Mg+Fe) in the mafic minerals accompanies decreasing Ca/(Ca+Na+K) in plagioclase -- a normal igneous differentiation trend. In the suite of anorthosites, however, plagioclase composition is nearly constant (<3 mole % variation) and is independent of mafic mineral composition which varies ∿25 mole % in the suite.

3) REE studies (4,5) have shown that despite differences in mineral composition, anorthosites and some Mg-rich cumulate rocks formed from liquids with similar REE patterns: specifically, light REE enrichment and small positive Eu-anomalies. The degree of REE fractionation inferred for these liquids is too extreme to be the result of a single stage of crystallization of an initially chondritic parent and still produce the observed cumulus olivine (6).

4) The crystallization sequence inferred for the primitive crustal rocks, olivine→aluminous-spinel→plagioclase→low-Ca pyroxene→high-Ca pyroxene, is also inconsistent with an initially chondritic Ca/Al ratio in the parent liquid at low pressure.

5) Examination of whole-rock Sm/Ti ratios shows that many of the Mg-rich cumulates, e.g., troctolite 76535, have a strong Ti depletion relative to Sm (7,8), yet lack textural evidence of ilmenite or other Ti-rich phase as a cumulus phase. This feature suggests that there are two subgroups of Mg-rich cumulates: those with strong Sm/Ti enrichments and those with near chondritic Sm/Ti,such as 72415.

6) Two of the Mg-rich cumulates have Rb/Sr internal isochron ages and I $^{87}Sr/^{86}Sr$ values of 4.54±.07, 0.69900±3 (76535) and 4.48±.10, 0.69900±4 (72415) respectively (9,10). It has not been possible to obtain isochron ages for the anorthosites. However, measured $^{87}Sr/^{86}Sr$ ratios calculated backwards 4.5 Gyr have a range of I values of 0.69894±3 to 0.69900±3 (11). These values indicate that some of the anorthosites are older than the dated Mg-rich rocks, while others formed contemporaneously.

MAGMA OCEANOGRAPHY REVISITED

LONGHI J.

7) This chronology is supported by the stratigraphy of the lunar crust suggested by studies of melt-rocks derived from basin-forming impacts (12). These studies indicate that the lunar crust is layered with the upper layers, which formed first, richer in ferroan anorthosite and the lower layers richer in Mg-rich cumulates.

All of these features are explicable in terms of a modified version of the "rockberg" model of crust formation(13). This model also has some interesting implications for the source regions of the mare basalts. If the moon was initially of chondritic composition, such as proposed by (14 - "TB"),and if the melt zone was on the order of 300 (15) to 500 (16)km deep, then following events and processes are proposed:

I) Pre-rockberg stage: Strong cooling and extensive crystallization in the upper layers of a strongly convecting magma ocean; rapid crystallization (mainly olivine) at the base. During this stage quenched crust, olivine, and pyroxene would tend to sink out of the upper layers, leaving behind suspensions of plagioclase floating in iron-enriched, differentiated liquids. Initially, convective energy and superheat available in strongly olivine-normative liquids was sufficient to remelt and assimilate these suspensions. Subsequent crystallization of these contaminated magmas produced differentiated liquids with more fractionated ratios of incompatible elements and with a heavier load of suspended plagioclase than in the first cycle. This process would repeat itself until convection in that region of the ocean became choked off by floating plagioclase. The result would be plagioclase with undifferentiated Ca/(Ca+Na+K) floating in an iron-rich liquid with highly fractionated incompatible element ratios and a positive Eu-anomaly; it is also possible that the crystallization sequence of the contaminated liquids changed from olivine → low-Ca pyroxene→plagioclase to olivine→plagioclase→low-Ca pyroxene(8). Accumulation of plagioclase produced floating anorthositic rockbergs, which coalesced eventually to form a continuous crust.

II) Rockberg stage: Growth of the rockbergs would have had two components : lateral and downward. The lateral component would be the result of continued plagioclase accumulation from differentiated, iron-rich liquids; the downward component would be the result of heat loss through the rockberg. The zone of melt beneath the rockberg would be chemically and thermally zoned between the "cold", plagioclase-rich rockberg and the "hot", olivine-normative magma ocean. Light REE enrichment and positive Eu-anomalies are probable features of liquids in this region. An inevitable consequence of the physical situation is the formation of liquids saturated with olivine and plagioclase ± aluminous spinel(17). Because the rockbergs have a very small mafic component, the Mg/Fe of the underlying liquid would be essentially that of the ocean. Foundering of the rockbergs could have trapped portions of such liquids and led to local accumulations of olivine and spinel within the crust, producing some of the Mg-rich cumulates, e.g., dunite 72415, spinel troctolite 67435.

Heat loss through the top of the magma ocean would have been quickly transferred to the base of the ocean by convection and crystal settling, thus inducing extensive crystallization. Filling in of the ocean at its base would have been more rapid than crustal growth during the rockberg stage. Because mafic crystals would settle into fractionating liquid at the bottom of the ocean as opposed to settling out of fractionating liquid at the top of the ocean, Mg/Fe fractionation for the ocean as whole would be much less efficient than for the upper layers. This is one reason for the hiatus in mineral composition between anorthosites and Mg-rich cumulates.

III) Continuous crust stage: Continued crystallization and infilling, primarily of olivine, at the base of the ocean would lessen the pressure at the

MAGMA OCEANOGRAPHY REVISITED

LONGHI J.

base until pyroxene saturation was reached (approx. at 240 km for an ocean initially 500 km deep of TB composition). Coprecipitation of olivine and low-Ca pyroxene would eventually lead to plagioclase saturation at depth (~150 km -(17)). At this point (67 mole % crystallization) the ocean would be effectively saturated with plagioclase, coalescence of the rockbergs, if not already completed, would rapidly come to completion, and downward growth of the crust would accelerate(18). Rocks formed at the base of the crust would be Mg-rich troctolites, norites, and eventually gabbros. As noted above, separation of a Ti-rich phase is required prior to the final formation of many of these rocks. The absence of cumulus ilmenite or other Ti-rich phase in these rocks suggests that some form of magma mixing operated during this stage as well, i.e., highly fractionated liquids,which had already separated ilmenite, mixed with and contaminated less fractionated liquids, undersaturated with ilmenite. These contaminated liquids would then crystallize troctolites and norites with fractionated Sm/Ti ratios, but no cumulus ilmenite. An important corollary is that ilmenite was crystallizing extensively, albeit locallly, while the ocean as whole was still relatively magnesian and deep. If subsequent accumulation took place, as seems probable, the source regions of the high-Ti mare basalts may be explained as a direct result of magma ocean crystallization without resorting to post-solidification settling of subcrustal ilmenite pods(19). Furthermore, similarity of REE patterns (except Eu) of some Mg-rich rocks, e.g., 78235, with KREEP has been noted (20), and KREEP also has a strong, positive Sm/Ti fractionation(7). It seems worthwhile, therefore, to examine the possibility that a magma mixing process similar to that which produced many of the Mg-rich cumulates eventually produced KREEP.

It is probable that some regions of the moon lagged behind others during development of the crust, i.e., anorthositic"continents" may have developed with a stage III regime beneath them, while other regions of strong convection may still have been in the pre-rockberg stage. Thus, rocks derived by different processes and from different liquids, such as anorthosites and troctolites, may have overlapping ages.

REFERENCES

(1) Taylor S.R. and Jakes P. (1974) Proc. Lunar Sci. Conf. 5th,p. 1287-1305. (2) Warner J.L. and Bickel C.E.(1978) Amer. Mineral.63, 1010-1015. (3) Warren P.H. and Wasson J.T. (1978) Proc. Lunar Planet. Conf. 9th, p. 185-217. (4) Laul J.C. and Schmitt R.A. (1975) Proc. Lunar Sci. Conf. 6th, p. 1231-1254. (5) McKay G. et al. (1979) Lunar and Planetary Science X, p. 804-806. (6) Longhi J. (1978) Proc. Lunar Planet. Conf. 9th, p. 285-306. (7) McKay G. et al. (1978) Proc. Lunar Planet. Conf. 9th, p. 661-687. (8) Longhi J. and Boudreau A.E. (1979) Proc. Lunar Planet. Sci. 10th, in press. (9) Papanastassiou D. and Wasserburg G.J. (1976) Proc. Lunar Sci. Conf. 7th, p. 2035-2054. (10) Papanastassiou D. and Wasserburg G.J. (1975) Proc. Lunar Sci. Conf.6th, p.1467 -1489. (11) Papanastassiou D. and Wasserburg G.J. (1976) Lunar Science VII, p. 665-667. (12) Ryder G. and Wood J.A. (1977) Proc. Lunar Sci. Conf. 8th,p.665-668. (13) Herbert F. et al.(1977) Proc. Lunar Sci. Conf. 8th, p.573-582. (14) Taylor S.R. and Bence A.E. (1975) Proc. Lunar Sci. Conf. 6th, p. 1121-1142. (15) Solomon S.C. and Chaiken J. (1976) Proc. Lunar Sci. Conf. 7th, p.3329-3243. (16) Taylor S.R. (1978) Proc. Lunar Planet. Conf. 9th, p. 15-23. (17) Warren P.H. and Wasson J.T. (1979) Lunar and Planetary Science X, p. 1304-1306 (18) Solomon S.C. and Longhi J. (1977) Proc.Lunar Sci. Conf. 8th, p. 583-599. (19) Kesson S.E. and Ringwood A.E. (1976) Earth Planet. Sci. Lett. 30, 155-163 (20) Winzer S.R. et al. (1975) Proc. Lunar Sci. Conf. 6th, p. 1219-1229.

THE APOLLO 15 HIGHLAND REGOLITH. D. S. McKay, SN6/NASA Johnson Space Center, Houston, TX 77058 and A. Basu, Indiana Univ. Bloomington, IN 47401

Introduction The lunar highlands at the Apollo 15 site are an important key to our understanding of early lunar history. The highlands of the Apennine Mountains are part of the uplifted scarp of the Imbrium Basin and may contain deep, early crustal material. Furthermore the Apollo 15 area contains rays and secondary crater clusters from the large craters Aristillus and Autolycus and is likely to contain highland ejecta from these impacts. Additionally, the intriguing problems of the origin of KREEP basalts (1) can be addressed by studying material from Apollo 15. Finally, the processes of regolith mixing and lateral transport are amenable to investigation at this site because of the proximity of mare basalt to the highland areas. We believe that regolith samples may contain a more varied assemblege of material than breccias because regolith potentially contains remnants of ancient breccias, primitive volcanic and plutonic rocks, and even interplanetary dust, some types of which may no longer exist in fragments large enough to be identified in breccias.

Technique We have analyzed, as part of a larger project of studying the entire Apollo 15 site (2), two of the most aluminous highland soils, 15221 and 15271. We have determined grain size by sieving and Coulter Counter, have made particle identification and counts on 6 grain size ranges from 20 to 500 micrometers, have analyzed a selection of pyroxenes on the electron probe, and have identified a representative number of grains in the one micrometer size range. Grain size and maturity data are given in Table 1, preliminary pyroxene analysis are presented in (2), modal data on 6 grain size fractions is presented in Table 3 and SEM/EDXA data are given in Table 4 which also shows mare-rich core sample 15010,1131 for comparison.

Discussion The samples are both relatively mature by all indicies. This has the disadvantage that much of the regolith material is tied up in agglutinates and vitric breccias but has the decided advantage that these samples are likely to contain very old components. The moon has certainly had a regolith since its earliest history and some highly diluted component of this regolith may still be preserved in its present mature regolith.

One of the most interesting results of our studies is a preliminary indication that the micron size particles differ considerably in modal abundance (Table 3) from even the finer fraction of the petrographically identified fragments (20 micrometers). The difference is mainly a pronounced increase in the plagioclase fraction in the highland soils. This difference is real and is documented by individual photographs of the grains and by EDXA spectra, although in some case we are not able to determine whether the plagioclase composition particles are crystalline. This difference in the micrometer size fraction may be related to the hint of a mode in the grain size data around 8 micrometers. Perhaps material finer than about 10 micrometers becomes progressively enriched in plagioclase and is derived either by a percularity in the fracture properties of plagioclase, or more interestingly by a different transportation mechanism selective to that grain size which has enriched these fine grain fractions in highland plagioclase. We are currently pursuing this problem.

From Table 2 it is interesting to note that identifiable ANT fragments are exceeded by both mare basalt fragments and KREEP basalt fragments. Furthermore, KREEP basalt is almost as abundant as mare basalt. Additional ANT may be present in the agglutinates and glass. The ropy glass fragments are unusually abundant and are more common in the coarser sizes as opposed to the green glass. Ropy glass may be ray material from large highland craters. Olivine shows a mode at about 100 micrometers perhaps reflecting the two populations noted chemically (2). Pyroxene analyses (2) show a minimum of identi-

THE APOLLO 15 HIGHLAND REGOLITH

D. S. McKay and A. Basu

fiable mare pyroxenes and a large number of pyroxenes which must be derived from KREEP basalts.

Conclusions (a) KREEP is an important component of the highlands at Apollo 15 and contributes perhaps an order of magnitude more pyroxene compared to the ANT suite. (b) It seems very likely that volcanic KREEP flows and perhaps their plutonic equivalents are present in the vicinity of the Apollo 15 site, perhaps underneath or interbedded with thin mare flows. We are actively searching for KREEP pyroclastics. (c) ANT suites may be mainly represented by coarse grained dunites or troctolites which are now present in the regolith as olivine fragments, ropy glasses, and glass dissolved in agglutinates. (d) Regolith may contain a distinct component of "exotic" material in the finest grain sizes less than 10 micrometers. There is some chemical evidence for this, particularly at the Apollo 17 site (3). At the Apollo 15 site the "exotic" material may be from the ANT suite rather than from a KREEP-rich source as at Apollo 17.

References:

(1) Spudis P. D. (1978) Proc. Lunar Planet. Sci. Conf. 9th, p. 3379-3394.
(2) Basu A. and McKay D. (1979) Proc. Lunar Planet. Sci. Conf. 10th (in press).
(3) Laul J. C., Lepe I. E., Vaniman D., and Papike J. (1979) Proc. Lunar Planet. Sci. Conf. 10th (in press).

Table 1. Maturity Indicies of Subcentimeter Soil

	15521	15271
$M_z(\phi)$	4.28	4.12
[1] I_s/FeO	63	63
% < 20 micrometers	26.9	23.4
Sorting coefficient	2.42ϕ	2.35ϕ

[1] Data from R. Morris

See Table 2 on Next Page

Table 3. Modal Analysis of Micrometer-Size Grains (%)

	15221,68 (highland)	15010,1130 (mare)
Plagioclase	46	21
Pyroxene	4	17
Silica phase	8	2
Olivine	1	1
Agglutinates + glass	39	57
Other	2	2
	100	100

Table 2. Condensed Modal Analysis (%)
Average of 15221,68 and 15271,115
Each Size Category Represents Approximately 600 Grains

Size (μm)	250-500	150-250	90-150	75-90	45-75	20-45	Weighted Average 20-500
Plagioclase	3.6	4.9	7.4	13.6	12.1	12.9	8.6
Pyroxene	4.4	4.1	8.5	11.6	16.0	21.1	12.8
Olivine	1.8	0.7	3.1	2.9	2.6	1.8	2.3
ANT	4.5	2.2	2.1	0.8	0.8	0.2	1.5
Mare Basalts	2.4	4.6	2.1	4.6	3.4	3.3	3.3
KREEP Basalts	3.5	2.2	2.2	1.9	2.6	1.5	2.2
Vitric Breccias	18.7	12.9	12.1	11.9	9.9	9.0	11.6
Annealed Breccias	2.7	3.2	1.8	2.0	3.1	0.8	2.1
Agglutinates	48.3	54.3	49.8	37.5	35.5	27.5	40.0
Ropy Glass	7.3	3.0	4.1	3.2	2.1	1.5	2.2
Green Glass	0.6	2.7	2.0	2.9	4.1	6.6	3.7
Other Glass	2.7	4.2	3.5	4.9	6.4	7.5	5.4

TRACE ELEMENTS IN PLAGIOCLASE FROM THE LUNAR HIGHLANDS

Meyer, Charles Jr. NASA/Johnson Space Center, Houston, TX 77058

It is useful to compare the trace element composition of plagioclase from the lunar highlands with a hypothetical composition of the first plagioclase that would have formed during the crystallization of a lunar magma ocean. High purity lunar anorthosites are the main reason for the concept of magma oceanology. (1,2,3). Of course, it is doubtful whether one can expect to identify pieces of the original plagioclase that floated from the lunar magma ocean. Metamorphic processes in the early hot crust and the extensive early bombardment of the crust probably reformed any original minerals. On the other hand, several very old ages have been reported for small pieces of plagioclase from lunar breccias (4,5,6). The ion microprobe is a useful technique to measure the trace element composition of these small inclusions and compare them with plagioclase from lunar anorthosites. In this way a larger number of pieces of the ancient lunar crust may be identified.

In this study, the ARL-IMMA was used to measure Li(7), Mg(24), K(39), Ti(49), Fe(54), Sr(88) and Ba(138) in 20 μm spots using a O(16) primary ion beam of 1 nanoampere. Standards analysed by isotope dilution were used to calibrate the measurements and Si(30) was used as an internal standard (7,8). Plagioclase inclusions in breccias were also analysed by line scan to study zoning and establish homogenity (figure 1). Reproducibility was poor for K and an Al_2^+ interference at 54 presented meaningful Fe analyses. An interference by $NaAlCaO_3$ at 138 limited Ba analyses to about 10 ppm. Ti is limited to about 50ppm because of hydride interference at 49 and NaMg interference at 47. Plagioclase in lunar anorthosites were analysed several months apart (a and b in Table) and the values were in good agreement.

Results — Ion Probe Analyses of Plagioclase (ppm)

	Li	Mg	Ti	Sr	Ba
Distribution Coefficient	0.5	.065*	.038	1.6	0.2
First Plagioclase	10 ppm	840 ppm	230 ppm	194 ppm	8 ppm
Anorthosites					
15362 a	1.5	300			40
b	2.2	288	91	200	26
15415 a	2.6	300			13
b	1.7	300	91	190	10
60025 a	1.5	500			20
b	1.3	448	85	197	11
60618	4	800			16
62237 a	4	700			10
b	2.7	370	75	203	10
62255 a	2.6	500			20
b	2.3	534	214	181	22
65315 a	2	600			10
b	1.8	616	150	208	8
67415 a	6	650			100
b	6	637	203	300	103
67075	3.2	300			16
69955 a	1.0	750			12
b	1.7	781	200	275	14

*Mole percent

TRACE ELEMENTS IN PLAGIOCLASE FROM THE LUNAR HIGHLANDS

MEYER, CHARLES JR.

Plagioclase Inclusions

		Li ppm	Mg ppm	Ti ppm	Sr ppm	Ba ppm
60315	a	6.6	700	182	317	53
	b	9.3	945	320	291	30
	c	10.4	1233	545	372	107
	d	13	1171	155	346	29
	e	9.2	822	246	288	16
	f	9.2	660	150	278	17
65015	a	6.5	600			
	b	7.0	550			
	c	7.8	800			
	d	8.6	730			
	e	4.5	700			
	f	4.2	500			
	g	5	400			
72435	a	13	534	412	333	150
	b	33	1360	600	440	230
	c	16	290	192	352	340
	d	9.7	1192	198	300	125
76215		10	800			90
77135		7	480			87
		14	290			130
78315		27	1400	440	900	30-120
14310		14	1000	166	250	180

In order to calculate the hypothetical composition of the first plagioclase to form from a lunar magma ocean, I have used distribution coefficients (plagioclase/liquid) from (9,10,11,12) and the composition of the liquid when plagioclase first forms (1188°C) from the model of Longhi(2).

The composition of Mg and Ti are less than calculated. This is probably due to metamorphic annealing. The value for Sr is in agreement with 15415 and 60025 because this is required by the model of Longhi. The values for Ba are in agreement, but then there are a range of Ba distribution coefficients!

Consider the Ti content of the first plagioclase. If only olivine preceeded plagioclase (2), the Ti content of the liquid would be about 1% and the Ti in the plagioclase would be about 230 ppm. On the other hand, if large amounts of pyroxene crystallized before the first plagioclase (3), then there would be considerably less Ti available at the time of first plagioclase formation. In this way, Ti might be a test of the various models of magma oceanology.

Consider the Li content of the first plagioclase. Li usually co-varies with the other incompatible trace elements (13). However, distribution coefficients for this element are not well known. From what little is known, the Li in lunar anorthosites seems too low. Perhaps it substitutes for Mg in early silicates or is depleted for the same reason Na is.

TRACE ELEMENTS IN PLAGIOCLASE FROM THE LUNAR HIGHLANDS

MEYER, CHARLES JR.

Old ages and low initial Sr have been found for small plagioclase inclusions in KREEP rich poikiolitic meltrocks 65015 and 72435 (14,15). These inclusions are neither isotopically nor chemically in equilibrium with a melt the composition of these rocks (7). Ion probe traverses show that they are unzoned and do not have diffusion gradients at the boundary with the melt. These poikiolitic meltrocks must have cooled rather rapidly, perhaps in a melt sheet of a medium size impact crater. The ion probe analyses show that these inclusions are higher in trace element content than the anorthosites analyzed.

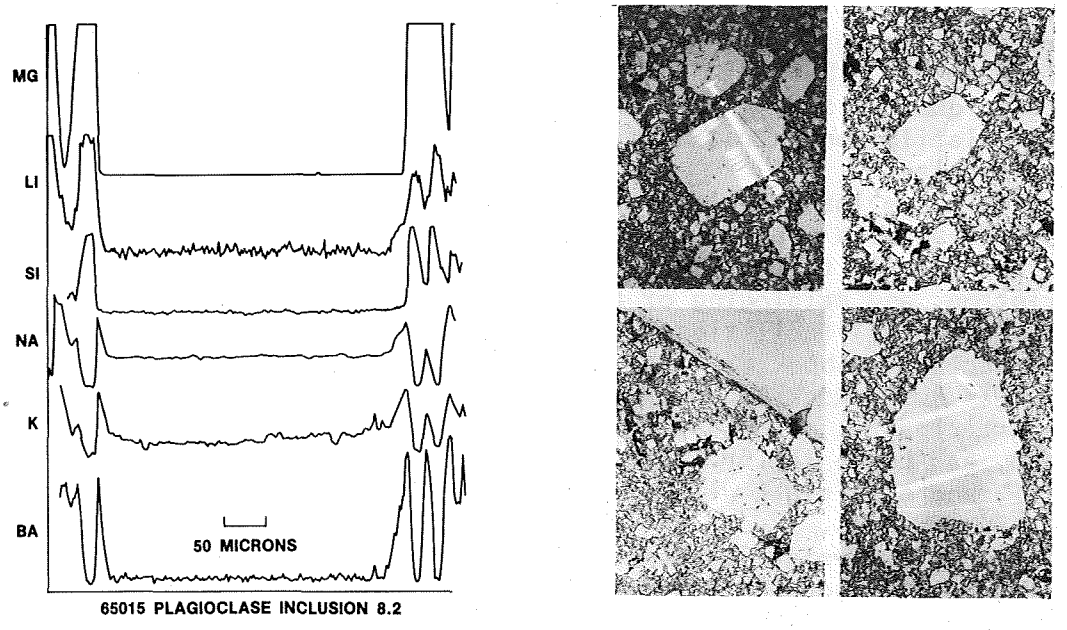

Figure 1. Line Profile by ion probe across plagioclase inclusions in 65015. Inclusions are 300-500 microns across.

1) Smith, et. al. (1970) PLSC 1st 897, Wood, et. al. (1970) PLSC 1st, 965
2) Longhi (1978) PLPSC 9th, 285, Hubbard et. al. (1971) EPSL 13, 71
3) Warren & Wasson (1979) Lunar Plant. Sci. X, 1304 (abs).
4) Jessberger, et. al. (1974) Nature 248, 199
5) Dominik & Jessberger (1978) EPSL 38, 407
6) Warren & Wasson (1977) PLSC 8th, 2215
7) Meyer 1974 PLSC 5th, 685
8) Meyer 1978 PLPSC 9th, 1551
9) Longhi et. al. (1976) PLSC 7th, 1281
10) Bougault & Hekinian (1974) EPSL 24, 249
11) McKay & Weill (1976) PLSC 7th, 2427
12) Phillpotts and Schnetzler (1970) GCA 34, 307
13) Dreibus et. al. (1976) PLSC 7th, 3383
14) Papanastassiou & Wasserburg EPSL 17, 52
15) Papanastassiou & Wasserburg PLSC 6th, 1477

RUSTY ROCK CONSORTIUM - VAPOR: PETROGRAPHIC FRAMEWORK FOR CLASTS OF 66095; R. W. Meyer, J. R. Garrison, Jr., and L. A. Taylor, Department of Geological Sciences, The University of Tennessee, Knoxville, Tennessee 37916

A most pronounced general fact concerning the moon is its great depletion in volatiles. The nature and origin of the volatile components still present in lunar rocks become then requisite data for modeling the outgassing and early evolution of the moon. Particularly noteworthy is the Apollo 16 anorthositic breccia 66095. This breccia, nicknamed "Rusty Rock" because of the abundance of FeOOH, contains anamolous abundances of the volatiles: Br, Cl, F, Bi, Cd, Pb, Tl, Zn, etc. It is the most volatile-rich of all lunar rocks. The relative proportions of volatiles in this breccia mirror those in many highland rocks, albeit of higher concentration. Rock 66095 is paramount both in its uniqueness and in its basic similarity to other terra breccias with lesser volatile concentrations, and it may be viewed as a paradigm for many other breccias.

Within the last couple of years, the importance of breccia "pull-apart" endeavors has been realized. Such an effort is now being performed on 66095. The first step in this endeavor has been undertaken, namely a complete mapping, description, and cataloging of the various portions of this rock as they exist in the Curatorial Facilities. This work has recently appeared in print as NASA Breccia Guidebook #2 (1). We have also established a well-rounded consortium -- Rusty Rock Consortium - VAPOR (Volatiles and Phases of Rust) -- with participants: E. Anders, S. Epstein, R. Housley, J. C. Laul, L. Nyquist, G. Reed, and L. A. Taylor. The "pull-apart" of breccia 66095 has begun (see also 5), and each clast will be attacked with the various expertises of the consortium members.

The unique (volatile-rich) rock 66095 is a large (1185g) medium gray, friable, partly shock-melted breccia composed of a fine-grained subophitic basalt matrix and of highly recrystallized to shocked, unannealed relict clasts of anorthosite, anorthosite-troctolite, plagioclase, and basalt. Despite the presence of numerous planar to slightly irregular fractures and blind veins filled with black glass (2), there is a lack of vesicles or cavities. The peculiar feature of this rock is the abundance (both on the surface and deeper within the chipped parent) of "rusty" stains of FeOOH, akaganeite, surrounding the FeNi metal grains (3). Since only water with a terrestrial signature (4) has been found present in the FeOOH phase, the addition of volatiles to this rock is postulated to have been an essentially anhydrous event.

The dispersion of elemental analyses of 66095 is a direct reflection of both the diversity of clast types and their distribution within the rock. Whole rock chemistry is a meaningless concept with the restricted sample sizes used. In fact, as pointed out by Garrison and Taylor (1) the REE data show Eu anomalies; however, both positive and negative anomalies are represented.

During our megascopic examination of 66095 for the guidebook, we (1) tentatively divided the clasts into three major types: 1) anorthosite-troctolite (40%), 2) plagioclase (both shocked and recrystallized = 35%), and 3) basalt (25%). Microscopic examination of thin sections coupled with EMP analyses have permitted us to further divide the first clast type into 1a) anorthosite, 1b) cataclastic anorthosite-troctolite, and 1c) coarse-grained anorthosite-troctolite. This five-fold clast classification scheme and the chemical data pertaining to the major phases are presented herein as a matrix along with other petrographic characteristics which provide a summary of the study.

Figure 1 is a plot of olivine versus plagioclase compositions (i.e., Fo vs. An). Each point represents the average of 10-30 individual analyses of

RUSTY ROCK 66095

Meyer, Garrison and Taylor

CLAST TYPE	TEXTURE	MODES	MIN COMPS
ANORTHOSITE	Coarse-grained Granulitic (various degrees of shock) Plag 10-500μm; Ol 1-100μm	Plag 90-100% Ol 0-10%	An 91-99 Fo 75-80
ANORTHOSITE-TROCTOLITE	Coarse-grained Equigranular Plag 450-1600 μm; Ol 20-200 μm.	Plag 90-95% Ol 5-10%	An 98 Fo 61-69
	Cataclastic - Stringers Plag 30-300 μm; Ol 5-200 μm	Plag 80-95% Ol 5-20%	An 91-98 Fo 78-81
PLAGIOCLASE	Coarse-grained (various degrees of shock up to Maskelynite) Plag .04-1cm	Plag 100%	An 91-99
BASALT	Fine-grained Porphyritic Plag 10-300 μm, Ol + Px 10-100 μm as Phenocrysts	Matrix <50% (Plag + Px)	An 92-95 Fo 74-76

each phase in one clast. The plagioclase clasts are monomineralic and cannot be included here; however, the feldspar in the plagioclase clasts are possibly bimodal in composition about An 95. The olivines in the 4 clast types containing them were analyzed for CaO. A plot of these data resulted in a delineation of the clasts as shown in Figure 2. There is a distinct difference in CaO contents of the cataclastic versus coarse-grained anorthosite-troctolite clasts. The cataclastic clasts actually consist of stringers and pods of coarse plagioclase and olivine which have been severly crushed. This type of crushed clast is very common in certain Apollo 16 cores (S. Nagle, Pers. Comm.). Investigation of these clasts continues.

Our first attempt at a modeling of the significance of the clasts in 66095 is discussed in an accompanying paper (5). Therein, we present a mixing model which can explain many of the features of volatile enrichment in 66095, as well as those in Apollo 16 rocks and soils, in general.

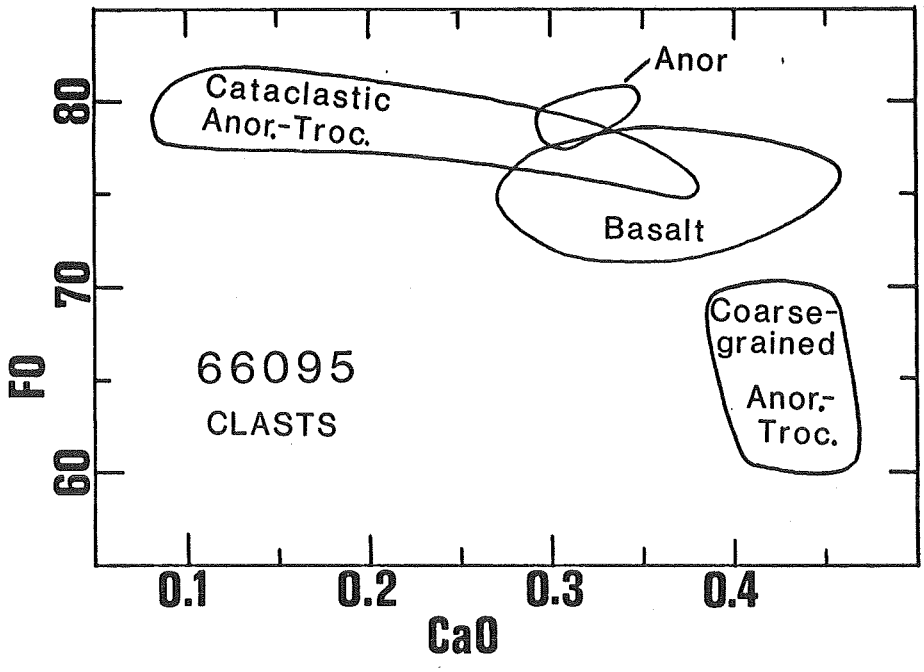

Fig. 1

RUSTY ROCK 66095

Meyer, Garrison and Taylor

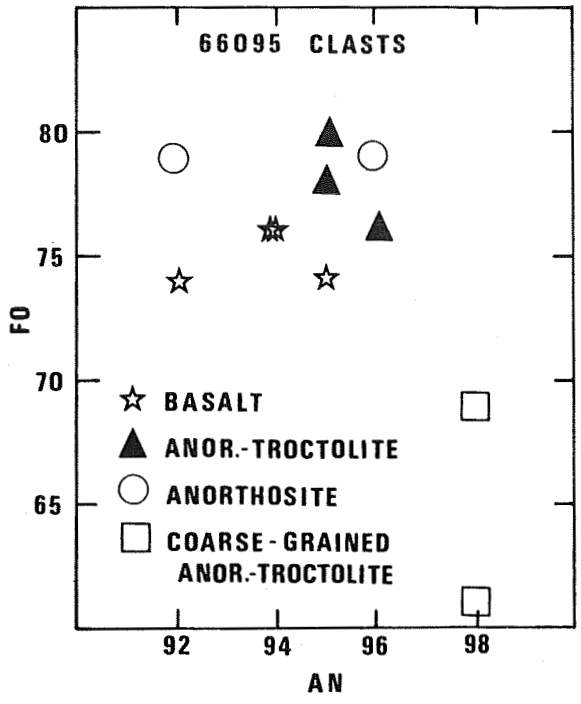

Fig. 2.

REFERENCES
(1) Garrison & L. Taylor, 1979, JSC 16198; (2) Bass, 1972, Apollo 16 PET; (3) L. Taylor et al., 1974, PLSC 5, 743; (4) Epstein & H. Taylor, 1974, PLSC 5, 1839; (5) Garrison & L. Taylor, 1979, this volume.

PATTERN RECOGNITION STUDIES ON HIGHLAND REFERENCE SUITE ROCKS AND RELATED LUNAR SAMPLES. C.B. Moore*, M.L. Parsons*, B. Rock*, and D.D. Pratt†. *Arizona State University, Tempe, AZ 85281, †Ripon College, Ripon, WI 54971

The chemical characteristics of analyzed highland reference suite rocks and related lunar samples were studied using pattern recognition techniques.

Pattern recognition is a computer based set of mathematical and statistical tools used to find correlations in large data bases (1). Each variable (in this case, the measured value for each element) is considered a separate dimension.

Major, minor, and trace elemental analyses for available highland suite rock samples were chosen from the computerized lunar sample data base tapes compiled by Warner at the NASA Johnson Space Center. Data was autoscaled (giving the values for each element a mean of zero and a standard deviation of one) and six pattern recognition techniques were investigated: hierarchical clustering (HIER), minimal spanning tree (TREE), eigenvector projections (KARLOV), nonlinear mapping (NLM), K nearest neighbors (KNN), and two dimensional plotting of variables (VARVAR). Results from these six methods were compared to define sample groups.

HIER. HIER (hierarchical clustering) produces a dendrogram by comparing intersample distances in n-dimensional space. Similarity values, based on these distances are shown with a value of one representing identical analyses.

KARLOV. Karhunen-Loeve eigenvector plots of the two axes in n-dimensional space which contain the most variance are used to visualize these categories and their relative positions.

TREE. A tree connecting samples similar in composition was constructed such that samples on opposite ends of the tree were most dissimilar. Distances shown are somewhat distorted due to the necessity to represent the n-dimensions into two, but again identical categories were found.

NLM. Nonlinear mapping reduces the data from n to two dimensions by minimizing relative intersample distance errors. Results were similar to those obtained above.

KNN. The k nearest neighbors in n-dimensions can be used to study, in more detail, the relationship between samples most similar in composition.

VARVAR. Plots of simple element versus element data can be made after selecting which analyses give the most separating information. The best species were found to be TiO_2 and Dy. A plot of these two species defined categories almost as well as the KARLOV plot, loosing some information along category boundaries.

The variety of mathematically independent techniques available with pattern recognition provides methods to not only define categories, but further to check those after they have been defined. Samples whose categories are unknown can then be added to determine their classification.

Utilizing the above methods, individual samples can be grouped with other samples with similar affinities. Samples from different mission sites did not overlap. Most groups contained rocks with the same petrologic name. An exception was an Apollo 16 group containing 67455, light matrix breccia; 67915, dark matrix breccia; 68415, feldspathic basalt. Pattern recognition indicated that they all had similar chemical affinities. The elements or species most important in the separation of categories in order of importance were Sm, MgO, TiO_2, Ce. (1) Pratt, D.D., Moore, C.B. and Parsons, M.L., (1976) Lunar Science VIII, p. 784-786.

PATTERN RECOGNITION STUDIES

Moore, C.B.

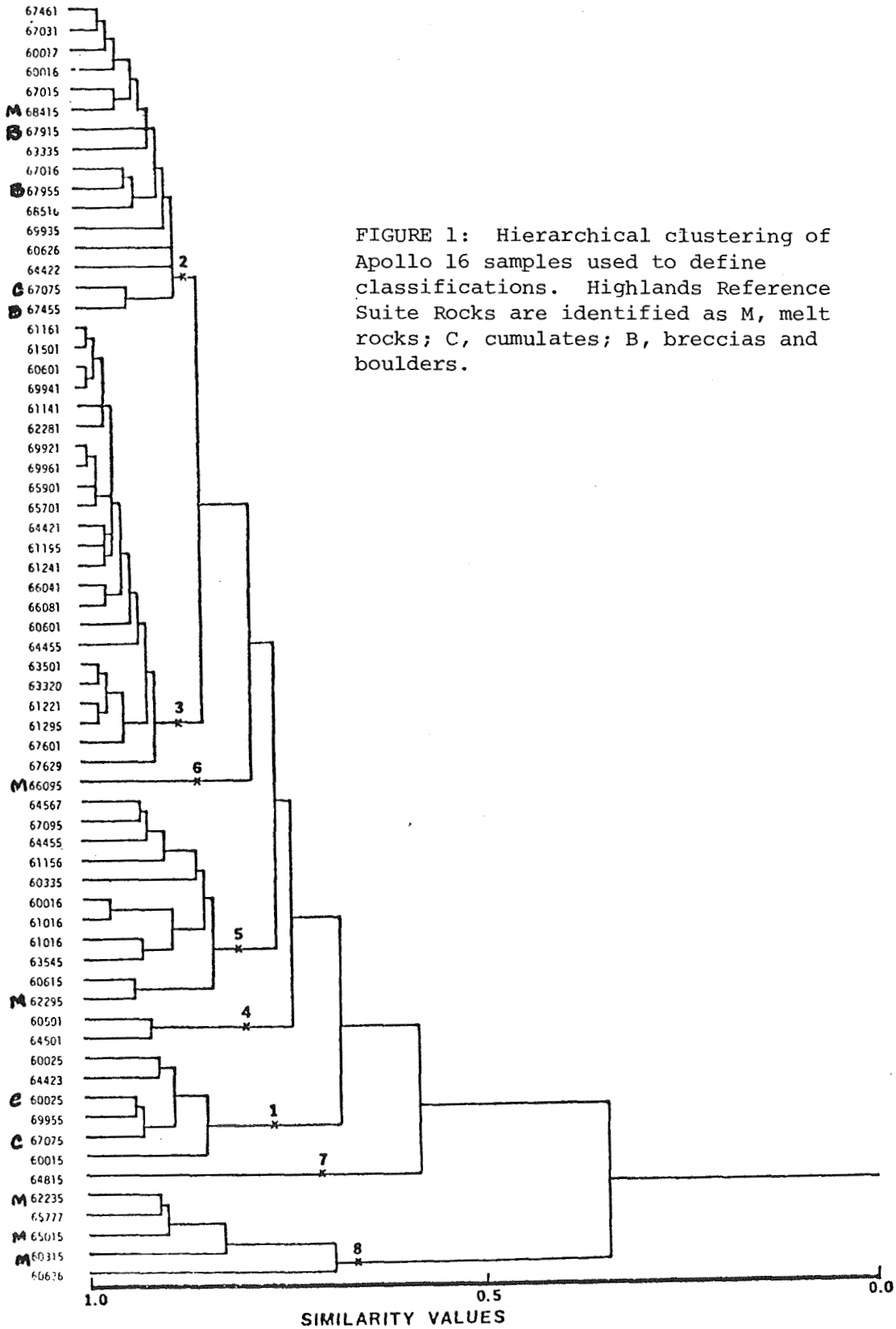

FIGURE 1: Hierarchical clustering of Apollo 16 samples used to define classifications. Highlands Reference Suite Rocks are identified as M, melt rocks; C, cumulates; B, breccias and boulders.

PRISTINE TROCTOLITES AS POSSIBLE SOURCE ROCKS FOR IGNEOUS APOLLO 15 KREEP. Marc D. Norman, Northrop Services, Inc., Houston, TX 77034

KREEP as a chemical component is present in most polymict lunar breccias and is primarily responsible for the incompatible element abundances in these rocks. Pristine fragments of igneous KREEP basalt occur in Apollo 15 soils and as clasts in Apollo 15 and 17 breccias. These are the only samples of genuine nonmare volcanics in the Apollo collection.

The purpose of this paper is to determine whether any of the rock types in the currently recognized suite of pristine highland rocks can represent a suitable source region for igneous Apollo 15 KREEP basalt. Geochemical models relating these pristine crustal cumulates to igneous Apollo 15 KREEP via simple partial melting mechanism will be tested. Apollo 17 KREEPy basalts will not be discussed. Walker et al. (1) have shown that partial melting of ANT-suite crustal rocks can produce liquids with major element chemistries similar to KREEP basalts. To date most of the proposed source rocks for KREEP have been polymict with chemistries produced by impact mixing of various lunar and extra-lunar materials. Since most of these breccias were apparently assembled during the "terminal cataclysm" ∿3.9-4.0 b.y. ago, they could not represent suitable source regions for roughly contemporaneous KREEP volcanics. However a fairly large collection of pristine rocks and clasts, most of which are probably samples of the ancient lunar crust, have been recognized and characterized (2,3,4,5,6). These samples could include suitable source regions for igneous KREEP basalts.

Variations in major and trace element chemistry in the suite of igneous Apollo 15 KREEP basalts have been reviewed by Irving (7) who concluded that low-pressure fractionation of plagioclase and low-Ca pyroxene could account for the observed range in compositions. The parent liquid probably had a composition near the olivine-plagioclase-pyroxene peritectic (point B, Fig.1). One fragment of Apollo 15 KREEP basalt (15102,2-11) has a bulk composition near the peritectic (Fig. 1) (7,9). This fine-grained fragment has a higher Mg/Fe and lower SiO_2 than other members of the Apollo 15 KREEP basalt suite and also has the same (Mg/Mg+Fe) atomic (Mg*) as that calculated for a parent to 15386 (10). 15102,2-11 is thus a plausible choice as a parent magma of the Apollo 15 KREEP basalt suite.

The largest and best-characterized sample of igneous Apollo 15 KREEP (15386) has a major element chemistry that places it along the pyroxene-plagioclase cotectic (Fig. 1). A composition along this line is not likely to represent a direct partial melt of an olivine-pyroxene-plagioclase source region. Rather it probably results during some intermediate stage of crystal-liquid fractionation. Assuming a genetic relationship between 15386 and 15102,2-11 which involved the separation of low-Ca pyroxene and plagioclase, the amount of fractionation can be calculated using a least-squares mixing program. 15386 composition is from (3), 15102,2-11 from (9), and minerals are core compositions from 15386. These calculations show that the removal of 27% low-Ca pyroxene and 20% plagioclase from 15102,2-11 gives a good fit to the 15386 composition (chi^2 = 1.08). Using these proportions of fractionating minerals and appropriate K_d's, the trace element

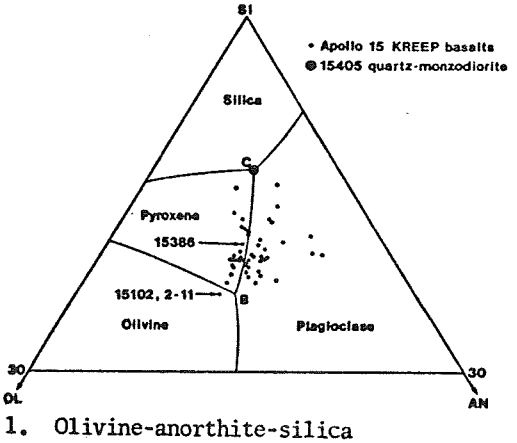

Fig. 1. Olivine-anorthite-silica pseudoternary phase diagram. Adapted from (7).

abundances of this 15386 parent liquid were calculated (plotted in Fig. 2 and 3 as 15386 Pcalc). These elemental abundances were then compared with those produced by melting various pristine highland rocks.

Several different types of pristine highland rocks have been recognized including anorthosites, troctolites (± spinel), norites, dunites, and a "feldspathic lherzolite". Because an olivine-pyroxene-plagioclase assemblage is required to produce peritectic (point B) liquids upon melting, only the troctolites are suitable as potential source rocks for Apollo 15 KREEP; anorthosites, dunites, and norites are excluded. Pristine norites have high SiO_2 (~50 wt %) and usually possess free silica and no olivine; thus they would not produce peritectic (point B) liquids upon melting.

Pristine troctolites do provide the necessary olivine-pyroxene-plagioclase assemblage but the amount of pyroxene is usually small (<5%). One particular pristine troctolite clast in breccia 15455 does contain a significant amount of low-Ca pyroxene (~11 mode %, 12.6 norm %) (4). This clast is especially attractive as a possible source rock since it is found in a breccia which was probably Imbrium ejecta (11) and was thus derived from a region spatially associated with the Apollo 15 KREEP basalts.

Trace elements. Figs. 2 and 3 show that most of the trace element characteristics of 15386 can be modeled by small degrees (7%) of equilibrium partial melting of the 15455 troctolite followed by fractionation of low-Ca pyroxene and plagioclase from the peritectic liquid (15386 Pcalc). The most

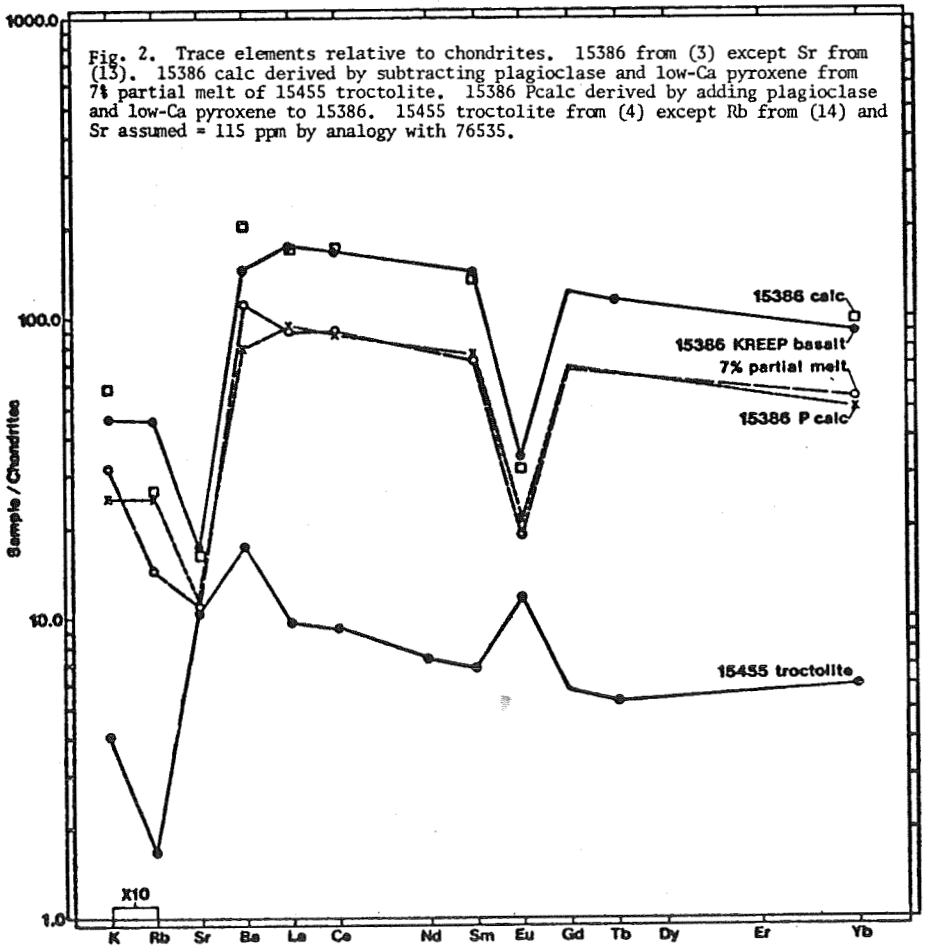

Fig. 2. Trace elements relative to chondrites. 15386 from (3) except Sr from (13). 15386 calc derived by subtracting plagioclase and low-Ca pyroxene from 7% partial melt of 15455 troctolite. 15386 Pcalc derived by adding plagioclase and low-Ca pyroxene to 15386. 15455 troctolite from (4) except Rb from (14) and Sr assumed = 115 ppm by analogy with 76535.

PRISTINE TROCTOLITES

Norman, M.D.

serious difficulties with the trace element model concern Rb and Ti, whose calculated abundances are low compared to Apollo 15 KREEP.

Although no Rb-Sr isotope data are available for the 15455 troctolite, it seems likely that the clast would possess a low $^{87}Sr/^{86}Sr$, similar to other pristine anorthosites and troctolites. Such a low ^{87}Sr abundance would rule out the troctolite as a source of the more radiogenic Apollo 15 KREEP basalt (12) unless disequilibrium processes were active.

Major elements. Although the 15455 troctolite has a Mg* = 0.83, the small amount of melting required by trace element data also produces a magma that is too Fe-rich (Mg* = 0.60) compared to that necessary for a peritectic melt parental to Apollo 15 KREEP basalt (Mg* = 0.72 (10)). (15102,2-11, the proposed parental composition, has an Mg* = 0.74.) For a troctolite to have been a suitable source region it must have had an Mg* = 0.90 (slightly lower with increasing amounts of pyroxene). Several pristine troctolites and spinel troctolites (e.g. clasts in 15445, 67435, 72705 and 76255) have olivine $\sim Fo_{90}$ so it is not unreasonable to assume that a source with the required Mg*, as well as appropriate modal and trace element abundances, could have existed.

Conclusions: (1) Most of the geochemical characteristics of igneous Apollo 15 KREEP can be successfully modeled by small degrees of melting of a source region approximating known pristine troctolites. Such a source would be mineralogically and chemically similar to the 15455 troctolite clast although somewhat more magnesian. (2) The major problem encountered by such a model appears to be the low Rb contents of pristine troctolites in general and the 15455 troctolite in particular. Such Rb-poor rocks probably could not have produced the more radiogenic KREEP basalts unless isotopic disequilibrium was involved.

Fig. 3. Transition metal abundances relative to chondrites. Symbols and sources of data same as Fig. 2.

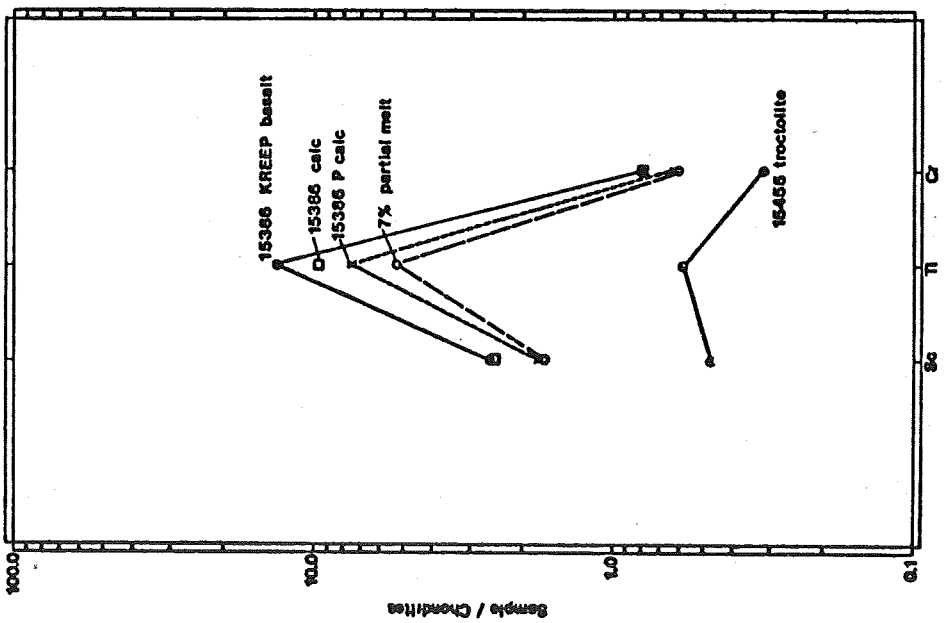

References: (1) Walker et al. (1973) EPSL 20, 325. (2) Warren and Wasson (1977) PLSC 8, 2215. (3) Warren and Wasson (1978) PLPSC 9, 185. (4) Warren and Wasson (1979) PLPSC 10, in press. (5) Anders (1978) PLPSC 9, 161. (6) Norman and Ryder (1979) PLPSC 10, in press. (7) Irving (1977) PLSC 8, 2433. (8) Powell et al. (1973) PLSC 4, 445. (9) Basu and Bower (1976) PLSC 7, 659. (10) McKay and Weill (1976) PLSC 7, 2427. (11) Ryder and Bower (1977) PLSC 8, 1895. (12) Nyquist et al. (1975) PLSC 6, 1445. (13) Hubbard et al. (1974) PLSC 5, 1227. (14) Ganapathy et al. (1975) PLSC 4, 1239.

AGE AND REE ABUNDANCES OF ANORTHOSITIC NORITE FROM 15455. L. Nyquist[1], H. Wiesmann[2], J. Wooden[2], B. Bansal[2], and C.-Y. Shih[2] ([1]NASA-Johnson Space Center, Houston, TX 77058; [2]Lockheed Electronics Co., Inc., Houston, TX 77058)

Anorthositic norites/gabbros are widely accepted as an important constituent of the lunar highlands crust. However, their chronology and petrogenesis is only poorly understood. This situation is due in large part to the obscuration of compositional and isotopic characteristics by impact processes. Low siderophile element contents and petrographic criteria indicate that the anorthositic norite clast in 15455 is pristine (1,2,3,4). Ryder and Bower (4) have concluded that 15455 and its twin 15445 are the best samples of deep crustal material excavated by the Imbrium event. We have begun a reexamination of the compositional and isotopic data for these rocks. The work reported here represents the first efforts of the Norite Consortium as well as a continuation of earlier studies by our PI-ship and also by the Imbrium Consortium.

Our sample 15455,228 was carefully selected in the RSPL to be free of matrix material and to be entirely anorthositic norite lithology. We received a 2.1 gm allocation which we subdivided for analysis by the various members of the Norite Consortium. A 1.1 gm portion was homogenized by crushing to pass a 100 mesh sieve. A 46 mg portion was analyzed for alkalis, alkaline earths, REE, and $^{87}Sr/^{86}Sr$. A second bulk sample from another 0.5 g portion was analyzed for Rb, Sr, $^{87}Sr/^{86}Sr$, Sm, Nd and $^{143}Nd/^{144}Nd$. Plagioclase and pyroxene mineral separates were prepared by mechanical means without exposure to liquids of any kind. These separates were analyzed for K, Rb, Sr and $^{87}Sr/^{86}Sr$.

Chondrite-normalized REE data for 15455,228 are shown in Fig. 1. Previous analyses of 15455,20 (5) and 15455,70 (6) are shown for comparison as are analyses of anorthositic norite 15445,17 (7) and 15445,104 (8). REE abundances are about 10x chondritic with the exception of 15455,20. We suggest that the 15455,20 abundances were severely biased by the selection of white material as described by (5). The abundance pattern is clearly dominated by plagioclase. The abundance patterns of the other samples are generally similar to each other. Slight variations in pattern shape are probably the result of variations in proportions of cumulus plagioclase and orthopyroxene, and trapped parental liquid. Of those samples with similar REE abundances, the abundance pattern of 15455,228 decreases most uniformly with increasing atomic number. We tentatively ascribe this to a high proportion of parental liquid in comparison to orthopyroxene. Opx tends to increase heavy REE abundances as for our analysis of 15445,17.

Modeling the REE abundances of the parent liquid will be a further goal of the consortium and was not attempted at this stage. However, we point out the potential significance of such modeling to the unification of our understanding of the geochemical evolution of the lunar crust and mantle. In Fig. 1 we show the range of REE abundances assumed by (9) to exist in the lunar magma ocean at the time of formation of cumulate source regions for the Luna 24 VLT basalts. These basalt source regions are thought by (9) to have formed at an early stage in magma ocean evolution. REE abundances, particularly those of Eu, suggest that the anorthositic norites formed at a similar stage in magma ocean evolution. The uniform heavy REE depletion of the hypothetical magma ocean which has been used (9,10,11) in modeling the formation of mare basalt cumulate sources has probably also been superposed upon the anorthositic norite abundance patterns.

A Rb-Sr internal isochron for 15455,228 provides direct evidence for the early formation of anorthositic norites. High quality plagioclase, whole rock, and pyroxene analyses (Table 1) define an age of 4.52 ± 0.10 AE ($\lambda(^{87}Rb)$ = 0.0139 AE^{-1}) and initial $^{87}Sr/^{86}Sr$ = 0.69903 ∓ 7 (Fig. 2). The deviations, Δ,

AGE AND REE ABUNDANCES OF ANORTHOSITIC NORITE FROM 15455

Nyquist, L. et al.

of the data from the best fit isochron are shown in the inset in Fig. 2, multiplied by 10^4. Previous data for 15445,17 (12) and recent data for 60025,26 and 61016,79 are shown for comparison. The isotopic systematics of highland rocks are often complex and thus this age should be interpreted with caurion. It is significant, therefore, that the isochron intercept is equal to LUNI (12) as defined by the Apollo 16 anorthosites. We would not expect this intercept if the location of the pyroxene datum which controls the age was due to an artifact. Alexander and Kahl (13) have reported complex $^{40}Ar/^{39}Ar$ age spectra for the matrix and noritic portions of 15455. They interpret the >400°C total age of the matrix, 3.92±0.04 AE, as the best estimate of the last major metamorphic event. A younger >400°C total age of the norite of 3.82±0.04 AE is interpreted to be a minimum age affected by Ar loss. A Sm/Nd analysis of bulk norite (Table 1) is consistent with a 4.52 AE solidification age of the norite. These data yield calculated initial $^{143}Nd/^{144}Nd$ I(Nd, 4.52±0.10) = 0.50596±11 and I(Nd, 4.56) = 0.50591±5 in agreement with I(Nd, 4.56) = 0.50589±2 for eucrites. The model age relative to "chondritic" evolution is T_{ICE} = 4.42±0.34 AE. The deviation, ε, in parts in 10^4 (17) of the norite $^{143}Nd/^{144}Nd$ from "chondritic" evolution is $\varepsilon(0)$ = -15.1±1.1 for present day values, $\varepsilon(3.92)$ = -1.87±1.1 at the time of metamorphism and $\varepsilon(4.52)$ = +0.13±1.1 at the Rb-Sr age. Thus, we tentatively accept the Rb-Sr age as the solidification age of 15455 anorthositic norite. We hope that further analyses will confirm and refine the age.

The coincidence of the 15455 initial $^{87}Sr/^{86}Sr$ with LUNI suggests the validity of including the Apollo 16 anorthosites in the regression. When all data obtained in our laboratory since 1973 for 60015, 60025, and 61016 are included the isochron becomes T = 4.50±0.10 AE, I = 0.699045 ∓ 26. If early data are excluded because of the possibility of instrumental drift and only the 1978 analyses of 60025 and 61016 shown in Fig. 2 are included, the regression becomes T = 4.48±0.11 AE and I = 0.69907 ∓ 4. The inclusion of the anorthosite data has little effect on the age, but defines the initial $^{87}Sr/^{86}Sr$ more precisely than is possible with the 15455 data alone because of the relatively radiogenic nature of 15455 plagioclase.

The Rb-Sr systematics of 15445,17 are similar to those of 15455,228 as shown in Fig. 2. At present we cannot attach significance to the slight displacement of the 15445 data above the 15455 isochron. The 15445 data were obtained between 1973 and early 1976 on a sample found to be susceptible to Rb leaching by heavy liquids and possibly acetone. The data shown in Fig. 2 are believed to be reliable; however, we plan to repeat the 15445 study on remaining material and without use of liquids.

The 4.52±0.10 AE Rb-Sr age for anorthositic norite 15455 is comparable to the 4.55±0.10 AE Rb-Sr age for dunite 72417 (14), the 4.61±0.07 AE Rb-Sr age of the troctolite 76535 (15), the 4.4 AE Rb-Sr and Sm-Nd ages of norite 77215 (18), and the 4.4-4.5 AE $^{40}Ar/^{39}Ar$ ages of some anorthosites (19,20). The 15455 age becomes 4.42±0.10 AE if $\lambda(^{87}Rb) = 0.0142\ AE^{-1}$ is used for comparison to ages obtained from the U-Pb system. This age is in satisfactory agreement with crustal differentiation at 4.47-4.51 AE as obtained from the upper concordia intersection for many crustal rocks (16). Anorthositic norites were apparently formed early in lunar history and their study should lead to better definition of lunar geochemical evolution.

Acknowledgements: We thank Linda Watts for her painstaking selection of matrix-free norite. We also thank G. Ryder for encouraging this investigation and for consultation during various stages of it.

AGE AND REE ABUNDANCES OF ANORTHOSITIC NORITE FROM 15455

Nyquist, L. et al.

Table 1. .Rb-Sr and Sm-Nd Results for 15455,228

Sample	Wt (mg)	Rb (ppm)	Sr (ppm)	$\frac{87_{Rb}}{86_{Sr}}$(a)	$\frac{87_{Sr}}{86_{Sr}}$(b)	Sm (ppm)	Nd (ppm)	$\frac{147_{Sm}}{144_{Nd}}$(a)	$\frac{143_{Nd}}{144_{Nd}}$ (b)
W. R. 1	46	1.133	137.9	0.0237±2	0.70062±7	2.13	7.79		
W. R. 2	46	1.065				1.502	5.379	0.1689±3	0.511024±53
Plag	5.5	1.299	167.2	0.0225±2	0.70047±4	-	-	-	-
PX	7.6	0.485	15.03	0.0934±8	0.70508±6	-	-	-	-

(a) Uncertainties are for last digit.

(b) Uncertainties are for last digit and are $2\sigma_m$. Sr normalized to $^{88}Sr/^{86}Sr = 8.37521$; Nd normalized to $^{148}Nd/^{144}Nd = 0.24308$.

References

(1) Warren P.H. and Wasson J.T. (1977) Proc. Lunar Sci. Conf. 8th, p. 2215-2235. (2) Ryder G. and Norman M. (1978) Catalog of Pristine Non-mare Materials, NASA, JSC 14565. (3) Ganapathy et al. (1973) Proc. Lunar Sci. Conf. 9th, p. 1239-1261. (4) Ryder G. and Bower J.F. (1977) Proc. Lunar Sci. Conf. 8th, p. 1895-1923. (5) Taylor S.R. et al. (1973) Proc. Lunar Sci. Conf. 4th, p. 1445-1459. (6) Philpotts J.A., private communication. (7) Hubbard N.J. et al. (1974) Proc. Lunar Sci. Conf. 5th, p. 1227-1246. (8) Blanchard D.P. et al. (1977) In Interdisciplinary Studies by the Imbrium Consortium, Vol. 2., p. 60. (9) Nyquist L.E. et al. (1978) In Mare Crisium the View from Luna 24, p. 631-655. (10) Nyquist L.E. et al. (1977) Proc. Lunar Sci. Conf. 8th, p. 1383-1415. (11) Nyquist L.E. et al. (1979) Proc. Lunar and Plan. Conf. 10th, in press. (12) Nyquist L.E. et al. (1973) Proc. Lunar Sci. Conf. 4th, p. 1823-1846. (13) Alexander E.C. and Kahl S.B. (1974) Proc. Lunar Sci. Conf. 5th, p. 1353-1373. (14) Papanastassiou D.A. and Wasserburg G.J. (1975) Proc. Lunar Sci. Conf. 6th, p. 1467-1489. (15) Papanastassiou D.A. and Wasserburg G.J. (1976) Proc. Lunar Sci. Conf. 7th, p.2035-2054. (16) Oberli F. et al. (1979) Lunar and Plan. Sci. X, p. 940-942. (17) Lugmair G.W. et al. (1976) Proc. Lunar Sci. Conf. 7th, p. 2009-2033. (18) Nakamura et al. (1976) ibid, p. 2309-2333. (19) Dominik B. and Jessberger E. (1978) Earth Plan. Sci. Lett. 38, p. 407-415. (20) Huneke J.C. and Wasserburg G.J. (1979) Lunar Plan Sci. X, p. 598-600.

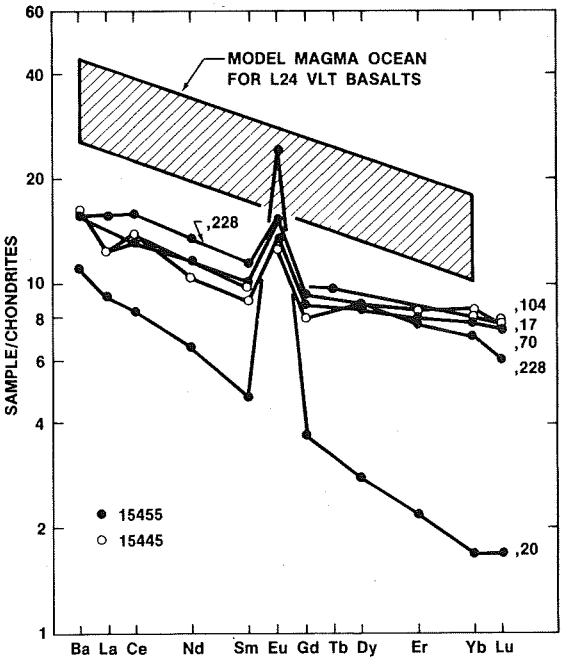

Fig. 1

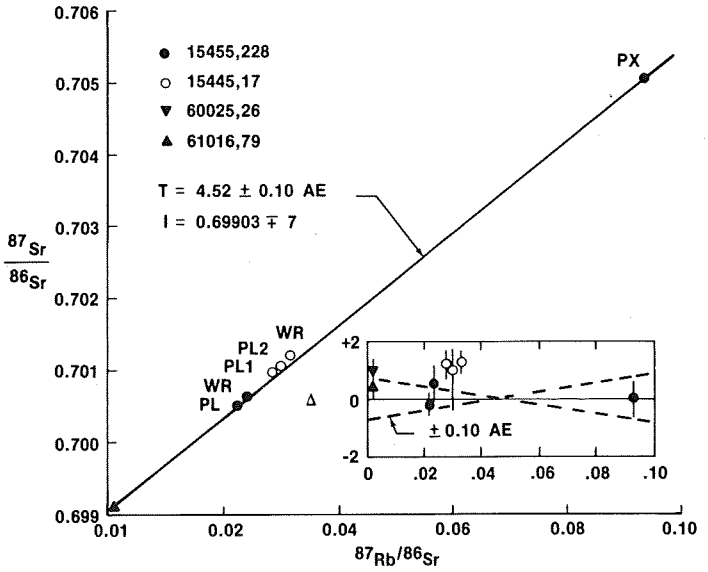

Fig. 2

FRACTIONATION IN THE STILLWATER COMPLEX: AN ANALOG FOR THE LUNAR CRUST AND UPPER MANTLE. L.D. Raedeke and I.S. McCallum, Department of Geological Sciences, University of Washington, Seattle, Washington 98195

Pristine lunar highlands rocks show two distinct fractionation trends on a $(Mg/Mg+Fe)^{ol \text{ or } opx}$ versus An^{plag} plot (see fig. 1 after Warren and Wasson (1)). Steele and Smith (2) first noted the near vertical fractionation trend for anorthositic fragments and pointed out that it "...is contrary to that for differentiation of terrestrial basaltic intrusions". They suggested that the trend may have resulted from the loss of Na from the lunar surface. Roedder and Weiblin (3) noted the existence of two trends, i.e., the near vertical trend in anorthosites and a trend with positive slope comparable to that observed for terrestrial layered intrusions, and concluded that "...the negative slope...requires...fractional crystallization of olivine and equilibrium crystallization of plagioclase, an obscure process that has been proposed but which we do not fully understand." Warner et al.,(4) expanded the data base, confirmed the finding of (3) and concluded "...the two suites are not cogenetic - they could not have formed from the same magma." However, they did propose formation by cumulate processes. Warren and Wasson (1) showed that the two trends remain even when only pristine samples are considered and they made the important observations that anorthositic rocks with cumulus olivine plot in the anorthosite trend and that there is a distinct compositional gap between the two trends. Drake (5) proposed that the near vertical trend is a consequence of crystallization from a lunar bulk composition that is poorer in silica than that of terrestrial layered intrusions. Longhi and Boudreau (6) noted that the displacement of the two series of rocks is such that they could not have formed from the same magmas and that the gap between the two series attests to separate magmatic processes. They modelled the fractionation trends by invoking both equilibrium and fractional crystallization processes along with magma mixing and assimilation. McKay et al.,(7) showed that rocks in both series crystallized from liquids with similar REE patterns.

We have recently identified remarkably similar trends in the cumulates of the Stillwater Complex (Fig. 2). A simplified section of the Banded zone is shown in Fig. 3. The dominant lithologies in the Lower Banded zone (LBZ) are "cotectic" norite and gabbronorite with minor anorthosite, troctolite and gabbro. Anorthosites are dominant in the Middle Banded zone (MBZ) while the Upper Banded zone (UBZ) is mainly "cotectic" gabbronorite. The "normal" fractionation trend in Fig. 2 is defined exclusively by samples from the LBZ and UBZ. This trend has been subdivided into an olivine $\pm$ opx/plag trend and a parallel cpx/plag trend which simply reflects the fact that $(Fe/Mg)^{opx} \sim 1.3 \times (Fe/Mg)^{cpx}$ at equilibrium (8). The sequence, proportions and compositions of cumulus minerals in the LBZ and UBZ are compatible with a process of fractional crystallization with both pyroxene and plagioclase accumulating on the floor of the chamber. Deposition from density currents was probably the dominant mechanism since Irvine (9) has shown that plagioclase can accumulate along with mafic phases even when it is slightly less dense than the magma.

The vertical trend in Fig. 2 is defined largely by data from anorthosites, but also includes points from troctolites and olivine gabbros of the MBZ. There is no systematic correlation between mafic mineral compositions and stratigraphic position in the MBZ. Note the absence of a compositional gap between the two trends. Cumulus plagioclase makes up $\sim$82% of the MBZ. Mass balance calculations indicate that the "excess" plagioclase was that which failed to accumulate on the floor of the magma chamber during the formation of the Ultramafic zone and the LBZ. The coarse grain size and uniform composition of plagioclase in anorthosites indicates an extended period of growth in a

FRACTIONATION IN THE STILLWATER COMPLEX

Raedeke, L.D. and McCallum, I.S.

relatively homogeneous, well mixed liquid. Plagioclase tends to "follow" the melt in a convecting system. This situation closely approached ideal equilibrium crystallization. Eventually plagioclase accumulated, trapping fractionated, but relatively homogeneous, intercumulus melt that crystallized as adcumulus plagioclase overgrowths and pyroxene oikocrysts. Processes of compaction, crystallization, reaction and infiltration metasomatism (10) produced trapped melt with a range of Fe/Mg values while the large volume of plagioclase effectively buffered its composition. Small scale subsolidus reequilibration homogenized mineral grains but did not erase the large scale compositional inhomogeneities.

Finally, the Stillwater data clearly show that it is not necessary to invoke different magmas. Six samples widely separated geographically and stratigraphically, have identical initial $^{143}Nd/^{144}Nd$ values (11). Insofar as the detailed stratigraphy is well known, the rocks are fresh and original textures preserved, the Stillwater Complex provides an excellent analog to test hypotheses proposed for the evolution of the lunar crust.

References: (1) Warren,P.H. and Wasson, J.T. (1977) Proc. Lunar Sci. Conf. 8th, p. 2215-2235. (2) Steele, I.M. and Smith J.V. (1973) Proc. Lunar Sci. Conf. 4th, p. 519-536. (3) Roedder, E. and Weiblin, P.W. (1974) Proc. Lunar Sci. Conf. 5th, p. 303-318. (4) Warner, J.L. et al. (1976) Lunar Sci. VII, p.915-917. (5) Drake, M.J. (1975) Proc. Lunar Sci. Conf. 6th, p. 293-299. (6) Longhi, J. and Boudreau, A.E. (1979) Proc. Lunar Sci. Conf. 10th, in press. (7) McKay, G.A. et al.(1974) Lunar Sci. X, p.804-806. (8) McCallum, I.S. (1968) PhD thesis, Univ. of Chicago, 175 p. (9) Irvine, T.N. (1979) Am. J. Sci., in press. (10) Irvine, T.N. (1978) Carn. Inst. Wash. Yb. 77, p.743-751. (11) DePaolo, D.J. and Wasserburg, G.J. (1979) G.C.A., 43, p. 999-1008.

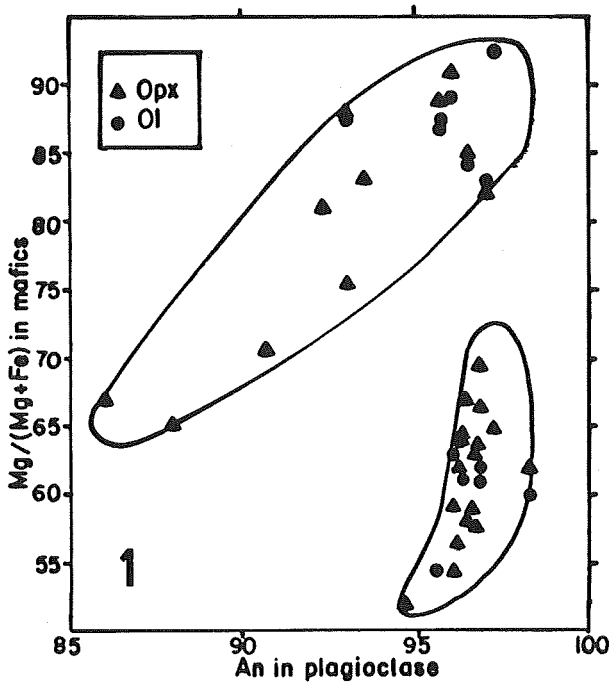

Figure 1. Mg/(Mg+Fe) in mafics vs. An in plagioclase among pristine nonmare lunar rocks. After Warren and Wasson (1).

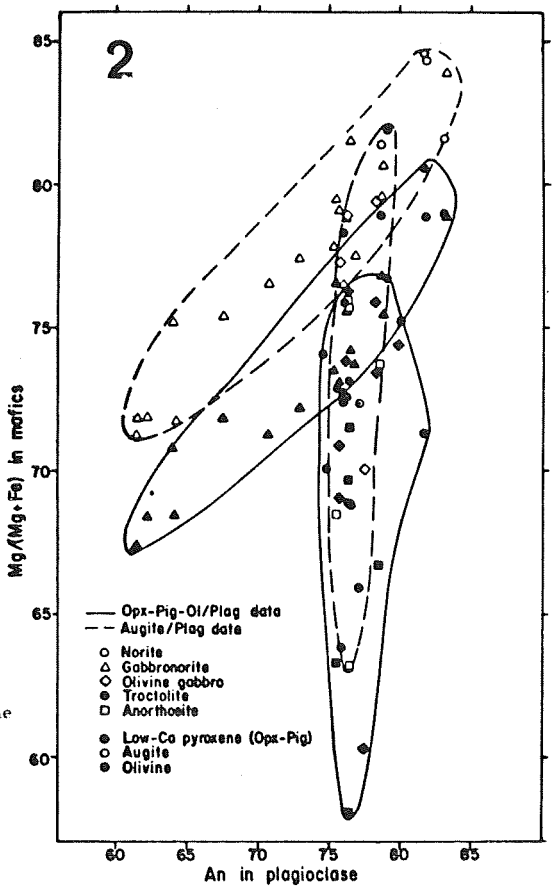

Figure 2. Mg/(Mg+Fe) in mafics vs. An in plagioclase among rocks of the Stillwater Complex.

Figure 3. Stratigraphic section and selected mineral compositions of the Banded zone of the Stillwater Complex.

FRACTIONATION IN THE STILLWATER COMPLEX

Raedeke, L.D. and McCallum, I.S.

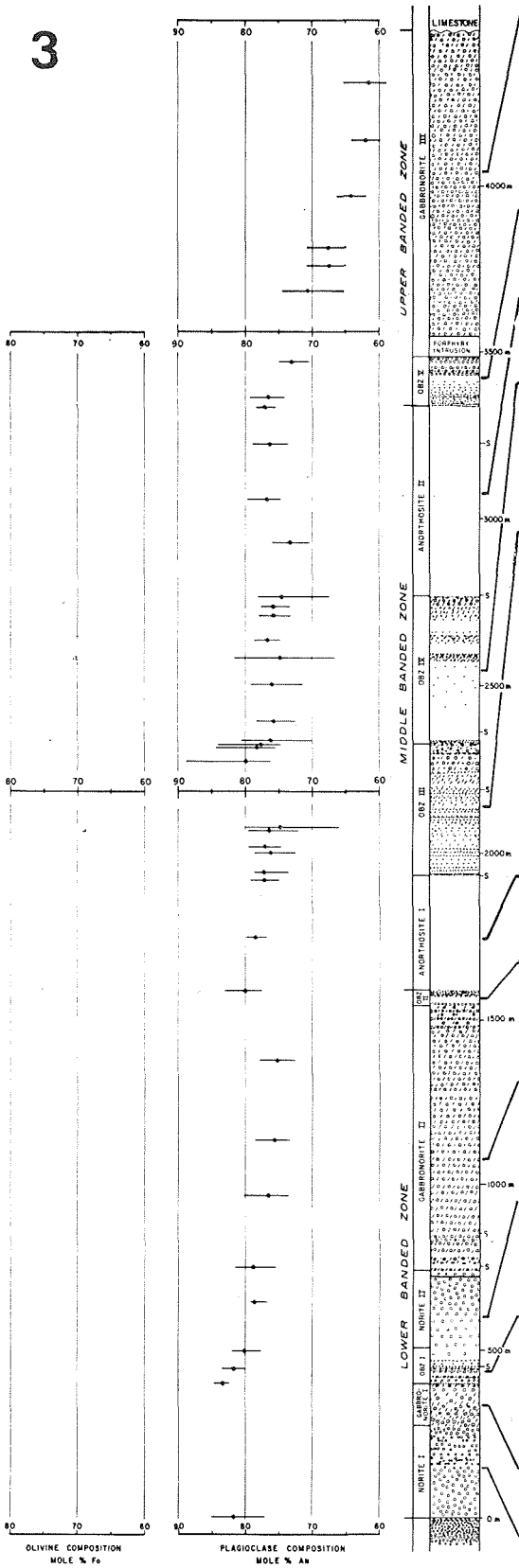

Gabbronorite III: Throughout this uniform subzone, plagioclase, augite and low-Ca pyroxene occur in approximately cotectic proportions. While planar lamination is almost always present, there is no preferred mineral orientation within the plane of layering. Below 3765 m, orthopyroxene is clearly a cumulus mineral. Between 3765 and 3975 m, orthopyroxene occurs as poikilitic crystals containing abundant "inclusions" of small rounded augites. Above 3975 m, orthopyroxene occurs as poikilitic crystals containing numerous sets of oriented "001" augite exsolution lamellae. These sets of lamellae outline domains corresponding to original cumulus pigeonite crystals. Insofar as there is no significant change in mineral proportions associated with these textural changes, we conclude that low-Ca pyroxene formed as a cumulus mineral throughout this subzone, the poikilitic texture being the result of postcumulus recrystallization accompanying the inversion reaction.

Olivine-bearing subzone V (OBZ V): The basal member of this unit is a well-banded troctolite containing varied amounts of plagioclase, normally in excess of cotectic proportions. Modally graded layering, cross bedding and cut-and-fill structures are locally present indicating strong current action during the deposition of this troctolite.

Anorthosite II: This uniform unit is the thickest anorthosite in the Banded zone. Postcumulus augite and inverted pigeonite make up 10-12% of the rocks and disseminated sulfides are concentrated in two narrow layers near the base and top of this unit. The average grain size of plagioclase is approximately twice that of plagioclase in two- and three-phase cumulates.

Olivine-bearing subzone IV (OBZ IV): The lower boundary of this subzone is placed at the base of a well banded troctolite and the upper boundary at the base of the second thick anorthosite. The sequence troctolite-anorthosite-anorthositic troctolite-olivine gabbro (+ gabbronorite) is repeated three times. The contact between troctolite and underlying olivine gabbro ranges from gradational to sharp, sinuous and discordant, whereas the upper contact between troctolites and overlying anorthosites is invariably sharp, planar and concordant. The uppermost troctolite is structureless, highly discordant, contains ameboidal olivine aggregates, and is virtually identical to the troctolite at the top of OBZ II.

Olivine-bearing subzone III (OBZ III): The predominant rock types in this 400 m of section are troctolite, anorthositic troctolite, anorthositic gabbro, olivine gabbro, and olivine gabbronorite. The various members are complexly interlayered, often on a centimeter scale. Olivine is present as a cumulus mineral through 80% of the subzone, but, except for eight narrow troctolite layers in which it comprises 40 modal percent, olivine abundances are low, making up between 1 and 10% of the cumulus mineral assemblage. The major units can be traced laterally but there are substantial lateral variations in the thickness, modes and textures of the thinner members. Two distinct cyclic sequences are repeated several times in the lower 275 m of this subzone: troctolite-anorthosite-anorthositic gabbro-olivine gabbro, and troctolite-anorthositic troctolite-olivine gabbro. Olivine gabbros and gabbronorites are usually isomodal with a well defined planar lamination. A distinctive feature of these rocks is the occurrence of polycrystalline aggregates of plagioclase (≈2X2X1 cm), the long axes of which are aligned parallel to the lamination. By contrast, the anorthositic gabbros commonly show an erratic layering defined by alternating mafic and felsic layers. The upper 125 m of this subzone are characterized by a four-phase cumulate. In some samples, small embayed olivines are present in the cores of orthopyroxenes, clearly indicating a reaction relationship. In other samples, however, coexisting orthopyroxene and olivine do not show the reaction relationship and both appear to be cumulus minerals.

Anorthosite I: This subzone is composed entirely of a uniform plagioclase cumulate with postcumulus augite and inverted pigeonite. The average grain size of the plagioclase is coarser and more uniform than in the two- and three-phase cumulates above and below. Disseminated sulfides occur in the upper 8 m of this unit and reach a maximum concentration in the upper 2 meters.

Olivine-bearing subzone II (OBZ II): The upper 8 m of this subzone is a remarkable association of gabbro, troctolite, and gabbroic pegmatite. The contact between gabbro and overlying troctolite is sinuous and discordant, in contrast to the planar and conformable contact between the troctolite and overlying anorthosite. Irregular patches of gabbro are enclosed within troctolite and vice versa. Olivine in the troctolite occurs as large (>10 mm) "ameboidal" grains with inclusions of plagioclase set in a matrix of relatively small (1-2 mm) plagioclase crystals.

Gabbronorite II: Varied proportions of cumulus augite, orthopyroxene and plagioclase are seen in the lower section with four interlayered anorthosite members, two of which contain sulfides. In the central part of this subzone, mineral proportions are near cotectic and planar lamination is well developed. The upper 50 m are composed of five well developed but laterally discontinuous cyclic units showing modally graded layering defined by an upward increase in plagioclase/pyroxene ratio.

Norite II: Rhythmic inch-scale layering is well developed in the basal anorthositic norites. Upward in the section, modal proportions become more pyroxene-rich, approaching cotectic values, and layering becomes correspondingly more uniform (isomodal). Toward the upper part of the norite the habit of the cumulus orthopyroxene changes from subrounded to highly elongate. A distinctive, laterally extensive, mafic layer (2 m thick) and a complementary anorthosite layer occur ≈20 m below the top of the subzone.

Olivine-bearing subzone I (OBZ I): The basal contact of this complex subzone is marked by the reappearance of cumulus olivine. The sequence troctolite-anorthosite-norite-gabbronorite is repeated five times with minor variations. The fourth troctolite contains abundant sulfides. The noritic members in the lower part of the subzone are characterized by a distinctive wispy banding; higher in the subzone layering in the norites becomes progressively more regular. This zone can be traced along strike for at leas 20 km, but individual members are laterally variable, both in thickness and mode. Modal proportions are highly varied and generally non-cotectic.

Gabbronorite I: The lower contact of this unit is placed at the first appearance of cumulus augite. Proportions of augite, low-Ca pyroxene and plagioclase are largely non-cotectic with plagioclase increasing up section. Layering is modally graded to isomodal. Pyroxenite inclusions are common in the upper 30 meters.

Norite I: Orthopyroxene and plagioclase are in approximate cotectic proportions in the lower uniform part of the unit, but plagioclase increases in abundance in the upper 100 m and layering becomes more pronounced. Layering is defined by alternating pyroxene-rich and plagioclase-rich layers with modally graded layering, scour-and-fill and slumping structures common near the top of the unit.

PHYSICAL PROCESSES IN THE FORMATION OF THE HIGHLAND SHELL.

S. K. Runcorn, School of Physics, University of Newcastle Upon Tyne

The early differentiation of the Moon, presumably beginning soon after 4.55 by, the time when the accretion of the Moon ended, was essentially complete by 4.4 by, with the formation of the anorthositic highland layer and the source region of the maria basalts. In understanding the physical processes involved in this process two problems require solution. The first is the nature of the heat sources and the depth to which melting and differentiation proceeded in the primeval accreted Moon (1). The palaeomagnetic evidence is critical here. If this was an early lunar magnetic field, as has been maintained (2) generated by dynamo action, an iron core must have been formed by melting at the centre soon after 4.4 by ago. Accretional energy is not a solution and Runcorn, Libby and Libby (1) have suggested that superheavy elements were responsible. In any case, that the early melting of the Moon presents a problem, which was not widely recognized hitherto, seems to be generally accepted.

The second question concerns the nature of the circulation which caused the transport of anorthosite crystals from the depth of the lunar mantle to form the highland layer. Was it an entirely radial, outward movement of material or did it involve some kind of circulation or convection, driven by thermal energy escaping from the Moon, or chemical segregation releasing potential energy. For this question a critical observation is the displacement away from the Earth of the centre of figure with respect to the centre of mass. The most plausible interpretation of this is that the thickness of the highlands on the far side exceeds that on the near side by some tens of kilometers, an idea which explains the absence of basaltic lava in the large far side basins. An explanation of this hemispherical asymmetry is that a single cell convection current, having a flow pattern described by a spherical harmonic of 1st degree, developed during the process of differentiation -- an old idea in geophysics originating with G. F. S. Hills. Support for this hypothesis comes from the shape of the maria surfaces, which are not consistent with formation in a gravitational field of the present Moon. The non-hydrostatic shape of the Moon today has been explained as distortion produced by a 2 cell convection pattern, one described by a second degree harmonic. If this pattern was not present at the time the maria basins filled with lava, then it is necessary to postulate any other pattern in the earlier history of the Moon and a single cell convection pattern is consistent with a simple evolutionary scheme. Similar asymmetries between two hemispheres is seen on Mercury, Mars and the Earth and may have a similar origin.

Directions of magnetization of areas of the highlands on the far side have been determined by Hood et al. (3) and of the Reiner γ by Hood et al. (4). Pole positions from the former are nearly 0°N90°E (5) and from the latter about 57°N171°E (6): these give early lunar orientations which place the maria in positions of significant symmetry. Polar wandering in the early Moon is postulated.

(1) Runcorn S.K. et al. (1977) Primeval melting of the Moon. Nature, 270, 5639, 676-681. (2) Runcorn, S.K. (1975) On the interpretation of lunar magnetism. Phys. Earth Planet. Inter. 10, 327-335. (3) Hood, L. et al. (1979) Evidence for a non-random magnetisation of the Moon. Geophys. Res. Lett. 5, 305-308. (4) Hood, L. L. et al. (1979) Lunar nearside magnetic anomalies. Proc. Lunar Sci. Conf. 10th. (5) Runcorn, S.K. (1978) The origin of lunar palaeomagnetism. Nature, 275, 430-432. (6) Runcorn, S. K. (1979) Proc. Lunar Sci. Conf. 10th.

LUNAR HIGHLANDS CHEMISTRY: EXPLORATION WITH Q-MODE FACTOR ANALYSIS.
Graham Ryder,[1] Cary Fico [2] and Robert Ehrlich [2]. [1]Northrop Services, Inc., Houston, Texas 77034, [2]Department of Geology, University of South Carolina, Columbia, S.C. 29208.

A significant group of highlands rocks has been recognized as endogenous (1,2,3) but most lunar highlands breccias are undoubtedly mixtures. To more fully understand the characteristics and evolution of at least the upper crust it is desirable to specify the individual primary components which have contributed to them. Because the function of Q-mode factor analysis in geochemistry and petrology is to resolve a data matrix such that each analyzed sample is viewed as a mixture of end-members, real or theoretical, it seems capable of providing information on the components of lunar breccias. The extended version of Q-mode factor analysis by Miesch (4) yields compositions of the end-members, the proportions of the end-members which must be mixed to match each analyzed sample, and the compositions of the resulting mixtures. These are all inspected for plausibility. We have initiated an attempt to better understand the chemistry of lunar breccias using this method.

In this initial effort we have used only the oxides of Al, Fe, Mg, Ca, Na, K, Ti, and Cr, to get a first look at the essential structure of the major and minor element data, and we have therefore only preliminary results and conclusions. Silica was disregarded because many analyses omit it and we desired to utilize as large a number of samples as feasible. Undoubtedly this supresses some significant variation. In work in progress we are including silica, as well as significant trace elements (including Sc, La, and Ni).

Problems: In "unmixing" chemical compositions numerically it is necessary to assume a reasonably small number of components of fixed composition. This may be unrealistic for while the breccias are mixtures, they are the result of the complex interaction of many processes. Plutonic processes both during the fundamental formation of the crust and later produced a spectrum of rock compositions; a large number of these has been identified. Differential assimilation and volatile movement into crystallized rocks may have modified their compositions. Volcanic activity probably produced a spectrum of compositions (note the varieties of mare basalts identified) and magma mixing during fractionation would have created additional complications. Impacts which produced breccias from this spectrum of rock compositions almost certainly dispersed volatiles. Assimilation of less refractory minerals by impact melts can lead to small scale exceptions to the concept that a melt is an ideal mixture of the rock compositions which went into it.The suggestion is that highlands breccias might be too complex for numerical analysis, that there are hundreds of end-members. However, identifications of the most important end-members and information about their variation is possible, as well as information as to how complex the breccias truly are.

Data base: The data base being used is taken from all analyses of highlands rocks and clasts published in the Proceedings and the Abstracts of the Lunar and Planetary Science References, as well as many analyses published elsewhere. By using Curatorial data packs, individual analyses were identified with specific lithologies and best-estimates calculated for each (5). In this way a comprehensive data base for highlands rocks from Apollo 15,16,17 and Luna 20 has been built. Apollo 14 samples have so far been omitted.

Extended Q-mode factor analysis method: The method is an extended form of that developed by Klovan and Imbrie (6)and is described in detail by Miesch (4,7,8). The particular form used here will be described more fully later. The data matrix considered is one where the rows represent rock samples and the columns represent chemical variables. Each row sums roughly to a constant (in our case, using percentages of oxides other than silica, about 55.) The Q-mode factor model is derived by conventional procedures: a similarity matrix is produced and the principal factors constructed from the eigenvalues and eigenvectors of the similarity matrix. The number of factors used in subsequent calculations is a matter of choice;the eigenvalues suggest how many may be reasonable. While the constant sum effect is normally adverse in petrology, in this case it is an asset and allows the principal factors to be computed in compositional terms, and each sample to be estimated or recomputed

HIGHLANDS CHEMISTRY...Q-MODE FACTOR ANALYSIS

Ryder, Graham

as a mixture of these factors or end-members (4). In the method used here, the end-members are first chosen as extremes of the sample population, but are modified during various necessary rotations of the axes of the principal factors to fit the factor solutions.

The communality (in Tables 1 and 2) is a measurement of how well a sample is explained by the model. High communalities indicate a good arithmetic fit, but do not necessarily mean that the model is petrologically reasonable. Coefficients of determination for each variable (element) are computed for each model, and indicate how well the original data set for that variable is explained by the model. High values indicate a good fit (maximum 1.000).

Results: The first data set consisted mainly of the Apollo 16 analyses, but also included Luna 20 and some Apollo 15 highlands analyses. The eigenvalues of the similarity matrix suggested that two factors could account for more than 99% of the total variation. The two factors calculated are shown in Table 1, along with the extreme samples the factors approximated. The coefficients of determination show that while the model accounts reasonably well for Al, Fe, Mg and Ca, it is poor for Cr and Ti, worse for K, and does not account for the variation in Na at all.

The recomputed estimates of the original data in many cases are similar to the original data; the worst fit among all the Apollo 16 samples is for 60615 (shown in Table 1). Factor 1 is essentially a typical anorthosite and is a reasonable and expected component of lunar breccias. Factor 2, a K, Ti-rich ultramafic composition is more surprising. It is unlike any known lunar sample, even 67667 on which it was based. It is probably unrealistic although it may itself represent a mixed component; Wasson et al (3) noted a rough correlation of ultramafic components with KREEP components in their analysis of highlands breccias. (In fact, Factor 2 is similar to the Wasson et al.(9) ultramafic component SCCRV but is not so extremely ultramafic and is much richer in alkalis). Because of its failure to account well for Ti, K, and Na the model is unsatisfactory. Nonetheless it does emphasize that the major element chemistry of highlands breccias is surprisingly simple and it is the minor elements which have the most variation.

The second data set contained 211 analyses from Apollo 15,16, and 17 and Luna 20. In this case 4 factors were chosen (Table 2) based on extremes among the sample analyses. Again one factor is a fairly pure anorthosite; the others approximate dunite, KREEPy basalt, and granite. The last factor is only a minor component (<5 %) in most samples. The model improves on fits for Al, Fe, Mg, and Ca compared to the two factor model but still does not account for K, Ti and Na satisfactorily.

Many samples can be estimated very well with the model (Table 2). Few samples have communalities below 0.9996, and one of the worst fits is the Luna 20 soil (comm. 0.9994). However, there are several reasons why this model cannot be considered to be particularly realistic, even though the communalities are high: 1) Factors 1 and 2 have negative scores for K_2O, an impossible situation, leading to negative K_2O values for some samples e.g. Luna 20 soil (other negative factor scores exist but are insignificant) 2) The model, even with the artificial K_2O in Factors 1 and 2, fails to account for K_2O in general.Na and Ti are also not explained. 3) Factor 4, even though minor, is radically different from any known endogenous rock type and Factor 2 has unusually high Na and Ti for a lunar ultramafic rock.

Conclusions: This initial effort emphasizes that while the major element chemistry of highlands breccias might be quite simple, and can be modelled as mixtures of a few components, this is not true of minor (and presumably trace) elements.While some of the inconsistencies with using a few factors might be explicable by the volatility of Na and (to lesser extent) K, this is not true of Ti. The suggestion is that while a few groups of rocks defined by major elements contribute to highlands breccias, the minor and trace elements within

HIGHLANDS CHEMISTRY...Q-MODE FACTOR

Ryder, Graham

these groups might be quite variable. Our continuing analysis using the extended Q-mode factor analysis method is intended to gain insight into these variations, and their significance in lunar crustal history.

1) Anders E. (1978) PLPSC 9th, p. 161-184
2) Warren P.H. and Wasson J.T. (1978) PLPSC 9th, p. 185-217
3) Norman M.D. and Ryder G. (1979) PLPSC 10th, in press
4) Miesch A.T. (1976) U.S.G.S. Prof. Pap. 574-G, 47 pp.
5) Ryder G. (1979) PLPSC 10th, in press
6) Klovan J.E. and Imbrie J.(1971) Jour. Int. Ass. Math. Geol. 3, p. 61-77
7) Klovan J.E. and Miesch A.T. (1975) Comp. and Geosciences 1, 161-178
8) Miesch A.T. (1975) Comp. and Geosciences 1
9) Wasson J.T. et al.(1977) PLSC 8th, p. 2237-2252

Table 1: 2 factor (end-member) model: 129 Mainly Apollo 16 and Luna 20 Samples,

	Factor 1	65235	Factor 2	67667	Variable	Coeff. of Determination
Al_2O_3	34.6	35.2	6.6	7.6	Al_2O_3	0.950
FeO	0.6	0.3	16.6	17.2	FeO	0.915
MgO	0.0	0.2	22.2	26.4	MgO	0.903
CaO	19.2	19.6	4.8	5.3	CaO	0.839
Na_2O	0.32	0.35	1.11	0.16	Na_2O	0.030
K_2O	-0.03	0.00	0.63	0.02	K_2O	0.238
TiO_2	-0.08	0.00	2.15	1.04	TiO_2	0.683
Cr_2O_3	-0.003	0.00	0.391	0.38	Cr_2O_3	0.743

Selected Comparisons of calculated (C) and actual (A) compositions in 2 factor model

	Apollo 16 soil		Luna 20 soil		60315		64475		60615		61016 dk.	
	C	A	C	A	C	A	C	A	C	A	C	A
Al_2O_3	26.5	26.7	22.8	22.7	17.8	17.2	27.7	28.3	20.5	21.5	23.7	25.1
FeO	5.2	5.5	7.4	7.4	10.2	9.3	4.6	4.6	8.7	5.8	6.8	5.1
MgO	6.4	6.3	9.3	9.7	13.3	13.3	5.4	5.6	11.1	14.0	8.6	10.7
CaO	15.0	15.5	13.1	14.7	10.6	10.4	15.6	15.9	12.0	12.1	13.6	14.3
Na_2O	0.54	0.46	0.65	0.40	0.79	0.60	0.52	0.49	0.72	0.39	0.63	0.33
K_2O	0.16	0.11	0.25	0.09	0.37	0.40	0.13	0.12	0.30	0.12	0.22	0.08
TiO_2	0.57	0.58	0.86	0.50	1.26	1.31	0.47	0.54	1.04	0.54	0.79	0.76
Cr_2O_3	0.11	0.12	0.16	0.16	0.23	0.21	0.09	0.07	0.19	0.14	0.15	0.10
Commun.	0.9998		0.9974		0.9991		1.0000		0.9802		0.9926	
Factor 1%	71.2		57.8		40.1		75.4		49.7		61.1	
Factor 2%	28.8		42.2		59.9		24.6		50.3		38.9	

TABLE 2: 4 factor (end-member) model: 211 Apollo 15,16,17 and Luna 20 samples.

	Factor 1	65327	Factor 2	72415	Factor 3	72275 bas.	Factor 4	73255 el.	Variable	Coeff. of Determination
Al_2O_3	34.1	34.4	1.7	1.5	13.9	13.5	28.5	12.3	Al_2O_3	0.938
FeO	0.4	0.3	10.7	11.3	15.4	15.0	7.7	3.1	FeO	0.958
MgO	0.3	0.3	40.5	43.6	10.4	10.0	0.0	0.2	MgO	0.988
CaO	19.2	19.7	0.47	1.1	11.0	10.5	-0.81	0.5	CaO	0.966
Na_2O	0.26	0.30	0.78	0.01	0.34	0.29	5.19	0.53	Na_2O	0.109
K_2O	-0.37	0.00	-1.18	0.00	0.46	0.25	12.16	7.55	K_2O	0.049
TiO_2	-0.01	0.00	0.57	0.03	2.01	1.40	1.01	0.26	TiO_2	0.559
Cr_2O_3	-0.01	0.00	0.32	0.34	0.39	0.46	0.07	0.01	Cr_2O_3	0.744

Selected comparisons of calculated (C) and actual (A) compositions in 4 factor model

	Apollo 16 Soil		Luna 20 Soil		60315		61016 dk		68415		72255		77017		15455 dk.	
	C	A	C	A	C	A	C	A	C	A	C	A	C	A	C	A
Al_2O_3	26.0	26.7	22.3	22.7	17.7	17.2	24.1	25.1	28.4	28.6	20.8	20.8	25.5	26.0	17.9	17.1
FeO	5.4	5.5	7.3	7.4	9.6	9.3	5.0	5.1	4.0	4.0	8.3	8.3	6.0	6.2	9.3	8.8
MgO	6.1	6.3	9.4	9.7	13.7	13.3	10.2	10.7	4.4	4.4	10.5	10.5	6.0	6.0	13.9	13.3
CaO	15.1	15.5	14.0	14.7	10.6	10.4	13.6	14.3	16.1	16.3	12.4	12.4	14.6	14.5	11.0	10.6
Na_2O	0.43	0.46	0.27	0.40	0.60	0.60	0.48	0.33	0.42	0.48	0.52	0.49	0.53	0.37	0.51	0.50
K_2O	0.07	0.11	-0.39	0.09	0.31	0.40	-0.15	0.08	0.05	0.07	0.23	0.25	0.39	0.05	0.05	0.15
TiO_2	0.60	0.58	0.81	0.50	1.06	1.31	0.44	0.76	0.43	0.31	0.93	0.79	0.70	0.75	1.00	1.35
Cr_2O_3	0.12	0.12	0.18	0.16	0.24	0.21	0.11	0.10	0.08	0.10	0.20	0.24	0.14	0.14	0.24	0.26
Commun.	1.0000		0.9994		0.9999		0.9998		1.0000		1.0000		0.9997		0.9997	
Factor 1%	63.2		50.8		29.4		61.7		73.2		41.0		58.1		32.4	
Factor 2%	7.9		13.2		22.1		21.0		5.5		15.2		6.4		23.2	
Factor 3%	26.6		37.7		44.6		15.2		18.9		40.6		31.1		42.5	
Factor 4%	2.3		-1.8		3.9		2.1		2.5		3.1		4.5		2.0	

VOLCANISM PRIOR TO THE TERMINATION OF THE HEAVY BOMBARDMENT: EVIDENCE, CHARACTERISTICS,AND CONCEPTS. Graham Ryder[1]and Paul Spudis[2], [1]Northrop Services Inc., P.O. Box 34416, Houston, Tx. 77034,[2]Department of Geology,Arizona State University, Tempe, Arizona 85281.

The intense, probably cataclysmic, heavy bombardment of the Moon which terminated ∿ 3.95 b.y. forms a convenient horizon in lunar chronology.At the same time, it obscures the record of the earlier period. Volcanism took place both following the terminal bombardment and during it,according to petrological and geochronological studies of both mare and non-mare pristine volcanic rocks.Potentially the post-heavy bombardment volcanism (mainly mare) is fully explorable, and many of its characteristics are already known (1,2)if not explained. However, it is of interest to assess the existence, nature, and importance of more ancient volcanism in constructing the lunar crust.

Evidence concerning ancient lunar volcanism can be sought directly and indirectly in sample studies and in remote sensing (particularly photogeological) studies. Furthermore, thermal models of the Moon, which probably cooled monotonically (3), would suggest that ancient volcanism was perhaps more common than the known later volcanism.Isotopic evidence e.g.(4,5) suggest that the source materials for mare and KREEP basalts were established and thus available ∿ 4.3 b.y. ago.

Samples of volcanics which were extruded during or just after the terminal heavy bombardment exist, and have a range of compositions.

APOLLO 15 KREEP/Apennine Bench Formation. Numerous particles and several small fragments of xenolith-free, meteorite-free (6,7) 3.9 b.y. old (8,9,10) KREEP basalts exist at the Apollo 15 site. Despite anti-volcanic model age arguments (e.g. 11) these are probably volcanic.The nearby Apennine Bench Formation is post-Imbrium but is older than the local mare basalts (12,13).Morphological and remote chemical studies permit and suggest its correlation with flows of Apollo 15 KREEP basalt (13,14).Thus, some KREEP basalts slightly postdate the Imbrium event; indeed their extrusion may have been triggered by it.

APOLLO 17 KREEPy basalts.Meteorite-free basalt occurring as clasts in the friable matrix of Boulder 1, Station 2 has been dated at 4.01 b.y.(15). It is mineralogically and chemically intermediate between KREEP and mare basalts (16) in many respects, suggesting that the distinction between KREEP and mare basalts may have been occasionally less obvious. Its source must be distinct from that of Apollo 15 KREEP basalt, both in trace elements and Sr-isotopes.

APOLLO 14 MARE basalts. Several high-alumina mare basalts found as clasts (or believed to have once been clasts) in the Apollo 14 collection have been described. Several (14053,14072,14321-clasts) have been individually dated at 3.95-4.0 b.y. (e.g. 17) and chemical data shows them to be meteorite-free(e.g. 18). Others, clasts in 14312, 14063, and 14082 may be inferred to be of similar age, but must first be inferred to be volcanic, as less chemical data exists. Although Apollo 14 breccias were once believed to have been Imbrium ejecta, this interpretation is now very doubtful and at least most of them(and hence the mare basalts) are probably pre-Imbrium (e.g.19).A remarkable feature of these Apollo 14 mare basalts is their great diversity of composition,including intermediate TiO_2 (∿ 7%) varieties.

APOLLO 17 boulder clasts. Several mare-like basalt clasts in the melt-matrices of the Apollo 17 boulders generally interpreted as Serenitatis impact melt ejecta and dated ∿3.95 b.y.have been described. The aphanitic melts(4.01 b.y.) of Boulder 1, Station 2 contain fragments of a probably volcanic olivine-normative basalt which is iron-rich, chrome-rich and low in titanium(20,21).No chemical analyses exist, other than microprobe defocussed-beam. Two small

VOLCANISM

Ryder, Graham

clasts of low-Ti mare basalt from the Station 6 boulder (∿3.95 b.y.(22)) have been briefly described (23). Three samples of basalt in 73255 (3.9-4.0 b.y?) have mare chemistry and low Ni contents (24), and may represent two different aluminous mare basalt groups unlike any other established types.If the interpretation of these boulder matrices as Serenitatis ejecta is correct,then these basalts attest to the production of pre-Serenitatis mare basalts in quite a variety.

This is about as far as direct sample evidence takes us. A few mare basalt fragments have been recognized in the Apollo 16 collection, but to the best of our knowledge none of these has been found to be older than 3.9 b.y. Many aluminous (>20 % Al_2O_3) basaltic-textured fragments occur in the Apollo collections, but most can be shown to be of impact origin, either with petrographic or siderophile evidence, and it is quite likely that all of them are.

Indirect evidence in samples occurs in the chemistry and mineralogy of breccias. For instance, pyroxene compositions in Apollo 16 LMBs include compositions similar to mare basalt pyroxenes and some of these LMBs are 4.1-4.2 b.y. old. However, such evidence is hardly conclusive, nor does it allow much characterization of ancient volcanism.Chemical evidence is more suggestive.The Apollo 14 breccias are higher in incompatibles than Apollo 15 KREEP basalt,are probably pre-Imbrium (19) and have ages of ∿3.9 b.y.They show considerable evidence of multiple reworking (in contrast to the dated mare clasts within them) and their impact histories and shock levels suggest an origin as pre-Imbrium near-surface accumulations of KREEP i.e. volcanics (14). Thus KREEP volcanism occurred prior to Imbrium as well as after it.Conversely, the existence of granulitic impactites which are meteorite-contaminated, ejecta blanket deposits free of KREEP materials, suggests that KREEP did not appear at the lunar surface until after the 4.2-4.3 b.y. age of the impactites (25). At best, KREEP could not have been so widely disseminated on the lunar surface at 4.2 b.y.ago as it was at 4.0 b.y. ago and it must have been lacking in some areas. Many authors have interpreted the ∿4.3 b.y. model ages of KREEP to mean that KREEP volcanics were extruded at this time, and subsequently were reworked by impact. However, the model age in itself does not signify volcanism, but the separation of Rb from Sr. If two-stage models are inappropriate, or if KREEP volcanics could have been produced with little separation of Rb from Sr, then there is no requirement for KREEP volcanism at 4.3 b.y.

The presence of a KREEP component in highlands breccias (whether of volcanic origin or not) is readily indicated by incompatible element abundances. However,mare basalts have no element abundances orders of magnitude different from highlands rocks (other than KREEP), and chemical evidence in favor of mare basalt components in breccias older than 4.0 b.y. is disputable (26).

Dating of lunar samples is consistent with a "stonewalling"effect of cratering, through which few samples older than ∿ 4.0 b.y. have passed.None of those older fragments which have been recognized have been volcanic, but such flows at the surface of the Moon would have been most extensively reworked and those later, lowland filling flows which were possibly preserved may well have been covered by the basin-filling mare flows. Some potential basalt-flooded highland plains may exist,despite the blow Apollo 16 dealt to such photogeological interpretations.The only areas in the lunar highlands which show saturation of large (>15 Km) craters are limited regions on the farside. There is an area south of Nectaris that is virtually free of any recognizable basin debris (27). This is one potential site of ancient plains volcanism. Schultz and Spudis (28) have documented the existence of craters which have excavated dark materials

VOLCANISM

Ryder, Graham

from below light highlands plains and Orientale ejecta. These dark-haloed craters have a wide distribution. The underlying low-albedo units are postulated to be ancient mare basalt flows. Obviously their absolute ages are unknown, but they may reflect pre-Imbrium volcanism masked by the heavy bombardment.

Considerations of extremely ancient volcanism so far unsampled require that two concepts be addressed. Firstly the term volcanism generally implies the extrusion of silicate liquid originally created by internal partial melting. This is difficult to apply very precisely to early lunar history if our understanding that the crust formed by crystallization of a magma ocean produced by accretion is essentially correct. Such a magma ocean may have released liquids as flows but these would not be volcanic in a strict sense. More importantly, one model for the origin of KREEP is that it is a residual from the magma ocean episode. If so, it is not truly volcanic, since it crystallized from an impact melt, a total melt not a partial melt. (Neither then are the anorthosites, norites etc., produced in this episode strictly igneous). However, any residues would probably have re-equilibrated internally to some extent prior to extrusion. Clearly the definition of volcanism must be flexible in the context of earliest lunar history, even if it is in principal straightforward to distinguish volcanics from non-fractionating melts produced in single impacts later in lunar history (29). Some basin-sized impacts may have penetrated pre-existing magma chambers and excavated lava (28); although the latter is ejecta, it is not impact melt. The line distinguishing volcanic from impact melt may sometimes be thin, and the overlapping of volcanic and basin-forming epochs complicates the problem tremendously.

Secondly, ancient volcanics may have been of extremely varied types, and the term "non-mare" as a group name is unfounded, if mare basalts are defined chemically. While we tend to consider volcanics as either KREEP or mare, some volcanics early in lunar history might not have been easily grouped with either e.g. there might have been volcanics with KREEP major elements but much lower abundances or different patterns of incompatibles, volcanics somewhat like rhyolites, or volcanics with high Mg/Fe ratios (however we are not suggesting that these particular volcanics did exist). We must retain open minds about ancient volcanism.

(1) Papike J.J. et al.(1976) Rev. Geophys. Space Phys. 14, 475-540
(2) Papike J.J. and Vaniman D.T. (1978) in Mare Crisium: The View from Luna 24, Pergamon Press, p. 371-401
(3) Hubbard N.J. and Minear J.W. (1975) PLSC 6th, p.1057-1085
(4) Tera F. and Wasserburg G.J. (1974) PLSC 5th, p. 1571-1599
(5) Lugmair G.W. et al.(1975) PLSC 6th, p. 1419-1429
(6) Dowty E. et al. (1976) PLSC 7th, p. 1833-1844
(7) Warren P.H. et al. (1978) PLPSC 9th, 653-660
(8) Papanastassiou D. and Wasserburg G.J. (1976) PLSC 7th, p. 2035-2054
(9) Turner G. et al.(1973) PLSC 4th, p. 1889-1914
(10) Carlson R.W. and Lugmair G.W. (1979) Lun. and Plan. Sci X, p. 178-180
(11) Delano J.W. and Ringwood A.E. (1978) PLPSC 9th,p.111-159
(12) Hackmann R.J. (1966) U.S.G.S. Misc. Geol. Inv. Map I-463.
(13) Spudis P.D. (1978) PLSC 9th, p. 3379-3394
(14) Hawke B.J. and Head J.W. (1978) PLPSC 9th, 3285-3309
(15) Compston W. et al. (1975) The Moon 14, p. 445-462
(16) Ryder, G. et al. (1977) EPSL 35 p. 1-13
(17) Mark R.K. et al. (1975) PLSC 6th, p. 1501-1507
(18) Morgan J.W. et al. (1975) Geochim. Cosmochim. Acta 39, p.261-264
(19) Hawke B.J. and Head J.W. (1977) PLSC 8th, p. 2741-2761
(20) Ryder G. et al. (1975) The Moon 14, p. 327-357
(21) Taylor G.J. et al. (1978) in Mare Crisium: The View from Luna 24, Pergamon Press, p. 357-370
(22) Turner G. and Cadogan P.H. (1975) PLSC 6th, p. 1509-1538
(23) Warner J.L. et al. (1976) Lunar Sci. VII, p. 915-917
(24) Blanchard D.P. and Budahn J.R. (1979) Lunar and Plan. Sci X, p. 134-136
(25) Warner J.L. et al. (1977) PLSC 8th, p 2051-2066
(26) Ryder G. (1979) PLPSC 10th, in press.
(27) Oberbeck V.R. and Morrison R.H. (1976) PLSC 7th, p 2983-3005
(28) Schultz P.H. and Spudis P.D. (1979) PLPSC 10th, in press.
(29) Simonds C.H. et al. (1976) PLSC 7th p. 2509-2528

PETROGRAPHY AND COMPOSITION OF LARGE LUNAR GLASS OBJECTS; R.B. Schaal, Lockheed Electronics Co., Inc., Houston, TX 77058; Karen H. Fryer, The Lunar and Planetary Institute, Houston, TX 77058; Friedrich Hörz, NASA-Johnson Space Center, Houston, TX 77058

INTRODUCTION

Because most lunar craters of all sizes, from less than 0.1 μm to 300 km were formed by projectiles with velocities exceeding 10 km/sec, impact melts were formed in each of those craters, creating a wide range of melt volumes. Melt volumes on the order of μm^3 occur in glass-lined microcraters, mm^3 in regolith agglutinates, and km^3 in megacrater melt sheets (1,2,3,4). Interpretation of the P/T conditions required to produce shock metamorphic effects and shock melts has been possible through investigation of shock products collected at terrestrial impact craters (5) and recovered from shock experiments (6). Our resulting understanding is that typical lunar impacts (>10 km/sec) create superheated "whole-rock" melts; thus, chemical variety observed in impact melts is controlled by the lithology of the targets, although textural diversity is caused by wide variations in a) melt volumes, b) ejection histories, c) cooling rates, and d) assimilation of shocked and unshocked ejecta debris.

This reasoning has lead to the general acceptance that microcrater glasses and homogeneous regolith glasses are derived primarily from distinct target rocks (1,2), that agglutinates are derived from fine-grained soils (3), and that large-scale impact melts, forming a diversity of texturally different rock types, are derived from a variety of monomict or polymict targets.

The objective of this study is to characterize a different group of lunar impact glasses, the "large glass objects (LGOs)," with intermediate volumes (cm^3), which occur in the following forms: a) thick drapings or coatings on rocks; b) large solid or hollow spheres, and c) veins penetrating rocks. We define "LGOs" as glasses with masses >>1 g or volumes typically greater than several cm^3 and macroscopically holohyaline textures. The LGOs are unique because their size implies that they were formed by cratering events larger than the "typical" lunar microcrater events and probably smaller than those which formed melt ponds. The LGOs appear to be the largest holohyaline impact melts available in the Apollo collection.

The purpose of this study is to distinguish between a polymict, regolith parental material and a monomict, pristine rock parental material and to address the questions of possible shock-induced selective volatilization and meteoritic contamination. We have formed a miniconsortium in order to obtain a) detailed petrographic descriptions, b) major-element chemical analyses via electron microprobe, c) trace-element determinations via instrumental neutron activation analysis (INAA) and d) ferromagnetic resonance measurements (FMR) of the LGOs.

This abstract presents only preliminary petrographic descriptions of five LGOs and major-element chemistry of only one. Additional studies including INAA and FMR are in progress and will be reported at the conference. Furthermore, additional LGOs have already been allocated for study.

PETROGRAPHY

Physical properties of five LGOs observed in thin section (TS) are listed in Table 1. Smooth surfaces and spherical shapes of 60095 and 65016, glass spheres, indicate that the melt cooled in free flight as ejecta droplets. TS 64455,70 and 65035,6 display glass coatings in contact with host rock and textures in the glass were attained by flow or splash of melt onto the host rock surface. Although 67115 is a glass-coated breccia, TS 67115,24 is an angular glass chip broken from the host. The crystallinity, schlieren, and vesicles in the LGOs indicate that the LGOs experienced molten flow and rapid cooling.

PETROGRAPHY AND COMPOSITION OF LARGE LUNAR GLASS OBJECTS

Schaal, R. B. et al.

Crystallinity. Each LGO except 65035 is holohyaline, indicating rapid cooling without primary crystallization. However, the 65035 coating has a microcrystalline microporphyritic texture indicating less rapid cooling and sequential crystallization.

Spherulites, nucleated on small crystal inclusions, vesicles, and outer glass surfaces, occur in each TS except 65035 but comprise less than 5% of each sample. The very fine-grained nature of the spherulites signifies rapid subsolidus crystallization with a large degree of supercooling (7).

Schlieren. Prominent schlieren, especially in glass coating 64455, give vivid evidence for flow of melt in the holohyaline samples. Color variations defining the schlieren are primarily attributed to the presence or absence of microscopic metal spherules (kamacite and troilite) and, possibly, to variations in abundances of Fe, Ti, Ni, or Cr in the glass. Schlieren in 64455 and 67115, glass coatings, spread throughout the length of the glass and, especially in 64455, display signs of swirling flow. Flow is enhanced by initially larger relative motion of fluid across stationary host rock, as represented by the flow schlieren composed of assimilated host rock material. Schlieren in 60095 and 65016, glass spheres, exhibit less contrast in color, extend shorter distances, and suggest that flow is more passive in ejected melt bodies.

Vesicles. Vesiculation is developed in each of the holohyaline samples (all but 65035) suggesting loss of volatiles and/or rock vapor from the melt. In 64455 vesicles are aligned in flow bands and schlieren appear to flow around vesicles, indicating that vesicles formed before cessation of flow. Vesicles in each sample are spherical; lack of deformation also implies concurrent growth of vesicles with flow in the melt.

The abundances of vesicles is different between the four holohyaline LGOs. Spherical LGOs, 60095 and 65016, contain more and larger vesicles than rock-coating LGOs, 64455 and 67115 (Table 1). This feature may signify that the glass coatings cooled more rapidly than the glass spheres, caused by efficient conductive cooling to the host rock.

COMPOSITION

The major element chemistry of the LGOs obtained with the electron microprobe provides sufficient evidence to distinguish the most likely candidates for their respective parental materials. A comparison of major element abundances in LGO 60095 with those in local soils and igneous rocks at the Apollo 16 site (Fig. 1) indicates that the local soil is most similar in composition and is the most likely parental material. Similar comparisons of the composition of other LGOs are presently in progress. However, conclusions based on major-element chemistry are tentative. Both INAA and FMR analyses are required to provide more definitive evidence for determining their parental materials.

REFERENCES

(1) Schaal R. B., et al. (1976) PLSC 7th, p. 1039-1054.
(2) Reid A. M., et al. (1972) PLSC 3rd, p. 363-378.
(3) Via W. N. and Taylor L. A. (1976) PLSC 7th, p. 393-403.
(4) Phinney W. C. and Simonds C. H. (1977) in "Impact and Explosion Cratering." Pergamon, p. 771-790.
(5) Grieve R. A. F., et al. (1977) in "Impact and Explosion Cratering," Pergamon, p. 791-814.
(6) Schaal R. B. and Hörz F. (1977) PLSC 8th, p. 1697-1729.
(7) Lofgren G. (1971) JGR 76, 5635-5648.

PETROGRAPHY AND COMPOSITION OF LARGE LUNAR GLASS OBJECTS

Schaal, R. B. et al.

TABLE 1. PHYSICAL PROPERTIES OF LARGE GLASS OBJECTS

THIN SECTION	1	2	3	4	5	6	7	8
60095,34	SPHERE	58.8 mm^2	11.0 mm	7.6 mm	1.2%	49-342 μm	19	10-88 μm
64455,70	COATING	30.0 mm^2	10.4 mm	10.0 mm	0.1%	12-200 μm	>50	12-106 μm
65016,10	SPHERE	31.9 mm^2	7.7 mm	5.7 mm	3.1%	24-683 μm	10	4-28 μm
65035,6	COATING	30.7 mm^2	7.5 mm	5.0 mm	0	0	12 grains	<2.5 mm
67115,24	COATING	15.1 mm^2	5.5 mm	3.7 mm	0.16%	10-85 μm	10	8-40 μm

1 TYPE OF SAMPLE; GLASS SPHERE OR GLASS COATING ON ROCK
2 AREA OF GLASS IN THIN SECTION, MEASURED ON PHOTOMICROGRAPH
3 LENGTH OF GLASS IN THIN SECTION, MAJOR AXIS
4 WIDTH OF GLASS IN THIN SECTION, MINOR AXIS
5 ABUNDANCE OF VESICLES, % OF GLASS AREA
6 SIZE OF VESICLES
7 ABUNDANCE OF METAL SPHERULES, TOTAL NUMER IN THIN SECTION
8 SIZE OF METAL SPHERULES

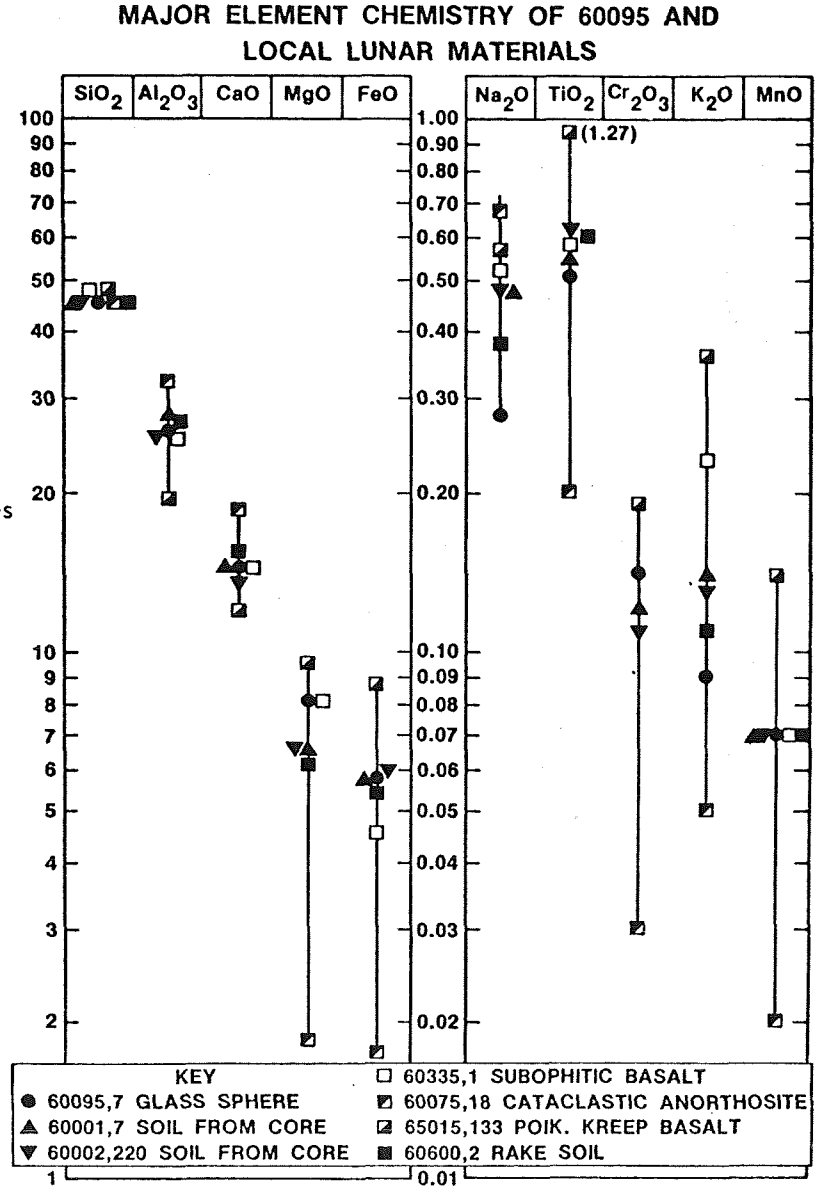

Fig. 1. Comparison of electron microprobe analyses of 60095 (average of 64 spots) with compositions of local lunar materials. Soils are most similar.

ARE THERE ANCIENT CLASTS IN LUNAR HIGHLAND ROCKS?

O. A. Schaeffer, A. E. Bence, and G. Eichhorn, Department of Earth and Space Sciences, State University of New York at Stony Brook, Stony Brook, New York 11794

Introduction. Most of the lunar highland rocks have been severely altered by impacts during the first 600 million years of the moon's existence. Whether the early bombardment represents gradual removal of relatively large objects left over after planet formation or whether the early bombardment was dominated by a very intense period around 4 G.y. ago is one of the unsolved problems of lunar chronology. From the systematics of Pb isotopes in lunar highland rocks it has been suggested (1) that either there was an intense bombardment 4 G.y. ago or else that the highland rocks were dominated by ejecta from the Imbrium event. ^{39}Ar - ^{40}Ar studies have yielded plateau ages in the interval 4.0 to 4.3 G.y. (2) and a suggestion of 4.5 G.y. old plagioclase clasts in 65015 (3) which is a noritic breccia containing abundant angular plagioclase clasts. If the ages are correct, these clasts would represent some of the earliest crystalline material in the lunar crust. One problem with these thermal release studies is the possibility that there may be excess argon in low-K minerals with high melting points, e.g. anorthite. Previously, in our initial ^{39}Ar - ^{40}Ar laser study of 65015,173, we reported that we had found 4.5 G.y. old material (4). On a re-examination of the three old plagioclase clasts identified, we noted that because of the extremely low K content, our correction for the blank at mass 39 was erroneous. (The blank is centered on a hydrocarbon mass displaced from the center of the ^{39}Ar mass peak.) We have now repeated the previous study on a one square centimeter polished surface of 65015,186.

Results and Discussion. The sample was irradiated by neutrons at the Brookhaven high flux reactor. A beam of light from a pulsed ruby laser was focused on the sample surface by a petrographic microscope. Each pulse resulted in melting and evaporating about 0.2 μg of material. Depending on the K-content, from 5 to 50 laser pulses were made to accumulate enough argon for an isotopic analysis. The results are listed in Table 1. The matrix ages of 3.87 ± .01 and 3.82 ± .01 G.y. are lower than the plateau age (3) of 3.96 ± .05 G.y., possibly due to slight argon loss in the laser study. The laser ages are total K-Ar ages and would be lower if mineral sites lost argon at low temperatures while the plateau age would not. Preheating the sample before laser work will show whether this is indeed the case.

The plagioclase clast laser ages vary from 3.73 ± .03 to 3.94 ± .04, the spread may be due to variable gas loss by the clasts. In any event, we find no samples with ages older than 4.0 G.y. One of the clasts was fairly large, allowing a laser analysis of the core and an intermediate zone. The core gave an age of 3.88 ± .03, while the intermediate zone gave an age of 3.85 ± .04, not appreciably different. We see no evidence for 4.5 G.y. old clasts in 65015,186. While our result casts some doubt on the previous result (3), it is possible that the ancient material in 65015 is rare and did not occur in our piece. On the other hand, it is also possible that the 4.5 G.y. old age reported for a clast in 65015 previously (3) was due to excess argon in a low-K high melting mineral phase.

Table 1. Argon isotopic analysis and age of various minerals from breccia 65015.

Mineral	40	39*	38*	37	36*	K/CA	40/39	AGE (G.Y.)
A	1413.7 ± 3.3	39.34 ± 0.22	2.41 ± 0.06	167 ± 2	1.48 ± 0.11	.128 ± .004	35.9 ± 0.2	3.87 ± 0.01
B	90.5 ± 0.9	2.81 ± 0.08	1.23 ± 0.09	145 ± 3	0.87 ± 0.07	.011 ± .001	32.1 ± 0.9	3.69 ± 0.04
C	701.1 ± 2.0	19.96 ± 0.16	1.94 ± 0.08	217 ± 6	0.93 ± 0.17	.050 ± .002	35.1 ± 0.3	3.83 ± 0.01
C	244.6 ± 1.3	7.21 ± 0.24	2.11 ± 0.10	287 ± 5	1.40 ± 0.17	.014 ± .001	33.9 ± 1.1	3.78 ± 0.05
D	110.4 ± 0.8	3.22 ± 0.05	1.86 ± 0.10	256 ± 2	1.06 ± 0.08	.007 ± .001	34.3 ± 0.6	3.79 ± 0.02
D	106.7 ± 0.6	2.92 ± 0.06	1.53 ± 0.09	210 ± 2	1.05 ± 0.08	.008 ± .001	36.5 ± 0.8	3.89 ± 0.03
D	190.6 ± 1.6	5.28 ± 0.09	1.49 ± 0.08	208 ± 3	1.02 ± 0.06	.014 ± .001	36.1 ± 0.7	3.87 ± 0.03
C	32.2 ± 0.8	0.82 ± 0.04	1.25 ± 0.07	159 ± 3	0.60 ± 0.06	.003 ± .001	39.3 ± 2.2	4.01 ± 0.07
C	13.8 ± 0.5	0.43 ± 0.03	2.61 ± 0.12	350 ± 2	1.58 ± 0.08	.001 ± .001	32.4 ± 2.7	3.71 ± 0.11
C	181.0 ± 0.6	4.81 ± 0.14	2.42 ± 0.12	304 ± 4	1.39 ± 0.14	.009 ± .001	37.7 ± 1.1	3.94 ± 0.04
C	31.1 ± 0.4	0.83 ± 0.04	1.53 ± 0.08	205 ± 4	0.96 ± 0.11	.002 ± .001	37.3 ± 2.0	3.93 ± 0.07
C	129.7 ± 1.5	3.90 ± 0.08	2.05 ± 0.06	251 ± 4	1.10 ± 0.06	.008 ± .001	33.3 ± 0.8	3.75 ± 0.03
E	88.6 ± 1.4	2.52 ± 0.08	1.13 ± 0.09	158 ± 3	0.74 ± 0.14	.009 ± .001	35.1 ± 1.2	3.83 ± 0.05
E	105.1 ± 0.4	2.92 ± 0.06	1.63 ± 0.06	247 ± 3	0.94 ± 0.09	.006 ± .001	36.0 ± 0.8	3.87 ± 0.03
A	1026.8 ± 2.4	29.38 ± 0.13	2.02 ± 0.14	175 ± 2	1.20 ± 0.05	.091 ± .003	35.0 ± 0.2	3.82 ± 0.01
C	17.2 ± 0.6	0.46 ± 0.03	0.82 ± 0.05	103 ± 4	0.44 ± 0.08	.002 ± .001	37.7 ± 2.5	3.94 ± 0.09
C	36.8 ± 1.7	1.06 ± 0.04	0.50 ± 0.07	58 ± 5	0.13 ± 0.09	.010 ± .001	34.6 ± 2.1	3.81 ± 0.08
C	10.5 ± 0.3	0.36 ± 0.02	1.14 ± 0.07	166 ± 4	1.14 ± 0.08	.001 ± .001	28.4 ± 2.0	3.50 ± 0.09
C	4.3 ± 0.3	0.20 ± 0.02	0.83 ± 0.05	113 ± 4	0.45 ± 0.08	.001 ± .001	21.6 ± 2.8	3.09 ± 0.18
C	6.5 ± 0.4	0.20 ± 0.02	0.71 ± 0.05	89 ± 2	0.56 ± 0.11	.001 ± .001	32.4 ± 3.9	3.71 ± 0.16

A, Matrix Sulfides; B, Plag.-Pyrox.; C, Plag. Clast; D, Center large Plag. Clast; E, Intermediate Zone large Clast.

ANCIENT CLASTS IN LUNAR HIGHLAND ROCKS

O. A. Schaeffer, et al.

References:

1. F. Tera, D. A. Papanastassiou, and G. J. Wasserburg (1974) Earth Planet. Sci. Lett. 22, 1-11.
2. G. Turner (1977) Phys. Chem. Earth 10, 145-195.
3. E. K. Jessberger, J. C. Huneke, F. A. Podosek, and G. J. Wasserburg (1974) Proc. Lunar Sci. Conf. 5th, 1419-1449.
4. O. A. Schaeffer, A. E. Bence, and G. Eichhorn (1978) Lunar Planet. Sci. IX, 1004-1006.

EVOLUTION OF INTERMEDIATE-AGE IMPACT BASINS ON THE MOON.
Peter H. Schultz, Lunar and Planetary Institute, Houston, TX 77058

The Orientale impact basin is often referenced as the prototype multi-ring basin owing to its well preserved state (1,2). Other large multi-ringed basins commonly are viewed as impact-degraded and lava-inundated remnants of the original Orientale-style morphology (3). However, volcano-tectonic modification of the major impact basins makes such a view a gross oversimplification. This statement is based on the contrasting states of presentation of a given lunar basin, the morphology of martian impact basins, and the complex interrelation between volcanism and tectonism in certain lunar craters.

The Nectaris and Crisium Basins illustrate several salient clues for recognizing the pre-mare basin morphology. The basin rings of Nectaris are delineated by the concentric arrangement of plateaus and massifs, as well as the prominent Altai scarp. The extremely degraded appearance of the basin is largely based on the absence of well-defined mountainous ridges. Yet, the Altai scarp exhibits 0.3 - 0.6 km relief and extends a distance of 800 km. Additionally, radial patterns and the Rheita Valley south of Nectaris have been interpreted as remnants of Nectaris ejecta deposits (4), yet the preservation of such structures is also inconsistent with any inferred degraded state of the concentric mountain rings. Similarly, the Crisium Basin exhibits fine-scale radial lineations, but the basin ring appears extensively degraded and broken. As around Nectaris, the prominent Crisium ring is typically composed of steep-sided plateaus, rather than subdued peaks and hummocks. The plateau surfaces are at approximately the same elevation (6.6 km - 7.2 km) and are separated by irregular valleys. The broken appearance of the basin ring is not simply the result of closely spaced superposed craters, and plateau profiles are not the style of degradation expected from long-term impact erosion.

Such contrasts between preserved features of relatively minor relief (ejecta scouring, secondary craters, scarps) and the absence or unusual appearance of mountainous rings suggest that the intermediate-age impact basins such as Crisium and Nectaris underwent rapid tectonic adjustments (5,6) and that the Orientale-style physiography may not have developed, or existed for only a short time (<0.1 b.y.). Recent studies (7,8,9) indicate that volcanism may have preceded at least the last major basin-forming event (Orientale). Consequently, initial basin morphology may have been profoundly affected by the evolution of the early lunar crust and mantle (6,10,11).

The style of volcano/tectonic modification of smaller lunar craters resemble elements of certain multi-ringed basins. The mare-filled crater Pitatus exhibits a Crisium-like flat-topped rim profile formed by interior and exterior concentric graben. Similarly concentric graben have created modified rim profiles in floor-fractured craters such as Gassendi, Doppelmayer, and Haldane (12). The crater Haldane, in particular, exhibits a four-ringed plan believed to reflect tectonic modification associated with basaltic volcanism (6,13). In general, such modification can resurrect the circular plan of a heavily degraded crater, increase its circularity along ring faults, create ridge or flat-topped rim

EVOLUTION OF INTERMEDIATE-AGE IMPACT BASINS

Schultz, Peter H.

profiles), and produce a marked contrast between preserved surface detail inside and outside the crater (12).

The flat-topped massifs surrounding both Nectaris and Crisium are proposed to be crustal blocks left in relief subsequent to subsidence along relatively well-defined concentric zones, rather than impact-battered remnants of an uplifted crater rim. The original "crater rim" in these and other intermediate-age basins may not have surface expression. Rather, the inner-ring massifs reflect the collapsed crust exterior to this transient marker (14) and may be largely erased by subsequent volcano/tectonic subsidence as in Crisium, Serenitatis and Humorum. Indirect markers of the original impact may be revealed by the distribution of vents and basalts within the inner basin. This view contrasts with interpretations where basin rings indicate nested-crater rims (15) or where other preserved elements of the original impact structures are sought. It extends interpretations where the outer ring reflects tectonic adjustment (5,6,8,10,16,17) to include the intermediate ring and even the inner rings.

The proposed model has several implications. First, the pre-lava filling morphology of impact basins may be significantly different from an Orientale model. Second, exposed ring structures may provide little indication of the original excavation basin in heavily modified structures. Third, samples from the major rings may not show evidence of strong shock effects. Fourth, the structural imprint of impact basins in the ancient lunar, martian, and even terrestrial crust may be long lasting and can be re-exposed during subsequent regional volcanism/tectonism.

References:

1. Moore H.J., Hodges C.A. and Scott D.H. (1974) *Proc. Lunar Sci. Conf. 5th*, p. 71-100.
2. Wilhelms D.E. (1973) *Apollo 17 Prelim. Sci. Rept.*, p. 29-29 to 29-34. NASA SP-330.
3. Head J.W. (1976) *Rev. Geophys. Space Phys. 14*, p. 265-300.
4. Stuart-Alexander D.E. (1971) U. S. Geol. Survey Misc. Geol. Inv. Map I-694.
5. Hartmann W.K. and Wood C.A. (1971) *The Moon 3*, p. 3-78.
6. Schultz P.H. (1976) *Moon Morphology*.
7. Ryder G. and Taylor G.J. (1976) *Proc. Lunar Sci. Conf. 7th*, p. 1741-1755.
8. Schultz P.H. and Spudis P.D. (1978) *Lunar and Planetary Science IX*, p. 1033-1035.
9. Schultz P.H. and Spudis P.D. (1979) *Proc. Lunar Sci. Conf. 10th* (in press).
10. Melosh H.J. and McKinnon W.B. (1978) *Geophys. Res. Letts. 5*, p. 985-988.
11. McGetchin T.R., Head J.W. and Schultz P.H. (1979) In *NASA TM-80339*, p. 168-169.
12. Schultz P.H. (1976) *The Moon 15*, p. 241-273.
13. Wolfe R.W. and El Baz F. (1976) *Proc. Lunar Sci. Conf. 7th*, p. 2903-2912.
14. Howard K.A., Wilhelms D.E. and Scott D.H. (1974) *Rev. Geophys. and Space Phys. 12*, p. 309-327.
15. Hodges C.A. and Wilhelms D.E. (1978) *Icarus 34*, p. 294-323.
16. Head J.W. (1977) In *Impact and Explosion Cratering*, p. 563-573.
17. McCauley J.F. (1977) *Phys. of Earth and Planet. Ints. 15*, p. 220-250.

LATERAL MIXING OF THE CRUST: EVIDENCE, MECHANISMS, AND IMPLICATIONS.

Peter H. Schultz and M. Mendenhall, Lunar and Planetary Institute, Houston, TX 77058

Descriptions of secondary cratering generally focus on single-body and two-body impacts into relatively homogeneous quartz-sand targets (1,2). The resulting craters clearly show that locally excavated debris dominate the ejecta deposits. However, several observations suggest that the color and spectral signature of primary crater ejecta remains at large distances from the source. First, spectra of ejecta deposits as far as 3R from the rim of several large craters (Picard, Aristillus) correspond to excavated debris from the primary crater (3,4). Second, spectra of primary crater material from Theophilus are identifiable in crater rays at distances greater than 1000 km (5). Third, geochemical data suggest that crater ray deposits contain observable quantities of non-local material (6). Fourth, dark crater rays from the lunar crater Dionysius (7) and numerous craters on Ganymede (8) suggest that primary crater ejecta deposits remain identifiable. Fifth, low-albedo deposits and lobate-bordered floor material within large basin secondaries require transport and survival of primary ejecta from the parent basin (9).

The survival of primary ejecta as a significant surface deposit may be understood if the impacting ejecta consisted of a complex of particles or a very weakly bonded projectile. This physical state of ejecta should be characteristic of certain target lithologies (e.g., highland crust) and for large impacts where comminution may increase with increased impact energy (10).

Preliminary laboratory-scale experiments have been made at relatively low velocities (30 m/s) in order to recognize trends for planned higher velocity experiments. Projectile masses remained approximately the same (55g - 70g) but the physical state included solid bodies, clustered multiple bodies (14 to 100), unbonded sand, and thinly crusted bodies containing different viscosity suspensions. Results clearly show the contrast between low-density and high-density systems at these low velocities. Single body projectiles formed well-defined craters with raised rims (aspect ratio of 1:5) with the projectile buried beneath the floor. Multiple-body projectile systems produced shallower, irregular craters with depths decreasing with an increasing number of projectiles. A projectile system of 100 bodies produced a slightly mounded, shallow floor (aspect ratio of 1:6). Individual projectiles exhibited little penetration below the crater floor and were concentrated around the central mound. Low-viscosity projectiles produced low-volume and extremely shallow craters (aspect ratios typically 1:10) with more pronounced central mounds. Craters became shallower with increased velocities. Projectile remnants draped the crater floor with little penetration.

At such low velocities, the cratering process is by compression and not by shock relaxation of the target. This behavior generally characterizes subsonic (<2 km/s) impacts, in contrast to hypervelocity impacts more generally described. Consequently, with increased target strength, the penetration by the projectile will be drastically decreased and ejecta will be primarily composed of fragmented projectile material. The observed central

mound represents target material left in relief as a result of lateral erosion. Similar phenomena have been described for laboratory-scale explosion craters (12).

These results confirm previous qualitative descriptions of the expected crater morphology and may have application to certain lunar secondary craters (11). In addition, they suggest that cratering efficiency (displaced mass/projectile mass) decreases with decreasing projectile strength. Consequently, low-velocity/low-density ejecta complexes may preserve primary crater debris in deposits near the surface. The importance of this process depends on the strength contrast between the impactor and target. It is important to note that these results do not underplay the importance of local mixing for single or double impactors in incompetent targets. However, they indicate that dilution of primary ejecta by locally excavated material may be less important for certain, and probable, low-velocity impact conditions.

Although vertical mixing currently appears to dominate regolith evolution (13), this observation largely reflects the dominant role of more frequent, small (<1 km) size craters. Catastrophic contributions of nonlocal material to the regolith necessarily result from ejecta of less frequent large craters. Prior to 3.9 AE, lateral transport of ejecta over much broader scales by basin-size impacts and their secondary craters must have occurred. The contribution of these nonlocal ejecta to near-surface deposits may be possible by weakly bonded and extended-system impacts and is perhaps partly responsible for the inferred light-plains veneer on ancient mare surfaces (14).

References:

1. Oberbeck V.R. (1975) *Rev. Geophys. Space Phys. 13*, 337-362.
2. Morrison R.H. and Oberbeck V.R. (1975) *Proc. Lunar Sci. Conf. 6th*, 2503-2530.
3. Pieters C.A., McCord T.B. and Adams J.B. (1976) *Geophys. Res. Letters 3*, 697-700.
4. Johnson *et al.* (1977) *Proc. Lunar Sci. Conf. 8th*, p. 1013-1028.
5. Saunders *et al.* (1976) *Lunar Science VII*, p. 761-763.
6. Andre *et al.* (1979) *Lunar Science X*, p. 38-40.
7. Schultz P.H. (1976) *Moon Morphology*, 628 pp.
8. Smith B.A. *et al.* (1979) *Science 204*, p. 951-972.
9. Schultz P.H. and Mendenhall M.H. (1979) *Lunar and Planet. Sci. Conf. X*, p. 1078-1080.
10. Schultz P.H. and Mendell W. (1978) *Proc. Lunar Sci. Conf. 9th*, p. 2857-2883.
11. Schultz P.H. (1978) *Lunar Science IX*, p. 1024-1026.
12. Pieketowski A. (1979) personal communication.
13. Hörz F. (1978) *Proc. Lunar Planet. Sci. Conf. 9th*, p. 3311-3331.
14. Schultz P.H. and Spudis P.D. (1979) *Proc. Lunar and Planet. Sci. 10th* (in press).

GEOLOGICAL CONTENT OF THE SKYLAB LUNAR MULTISPECTRAL SCANNER DATA.
C. Ronald Seeger, Western Kentucky University, Bowling Green, Kentucky 42101.

Seeger, et al. (1) previously reported on the Skylab S-192 multispectral scanner interpretation in terms of potential for lunar geology/geochemistry, and the data processing and filtering involved. This report is to convey the geologic content of this data. Details of the data processing and filtering are published elsewhere (2).

As before, the data from LUNARCAL V (SKYLAB IV) was processed by IBM including the filtering, and clustered. Prior to clustering each pixel was divided by the readings in Band 4 (centered at .56 μm) in order to minimize the effects of albedo, which had been a major determinate in previously clusterings, and thus to cluster as much as possible on spectural characteristics. Then each of the 2388 valid pixels on the lunar nearside was classified as to cluster type and a cluster class map produced. This map is the basis for the characterization map which will be available at the meeting.

Figure 1 shows the "spectral" characteristics of the cluster means for the 17 cluster classes in the 12 wavelength bands on the observed lunar disk. They are relative to the MS-2 location in Mare Serenetatis (3). They are also normalized to .56 μm (e.g., .56 μm = 1).

Using the data represented by Figure 1, it is possible to characterize the lunar nearside in a way quite similar to other studies (4) with some omissions and additions. This characterization system is given on Table 1.

The characterization features listed on Table 1 were determined as follows (the wavelengths of the band passes are shown of Figure 1): 1) and 2) are obvious; 3) "Blueness" is determined by the relative radiance observed in Band 1 to Band 4 compared to that for MS-2 (cluster class L); 4) albedo is the true counts in Band 4 for each cluster class separated when the standard deviation of the mean does not overlap the true counts of another cluster class; 5) 1 μm absorption refers to the well known pyroxene (and glass) band at ~0.9-1.0 μm. Band 8 peaks at 0.96 μm, so the strength of the absorption relative to MS-2 is calculated as follows: [(Band 5 + Band 6) /2 + Band 9] /2 - Band 8. Thus, a minus number means less absorption than Mare Serenetatis, MS-2; 6) IR. Band 12 should contain components of both reflected solar and emitted thermal infrared (5), so the true counts in Band 12 were ranked and divided into obvious groups; 7) Adams and Charette (8) report that the relative heights of the "shoulders" on either side of the 0.9 μm absorption band characterize certain highland rock types, so the calibrated true count heights of Band 6 (Left) VS Band 9 (Right) was compared; 8) Band 2 exhibited positive and negative anomaly patterns compared to MS-2. There are reported.

Discussion. These results provide additional areal and spectral coverage to previous similar studies (4). They are consistent with these studies. The general conclusion of our previous reports (1), e.g., there is considerable heterogeneity in the lunar highlands materials, is unchanged. Also, the special conclusions of those reports (1) are reconfirmed.

This work allows the characterization of most of the geologic units mapped on the lunar near side (6, 7) as to spectral class. This is tabulated on Table 2.

Conclusions. A few of the preliminary conclusions which can be drawn are: a. Copernican class craters expose more highlands type materials than mare types. An especially strong component of anorthositic gabbro (8) type is present in the Tycho materials; b. Conversely, Eratosthenian crater materials as mapped (6) are mostly of mare type in the mare and highland type in the highlands; c. Hevelius Formation is of highland type and indeed like

Seeger, C. R.

FIGURE 1 AT RIGHT

TABLE 1. CLUSTER CLASS CHARACTERIZATION FEATURES

Cluster Class	A	B	C	D	E	F	G	H	I
1.	H (B)	H	M	H (B)	M	H	M	M (B)	M
2.	354 14.8	79 3.3	187 7.8	77 3.2	103 4.3	139 5.8	81 3.4	126 5.3	44 1.8
3.	.942	1.001	.966	.903	1.022	.978	1.100	.938	.897
4.	8	10	3	7	1	9	6	5	2
5.	-.084	-.100	-.014	-.132	+.012	-.119	+.042	-.100	-.047
6.	6	9	2	4	2	7	4	4	1
7.	Slight Left 1.0	Slight Left 1.2	-	Slight Left 1.7	-	Left 2.2	Slight Right 0.4	Slight Right 0.4	-
8.	-	Pos.	-	Neg.	Pos.	-	-	-	Neg.

TABLE CONTINUED

	J	K	L (MS-2)	M	N	O	P	Q
1.	H	H	M	M	B	B	M	M
2.	212 8.9	199 8.3	222 9.3	82 3.4	124 5.2	166 6.9	67 2.8	126 5.2
3.	.976	.981	1.000	1.006	1.015	.936	1.043	1.024
4.	11	10	2	3	8	8	4	5
5.	-.061	-.090	Strong	-.026	-.013	-.070	-.027	+.016
6.	7	8	2	2	6	5	3	4
7.	Left 4.3	Slight Left 1.5	-	-	Left 2.2	Left 3.3	-	-
8.	-	-	-	-	-	-	-	-

1) Location: M-Mare, H-Highlands, B-Both or Bordering; 2) Number Pixels (2388), percent of disk covered; 3) "Blueness"; 4) Albedo (1 Darkest); 5) 1 μm absorption (-less than MS-2); 6) IR (9 Highest); 7) High "Shoulder", percent; 8) Band 2 anomaly.

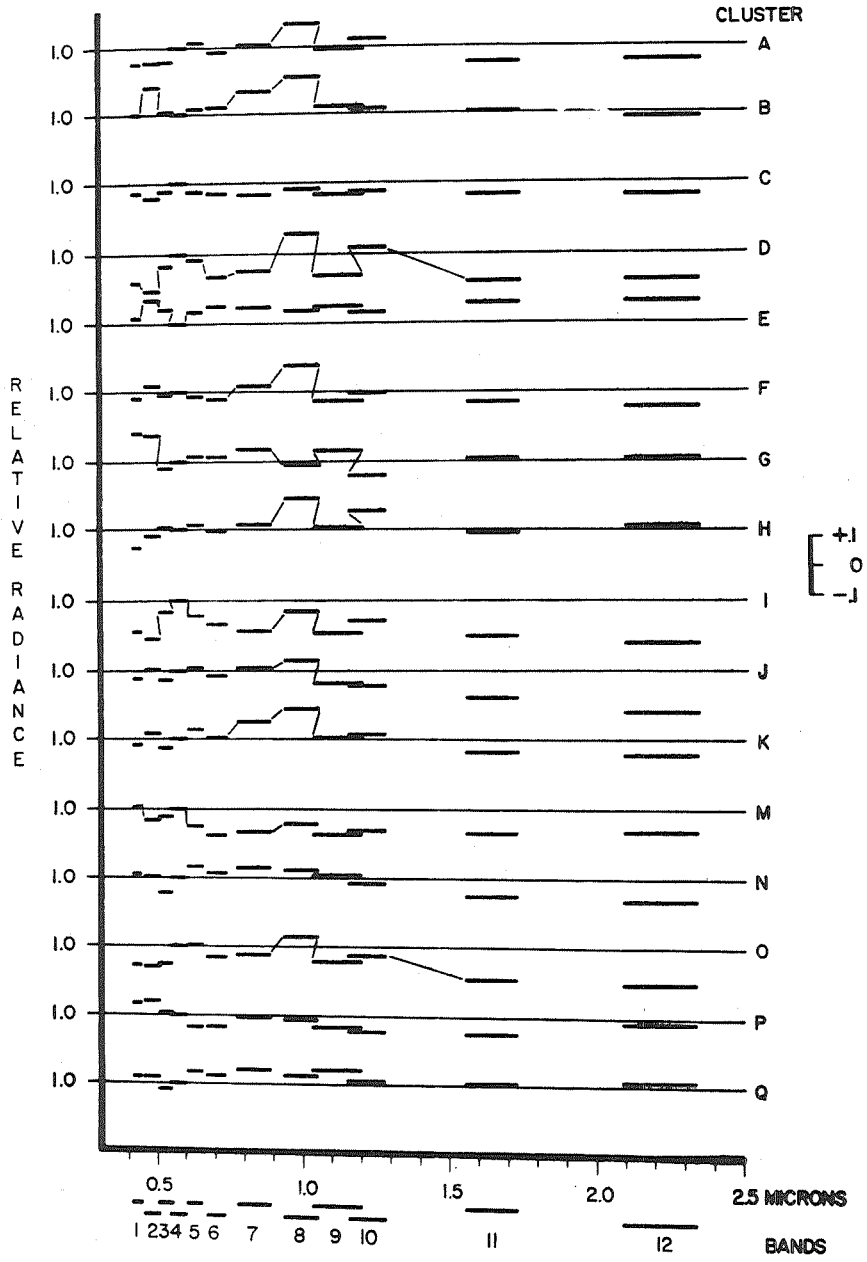

GEOLOGIC...SKYLAB...LUNAR...MULTISPECTRAL

Seeger, C. R.

TABLE 2. RELATIVE COUNTS OF CLUSTER CLASS OCCURRENCES IN MAPPED UNITS OF LUNAR NEARSIDE (WILHELMS AND MCCAULEY, 1971, 6)

	CLUSTER CLASS																
Relative Counts in Mapped Unit (total)	A	B	C	D	E	F	G	H	I	J	K	L	M	N	O	P	Q
Cc_2 (21)	-			-						16					3		
Cc_1	25	6		3		11		13		9	29	4			8		
Cc (total) (153)	26	6	-	4		11	-	13		25	29	4	-	-	11	-	7
CId (31)	-			-	8		-	-	4	-		4		-	-		7
Emp (18)			4			2		3					9				
Ec (mare 22)					-		6					-		-		4	5
Ec (highland 45)	15			-				7		4	7			-	5		
Ihe (16)	3									10		-		-	-		
If (44)	22		-		-		-	12			-	-					-
Ia/ (44)	6	-	-			-		-		-	11	-		7	-		6
Iap (29)	5							8			5			4			7
Ip (82)	23			10	-	-		4		7	7	-		11	10		5
Ihf (53)	21	-			-		-	10			4	6			5		-
Ihp (62)	27	4			7	-	-	-		-	6	-			4		-
IpIt (81)	18	-	4	8		6		-		15	7			-	17		
Ic_2 (58)	14	-		-		9	5			-	8		-	7	6		-
Ic_1 (72)	16	-	-	6		6		13		5	19	-	-		-		-
pIp (16)		5				5				3	3						
pI_j (N_j) (25)		-				19				-	-						
pIr (26)	8			-				9			-		-	-	4		
pIr (Crisium) (19)*	-	9									8						-

*now mapped pNb_m and $_pNbr$ (Wilhelms and El-Baz, 1977, 7).

Cc_2 of Tycho (6); d. Fra Mauro formation shows mixed characteristics of both mare and highlands; e. The undivided Terra units (IpIt) (6) show a variety of spectral types; f. Spectral differences can be observed between Ip and pIp, Ic_2 and Ic_1, and pIr around Mare Crisium and pIr in other locations; g. Janssen Formation has a spectrum dominated by Cluster Class F (Table 1).

References: (1) Seeger, C. R., Potter, A. E., and Wolfe, R. H. Jr., (1977) Lunar and Planet. Sci. IX, p. 1044-1046. (2) Wolfe, R. H, Jr., and Wheeler, S. G., (1979), NASA New Technology Report, NAS 9-14350, manuscript in preparation. (3) McCord, T. B., Charette, M. Johnson, T. V., Lebofsky, L. A., Pieters, C. and Adams, J. B. (1972), J. Geophys. Res., 77, p. 1349. (4) Pieters, C., (1977) Lunar and Planet. Sci. IX, p. 898-900; Science News 111, (1977) cover; Solderblom, L. A. (1977), Proc. Lunar Sci. Conf. 8th, Plate 7; Pieters, C., (1978) Proc. Lunar Plant. Sci. Conf. 9th, p. 2825-2849; (5) McCord, T. B., and Adams, J. B., (1973), The Moon 7, p. 454; (7) Wilhelms D. E., and El-Baz, F. (1977), Geol. Map, East Side Moon, U.S.G.S. Map I-948; (6) Wilhelms, D. E., and McCauley, J. F., (1971), Geol. Map, Near Side of the Moon, U.S.G.S. Map I-703; (8) Adams, J. B., and Charette, M. P., (1975), The Moon, 14, p. 483-489.

LOW SPEED (8 km/sec) IMPACT-ACCRETIONAL HEATING AND EARLY FRACTIONATION OF THE MOON. C. H. Simonds, Northrop Services, Inc., Houston, TX 77034

Wood (1), Taylor (2) and Longhi (3), among others, propose that a total melt of ultramafic "whole moon" composition separated into anorthositic troctolitic and ultramafic compositions by fractional crystallization during the first $3x10^8$ y of lunar history. Impact (accretional) heating is one mechanism proposed to melt the outer few hundred km of the moon. Impact melt, which forms in the few seconds following collision, is typically a total melt. Wetherill (4,5) concludes that the projectiles, which presumably do the heating, are on the order of a hundred km across, impact at about 8 km/sec, and most hit within the first 10^8 years of lunar history. This abstract attempts to apply what is known about impact melting and crystallization of impact melts to evaluate the total melting followed by fractional crystallization hypothesis. Four bodies of relevant information on what impact can do are available: 1) observations of terrestrial craters with melt sheets probably formed by high speed (24.6 km/sec) impacts; 2) observations of lunar, particularly Serenitatis, impact melts formed by projectiles of unknown velocity; 3) hydrodynamic calculations of the flow of debris within a crater; and 4) shock physics calculations of the effect of impact velocity on melt production.

Terrestrial craters--Shoemaker (6) and Grieve and Dence (7) argue that meteorites in Apollo asteroid-like orbits make most of the Phanerozoic craters and that their mean impact velocity with earth is 24.6 km/sec. Geochemical studies of large craters in crystalline rocks suggest that their impact melts are total melts of the target and that the melt sheets did not fractionate by crystal liquid separation. Major and lithophile trace element analyses of the 400-600 km^3, 65 km diameter Manicouagan, Quebec melt sheet (8, 9) show that the composition of all samples of the sheet can be duplicated by simple mixture of the target lithologies which include meta-gabbro and anorthosite, tonalite and granodiortes. The mixing is so complete that one gram samples of melt have a SiO_2 content of 57.7 ± 1.2% although the target ranges from 42 to 72% SiO_2. Samples collected along vertical traverses through the >100 m thick lower portion of the melt sheet show no cryptic layering or other evidence of fractionation. Major element analyses (10) show a similar pattern of total melting for the 80 m thick lower part of the sheet at the 25 km diameter Mistastin, Labrador structure. Simonds et al. (11) analyzed melt rocks from throughout the lower 130 m of the melt sheet at the 28 km diameter West Clearwater, Quebec structure and again conclude that the melt is a total melt of the target with no subsequent fractionation within the melt sheet.

Field and petrographic studies of the melt sheets at the above mentioned craters and other structures reveal much of them to be so fine grained and filled with debris that the melts quickly cooled and become too viscous to allow any crystal settling. The solid debris ranges from angular crystal fragments <40 μm across to blocks >10 m across. Undigested debris is concentrated (10-50% by volume) in the top and bottom 10-20 m of the melt sheet, but even the coarsest grained samples from the interior of the melt sheets have a few % plagioclase with patchy or other complexly zoned cores suggesting the remnants of incompletely digested debris. The composition of these relict clasts suggests that they are only the most refractory phases. The small fragments of less refractory phases (e.g. garnet, amphibole, biotite) have been completely digested. The relict material is only a fraction, potentially a small fraction, of the solid debris initially mixed with the melt. Large blocks of dense amphibolite are exposed in cliffs ten meters above the base of the Manicouagan melt sheet and isolated samples of basement lithologies

collected from lichen and moss covered outcrops over 50 m up into the melt sheet. Such observations suggest that such blocks occur throughout the melt sheet. The suspended blocks imply that the melt sheet's viscosity quickly becomes too high to allow the blocks to settle to the bottom of the sheet.

As argued by Simonds (12) and Simonds et al. (11, 13) the lack of shock features in the fine debris suggests an upper limit of about 300°C for the shock induced heating of the debris prior to incorporation into the melt. He has further argued that the cold clasts lowered the melt's temperature sufficiently that the melt quickly began to crystallize. Lofgren (14) duplicated textures of lunar impact melt rocks and suggests a different formation mechanism for the fine grain size of impact melts. In his view, the rapid heating of the melt does not allow sufficient time for breakdown of all small crystallites, thus the impact melts are full of nuclei to promote crystallization. Both authors agree that the textures of impact melt rocks suggest rapid crystallization of very small grains and rapid increases in viscosities. The observations of suspended blocks of dense rock in the melt sheets supports this proposition, and if the large blocks cannot separate from the melt, certainly the small crystals cannot. Thus crystal fractionation (crystallization and separation of melt from crystals) seems intrinsically difficult in impact melts.

Lunar impact melts--Typical 3.9 billion year old impact melt rocks from the moon are fine grained (plagioclase 10-50 μm) clast laden melt rocks texturally similar to the rocks from the marginal 10-20 m of terrestrial melt sheets. The coarser lunar impact melt rocks (e.g. 14310, 68415) are similar to, but less abundant than, the medium grained rocks with largely digested clasts in the terrestrial melt sheets. There are no suites of samples in the lunar collection where target and impact melt rock can be compared directly. The only reasonably complex sampled lunar melt sheet is the source of the boulder samples at Apollo 17. The boulders all rolled down from a line of boulders about 400 m up the sides of the 2 km high massifs. This melt sheet is believed to have been formed by the Serenitatis event and appears to be only a few tens of meters thick. The composition of the boulders are very restricted with no evidence of a crystal fractionation trend in the analyses.

Turbulent flow of impact melt within a crater--Numerous numerical models for the cratering process for high velocity impacts (15, 16) suggest that impact melt flows outward and downward forming a lining on the expanding transient cavity. The flow along the base of the melt sheet allows less shocked debris to come in contact with the melt which is still moving at high velocities. Reynolds numbers for the flow of the melt across the relatively slow moving fractured basement at the margin of the excavation are $>10^5$ and thus flow should be turbulent. Increasing the dimensions of a crater to those produced by Wetherill's 100 km projectiles should increase the dimensional terms used to calculate the Reynolds number and, hence, increase the tendency to turbulent flow. The only reason for less turbulent flow in the accretional period craters would be the more modest impact velocities. However, so long as the flow is turbulent, melt sheets in basin scale craters should be as filled with cold clastic debris as the smaller craters. Since these sheets seem prone to rapid crystallization as the cold debris raises the sheet viscosity by crystallization, the large pools of melt should not fractionate by crystal settling any better than the sheets with volumes of several hundred km^3 already studied on earth or moon.

Impact melting as a function of impact velocity--Impact melting by the accreting planetesmals is inhibited by their relatively modest impact velocities and resulting peak shock pressures. Kieffer and Simonds (17) calculated peak shock pressure as a function of impact velocity for a range

of meteorite and target combinations. Impact of a stony projectile (modeled with the physical properties of diabase) into a stony target will set up a peak shock pressure of about 900 kb for impacts with a velocity of 8 km/sec. This is 150-200 kb more than required for total melting of granite but less than the 1000 kb required for total melting of basalt. In contrast, the impact of a 24.6 km/sec stony meteorite will have a peak shock pressure of >7000 kb. Since the peak shock pressure attenuates as a function of radius to about the 3.4 power, individual planetesmal impacts will make very little impact melt.

Summary--Formation of the lunar crust by crystal fractionation of huge masses of impact melt produced during accretion is a problem. High speed (24.6 km/sec) impacts demonstrably produce total melts which crystallize rapidly and do not fractionate, and low speed (8 km/sec) impacts produce relatively little melt because their peak shock pressures only marginally exceed that required for impact melting.

Concluding speculations--Since the lunar crust has been demonstrated to have fractionated during the first few hundred million years of its existence and projectiles traveling at 8 km/sec have the kinetic energy equivalent to the heat required to melt about 12 times their mass, it is probable that impact heating had something to do with the melt formation. The author wishes to emphasize the point made by Wetherill (4) that melting can take place by the cumulative effect of impacts slowly raising the temperature of the crust over the hundred million years of accretion in a very heterogenous manner similar to the process modeled by Kaula (18) and Kaula and Randsford (19). If the accretional heating of the lunar crust is due to the cumulative effect of impacts over a time span equal to that extending from the Cretaceous to the present, then partial melting, rather than total melting, will take place at some depth below the surface. If the melt can be separated from the residue and the melt can then fractionally crystallize, a wide range of compositions can result. Could it be that the often mentioned analogues for the moon's early fractionation, the gabbroic layered intrusions (Skaergaard, Bushveld, Stillwater) are compositional as well as process analogues to the moon's early crust?

(1) Wood J.A. et al. (1970) Science 167, p. 602-604. (2) Taylor S.R. (1975) Lunar Science: A Post Apollo View, Pergammon Press, p. 372. (3) Longhi J. (1977) Proc. Lunar Sci. Conf. 8th, p. 601-621. (4) Wetherill G.W. (1976) Proc. Lunar Sci. Conf. 7th, p. 3245-3257. (5) Wetherill G.W. (1977) Proc. Lunar Sci. Conf. 8th, p. 1-16. (6) Shoemaker E.M. (1977) Impact and Explosion Cratering, Pergammon Press, p. 617-628. (7) Grieve R.A.F. and Dence M.B. (1979) Icarus 38, p. 230-242. (8) Floran R.J. et al. (1978) J. Geophys. Res. 83, p. 2737-2760. (9) Grieve R.A.F. and Floran R.J. (1978) J. Geophys. Res. 83, p. 2761-2771. (10) Grieve R.A.F. (1975) Geol. Soc. Am. Bull. 86, p. 1617-1629. (11) Simonds C.H. et al. (1978b) Proc. Lunar Planet. Sci. Conf. 9th, p. 2633-2658. (12) Simonds C.H. (1975) Proc. Lunar Sci. Conf. 6th, p. 641-672. (13) Simonds C.H. et al. (1978a) J. Geophys. Res. 83, p. 2773-2788. (14) Lofgren G.E. (1977) Proc. Lunar Sci. Conf. 8th, p. 2079-2095. (15) O'Keefe J.D. and Ahrens T.J. (1976) Proc. Lunar Sci. Conf. 7th, p. 3007-3025. (16) Orphal D.L. (1977) Impact and Explosion Cratering, Pergammon Press, p. 897-906. (17) Kieffer S.W. and Simonds C.H. (1980) Rev. of Geophys. and Space Phys., in press. (18) Kaula W.M. (1979) J. Geophys. Res. 84, p. 999-1008. (19) Ransford G.A. and Kaula W.M. (1979) Lunar and Planet. Sci. X, p. 998-1000.

INTERPRETATION OF NON-MARE AND MARE SAMPLES IN TERMS OF NEW MODEL FOR SEQUENTIAL EPISODIC DIFFERENTIATION OF A GROWING MOON. J.V. Smith and E.C. Hansen, Dept. of Geophysical Sciences, University of Chicago, Chicago, Ill. 60637.

Some petrochemical paradoxes are resolved by a new model [1] in which the Moon underwent crystal-liquid differentiation into a core(?)-mantle-liquid-crust during growth, followed by successive episodes of further accretion and crystal-liquid differentiation as envisaged in [2,3]. This type of model is plausible if accretion [4] occurred from hot debris produced during capture of several earth-orbiting moonlets or of sun-orbiting planetesimals of moderate size (radius >500km?) during addition of the final one-half of its volume.

Fig. 1 shows symbolic cartoons of three stages of final accretion. In stage 1, the infant Moon has differentiated into a small FeS-rich core, a mantle zoned outwards from Mg-rich olivine-rich rocks to relatively Mg-poor cumulate rocks containing pyroxene and plagioclase as well as trapped liquid, a residual liquid rich in Fe and the large-ion-lithophile elements, and a crust composed of plagioclase-pyroxene-rich rocks, similar to an original proposal for the entire Moon [5]. Next, a thick coating of hot debris is accreted, and intermingled with the crust and residual liquid of stage 1. Because anorthositic cumulates are more refractory and lighter than plagioclase-rich rocks containing abundant pyroxene and olivine, some anorthositic components are expected to survive and "float" in the new outer zone. This zone precipitates a new set of cumulates ranging outwards from Mg-rich olivine-rich rocks to relatively Mg-poor cumulate rocks containing liquid trapped between pyroxene and plagioclase, a new residual liquid even more enriched in Fe and LIL elements than in stage 1, and a new crust of plagioclase-pyroxene-rich rocks enclosing surviving anorthositic relics (symbolic stage 2). This process of successive accretion and differentiation could be repeated to give a sequence of zoned cumulates in the lunar mantle. It is not necessary for the accreted material to vary in chemical composition, but chemical diversity is possible. Finally in symbolic stage 3, the last major phase of accretion occurs, and the new material differentiates into zoned cumulates which cap the already zoned mantle and a crust which consists of new plagioclase-pyroxene-rich rocks and basalts intermingled with surviving anorthositic relics. Any Fe-S-rich immiscible differentiates will tend to sink. Erratic convection will considerably modify the neat concentric zoning of the model, but homogenization of the entire mantle is not envisaged. Accretion is completed within 100my to satisfy isotopic and thermal constraints.

Development of the Moon continues (stage 4) and bombardment of the crust ultimately results in formation of the ringed mare basins about 4by ago. Melting of trapped cumulates [5] in the zoned mantle produces diverse magmas, of which some are represented by mare basalts sampled in the Apollo and Luna missions, and some of which may be intermingled with highlands rocks.

We now interpret the properties of mare and non-mare rocks in terms of this model.

Multiple differentiation permits formation at some hundreds of kilometers depth of zones of advanced cumulates and trapped liquids enriched in Fe, Ti and LIL elements, thereby allowing (a) deep-seated retention of radioactive species to provide the heat sources for the mare-basalt magmas, and (b) satisfaction of the phase-equilibrium data for simultaneous coexistence at substantial pressure of each mare-basalt liquid with residual minerals [6]. The trace-element characteristics of mare basalts listed by [6,7] can be explained by varying the proportions of olivine, clinopyroxene and plagioclase

in the source regions; hybridism of magmas [8] and assimilation of exotic oxide minerals [9] is also needed for some basalts, as well as near-surface crystal separation [6]. Details will be given elsewhere. The depths in the cartoons are schematic, and discussion of the geophysical and geochemical controls will be given elsewhere; in particular a core is not necessary, and mare-basalt chemistry is apparently not constrained by residual garnet.

We now suggest very tentatively that the distinction between anorthosites and Mg-rich plutonic rocks [10,11] results because the former are survivors of successive crusts of the growing Moon whereas the latter formed mainly in stratiform plutons of the final crust. The Mg-rich plutonic rocks follow a normal differentiation sequence (Hansen et al., this vol.) in which Fe/Mg (mafic silicate) increases with Na/Ca (plagioclase), as expected for gravity-controlled crystal-liquid differentiation. The anomalous trend for anorthosites [12,13] is tentatively attributed to the proposed complex history of crustal survivors. In spite of the apparent calm unavoidably implied by simple cartoons (Fig. 1), the infant moon would have a turbulent history. Because Ca and Na would hardly enter into the cumulate minerals dropping into the growing mantle, the Ca/Na ratio of the crust-plus-liquid portion would change little during growth from an infantile to an adolescent Moon. However the Fe/Mg ratio of the liquid would tend to increase because of the sinking of cumulate minerals with high Fe/Mg, and then decrease as new material was accreted (assuming near-homogeneity of accreting material). Erratic fluctuations should occur, especially as small bodies would be impacting the surface as well as the occasional accretion of debris from big planetesimals or moonlets [the Mg-rich highlands component identified by several geochemists]. Anorthosites would form from liquids with nearly constant Na/Ca but variable Fe/Mg. Only the feldspar-rich rocks of the temporary crusts would survive further accretion. Prolonged high-temperature metamorphism would be expected for surviving relics, probably with exsolution of mafic minerals from the plagioclase [14]. The high Fe/Mg ratio of the anorthites from the anorthosites indicates a high Fe/Mg ratio of the inferred coexisting liquid [15]. Particularly important from the viewpoint of trace-element geochemistry is the general complementary nature of the REE distribution between anorthosites and mare basalts which is consistent with the present model. The relative amounts of K and REE in the anorthositic and Mg-rich plutonic rocks are also consistent, as explained elsewhere.

We thank I.M. Steele and I. Baltuska for technical help and NASA for grant 14-001-171.

1. J.V. Smith 1979 submitted Nature. 2. G.W. Wetherill 1975 Lunar Science Institute Contrib. 234, 184. 3. J.V. Smith 1974 Lunar Science V, 718. 4. J.V. Smith 1979 Mineral. Mag. 43, 1. 5. J.V. Smith, A.T. Anderson, R.C. Newton, E.J. Olsen, P.J. Wyllie 1970 J. Geol. 78 381. 6. J.J. Papike, F.N. Hodges, A.E. Bence, M. Cameron, J.M. Rhodes 1976 Rev. Geophys. Space Phys. 14, 475. 7. S.R. Taylor, A.E. Bence 1975 Lunar Sci. Inst. Contr. 234, 159. 8. J.W. Delano, A.E. Ringwood 1979 Lunar Planetary Sci. X, 286. 9. A.T. Anderson 1971 Geochim. Cosmochim. Acta 35, 969. 10. P.H. Warren, J.T. Wasson 1977 PLSC 8 2215. 11. J.L. Warner, C.E. Bickel 1978 Am. Min. 63 1010. 12. I.M. Steele, J.V. Smith 1973 P4LSC, 519. 13. E.C. Hansen, I.M. Steele, J.V. Smith 1979 Lunar Planetary Sci. X, 497. 14. J.V. Smith, I.M. Steele 1974 Am. Min. 59 673. 15. J. Longhi et al. 1976 PLSC 7 1281.

INTERPRETATION OF NON-MARE AND MARE SAMPLES

Smith, J.V. et al.

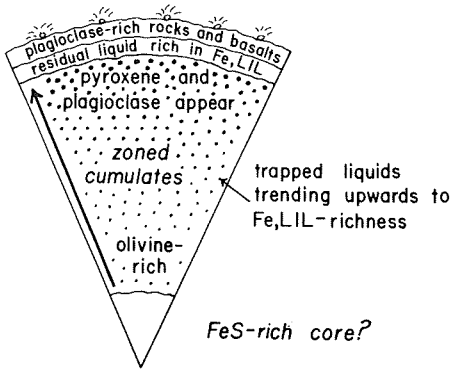

Symbolic stage 1

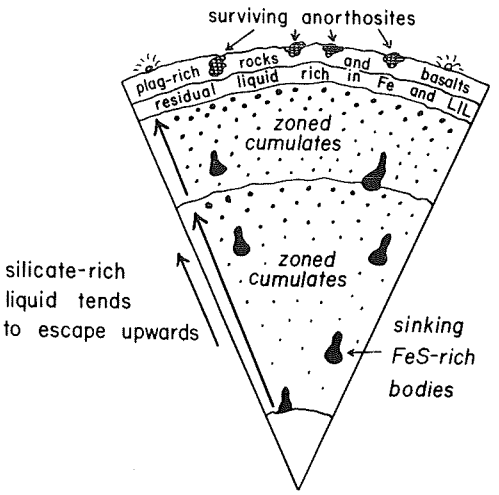

Symbolic stage 2

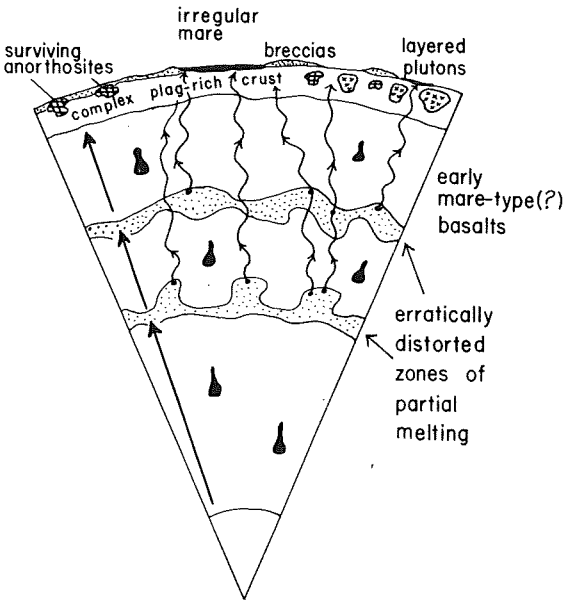

Symbolic stage 3

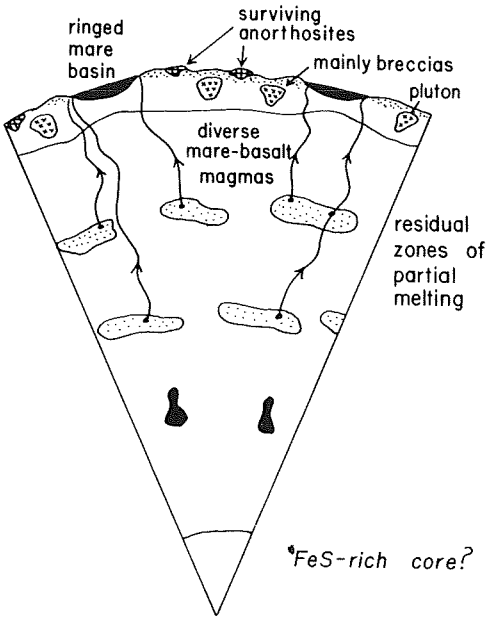

Symbolic stage 4

Fig. 1 Cartoons of four symbolic stages in growth of the Moon. Stages 1 and 2 occur within 100my of -4.5x10^{9}yr. Stages 3 and 4 represent the periods of formation of irregular and ringed mare, respectively. Irregular movement of the mantle is envisaged.

GEOPHYSICAL EVOLUTION OF THE LUNAR CRUST AND LITHOSPHERE. S. C. Solomon, Department of Earth and Planetary Sciences, Massachusetts Institute of Technology, Cambridge, MA 02139.

Introduction. The crust of a planet is a chemically distinct surficial layer which has been produced by some form of igneous differentiation from the underlying silicate mantle. The lithosphere of a planet is an outer layer of low temperature and high mechanical strength overlying a hotter, weak asthenosphere. Whereas the concept of a crust is the more important for questions of chemistry and petrology, the concept of a lithosphere is the more significant for many physical processes of planetary evolution. This paper presents a synthesis of geophysical information on the crust and lithosphere of the Moon, and on the variation of their large-scale properties with space and with time. The subject is treated within three broad and overlapping topics: (i) the physical structure of the crust, (ii) the evolution of lunar isostasy with time, and (iii) the global and regional thermal evolution of the lunar lithosphere.

Crustal Structure. The lunar crust is known to be about 55 km thick on the central nearside within the Apollo 12-16 network and to consist of several distinct layers that may differ primarily in physical properties (porosity, crack density) rather than in chemistry or petrology [1]. The lower 35 km of the crust has the nearly uniform P wave velocity of 6.7 km/sec, consistent with the measured velocities of several lunar highland (and mare) samples.

The global crustal structure may be determined from gravity and topographic data, if assumptions are made about crustal composition. A widely held view is that the lunar crust, exclusive of the volumetrically minor mare basalt deposits [2], is on the average broadly similar in constitution to the surface and near-surface rocks of the lunar highlands, or roughly anorthositic gabbro in composition [3]. The strongest argument in favor of this view is the correlation of surface abundances of several elements (Al, Fe, Th) with elevation in isostatically compensated non-mare regions [4-6], suggesting that surface chemistry may be representative of the composition of the bulk of the underlying crustal column.

Crustal thickness variations on the Moon may be determined for three simple models for isostatic compensation: (i) simple Airy, or constant crustal density, models [7-8]; (ii) Airy models with superisostatic mare fill [8], and (iii) Pratt, or variable density, models [6,8]. The models give widely different predictions for the magnitude of crustal thickness variations, yet cannot be distinguished on the basis of gravity and topographic data [8]. The relationship between elevation and bulk density calculated from surface chemistry [6,9] suggests that the relative importance of Airy and Pratt compensation mechanisms may vary regionally among highland crustal provinces.

Lunar Isostasy vs. Time. The change in isostatic response of the Moon to surface loads shows a clear signature of the steady cooling of the Moon's outer portions. Pre-Imbrian

GEOPHYSICAL EVOLUTION

Solomon, S.C.

(> 3.9 b.y. old) highland topography is generally completely compensated isostatically, with at most a few limited regions with incomplete compensation [8, 10-11]. By 3.8 b.y. ago, however, the Moon had developed a lithosphere of sufficient strength so that neither the Apennine mountains nor the Orientale basin were completely compensated [12-13]. The lunar mascons [14], excess or superisostatic masses located within major basalt-filled impact basins, indicate a lithosphere of significant strength dating from the time of mascon formation. The response of the Moon to mascon loads has been that of a plate of finite elastic strength [15-16]. There has been lithospheric subsidence and associated tectonic failure, including the formation of mare ridges within the load region and concentric rilles outward of the ridges [17], but a substantial fraction of the original load has remained supported until the present day.

Lithosphere Thickness vs. Space and Time. The tectonic history of the lunar surface provides strong constraints both on the global thermal evolution of the Moon and on the variation of the effective thickness of the elastic lithosphere with space and time. The principal tectonic constraints are: (i) that the Moon lacks large scale tectonic features except those associated with vertical crustal motions and lithospheric flexure induced by volcanic loading [16], and (ii) that lunar graben are all older than 3.6±0.2 b.y. ago [18] even though mare basin subsidence and mare ridge formation continued until much younger times. The first observation restricts the accumulated thermal stress in the lunar lithosphere since the time of heavy bombardment to be less than that necessary to cause widespread failure. Neither this stress level nor its dependence on rate of stress accumulation are known for certain; an upper bound of 1 kbar stress change or, roughly equivalent, a 1 km change in lunar radius [19], is in accord with the strength of the lunar lithosphere estimated both from laboratory data and from a fit of stress models to lunar rilles and mare ridges [20]. This limit can be satisfied only by thermal history models starting with the outer portions of the Moon hot and the deep interior relatively cold [19,21]. The observation that rilles formed only prior to 3.6±0.2 b.y. [18] indicates that global horizontal surface stress was sufficiently compressive after that time so that continued mare subsidence and lithospheric flexure did not lead to further extensional failure.

The radial positions of rilles and ridges and the current gravitational and topographic data from mascon maria have been used [16,20] to infer the thickness of the elastic lithosphere and its variation with space and time. At the time of rille formation, 3.6-3.8 b.y. ago, the elastic lithosphere beneath the mascon maria was 25 to 75 km or more thick, a range of values requiring substantial lateral heterogeneity in the temperature field within the lunar crust and upper mantle. At the time of younger mare volcanism ($\sim$ 3.0 b.y. ago) in several mascon maria, a substantially thicker ($\sim$ 100 km) elastic lithosphere is evident in the response of the Moon to the additional load.

The areas of relatively thin (25-50 km) elastic lithosphere at 3.6-3.8 b.y. ago include the central and western mare basins

GEOPHYSICAL EVOLUTION

Solomon, S.C.

(Serenitatis, Imbrium, Humorum, and particularly Orientale and Grimaldi), whereas relatively thicker (>75 km) lithosphere lay beneath Crisium, Smythii and Nectaris [20]. The areas of thinner lithosphere can be broadly correlated with the presence of the largest mare volcanic complexes [22], with identified sites of non-mare volcanism [23], and with high levels of KREEP material [24], suggesting that all of these phenomena are linked through the heterogeneous thermal structure of the lunar crust and upper mantle.

References. [1] Toksöz M. N. et al. (1974) Rev. Geophys. Space Phys. 12, 539-567. [2] Head J. W. (1976) Rev. Geophys. Space Phys. 14, 265-300. [3] Adler I. et al. (1973) Proc. Lunar Sci. Conf. 4th, p. 2783-2791. [4] Metzger A. E. et al. (1977) Proc. Lunar Sci. Conf. 8th, p. 949-999. [5] Schonfeld E. (1977) Proc. Lunar Sci. Conf. 8th, p. 1149-1162. [6] Solomon S. C. (1978) Proc. Lunar Planet. Sci. Conf. 9th, p. 3499-3511. [7] Bills B. G. and Ferrari A. J. (1977) J. Geophys. Res. 82, 1306-1314. [8] Thurber C. H. and Solomon S. C. (1978) Proc. Lunar Planet. Sci. Conf. 9th, p. 3481-3497. [9] Haines E. L. and Metzger A. E. (1979) Lunar Planet. Sci. X, p. 488-490. [10] O'Keefe J. A. (1968) Science 162, 1405-1406. [11] Ferrari A. J. (1977) J. Geophys. Res. 82, 3065-3084. [12] Sjogren W. L. and Smith J. C. (1976) Proc. Lunar Sci. Conf. 7th, p. 2639-2648. [13] Ferrari A. J. et al. (1978) J. Geophys. Res. 83, 2863-2871. [14] Muller P. M. and Sjogren W. L. (1968) Science 161, 680-684. [15] Kuckes A. F. (1977) Phys. Earth Planet. Int. 14, 1-12. [16] Solomon S. C. and Head J. W. (1979) J. Geophys. Res. 84, 1667-1682. [17] Muehlberger W. R. (1974) Proc. Lunar Sci. Conf. 5th, p. 101-110. [18] Lucchitta B. K. and Watkins J. A. (1978) Proc. Lunar Planet. Sci. Conf. 9th, p. 3459-3472. [19] Solomon S. C. (1977) Phys. Earth Planet. Sci. 15, 135-145. [20] Solomon S. C. and Head J. W. (1980) Rev. Geophys. Space Phys., in press. [21] Cassen P. et al. (1979) Phys. Earth Planet. Int. 19, 183-196. [22] Whitford-Stark J. L. and Head J. W. (1977) Proc. Lunar Sci. Conf. 8th, p. 2705-2724. [23] Wood C. A. and Head J. W. (1975) Origins of Mare Basalts, p. 189-193. [24] Trombka J. I. et al. (1977) NASA SP-370, p. 153-182.

THE EXTENT AND DURATION OF LUNAR KREEP VOLCANISM. P. D. Spudis, Department of Geology, Arizona State University, Tempe, AZ 85281.

The general term "highland volcanism" has come to include those volcanic events that predate the major basins and subsequent mare basalt flows. Although various types of ancient volcanic rock clasts have been returned by the Apollo missions (e.g., high alumina basalt clasts in Apollo 14 breccias), highland volcanism is represented primarily by KREEP, a volcanic product containing large quantities of incompatible elements (1). Recent work has demonstrated that early KREEP volcanism (~4.3 AE) (2) was probably complemented by contemporaneous early mare volcanism (*mantle* derived magmas) (3,4). Thus, both mare and KREEP basalts may constitute portions of the highland crust. However, KREEP is distinct in chemistry and source region from the more common mare basalts and are important in assessments of highland volcanism due to their petrologic significance and relation to lunar thermal history. The Apollo gamma-ray spectrometer experiment (5) measured the natural radioactivity of the lunar surface and this data may be expressed in terms of elemental concentration of U and Th. KREEP basalts contain high concentrations of Th (10-15 ppm) (1,6) and a common assumption is that a map of Th concentration is a map of the distribution of KREEP basalt (e.g., 2). However, several other lunar rock types contain significant quantities of Th, from low-K Fra Mauro basalt (5-7 ppm) (6) to unusual "granite" clasts that may contain as much as 20 ppm Th (7,8). Thus, a map of Th content does not *uniquely* determine the presence of KREEP basalt, but must be considered in the context of other elemental abundances as well as regional geologic considerations such as the presence of crater and basin ejecta blankets, light plains, and local mare concentrations. When these factors are taken into consideration, orbital remote sensing offers the best possibility for mapping the location and geologic setting of KREEP on a moonwide basis.

High concentrations of Th occur near the Apollo 14 and 15 landing sites and on the Aristarchris plateau (9,11). KREEP was first defined from returned samples (1) and was thought to represent the chemical character of Imbrium basin ejecta (12). Subsequent study of the igneous phase chemistry of KREEP (13) demonstrated its volcanic origin and studies of cratering mechanics (e.g., 14) suggested mainly local landing site origins for this rock type (15). Timing and duration of KREEP volcanism is based mainly on radiometric dating of lunar samples. It is generally agreed that KREEP volcanism commenced at about 4.3 AE (possibly as late as 4.1 AE) (9,10); however, KREEP volcanism may have continued for some time *after* the Imbrium basin impact (9,16) with the Apollo 15 KREEP samples being the youngest *volcanic* KREEP rocks known (~3.9 AE) (17). It thus seems fairly certain that KREEP volcanism was active between 4.2-3.9 AE, a time when the Moon was undergoing terminal heavy bombardment (6). Thus, direct morphologic evidence for KREEP volcanism is rare (being preserved only in the Apennine Bench region (1,16)) and orbital chemical data is the primary source of information regarding its distribution.

Because the highest radioactive levels seen from orbit occur in the Imbrium-Procellarum region (18), it has long been assumed that KREEP volcanism was primarily confined to this area (e.g., 5,9). New reduction of the orbital gamma-ray data (18,19) and photogeologic studies (4) suggest KREEP volcanism may have been much more widespread. The radioactive highs seen on the lunar farside are of low magnitude, generally corresponding to 2-5 ppm of Th (18,19). It may be argued that these concentrations correspond not to KREEP basalt but to low-K Fra Mauro (LKFM) basalt, a major component of Apollo highland polymict breccias (6). However, LKFM as seen from orbit (20) is primarily associated with deeply derived basin ejecta, such as the Imbrium basin Apennine Mountains (20) and none of the farside radioactive highs display photogeologic evidence of pristine basin ejecta deposits (21,22). These regions do display areas of ancient highland plains that probably either mantle or incorporate significant quantities (up to 20%) of medium-K KREEP basalt, which is presumed to be of volcanic origin on petrologic grounds (1,13).

The most prominent farside radioactive high is the Van De Graaff anomaly (approximate location: 25°S, 175°E) corresponding to 2.3 ppm Th and 1300 ppm K (18). This region is just within

the outer ring of the largest multiringed basin on the Moon, the South Pole-Aitken basin (22,23) and contains concentrations of both Imbrian and Nectarian age highland plains (22). This region has long been noted as a prominent magnetic anomaly (24), and contains several mare filled craters, such as Aitken, that occur in the vicinity of the anomaly. This region is also remarkable in that large portions of the highland intercrater terrain have a "grooved" appearance that has been attributed to the antipodal effects of the Imbrium basin, either through basin ejecta deposition (22) or the seismic effects of the basin impact (25). It is known from the study of volcanically modified craters elsewhere on the Moon (26) that dike swarms are likely to occur in the vicinity of floor-fractured and mare flooded craters. It is possible that the seismic effects of the Imbrium impact responsible for the production of grooved terrain in the Van De Graaff region (25) also produced a zone of crustal fracturing that resulted in emplacement of a dike swarm, responsible for the magnetic anomaly (24). The orbital chemistry suggests the presence of KREEP-like material and this may have been derived by the volcanic emplacement of KREEP basalt contemporaneous with this dike forming episode.

Two additional radioactive highs occur in the Mare Marginis (10°N, 90°E) and Balmer (15°S, 70°E) regions (19). The Balmer anomaly, corresponding to 4.0 ppm Th (19) occurs in a region of highland light plains that contain numerous dark halo craters (4). In this region, a basaltic lava flow having KREEP affinities has probably been mantled by later Imbrian age light plains (21); subsequent impact cratering has exposed these buried KREEP basalts in the ejecta of dark halo craters (4). The Mare Marginis anomaly is more interesting in that it contains a high Th content (3.4 ppm) (19) centered on the mare material, and is surrounded by highlands that contain very low Th concentrations (0.5-0.7 ppm) (19). This suggests that the high Th content is *not* derived from vertical mixing of a buried KREEP basalt unit, but reflects the Th content of the *lavas* of Mare Marginis. It would appear that the lavas of Mare Marginis contain Th contents intermediate between mare and KREEP basalts and similar samples may be represented in the Apollo collection by unusual "KREEP-y" basalts found in an Apollo 17 boulder (27). It appears that this region of the Moon underwent a protracted period of KREEP volcanism with the Balmer pre-Imbrian lavas (*buried* by Imbrian age light plains) succeeded by subsequent "KREEP-y" Imbrian age mare volcanism in Mare Marginis.

The regions of farside KREEP concentration occur in areas of thin (within the 60 km isopach) farside crust as mapped by gravity data (28) in addition to occupying geologically old topographic lows (29). Earlier studies (30,31) suggested an inverse correlation of Th content with crustal thickness and it is important to emphasize that this relation holds for the farside as well as the Imbrium-Procellarium region. This observation supports the presence of ancient basin-filling volcanic deposits subsequently reworked by late stage impact processes. It now appears that all observable KREEP-rich areas on the Moon occur near regions where the crustal thickness is 60 km or less.

KREEP-rich regions on the Moon are more widely distributed than previously believed. It is apparently of limited extent on the lunar farside, due to the greater average thickness of the crust, the same reason most mare basalt deposits are concentrated on the lunar nearside (32). KREEP-rich anomalies occur in regions of relatively thinner farside crust that were overflown by Apollo orbital chemical instruments. This suggests that KREEP volcanism was a moonwide episode in early lunar history and was not strictly confined to the Imbrium-Procellarum regions, although major concentrations are found there. It is unlikely that much morphologic evidence for this early phase of highland volcanism is preserved but integrative studies of remote sensing and photogeologic data have successfully identified ancient regions of KREEP volcanism. The suggestion that KREEP volcanism was not limited to a small region of the Moon increases the importance of this process to the petrologic evolution of the highland crust.

KREEP Volcanism

Spudis, P.D.

REFERENCES

1. Meyer C. (1977) Phys. Chem. Earth 10, 239.
2. Schonfeld E. and Meyer C. (1972) PLSC 3, 1397.
3. Ryder G. and Taylor G. (1976) PLSC 7, 1741.
4. Schultz P.H. and Spudis P.D. (1979) PLPSC 10, (in press).
5. Arnold J. *et al.* (1972) Apollo 15 PSR, 16-1.
6. Taylor S.R. (1975) Lunar Science, Pergammon Press.
7. Ryder G. (1976) EPSL 29, 255.
8. Nyquist L.E. *et al.* (1977) Imb. Consort. 2, 30.
9. Hawke B.R. and Head J.W. (1978) PLPSC 9, 3285.
10. Warner J.L. *et al.* (1977) PLSC 8, 2051.
11. Zisk S. *et al.* (1977) Moon 17, 59.
12. LSPET (1971) Science 173, 681.
13. Walker D. *et al.* (1972) PLSC 3, 797.
14. Morrison, R. and Oberbeck V. (1975) PLSC 6, 2503.
15. Hawke B.R. and Head J.W. (1977) PLSC 8, 2741.
16. Spudis, P.D. (1978) PLPSC 9, 3379.
17. Nyquist L. *et al.* (1975) PLSC 6, 1445.
18. Adler I. and Trombka J. (1977) Phys. Chem. Earth 10, 17.
19. Haines E. *et al.* (1978) PLPSC 9, 2985.
20. Hawke B.R. (1978) Lun. Planet. Sci. IX, 474.
21. Wilhelms D. and El-Baz F. (1977) USGS Map I-948.
22. Stuart-Alexander D. (1979) USGS Map I-1047.
23. Wilhelms D. *et al.* (1979) USGS Map (in press).
24. Sharp L. *et al.* (1973) Moon 7, 322.
25. Schultz P.H. and Gault D.E. (1975) Moon 12, 159.
26. Schultz P.H. (1976) Moon 15, 241.
27. Ryder G. *et al.* (1977) EPSL 35, 1.
28. Bills B. and Ferrari A. (1976) PLSC 7, Frontispiece.
29. Kaula W. *et al.* (1974) PLSC 5, 3049.
30. Schonfeld E. (1977) PLSC 8, 1149.
31. Metzger A.E. (1977) PLSC 8, 949.
32. Soloman S. (1975) PLSC 6, 1021.

TRACE ELEMENTS IN HIGHLAND PLAGIOCLASE: ION PROBE ANALYSES OF LI, NA, MG, TI, SR AND BA. I.M. Steele and J.V. Smith, Dept. of the Geophysical Sciences, University of Chicago, Chicago, Ill. 60637.

Plagioclase is the most abundant mineral in highland rocks whose isotope geochemistry indicates original crystallization during early differentiation of the Moon. A plot of *mg* (= Mg/(Mg+Fe) atomic) of mafic minerals vs. *ab* (= Na/(Na+Ca) atomic) of plagioclase yields a normal trend for Mg-rich plutonic rocks, but an enigmatic trend for anorthositic ones [1,2,3]. In [4] we showed that the same trends appear when only plagioclase is used to give plots of *mg* vs. *ab* and K_2O vs. *ab*. We now present corresponding plots for trace and minor elements (Li, Na, Mg, Ti, Sr, Ba) in plagioclase measured with an ion probe.

Experimental An AEI IM-20 ion probe was operated with a mass-analyzed 20kV O^-beam of 10na focused to about 30μm diameter. All data were obtained at low mass resolution using ion counting. No corrections were made for Ca interference at ^{24}Mg and ^{88}Sr because of its smallness and the near-constant matrix. No significant interferences are present at ^{7}Li and ^{138}Ba according to semi-quantitative measurement of isotopic ratios. ^{49}Ti was measured in preference to ^{47}Ti because of a mass interference of $NaAlSiO^{++}$ at m/e 47 and consistently high 47/49 isotopic ratios. All six elements showed peaks well above background with detection levels very much less than concentrations present in lunar plagioclase. Constancy of operating conditions was checked by replication on 15362. Fig. 1 shows a good correlation between electron and ion probe measurements for Mg, except for 76535 whose electron probe analysis is believed to be wrong. A good correlation also occurs for Na. Absolute calibrations for Li, Ti, Sr and Ba were not attempted and only relative count rates are reported. Approximate levels may be obtained by using concentration levels in [5] for 15415: Li 2, Sr 178, Ba 6.2, Ti 90ppmw.

Discussion Figs. 2-5 show count rates of Sr, Ti, Ba and Li plotted respectively against Na for 12 highland plagioclases (2 x 10^6cts/sec ^{23}Na = 5 mol.% Ab). Solid and open symbols (key in Fig. 2) distinguish between anorthositic and mafic-rich samples [4]. Sr vs. Na (Fig. 2) shows a simple positive correlation and no obvious separation of symbol types with the exception of peridotite 67667 (~1200ppm Sr) which has been recognized as a unique lherzolitic type [2]. Ti vs. Na (Fig. 3) shows considerable scatter. Most anorthosites, norite 78235 and troct. 76535 fall at low Ti, while 67667 peridotite, 60619 granoblastic anorthosite and 15689 norite fall at distinctly higher Ti perhaps indicating derivation of the latter from Ti-rich liquids (?? related to mare basalts). The range in Ti is similar to that determined for Apollo 14 rocks [5]: note scatter for 14306 breccia. Ba vs. Na (Fig. 4) shows a neat linear trend for anorthosites which correlates positively with Na as expected for crystal-chemical control [6]. One datum for 67637 and three for 14306 lie at much higher Ba, as do data for all the non-anorthositic specimens. An obvious speculation is that the Ba content of the plagioclase is inherited from its parent magma, and that the magmas responsible for the anorthositic specimens were much poorer in Ba (after normalization for Na content) than those responsible for the mafic-rich specimens. Li vs. Na (Fig. 5) shows a remarkable series of positive linear trends for most specimens, suggestive of a distinctive parent liquid for each rock. Five crystals from the 14306 breccia have very high Li, and one has low Li. The anorthositic specimens tend to have low Li, but there is a 3-fold range.

It is obvious that the simple two-fold classification based on *mg*-*ab* plots can be extended to a richer classification when trace elements in

plagioclase are considered. Polymict specimens should be identifiable from systematic analysis of many grains. In spite of the distinctive nature of each specimen (Fig. 5), the cataclastic anorthosites tend to form a single cluster with respect to Li, Ti, Sr and Ba, thereby indicating a generally similar geochemical history. The other specimens generally show higher levels of trace elements, and scatter more widely than for anorthosites. Since the effects of metamorphism have not been considered, some caution is needed in utilizing for lunar modeling the simplest implication of the above data: namely that the anorthositic plagioclases crystallized from liquids less enriched in Ba (especially), Li (mostly) and Ti (mostly) than the plagioclases from the Mg-rich plutonic trend. Analyses of plagioclase from further rocks (including granulitic impactites) are scheduled, and analyses of mafic silicates are beginning.

We thank E.C. Hansen, O. Draughn, I. Baltuska and R. Draus for technical help, and NASA for grant 14-001-171.

1. J.L. Warner, C.E. Bickel 1978 Am. Mineral. 63 1010. 2. P.H. Warren, J.T. Wasson 1978 PLPSC9 185. 3. E.C. Hansen, I.M. Steele, J.V. Smith this vol. 4. E.C. Hansen, I.M. Steele, J.V. Smith 1979 PLPSC10 in press. 5. C. Meyer, D.H. Anderson, J.G. Bradley 1974 PLSC5 685. 6. J.V. Smith, Feldspar Minerals, Vol. 2, 1974, Springer.

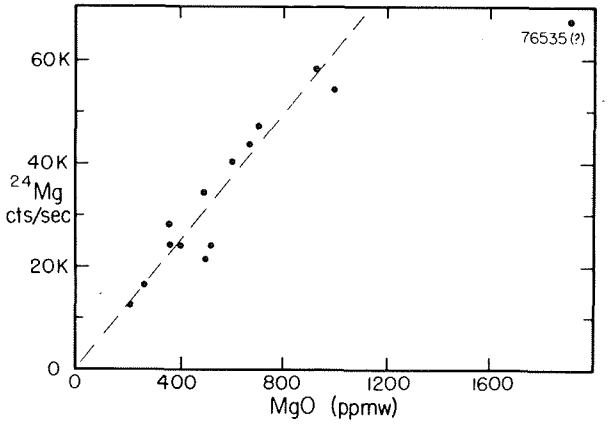

Fig. 1. Ion probe count rates for ^{24}Mg vs. ppmw MgO from electron probe. The electron probe analysis for 76535 is probably wrong.

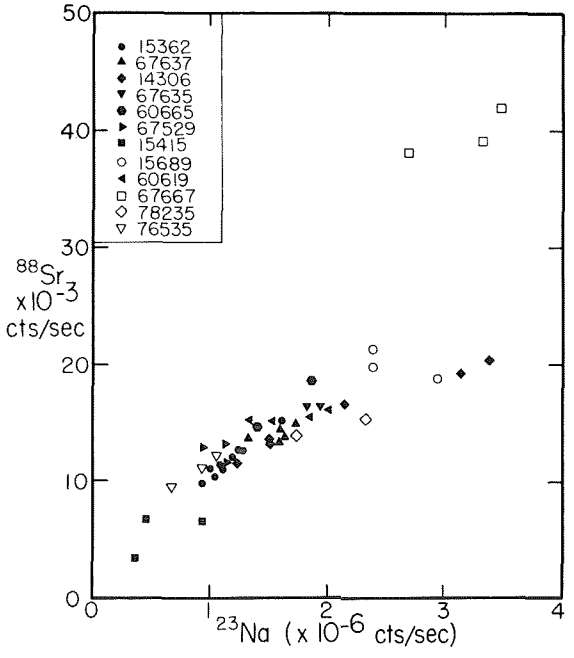

Fig. 2. Ion probe count rates for ^{88}Sr vs. ^{23}Na.

TRACE ELEMENTS IN HIGHLAND PLAGIOCLASE:

Steele, I.M. et al.

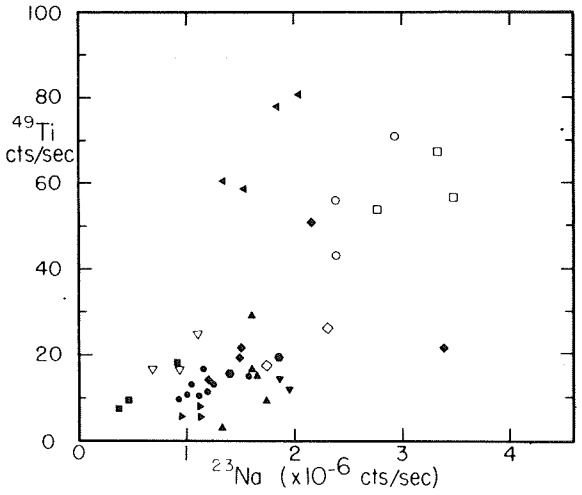

Fig. 3. Ion probe count rates for ^{49}Ti vs. ^{23}Na.

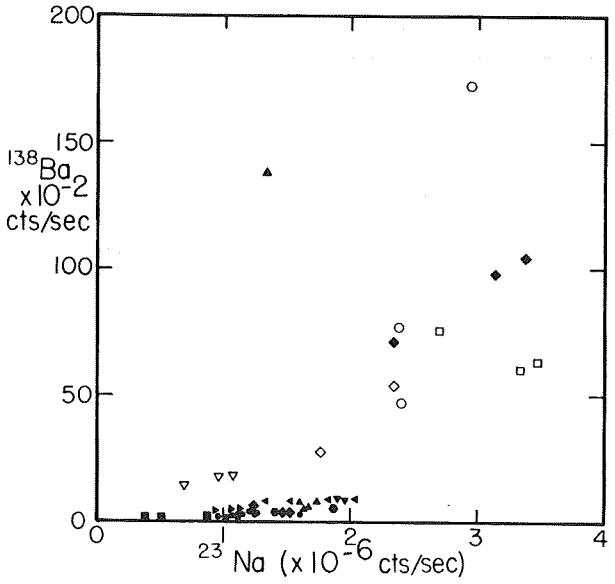

Fig. 4. Ion probe count rates for ^{138}Ba vs. ^{23}Na.

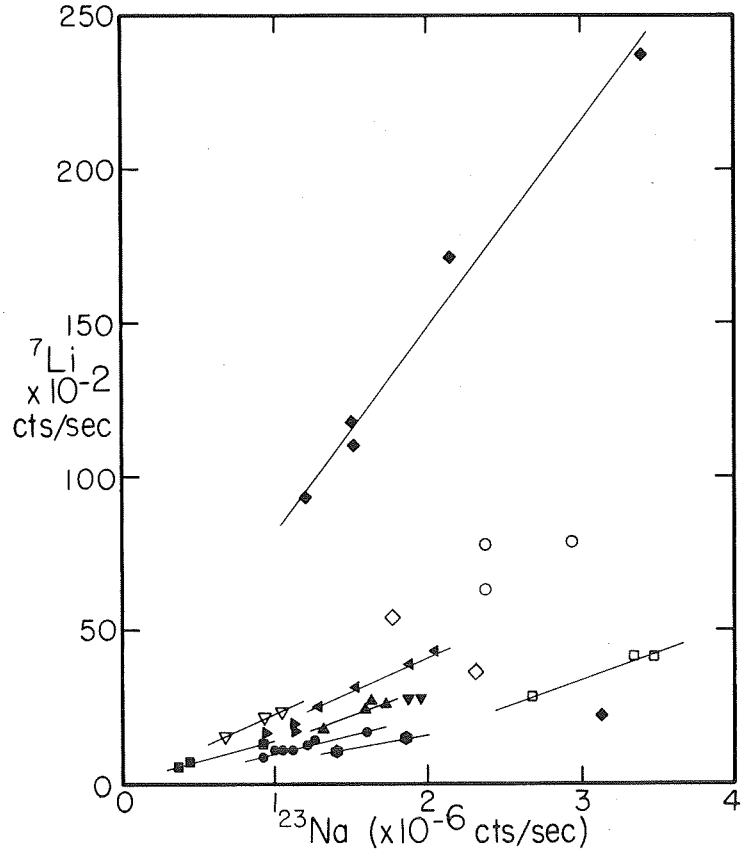

Fig. 5. Ion probe count rates for ^{7}Li vs. ^{23}Na.

PROBLEMS OF THE CLASSIFICATION AND NOMENCLATURE OF LUNAR HIGHLAND ROCKS - A STATUS REPORT. D. Stöffler and H.-D. Knöll, Institute of Mineralogy, University of Münster, D-44 Münster, Germany

A major contribution to the better understanding of ancient planetary crusts is to be expected from the 1979 "Lunar Highlands Initiative" of the Lunar and Planetary Sample Team. One of many important objectives of this research project on the lunar crustal rocks is the establishment of a unified classification and nomenclature of rocks which is acceptable by the lunar scientists and understandable for all Earth and planetary scientists. Such a unified systematics of lunar rock materials is necessary for a successful interdisciplinary team work during this project.

Recently, new proposals for the classification and nomenclature of the highland rocks have been made (1,2). The problems of the diverse classification systems presently in use and the need for their improvement and unification have been discussed repeatedly (2,3). A "Nomenclature Committee" formed by LAPST at the 10th Lunar and Planetary Science Conference (members: O.B.James, U.Marvin, H.-D.Knöll, C.H.Simonds, P.H.Warren and D.Stöffler (chairman)) has been engaged in this matter and has made extensive proposals which will be presented to this Conference after a final agreement has been reached immediately prior to the Conference at Houston.

In connection with the work of the nomenclature committee this paper intends to discuss some general principles and problems of the highland rock systematics in order to stimulate further discussions by the planetary science community outside the committee. This may help to achieve a most widely acceptable classification and nomenclature by the time of the Conference on the Lunar Highlands Crust.

The highland rocks consist of displaced and metamorphosed lithic units which are parts of composite, texturally complex, polygenetic breccia formations. Both magmatic and impact processes are important for the formation of these rocks. Considering the high frequency of impact craters in the lunar highlands it appears reasonable if not mandatory to use informations from terrestrial impact craters in crystalline bedrocks as a framework for a textural classification of the highland rocks. A textural analysis is a necessary presupposition for any subsequent chemical and physical analysis. Without such an analysis the petrogenesis and the chronology of a sample cannot be fully understood.

The texture of a highland rock sample is either heterogeneous or homogeneous. Homogeneous textures are represented by igneous textures of plutonic and volcanic origin and by metamorphic textures resulting from thermally induced solid state recrystallization. The heterogeneous textures are breccia textures. One type of breccia texture is cataclastic. It is formed by in-situ brecciation of a single lithology (monomict cataclastic rock). Another type of breccia texture consists of two textural components. One component is termed matrix, the other one is represented by fragmental inclusions within this matrix which are called clasts.

The matrix can be produced by fragmentation and mixing of different lithologies. This leads to a clastic matrix texture. Consequently, breccias with clastic matrix are polymict or polylithologic. The boundary between larger clasts and the fine-grained matrix may be arbitrarily set at 20 - 25 μm.

CLASSIFICATION OF LUNAR HIGHLAND ROCKS

Stöffler, D.

Melting produces another type of matrix material which is characterized by a variety of crystallization textures. They may range from holocrystalline to holohyaline (vitric). Most frequently observed types of crystalline matrix textures are granular, ophitic, subophitic, poikilitic and porphyritic. Spherulitic, dendritic, fibrous and other devitrification textures are also quite abundant. Metamorphic matrix textures which are typically granoblastic to poikiloblastic are formed by thermally induced recrystallization of all other types of breccia textures. The second component of a breccia are rock and mineral clasts which are incorporated into the various types of matrix. The clast population of a breccia may also comprise vitric or crystallized melt bodies or fragments thereof.

The criteria which have to be fulfilled by an appropriate classification system may be summarized as follows:

1. The prime criterion for classification must be such that it can be determined with a standard microscopic examination
2. Textural and/or structural properties of a sample must serve as prime criterion for the classification. Compositional or other properties may be used in subsequent order for subclassifying the main textural groups
3. Equivalent and consistent criteria must be used for each order of rock classes or subclasses. The same holds for the terminology
4. The nomenclature of highland rocks must be understandable for non-geologists of the planetary science community as well as for terrestrial geologists.
5. The classification should allow later additions or changes without changing the principles of the whole classification system

A comparison of the proposals for the classification of lunar highland rocks is given in Table 1. The proposal of (2) was presented to the members of the "Nomenclature Committee" as a basis for discussion. This proposal was further developed by (5) making in part use of important suggestions by O.B.James and C.H.Simonds. The other members essentially agreed with (2).

A proposal for the nomenclature is given in Table 2. The most detailed suggestions were made by P.H.Warren. Several alternative names are listed in Table 2. The subclassification of the main rock classes of Table 1 and 2 should be made according to the following criteria: (1) clast-content, (2) composition of matrix and/or clasts, (3) matrix texture, (4) matrix grain size, and (5) mesostasis content. A corresponding modifier could be used in connection with the root names.

References (1) McGee P.A., Simonds C.H., Warner J.L. and Phinney W.C. (1979) Introduction to the Apollo collections: part II lunar breccias, L.B. Johnson Space Center, Houston; (2) Stöffler D., Knöll H.-D., and Maerz U. (1979) Lunar and Planetary Science X, 1177-1179, The Lunar and Planetary Institute, Houston; (3) Prinz M. and Keil K. (1977) Phys. Chem. Earth 10, 215-237; (4) Warren P.H. (1979) written communication; (5) Stöffler D., Knöll H.-D.,and Maerz U. (1979) Proc. Lunar Planet. Sci. Conf. 10th,in press

CLASSIFICATION OF LUNAR HIGHLAND ROCKS

Stöffler, D.

Table 1: Comparison of proposals for the classification of lunar highland rocks

(1)	(2)	(4)
	Igneous rocks Plutonic rocks *Volcanic rocks*	Igneous rocks Plutonic rocks Volcanic rocks
		Metamorphic rocks
	Impact rocks cataclastic impact breccias	Breccias Monolithologic cataclastic rocks metamorphic cataclastic rocks
Black and white breccias		Dilithologic dike breccias
		Polylithologic
Fragmental breccias dark matrix breccias light matrix breccias	regolith breccias	regolith breccias clastic matrix breccias
	clastic impact breccias suevitic impact breccias	melt-free melt-bearing
Crystalline breccias impact melt breccias clast-free clast-bearing clast-rich	crystalline impact breccias	crystalline matrix breccias
	vitric impact breccias = *impact glass*	hyaline matrix breccias
granulitic impactites		metamorphic matrix breccias

Table 2: Proposals for the nomenclature of lunar highland rocks

(5)	present proposal	alternative names
Igneous rocks Plutonic rocks Volcanic rocks	commonly used names according to IUGS nomenclature or similar nomenclature, e.g. Prinz *and Keil*, 1977	
	igneous rock names as above with prefix meta-	
Breccias	Breccias	
monomict (impact) breccias	cataclastic and meta-cataclastic rocks[1)] [1)] igneous or other rock names	
	dike breccias	dilithologic breccias or (pseudo)tachylitic breccias or veined breccias
micro-polymict (impact) breccias	micro-regolith breccias	microbreccias or soil breccias
fragmental (polymict) (impact) breccias suevitic (polymict) (impact) breccias	fragmental breccias	clastic breccias
pseudovolcanic (polymict)(impact) breccias	crystalline breccias	impact melt breccias or pseudovolcanic breccias
impact glass	impact glass	vitric breccias
	metamorphic breccias	granulitic breccias

note: "breccia" could be replaced by "impact breccia" if necessary

LUNAR HIGHLAND ROCKS WITH EVOLVED COMPOSITIONS: FRACTIONAL CRYSTALLIZATION OR LIQUID IMMISCIBILITY? G. J. Taylor, R. D. Warner, and K. Keil, Dept. of Geology and Inst. of Meteoritics, Univ. of New Mexico, Albuquerque, NM 87131 USA

A small percentage of lunar samples (mostly clasts in breccias) have high contents of incompatible elements and high Fe/Mg. These evolved rocks, which petrologically are quartz-monzonites to granites, have attracted considerable attention because of the role they may have played during the evolution of the lunar crust, particularly late in the crystallization of the magma ocean. Interpretations have tended to fall into two categories: those suggesting that the petrogenesis of evolved lunar rocks involved fractional crystallization (FC) followed by silicate liquid immiscibility (SLI) (1-6) and those favoring FC alone (7-11). In most cases, single rock specimens do not contain a whole sequence of clasts with evolved compositions. This has made it difficult to deduce the histories of evolved rocks. There are a few cases, however, where a sequence of rock compositions or a possible immiscible-melt pair occurs in one sample. This paper describes three such samples, 77538, 12013, and 15405, plus a monzonitic lithology in rock 67915, and evaluates the roles SLI and FC have played in their evolution.

77538: Breccia 77538 contains high-Fe and high-Si clasts (6). The high-Si clasts consist mostly of silica and K-feldspar ($An_{1-4}Ab_{5-8}Or_{88-93}$), frequently intergrown in a barred texture, with smaller amounts of sodic plagioclase ($\sim An_{68}Ab_{30}Or_{3}$), fayalitic olivine ($FO_{4-13}$), ferroaugite (Fig. 1), ilmenite, metal, troilite, and a Ca-phosphate mineral. The high-Fe clasts are made mainly of ferroaugite and a smaller amount of ferropigeonite (Fig. 1) that enclose blebs of silica and fayalitic olivine (FO_{12-17}); troilite, metal, and ilmenite are also present. Bulk compositions (Table 1) of the two types of clasts are strikingly different; compared to the high-Si clasts, the high-Fe clasts are greatly enriched in Fe, Mg, Ca, and P, and depleted in Si, Al, Na, and K.

12013: This complex black and gray breccia has recently been restudied (4). The gray breccia contains lithic (mostly feldspathic basalts) and mineral clasts, including a lithology called felsite (4). Felsite is composed of $\sim$ 50% K-feldspar and $\sim$ 40% silica, with ilmenite, pyroxene (Fig. 1), K-rich glass, and trace amounts of whitlockite, zircon, and zirconolite. The black breccia contains lithic (including felsite) and mineral clasts in an aphanitic groundmass. This groundmass, which has reacted with many mineral clasts, is thought (4) to represent the composition of a melt that is possibly genetically related to the felsite. It is composed of 40-50% plagioclase (An_{90-67}), 40-50% low-Ca pyroxene (Fig. 1), $\sim$ 5% ilmenite, $\sim$ 5% phosphate minerals, and trace amounts of Zr minerals. The bulk composition of the black-breccia groundmass is significantly different from that of the felsite (Table 1), containing more Ti, Fe, Mg, Ca and P, and less Si, K and Ba; Al and Na are approximately equal in each lithology.

15405: Melt rock 15405 contains a suite of KREEP basalts, quartz-monzodiorite (QMD), and granite clasts set in a fine-grained, KREEP-rich, igneous-textured matrix (10). The QMD lithology has a coarse-grained basaltic texture and consists of $\sim$ 35% each of pyroxene (Fig. 1) and plagioclase ($An_{82}Ab_{17.5}Or_{0.3}$ to $An_{50}Ab_{44}Or_{6}$), $\sim$ 10-15% each of silica and K-feldspar, $\sim$ 0.5-1.5% each of ilmenite, zircon and whitlockite, and minor amounts of metal and chromite. The granite lithology is coarse-grained (crystals > 1 mm), but somewhat crushed. It consists of approximately equal amounts of plagioclase ($An_{88}Ab_{11}Or_{1}$ to $An_{61}Ab_{33}Or_{6}$), pyroxene (Fig. 1), a

silica mineral, and K-feldspar, with minor amounts of ilmenite, troilite, metal, chromite, and a phosphate mineral (10). Bulk compositions (Table 1) of the QMD (12) and the granites (10) are not as strikingly different from one another as were the pairs described above; the QMD contains less Si, K and P, and more Al, Fe, Mg, Ca and Na than does the granite.

67915: This rock is a feldspathic breccia (13,14). It contains a variety of clast types, one of which has been called a sodic ferrogabbro (SFG). SFG clasts are generally coarse-grained (crystals up to 1 mm) but cataclastic. They consist of plagioclase ($An_{69}Ab_{28}Or_3$ to $An_{54}Ab_{37}Or_9$), ferroaugite and ferropigeonite (Fig. 1), ilmenite, silica, and K-feldspar, with minor amounts of troilite and a phosphate mineral. The silica and K-feldspar are not intergrown as they are in many evolved rocks; instead, they occur as separate, equant crystals. We determined the bulk composition of a 4x6 mm SFG clast (Table 1) by the broad-beam microprobe technique. Although the relatively high porosity of the section resulted in a low total, it appears that the SFG is similar in composition to the QMD in 15405. (We are in the process of determining the bulk composition of the SFG lithology in 67915 by modal analysis combined with average mineral compositions.)

Criteria have been established that allow us to assess whether FC or SLI has been the dominant process in producing the evolved rock types described above. During FC, the more evolved composition usually has higher Na/Ca, Fe/Mg, P, and K; this, of course, is affected by the details of the crystallization sequence. Experiments (2) and observations of natural systems (13,15-18) have shown that SLI acts in a drastically different manner: the high-Si melt is enriched in Si, Al, Na, and K, whereas the high-Fe melt is enriched in Fe, Mg, Ti, Ca and P (Table 2). (Trace elements are also extremely useful in distinguishing between FC and SLI, but such data are available only for 12013 and the 15405 QMD, so we will confine our observations to major elements only.) Although all the melt pairs described above plot near the immiscible-melts field in Fig. 2, only the 77538 pair seems to be unambiguously derived by SLI: compared to the high-Si melt, the high-Fe melt contains significant enrichments in Fe, Mg, Ti, Ca and P and marked depletions in Si, K, Na and Al (Tables 1, 2). The melt pair in 12013 might have formed by SLI (4), but the data are ambiguous: K is low and Fe, P, Mg, and Ti (Tables 1,2) are high in the high-Fe melt (black-breccia groundmass), but, as noted by (19), Al and Na are enriched in the high-Fe melt, opposite to the trend expected. However, because the melts in 12013 are clast-laden and show evidence of assimilation of mineral clasts, their present compositions might not reflect the original ones, which could have been derived by SLI (19). The QMD and granite in 15405 are certainly not an immiscible pair: Al, P, K, and Na are all much too high and Fe too low (Tables 1,2) for the QMD to have formed with the granite by SLI. We agree with Ryder (10; see also 7,9) that both the QMD and granite in 15405 formed by FC of a KREEP-basalt magma. Rutherford et al (5) suggested that the 15405 granite formed by SLI near the end of crystallization of a KREEP-basalt parent, but the high P and K contents (Table 1) of the granite argue against this idea. (Rutherford et al (5) did not suggest that the QMD was the corresponding high-Fe melt that formed with the granite; they proposed instead that it might have formed by impact-melting or by mixing of immiscible granite melt and plagioclase fractionated from the high-Fe melt, but there is no textural evidence for either of these possibilities.) The similarity in composition between the SFG in 67915 and the QMD in 15405 (Table 1) suggest that it, too, formed by FC of a KREEP-basalt magma. We

conclude that some lunar granites formed by FC only and that others formed by FC followed by SLI. (1) Crawford, M. L. and Hollister, L. (1977) Proc. Lunar Sci. Conf. 8th, p. 2403-2417. (2) Hess, P. C. et al (1975) Proc. Lunar Sci. Conf. 6th, p. 895-909. (3) Hess, P. C. et al (1978) Proc. Lunar Planet. Sci. Conf. 9th, p. 705-724. (4) Quick, J. E. et al (1977) Proc. Lunar Sci. Conf. 8th, p. 2153-2189. (5) Rutherford, M. J. et al (1976) Proc. Lunar Sci. Conf. 7th, p. 1723-1740. (6) Warner, R. D. et al (1978) Proc. Lunar Planet. Sci. Conf. 9th, p. 941-958. (7) Irving, A. (1977) Proc. Lunar Sci. Conf. 8th, p. 2433-2448. (8) Lovering, J. F. and Wark, D. A. (1975) Proc. Lunar Sci. Conf. 6th, p. 1203-1217. (9) Nyquist, L. E. et al (1977) Lunar Sci. VIII, p. 738-740. (10) Ryder, G. (1976) Earth Planet. Sci. Lett. 29, p. 255-268. (11) Ryder, G. et al (1975) Proc. Lunar Sci. Conf. 6th, p. 435-449. (12) Taylor, G. J. (1976) Interdisciplinary Studies by the Imbrium Consortium, Vol. 1.(13) Weiblen, P. W. and Roedder, E. (1973) Proc. Lunar Sci. Conf. 4th, p. 681-703. (14) Roedder, E., and Weiblen, P. W. (1974) Proc. Lunar Sci. Conf. 5th, p. 308-318. (15) Roedder, E. and Weiblen, P. W. (1970) Proc. Apollo 11 Lunar Sci. Conf., p. 801-837. (16) Roedder, E. and Weiblen, P. W. (1971) Proc. Lunar Sci. Conf. 2nd, p. 507-528. (17) Roedder, E. and Weiblen, P. W. (1972) Earth Planet. Sci. Lett. 13, p. 272-285. (18) Roedder, E. and Weiblen, P. W. (1973) Proc. Lunar Sci. Conf. 3rd, p. 251-279. (19) Rutherford, M. J. and Hess, P. C. (1978) Lunar Planet. Sci. IX, p. 987-989.

Table 1. Bulk chemical compositions (wt.%) of lunar samples with evolved compositions

	77538		12013		15405		67915
	high-Fe	high-Si	dark-breccia	felsite	Quartz monzodiorite	Granite	Sodic ferrogabbro
Ref.	6	6	4	4	12	10	
SiO_2	50.3	74.0	50.1	73.1	57.4	68.1	60.8
TiO_2	2.82	0.54	2.2	0.6	1.1	0.90	2.6
Al_2O_3	0.96	12.5	13.2	12.1	13.2	10.2	12.9
Cr_2O_3	0.17	<0.01	0.13	<0.1	—	0.06	<0.05
FeO	31.3	2.21	12.3	1.5	11.2	7.0	9.2
MnO	—	—	0.15	<0.1	—	0.12	0.1
MgO	4.3	0.08	7.4	0.5	3.4	1.5	2.8
CaO	9.8	1.86	9.5	1.5	9.0	4.9	9.1
Na_2O	0.12	0.90	1.9	1.4	1.0	0.79	1.6
K_2O	0.29	7.6	0.06	6.7	1.9	3.4	0.61
P_2O_5	0.28	0.07	1.2	0.2	0.4	0.52	0.23
BaO	—	—	0.03	0.73	—	0.45	—
ZrO_2	—	—	0.3	<0.1	—	—	—
S	0.63	0.13	<0.01	<0.1	—	—	—
Total	100.97	99.89	98.47	98.13	99.0	97.82	99.94*

* Normalized; sum originally 91.6.

Table 2. Elemental ratios (element or ratio in high-Fe composition/element or ratio in high-Si composition) in evolved lunar rocks.

	77538	12013	15405	Exp [1]	Basalts [2]
K_2O	0.04	0.001	0.56	<0.36	<0.06
P_2O_5	4.0	6.0	0.77	>4.6	>3.0
TiO_2	5.2	3.7	1.2	>2.5	>5.0
K_2O/P_2O_5	0.01	<0.001	0.7	<0.08	<0.02

1) Ref. (2)
2) Refs. (13, 15-18)

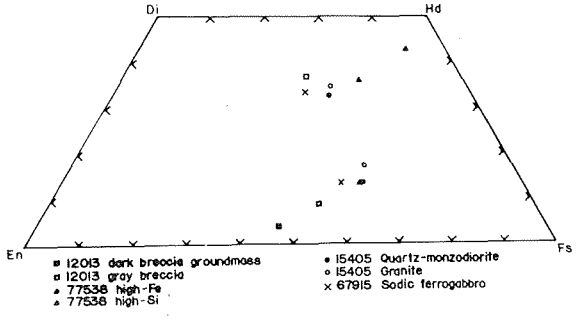

Fig. 1. Average pyroxene compositions in evolved lunar rocks (4,6,10,12).

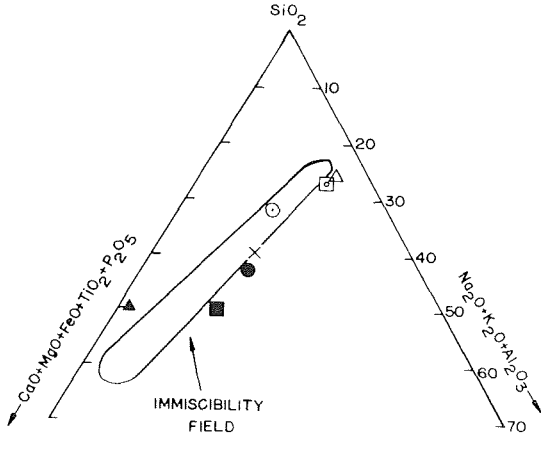

Fig. 2. Bulk comopsitions of evolved lunar rocks. Immiscibility field from (2,13-18).

THE 67915 CONSORTIUM: SEARCHING FOR PIECES OF THE ANCIENT LUNAR CRUST. G. J. Taylor[1], R. Warner[1], K. Keil[1], J. Geiss[2], K. Marti[3], E. Roedder[4], R. A. Schmitt[5], and P. Weiblen[6]. [1]Univ. of New Mexico, Albuquerque, [2]Univ. of Berne, Switz., [3]Univ. of Calif., San Diego, [4]U.S.G.S, Reston, [5]Oregon State Univ., [6]NASA Headquarters, Washington, D.C.

Our consortium was organized to extract and study clasts from breccia 67915. Our goal was to select clasts that survived the final intense bombardment of the moon and, therefore, carry important chronological and petrological information about the processes that took place during the first half-billion years of lunar history. The consortium intends to study the mineralogy, petrology, bulk compositions (major and trace elements), and ages (^{40}Ar-^{39}Ar, Nd-Sm, ^{244}Pu-Nd-Xe, and exposure ages) of separated clasts, as well as *in situ* studies of clast-breccia interaction. We chose 67915 because previous studies (1,2) had shown that it contained an interesting assemblage of clasts. This report briefly summarizes work to date including data we reported previously (3); we anticipate that much more data will be available at the time of the Conference on the Lunar Highlands Crust.

Breccia 67915 was hammered off South Boulder, which might be ejecta from the bottom of North Ray Crater (4). The rock is composed of two main lithologies, both of which are polymict breccias. One is white to very light gray macroscopically and is made up of numerous rounded clasts. These clasts range in size from < 1 mm to ∿ 1 cm and are predominantly fine-grained, hornfelsic ANT breccias. The other main lithology is gray macroscopically and seems to form the matrix of the rock. This gray breccia is composed mostly of gray clasts ranging in size from < 1 mm to ∿ 3 cm. These clasts are fine-grained, clast-bearing melt rocks. Both white and gray areas of the rock are cut by numerous veins of glass; these may have been produced when the rock was excavated from North Ray Crater. Chemical analyses (5-9) indicate that both white and gray clasts have similar compositions, containing 80 to 85% normative plagioclase. Abundances of REE are low (∿ 10 times chondritic) and there is a positive Eu anomaly. Siderophile-element contents are high in both white and gray clasts, averaging ∿ 10^{-2} times Cl abundances (10). Ir/Au and Re/Au ratios are higher than in other Apollo 16 breccias, suggesting a distinct source for the siderophile elements. Combining these data with the notion that 67915 represents the deepest material from North Ray Crater (4), Krahenbuhl et al. (10) suggested that 67915 originated as ejecta from the Nectaris basin.

Although white and gray clasts make up 95% of the rock, several other types of clasts are also present. Brief descriptions of those under study by the consortium follow. Two types of possibly pristine *troctolitic anorthosite* occur. One variety (represented by *67965,26*) seems to have a cumulate texture, with large (∿ 1 mm) plagioclase crystals surrounded by intercumulus olivine (see Fig. 2 of ref. 2). The two clasts of this lithology studied so far (,26 and ,12-1, ref. 2) are strongly shocked: plagioclase is partly isotropic and olivine is mosaicized. The two clasts have the same olivine compositions, Fo_{55}; plagioclase has a composition of An_{98} in one and An_{93-96} in the other. The severe shock might hinder ^{40}Ar-^{39}Ar measurements. (A plagioclase separate from 67915,26 has been prepared for both Ar-dating and INAA.; in addition, a subsample of the bulk clast was forwarded to Oregon State for INAA.) The other type of troctolitic anorthosite is represented by clast 67915,67. It has a granular texture, with plagioclase grains up to 0.6 mm across and olivine up to 0.4 mm. Olivine is homogeneous

and has a composition of Fo_{75}. Plagioclase has a composition of An_{95}. (Subsamples have been prepared for Ar dating and INAA.) A second interesting lithology in 67915 was discovered by Weiblen and Roedder (1), who called it a sodic ferrogabbro. The consortium is studying several such clasts. This rock type is characterized by the presence of sodic plagioclase ($An_{69}Ab_{28}Or_3$ to $An_{54}Ab_{37}Or_9$), iron-rich pyroxene, and ilmenite (∿ 5% of the rock), with lesser amounts of silica and K-feldspar. The pyroxene appears to have crystallized with two distinct compositions: a ferropigeonite with ∿ $En_{34}Fs_{52}Wo_{14}$ and a ferroaugite with ∿ $En_{31}Fs_{35}Wo_{34}$. Sodic ferrogabbro clasts are usually brecciated, but monomict. Because plagioclase and pyroxene crystals between 0.5 and 1.0 mm in size are common, we infer that the original texture was coarse grained. For a discussion of the sodic ferrogabbros in the context of evolved rock-types from the lunar highlands, see (11). (A plagioclase concentrate, containing ∿ 5% silica and perhaps some K-feldspar, has been prepared for Ar-dating and INAA. A subsample was also selected for INAA.)

^{40}Ar-^{39}Ar data have been reported for eight clasts from 67915 (3,12). Table 1 summarizes the results. Three points emerge from a study of the data in Table 1. First, there are as yet no well-defined ages older than ∿ 4.0 b.y. This is not too surprising because all but one of the clasts dated are white or gray breccias and, therefore, obviously not pristine. Second, most samples show significant gas loss. This is consistent with the shocked nature of many clasts in 67915 and with the presence of numerous glass veins. The gas loss may be associated with heating during the excavation of North Ray Crater. Third, some clasts do give good plateau ages, around 3.9 to 4.0 b.y. This indicates that the younger shock event(s) did not totally disturb the chronology of clasts in 67915. Consequently, the search for clasts with ages > 4.0 b.y. can be undertaken with at least a glimmer of hope.

(1) Weiblen, P. W. and Roedder, E. (1973) Proc. Lunar Sci. Conf. 4th, p. 681-703. (2) Roedder, E. and Weiblen, P. W. (1974) Proc. Lunar Sci. Conf. 5th, p. 303-318. (3) Marti, K. et al. (1978) Lunar Planet. Sci. IX, p. 696-698. (4) Apollo Lunar Geology Investigation Team (1972) Interagency Report: Astrogeology 51. (5) Duncan, A. R. et al. (1973) Proc. Lunar Sci. Conf. 4th, p. 1097-1113. (6) Jangnhorbani, M. et al. (1973) Proc. Lunar Sci. Conf. 4th, p. 1115-1126. (7) Nakamura, N. et al. (1973) Proc. Lunar Sci. Conf. 4th, p. 1407-1414. (8) Wanke, H. et al. (1976) Proc. Lunar Sci. Conf. 7th, p. 3479-3499. (9) Rose, H. J. et al. (1975) Proc. Lunar Sci. Conf. 6th, p. 1363-1373. (10) Krahenbuhl, U. et al. (1973) Proc. Lunar Sci. Conf. 4th, p. 1325-1348. (11) Taylor, G. J. et al. (1979) This volume. (12) Kirsten, T. et al. (1973) Proc. Lunar Sci. Conf. 4th, p. 1757-1784.

67915 CONSORTIUM

Taylor, G. J. et al.

Table 1. Summary of ^{39}Ar-^{40}Ar age data on clasts from 67915

Clast No.	Petrography	Age(b.y.)	Ref.	Comments
67915,41a	light-gray breccia		12	Continuous increase in apparent age with fraction of ^{39}Ar released
67915,41b	White, aphanitic		12	Semi-plateau with age > 4.2 b.y., but 1500° fraction has apparent age of 4.65 b.y.
67915,41c	White to light-gray, coarser-grained than clast b	3.91±.05	12	Good plateau for last 40% of ^{39}Ar released
67915,41d	Friable matrix of breccia	3.99±.05	12	Good plateau for just 60% of ^{39}Ar released last
67915,34W	Large plag. crystals in a much finer-grained matrix (white clast)	4.0±.1	3	Plateau for last 40% of ^{39}Ar released.
67915,13DW	Slightly recrystallized ANT breccia (white clast)	~4.0	3	Continuous increase in apparent age with fraction of ^{39}Ar released; final 50% has age > 3.7 b.y.
67915,34B	Fine-grained, plag. rich melt rock	~ 3.5	3	Poorly-defined plateau that comprises 40% of the ^{39}Ar and has a slight dip in it.
67915,34S	Sodic ferrogabbro	> 3.2	3	Plag. separate; continuous increase in apparent age with fraction of ^{39}Ar released. No plateau.

CONCEPTS OF THE CHEMICAL COMPOSITION OF THE LUNAR HIGHLAND CRUST.
S.R. Taylor, Research School of Earth Sciences, Australian National University, CANBERRA, Australia.

Initial observation with low-powered telescopes revealed that the highlands were elevated, relative to the maria (1). This led to analogies, both for density and composition, to the terrestrial continents. A crucial step was to resolve the nature of the large craters. If these were of volcanic origin (2), then lunar magmas would possess different properties to those on Earth. The resolution of the crater problem was accomplished effectively by Gilbert (3) and Baldwin (4), but the concept of widespread volcanism on the lunar highlands continued, finally influencing the selection of the Apollo 16 landing site. The terrestrial continent analogy suggested the possibility that the lunar highlands were of granitic composition (5,7). This concept was not inconsistent with visual observation, and was reinforced by two factors: (a) Detailed mapping of the highlands revealed the presence of light plains units (6), of varying stratigraphic age, which would be consistent with deposition by a mechanism analogous to terrestrial ignimbrite eruptions. The highly viscous lavas required to generate such ash-flow deposits would necessarily be acidic, analogous to terrestrial dacites or rhyolites in composition (5,7,8). (b) This concept was agreeable to those workers who wished to derive tektites from the moon (9,10),since it provided an acidic source material. The distinctions between the composition of terrestrial rhyolites and tektites were ignored, since such differences might not apply to lunar acidic rocks (5).

The first direct analysis of the lunar surface by Surveyor VII, on the rim of Tycho, revealed a totally different composition, similar to terrestrial high-alumina basalt (11), and widely different from granitic compositions. The first clue to the mineralogical nature of the highlands came from the discovery of anorthosite fragments in the Apollo 11 soil samples (12). This immediately suggested a possible resolution to a major geochemical dilemma by providing a sink for europium. Thus began the "magma ocean" concept.

The next surprise was the discovery at the Apollo 12 site of the light grey fines (eg 12033) and rock sample 12013, both enriched to an extraordinary degree in large ion lithophile elements (13). The evidence for an extreme degree of element fractionation, reminiscent of the concentrations observed in terrestrial pegmatites, was dramatically reinforced by the Apollo 14 sample return from Fra Mauro (14). The existence of large areas of K-rich material (KREEPUTH) at the lunar surface, indicated by the gamma-ray orbital data, led to new concepts of the origin of the highland crust. Since the Fra Mauro site was on the Imbrium ejecta blanket, these unusual compositions focussed attention on possible sources, either local, or from within the Imbrium basin. The nature and origin of the ejecta blankets, and the depth of excavation of the large ringed basins became matters of concern to geochemists. The recognition of the high content of local material in large ejecta blankets was aided by the marked lateral differences in Al/Si ratios recorded by the orbital XRF experiment (15,16).

Attempts to explain the chemical composition of the crust with its high contents of refractory elements led quickly to the development of heteogeneous accretion models (17). The late addition of a layer rich in refractory elements at first appeared to pose fewer problems than those caused by melting and cooling of large volumes of the moon, since this was

required to happen at a very early stage of lunar history. The geochemical debate over homogeneous versus heterogeneous accretion, which led to some extremely high-alumina moons (18), was eventually resolved in favour of homogeneous models (or homogenisation after accretion) (19). The key evidence was the recognition that the ratios of volatile/refractory elements were similar in mare basalts (derived from the deep interior) and in the highlands crust (20). This linking of the highlands chemistry with that of the source regions of the mare basalts provided a ready explanation for the europium anomalies, and many other geochemical problems.

Meanwhile the sampling problem persisted. How representative of the crust were the surface samples, and how might they be related to the Al/Si and Th values derived from the orbital geochemistry experiments? A solution to this problem was proposed by the Apollo soil survey (21), who advanced the proposition that the formation during impact of glass spherules (whose composition could be rapidly determined by microprobe analysis) would be representative of the principal components of the highlands crust. This approach still appears to represent the only viable way to accumulate enough statistical data (utilising the natural sampling process) to evaluate bulk surface compositions and to relate these to the orbital chemical data.

The observation that many of the refractory trace elements were correlated (22) in lunar highlands samples of differing composition, and from different landing sites, enabled estimates to be made for the abundances of many trace elements and to relate these, via the gamma-ray thorium abundances, to moon-wide compositions. By this means, average lunar highland surface compositional estimates can be achieved (23).

The next step is less readily taken. How representative is this surface composition of the bulk highland crust, to depths of 60-100 km? How reliable are the geophysical estimates of crustal thickness? Does the crust vary laterally in chemistry, or thickness? From what depth are samples brought to the surface by the large impacts which form the ringed basins? How much mixing and homogenisation has resulted from these and smaller collisions? The answers to such questions will provide basic information about the initial depth of melting to form the magma ocean, and on the bulk composition of the moon, via element balance calculations.

Current models for the origin of the highland crust are largely based on magma ocean crystallisation during which plagioclase floats with possible formation of "rockbergs". Little difficulty is experienced in producing this stage ("The plagioclase has clearly risen to the top," 24). Less progress has been made with the two other basic geochemical problems.

The question of local versus moon-wide origin for the high concentrations of KREEP appears to be resolved by the Sm-Nd systematics which indicate a large scale uniformity (25), consistent with the model that these element abundances represent the final or residual stages of crystallisation of the magma ocean. These residual melts can be expected to pervade the highland crust. The combination of intrusion and mixing by impact, with some localised partial melting appears adequate to produce the observed distribution (26). The observation of the parallel nature of the REE patterns (22), and the correlations among the trace elements provides evidence for the importance of mixing mechanisms with the highland crust.

The second geochemical problem concerns the origin of the "primitive" Mg-rich component. This could represent an original frozen crust, trapped interstitial liquid or be contributed in part by the continuing bombardment.

CHEMICAL COMPOSITION HIGHLAND CRUST

Taylor, S.R.

The concept of three initial components (plagioclase, residual precursor - KREEP liquid, and a more primitive Mg-rich component) appears adequate to account for the geochemical characteristics of the highland crust. Most of the petrographic complexities result from the extremely turbulent crystallisation and brecciation history of this material during the continuing bombardment of the moon by large projectiles.

(1) Galilei, G (1610) Nuncius Siderus, Padua.
(2) Spurr, J.E. (1948) Geology applied to Selenology III (Rumford)
(3) Gilbert, G.K. (1893) Phil. Soc. Wash. Bull. 12, 241.
(4) Baldwin, R.B. (1949) The Face of the Moon (Chicago)
(5) Walter, L.S. (1965) Ann. N.Y. Acad. Sci. 123, 367
(6) Wilhelms, D.E. (1970) U.S. Geol. Surv. Prof Paper 599 F.
(7) O'Keefe, J.A. and Cameron W.S. (1962) Icarus, 1, 271
(8) O'Keefe, J.A. Lowman P.D. and Cameron W.S. (1967) Science, 155, 77
(9) Lowman. P.D. (1963) Icarus, 2, 35
(10) O'Keefe, J.A. (1976) Tektites and their Origin (Elsevier)
(11) Jackson, E.D. and Wilshire. H, (1968) J.G.R. 73, 7621
(12) Wood, J.A. et al. (1970) Proc. Apollo 11 Lunar Sci. Conf. 965.
(13) LSPET (1970) Science, 167, 1325
(14) LSPET (1971) Science 173, 681
(15) Adler. I. et al (1973) Proc. Lunar Sci. Conf. 4th, 2783
(16) Hörz, F. (1974) Lunar Sci V, 357
(17) Gast, P.W. (1972) Moon, 5, 121
(18) Anderson, D.L. (1973) E.P.S.L. 18, 301
(19) Brett P.R. (1973) G.C.A. 37, 2697
(20) Duncan, A.R. et al (1973) Proc. Lunar Sci 4th. 1097
(21) Reid, A.M. (1974) Moon, 9, 141
(22) Taylor, S.R. et al (1973) G.C.A., 37, 2665
(23) Taylor, S.R. (1975) Lunar Science, A Post Apollo View (Pergammon)
(24) Walker, D. and Hays J.F. (1977) Geology, 5, 426
(25) Lugmair, G.W. and Carlson, R.W. (1978) Proc. Lunar Sci. Conf 9th. 689
(26) Reid, A.M. et al (1977) Proc. Lunar Sci. Conf. 8th, 2321

MARE-TERRA DIFFERENCES IN INFRARED/RADAR ANOMALY OCCURRENCES: IMPLICATIONS ABOUT CRATER AGING;

T.W. Thompson and J.A. Cutts, Planetary Science Inst., Pasadena, CA 91101, R.W. Shorthill, Univ. of Utah Research Inst., Salt Lake City, UT 84108, S.H. Zisk, NEROC, Haystack Obs., Westford, Mass. 01886

INTRODUCTION

In a previous study, 1310 craters were cataloged as radar and/or infrared anomalies (Thompson, et al., 1979). Here, mare-terra differences of larger (diam. > 10km) craters is examined and the implications for lifetimes of rocks in the near subsurface are explored.

These inferences about surface and subsurface rocks are based upon an earlier study of 51 craters by Thompson, et al. (1974). Briefly, an infrared anomaly is a crater which remains warmer than its environs during a lunar eclipse implying excess surface rocks larger than 10cm diameter. A radar anomaly is a crater which backscatters more power than its environs, implying excess surface or subsurface rocks, where the rock size must be 0.25 to 10 wavelengths and the rock must be within 30 wavelengths of the surface. Thus, 3.8cm radar echoes are controlled by 1cm to 40cm rocks buried no deeper than 1.1 meter; the 70cm radar echoes are controlled by 15cm to 7.0cm rocks in size buried no deeper than 21 meters.

Here, various combinations of these infrared and radar anomalies will be examined. Thus it is useful to identify crater signatures with a 3-letter index XYZ, where X is the infrared behavior, Y is the 3.8cm radar behavior and Z is the 70cm radar behavior. The letters X, Y, Z will be B = bright = an anomaly or F = faint = no anomaly. For example, a BBF crater is an infrared and 3.8cm radar anomaly accompanied with an average 70cm radar signature.

CRATER EVOLUTION MODEL

The various combinations of infrared and radar signatures can be related to models of crater evolution. It is assumed first that the youngest craters are all BBB (bright at all wavelengths) craters based upon observations of the rayed craters Tycho, Aristarchus, Kepler, Copernicus, and Langrenus. Similarly, the oldest craters are FFF (faint at all wavelengths) craters based upon the observations of older terra craters.

Between the youngest and oldest craters, there are six possible anomaly combinations for intervening states. The process which modifies these anomalies is meteoritic impact, which erases the excess surface and subsurface rocks, the source of the infrared and radar anomalies. Thus, one expects the excess surface rocks and the infrared anomaly to disappear first. Then the excess centimeter (near surface) rocks and the 3.8cm radar anomaly should disappear at the second step. The last anomaly to disappear should be the long wavelength radar since it penetrates deeeper into the subsurface. This crater evolution model, as shown in Figure 1, predicts that the BBB, FBB and FFB craters will be abundant and the FBF, BFB, BBF, and BFF craters will be scarce or non-existent.

IR/RADAR DATA

It is useful to compare this crater evolution model with

the observed distributions of craters which are infrared and radar anomalies. Mare-terra differences in these distributions are important here since the time of mare formation is known from age-dating of Apollo samples. The IR/radar data are summarized in Table 1 and Figure 2.

The BBB (bright at all wavelengths) crater, which has excess surface rocks of all sizes, appears equally frequently in the mare and terra. The FBB (faint IR, bright radar craters) craters, which have excess subsurface rocks of centimeter and meter sizes, appear in both mare and terra with terra craters occuring with 3 times greater density. It is likely that BBB craters are post mare in ages, while the FBB craters are contemoraneous with the mare emplacement. Some terra FBB craters should be premare in age to account for the mare-terra differences in these FBB craters.

The FBF craters, which has excess subsurface rocks of centimeter size, and FBB craters, which has excess subsurface rocks of meter size, appear almost exclusively in the terra. Thus, these FBF and FFB craters appear to be premare in age. The BFB, BBF, and BFF craters are bright in the infrared and faint at one or both radar wavelengths, which implies surface rocks with peculiar size distributions. As expected these BFB, BBF, and BFF craters occur relatively infrequently.

Also, all anomalies taken together have a frequency distribution which closely matches that for Imbrian craters plotted by Wilhelms, et al. (1978). This implies the oldest radar anomalies are no older than the Imbrium basin. In summary, the infrared and radar data suggest crater lifetimes shown in Table 1.

DISCUSSION

The observed occurences of craters which are infrared and radar anomalies both agree and disagree with evolutionary model described above. As expected, the infrared anomaly is the first anomaly to disappaear and the BBF, BFB, BFF craters are rare. However, FBF craters occur unexpectedly frequently. Also, the FBB and FBF craters are unexpectedly premare in age. It is concluded that excess subsurface rocks of centimeter size have longer lifetimes than expected. One notes here that regolith formed on a premare feature should be deeper than 10 meters while the radar penetration depth at 3.8cm wavelength is only 1.1 meter.

REFERENCES

Thompson, T.W. et al., (1974), The Moon, 10, 87-117.

Thompson, T.W. et al., (1979), accepted for publication in The Moon and Planets.

Wilhelms, D.E., Oberbeck, V.R., and Aggarwal, H.R., (1978), Proc. Lunar Sci. Conf. 9th, 3, 3735-3762.

MARE-TERRA DIFFERENCES...

Thompson, T.W. et al

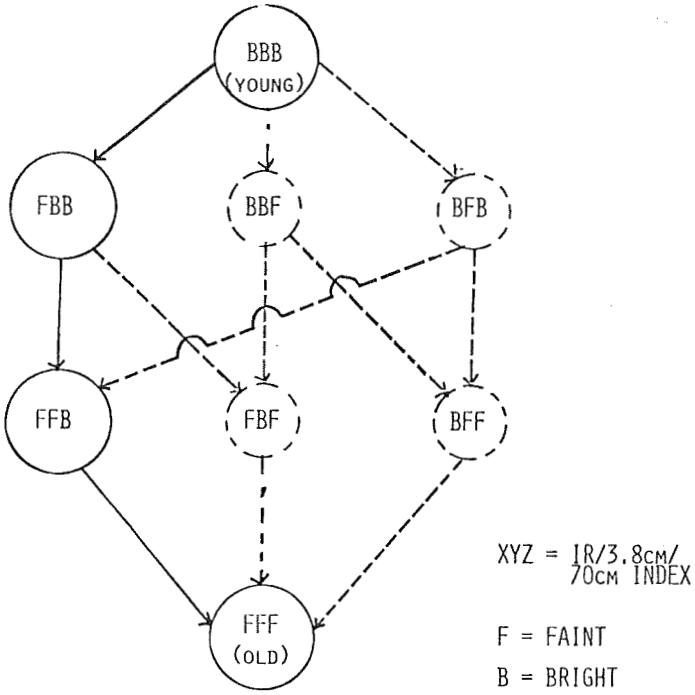

Figure 1: Idealized model of the evolution of the IR/radar signatures of craters caused by lunar surface processes.

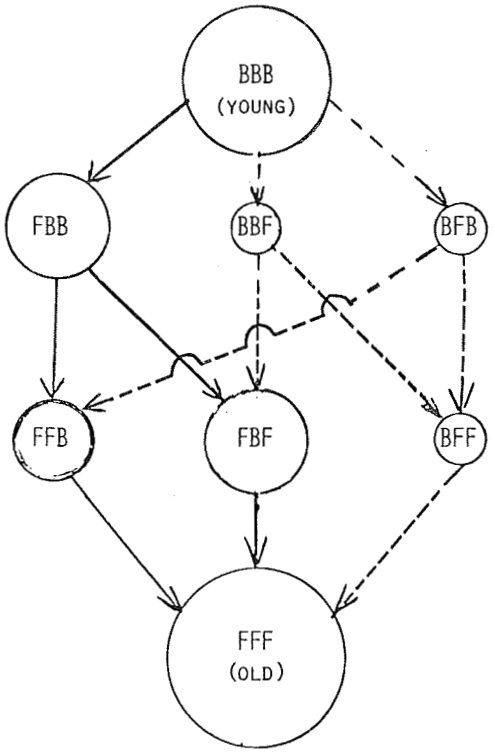

Figure 2: Observed abundances of IR/radar craters on the moon (circle diameter denotes abundance).

TABLE 1

ANOMALY TYPE	BBB	FBB	FBF	FFB	BFB + BBF + BFF	ALL
IMPLIED SURFACE CONDITIONS	EXCESS SURFACE ROCKS OF ALL SIZES	EXCESS SUBSURFACE ROCKS OF ALL SIZES	EXCESS SUBSURFACE ROCKS OF CENTIMETER SIZES	EXCESS SUBSURFACE ROCKS OF METER SIZES	UNEXPECTED EXCESS SURFACE ROCKS WITH PECULIAR SIZES	----
NUMBER OF MARE CRATERS DIAM.>11.3KM PER $10^6 KM^2$	13.6	3.9	0.9	0.9	2.0	21.4
NUMBER OF TERRA CRATERS DIAM.>11.3KM PER $10^6 KM^2$	18.3	14.6	11.9	5.6	3.7	54.1
IMPLIED AGE	POST MARE	CONTEMPORANEOUS WITH MARE FORMATION	PRE-MARE AND POST IMBRIUM BASIN		MARE AREA = $4.4 \times 10^6 km^2$ TERRA AREA = $5.4 \times 10^6 km^2$	

SILICATE MINERALOGY OF HIGHLAND MELT ROCKS. D.T. Vaniman and J.J. Papike, Department of Earth and Space Sciences, SUNY, Stony Brook, N.Y. 11794

Lunar highland "melt rocks" include impact melt and volcanic compositions that can be divided into six groups by cluster analysis [1]. High-K KREEP - anorthosite mixtures and anorthosite rich (>63% normative An) melt rocks form three of these groups, but are not represented by large melt rock samples[2,3]. The remaining three groups are: anorthositic gabbro (ANG) melt rocks which plot within the anorthite field of the Walker et al. pseudoternary [4], low-K Fra Mauro (LKFM) rocks which plot at or near anorthite-olivine cosaturation, and intermediate-K Fra Mauro (IKFM) rocks which are part of a pyroxene-plagioclase fractionation series [5]. In Fig. 1 representative melt-rock compositions compiled from the literature are plotted in the Walker et al. [4] pseudoternary. In table 1 the LKFM group has been divided into poikilitic- and subophitic/intergranular - textured series, and the ANG group has been divided into olivine-free and olivine-bearing series. These subdivisions are important in the cooling-rate distinctions made later in this abstract. The silicate mineralogy of highland melt rocks reveals (1) crystallization from melts of highland compositions and (2) variations in the crystallization and cooling histories of specific highland compositions.

Table 1

Melt Rock Groups and sub-groups

Anorthositic Gabbro (ANG)	
Olivine-free	
	63549
	65055
Olivine-bearing	
	67559
	68415
	68416
	60335
	66095
Low-K Fra Mauro (LKFM)	
subophitic/intergranular-textured	
	14276
	14310
	64455
	62295
poikilitic-textured	
	60315
	62235
	65015
	77135
Intermediate-K Fra Mauro (IKFM)	
	15386
	15434

(I) Feldspar Compositions. The most refractory (An-rich) feldspars in highland melt rocks range from An_{98} (68415, 66095) to An_{76} (14068). Fig. 2 shows the correlation between the most refractory feldspar compositions (excluding feldspar clasts) and the normative An composition of the host rock. Horizontal bars represent the range of host rock compositional estimates (vertical marks) and are not individual compositional error bars. There is a non-linear relationship between An-content of the host rock and An-content of the first-formed plagioclase. The two samples which deviate most from the plotted curve are 62295, a troctolitic melt rock, and the sample 64455 which contains some maskelynite as well as feldspar. Reasonable adherence to this curve is found in both quickly cooled samples (subophitic/intergranular-textured LKFM and olivine-free ANG) and slowly cooled samples (poikilitic-textured LKFM and olivine-bearing ANG), suggesting a bulk compositional control which is not seriously offset by variations in cooling rate.

(II) Olivine: High K_D^{ol-liq} Values. Olivine compositions in terrestrial basalts and lunar mare basalts have a common $K_D^{ol-liq} = (X_{Fe}^{ol} X_{Mg}^{liq} / X_{Mg}^{ol} X_{Fe}^{liq})$ of 0.3-0.34 [6,7]. Table 2 shows that K_D^{ol-liq} estimates from highland melt rocks based on most refractory (most Mg-rich) olivine analyses indicate a higher K_D^{ol-liq} of 0.5-0.7 (av. 0.6). The high values of K_D^{ol-liq} in highland melt rocks are not due to undercooling during rapid crystallization, because the 0.6 value is found in rocks with evidence for slow cooling (poikilitic rocks such as 65015 and 77135) as well as in rocks that crystallized rapidly (skeletal-olivine rock 62295). Within rocks of specific ANG composition, olivine may be present in some (67559, 68415) and absent in others (63549, 65055). In this instance

Table 2

Olivine K_D^{ol-liq} Compositions

	Mg/(Mg+Fe) rock	maximum Mg/ (Mg+Fe) olivine	K_D^{ol-liq}
ANG			
68415	0.65	0.73	0.69
60335	0.76	0.84	0.60
66095	0.69	0.77	0.66
LKFM subophitic/intergranular			
64455	0.75	0.83	0.61
62295	0.81	0.88	0.58
poikilitic			
62235	0.66	0.81	0.46
65015	0.66	0.77	0.58
77135	0.71	0.80	0.61

the absence of olivine may be due to rapid cooling: olivine-free ANG has smaller grain sizes (<0.5 mm) than olivine-bearing ANG (>0.5 mm), evidence of a more rapid cooling rate in the olivine-free samples. Experimental cooling-rate studies of this highland melt rock composition would help to test the significance of olivine appearance as a cooling-rate indicator and aid in the development of thermal models for lunar impact-melt sheets.

(III) Pyroxene: Variations with Bulk-rock Composition and Cooling Rate. Variations in pyroxene structural state and composition are more likely to reflect cooling-rate differences than differences in melt rock bulk compositions. A notable exception is the higher Cr content (0.03 cations/6 oxygens) of pyroxenes in the IKFM melt rocks and the lower Cr content (<0.02 cations) in the other melt rocks. This variation in Cr content reflects the difference in bulk rock compositions (which possibly reflects the volcanic rather than impact-melt origin of IKFM): the Cr content in IKFM is 0.3 wt. %, whereas the Cr content of other melt rocks is less than 0.2 wt. %.

Cooling-rate variations lead to striking differences in the pyroxene compositions of rocks which are similar in bulk composition. Fig. 3 shows the difference between orthopyroxene-pigeonite-augite zonation in subophitic/intergranular-textured LKFM (quickly cooled), and the poorly zoned pigeonite/orthopyroxene plus augite pairs of poikilitic-textured LKFM (slowly cooled). Other indications of cooling-rate differences may be found in Ti/Al zonation (Fig. 4b): pyroxenes in subophitic/intergranular LKFM are zoned from high Al contents (0.14 cations) toward a restricted range of Ti, Al content in Fe-rich augites (Al = 0.4-0.7 cations, Ti = 0.2-0.3 cations), but poikilitic LKFM has little pyroxene zonation. Compositions above the line of Al/Ti ratio = 2 (stippled area) have Na contents at or slightly above microprobe detection limits (0.01 cations/6 oxygens), suggesting the presence of an $NaTi(Al,Si)O_6$ or $NaTi_{0.5}R^{2+}_{0.5}Si_2O_6$ substitution in augites of the more slowly cooled LKFM. The correlation of this Na-Ti substitution with slowly cooled augite is also found in the ANG melt rocks (Fig. 4a) where the olivine-free samples (i.e., rapidly cooled, as discussed above) have high-Ca pyroxenes that plot below the Al/Ti = 2 line, but the olivine-bearing samples (cooled more slowly) have Na-bearing augites that plot above the Al/Ti = 2 line (stippled area) as do the more slowly cooled augites in poikilitic LKFM. Note that the low-Ca pyroxene trend of olivine-free ANG preserves a higher initial Al content (0.20 cations) than the comparable trend in olivine-bearing ANG melt rocks (maximum Al content = 0.12 cations), further evidence of more rapid crystallization in the olivine-free samples. Figure 4c shows the Ti/Al systematics for the IKFM samples. A comparison of figures 4a,b,c shows that the maximum initial Al content of low-Ca pyroxene in the most rapidly cooled samples decreases from 0.20 cations in olivine-free ANG, to 0.15 cations in subophitic/intergranular LKFM, to 0.12 cations in IKFM. This variation correlates with decreasing bulk rock Al content, indicating a compositional control preserved only in the initial pyroxene compositions of the most rapidly cooled samples and overprinted by distinctive cooling-rate variations.

[1] Naney M.T. et al. (1977) Lunar Science VIII, p. 717-719. [2] Vaniman D.T. and Papike J.J. (1978) Geophys. Res. Lett. 5, p. 429-432. [3] Curatorial Branch, JSC (1979) Lunar Highlands Newsletter vol. 1, no. 2. [4] Walker D. et al. (1972) Proc. Lunar Sci. Conf. 3rd, p. 797-817. [5] Irving A.J. (1977) Proc. Lunar Sci. Conf. 8th, p. 2433-2448. [6] Roedder E. and Emslie R.F. (1970) Contrib. Mineral. Petrol. 29, p. 275-289. [7] Longhi J. et al. (1978) Geochim. Cosmochim. Acta 42, p. 1545-1558.

Mineralogy, Highland Melt rocks

D.Vaniman

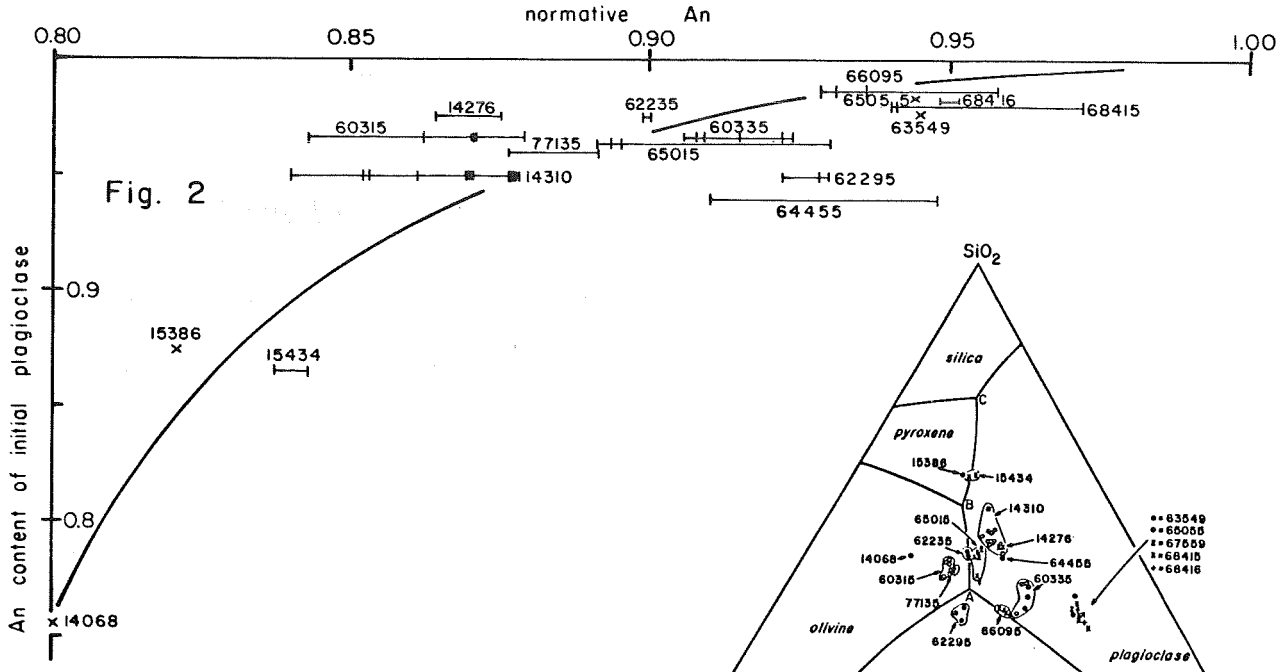

Fig. 2

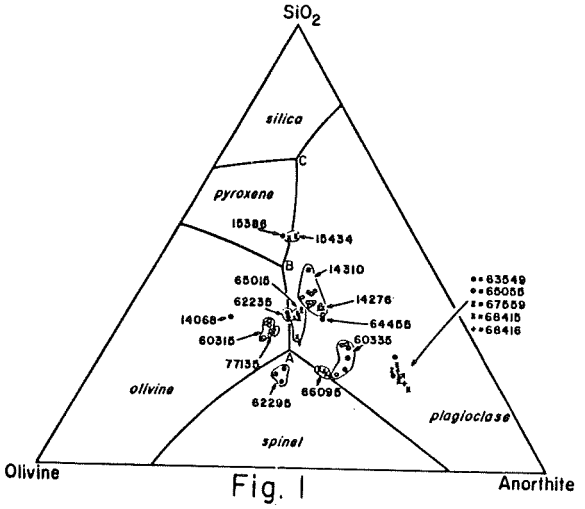

Fig. 1

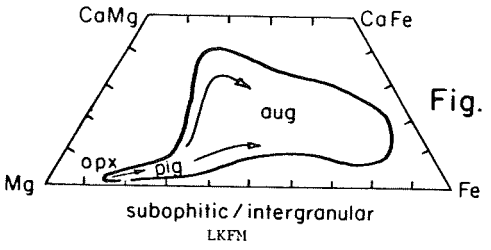

Fig. 3

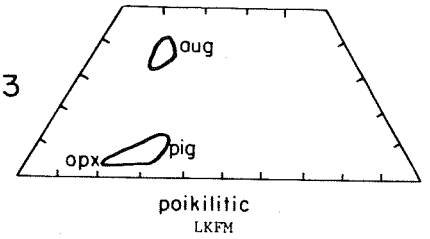

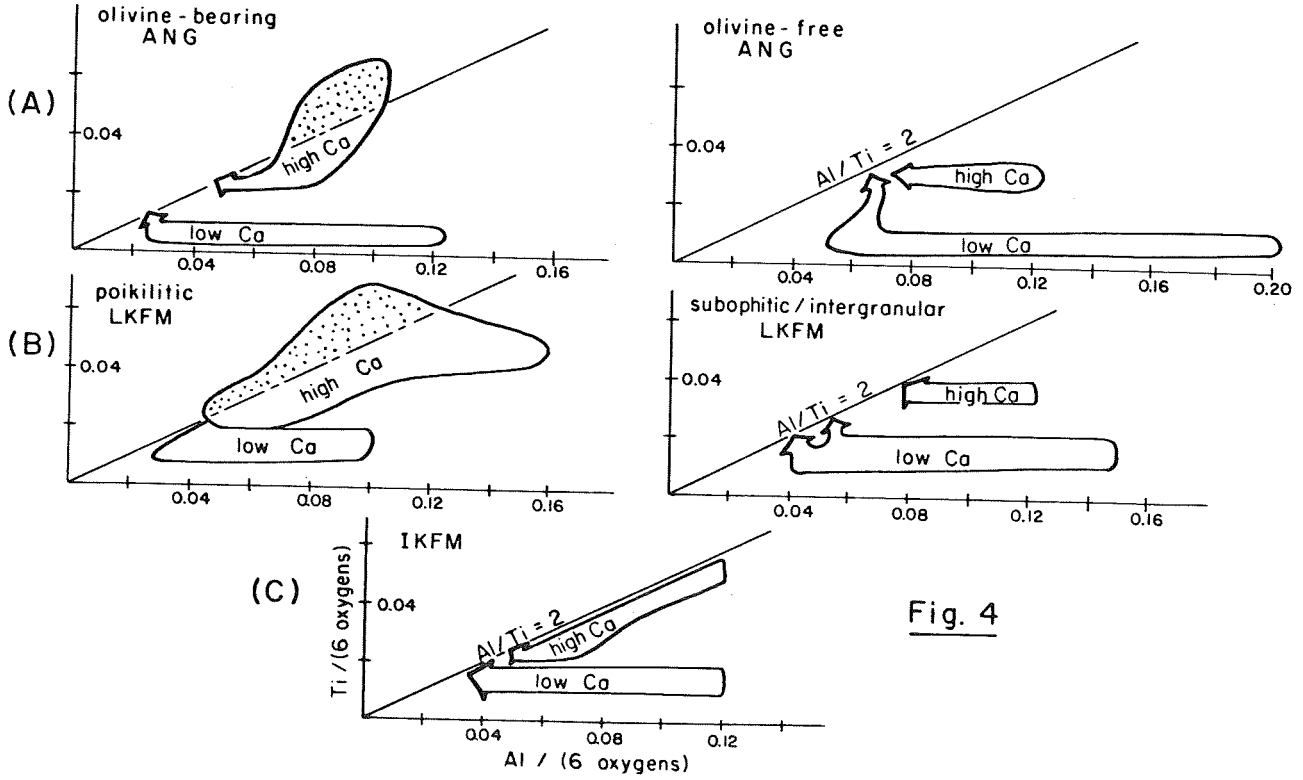

Fig. 4

THE LUNAR MAGMA OCEAN REVISITED

D. Walker, Hoffman Laboratory, Harvard University, Cambridge, Mass. 02138

The concept that the outer regions of the moon were molten penecontemporaneously with, and perhaps as a consequence of, lunar formation has proven to be a remarkably durable theme in lunar sample studies. This concept was originally inspired by the discovery of anorthositic samples associated with the lunar highlands, and the realization that the roughly isostatically compensated topographic contrast between mare and highlands was consistent with a considerable thickness of anorthosite in the highlands (1,2). To form the requisite amount of anorthosite as a globe-encircling flotation product requires an ocean of magma. The durability of the magma ocean model, with its floating and sinking cumulate solidification products, is a consequence of the model's ability to provide a broad outline for understanding such lunar characteristics as the mare/highlands contrast and the early lunar separation of complementary chemical reservoirs subsequently tapped by Fra Mauro and mare volcanism (3).

The magma ocean has become firmly entrenched in lunar thought. Indeed, the popularity of the model has spilled into terrestrial petrogenesis (4). For the infered terrestrial magma ocean, the principal ambition has been to discover some trace of the solidification products which are either absent or unrecognized. However in the wake of enthusiasm over the magma ocean model, minor inconsistencies in the model bob up from time to time. A number of anorthositic norite highlands samples do not possess the positive Eu anomaly (5-9) which might be expected of material supposed to be complementary to mare basalt source regions (10). Primordial Rb/Sr ages have been obtained on the dunite and troctolite samples (11,12) most likely to be direct magma ocean solidification products of any lunar samples recovered. This is difficult to understand if these rocks were in fact crystallized from a deep ocean which took $\sim$200 my to solidify, much less reach isotopic closure. (Note however the discrepancy of the Nd/Sm age of the troctolite which is much less primitive (13).) Seismic evidence (14) and inspection of basin-rim ejecta (15,16) are convergent in being consistent with a lunar crust composed of a large fraction of noritic or low-K Fra Mauro material rather than anorthosite or anorthositic norite. If the lunar crust is largely noritic or low-K Fra Mauro in composition, then the original incentive for calling on a lunar magma ocean disappears as no anorthositic layer of global proportions need be accounted for.

From the perspective of 10 years of lunar sample research, three questions may profitably be asked to help focus the objectives of the reinspection of lunar highlands petrogenesis now in progress. (A) What is the best estimate of the lunar highlands crust composition, or is it too heterogeneous to make a meaningful estimate? (B) Is the magma ocean model a necessary consequence of, or even consistent with, our present understanding of the highlands rock types? In order to answer this question we must ask the third question: (C) What rock types do we expect as products of the solidification of a magma ocean?

Magma oceanography has become a subdiscipline of lunar science which endeavors to answer this third question. Unfortunately this cottage industry has been too productive and we have more answers than oceans. (1-3, 17-29). Early attempts to model the solidification products of a magma ocean leaned heavily on sample constraints and were subsumed in later models. A common feature of all the models is feldspathic upper and mafic lower cumulate horizons. The plethora of postulated solidification

MAGMA OCEAN REVISITED

D. Walker

products differ in the details of the distribution and constitution of these horizons. The diversity of models stems in part from the range of ocean compositions selected. However an even more varied range of solidification products depending on the groundrules chosen for the solidification and differentiation process may be encountered for any particular ocean composition. This artificial diversity results from the various treatments of the boundary layer at the top of the solidifying ocean. Is there a crust? How rapidly does it form? What is the mode of heat transport in the ocean just beneath the crust? Depending on the manner in which the boundary layer is treated, the solidification products may range from largely undifferentiated (21) to intricately and discretely layered series of cumulates (29). Consequently the dynamics of heat and mass transfer at the top of a magma ocean must be understood before meaningful comparisons of models and rocks can be made. This aspect of magma oceanography seems to have received no satisfactory treatment at the present time.

References: (1) Wood et al. (1970) Proc. Apollo 11 Lunar Sci. Conf., p. 965-988. (2) Smith et al. (1970) ibid., p. 897-925. (3) Taylor & Jakes (1974) Proc. Lunar Sci. Conf. 5th, p.1287-1305. (4) Goles & Seymour (1978) EOS,59, p. 1214. (5) Haskin et al. (1973) Proc. Lunar Sci. Conf. 4th, p. 1275-1296. (6) Hubbard et al. (1973) ibid., p.1297-1312. (7) Brunfelt et al. (1973) ibid., p. 1209-1218. (8) Laul & Schmitt (1973) ibid., p. 1349-1367. (9) Philpotts et al. (1973) ibid., p. 1427-1436. (10) Wakita & Schmitt (1970) Science, 170, p. 969-974. (11) Papanastassiou & Wasserburg (1975) Proc. Lunar Sci. Conf. 6th, p. 1467-1489. (12) Papanastassiou & Wasserburg (1976) Proc. Lunar Sci. Conf. 7th, p. 2035-2054. (13) Lugmair et al. (1976) ibid., p. 2009-2033. (14) Liebermann & Ringwood (1976) Lunar Science VII, p.489-491. (15) Ryder & Wood (1977) Proc. Lunar Sci. Conf. 8th, p. 655-688. (16) Charette et al. (1977) ibid., p. 1049-1061. (17) Hodges & Kushiro (1974) Proc. Lunar Sci. Conf. 5th, p. 505-520. (18) Hubbard & Minear (1975) Proc. Lunar Sci. Conf. 6th, p. 1057-1085. (19) Taylor & Bence (1975) ibid., p. 1121-1141. (20) Hollister (1975) ibid., p.1159-1178. (21) Walker et al. (1975) ibid., p.1103-1120. (22) Wood (1975) ibid., p. 1087-1102. (23) Drake (1976) Geochem. Cosmochim. Acta, 40, p. 401-411. (24) Longhi (1977) Proc. Lunar Sci. Conf. 8th, p. 601-621. (25) Kesson & Ringwood (1977) ibid., p. 411-431. (26) Herbert et al. (1978) Proc. Lunar Sci. Conf. 9th, p. 249-262. (27) Minear & Fletcher (1978) ibid., p. 263-283. (28) Longhi & Boudreau (1979) Proc. Lunar Sci. Conf. 10th, in press. (29) Warren & Wasson (1979) ibid.

MAJOR AND TRACE ELEMENT SYSTEMATICS OF LUNAR HIGHLAND SAMPLES.

Heinrich Wänke, Gerlind Dreibus and Herbert Palme
Max-Planck-Institut für Chemie, Abtlg. Kosmochemie, 65 Mainz, F.R.Germany

Lunar highland samples are generally thought to be mechanical mixtures of components of highly different origin: a.) An anorthositic component; b.) Residual liquid from early lunar differentiation processes. Since the two components are not sufficient to explain the major element chemistry of highland samples a c.) Mg-rich component is required. This Mg-rich component can only be explained as a very primitive trapped liquid[1)] or as primary material which was either added to the moon after a solid crust had already formed or which somehow has escaped any larger fractionation processes[1-3)]; d.) The KREEP-component, rich in incompatible elements, does not significantly contribute to the major element chemistry of highland rocks.

For the compatible mafic elements lunar highland breccias represent probably the least fractionated lunar samples. Constant Fe/Sc and Mg/Cr ratios are observed which fall close to the ratios observed in the earth's mantle (Figs.1,2).

In the case of moderately volatile and volatile elements, evidences for mobilization and redistribution in lunar highland samples have been reported by a number of authors. Clearly both siderophile and non-siderophile elements were subject to such processes. However, the resulting element patterns cannot easily be explained in a general way. If we keep in mind the large differences in vapour pressures of the elements involved, it is understandable that no uniform enrichment patterns are observed in most samples. Highland samples highly enriched in elements like Zn, Cl, e.g. 65315 are not enriched in Na and K, while samples clearly enriched in Na and K such as 67095 show no enrichment of elements with considerably higher volatility.

The three element plot in Fig. 3 reveals the redistribution of Na. In lunar highland breccias the two feldspathic elements Na and Eu are in part contributed by the anorthositic component but also by the KREEP component, while La is almost exclusively supplied by the KREEP component. The Na/Eu ratio of 3500 extrapolated for La/Eu = 0 (KREEP-free samples) is identical to the Na/Eu ratios determined in lunar anorthosites. Since the plag./liquid partition coefficient for Eu is slightly larger than 1, one can calculate Eu concentrations of around 0.6 ppm for the parent liquid of the anorthosites. This is 4 x the concentration of Eu in the bulk moon[4)]. Crystallization of ol and px (both minerals do not take up Eu) are responsible for this enrichment. Since Na is also not taken up by ol and px to a large extent, the Na/Eu ratio of 3500 should closely reflect the Na/Eu ratio of the original magma ocean. Comparing the Na/Eu ratio of 3500 with the K/La ratio of 70 as observed for mare basalts as well as for KREEP-rich and KREEP-poor highland samples, we obtain a K/La ratio of 10.9 for the lunar magma ocean (La/Eu = chondritic).

Samples 60335 and 67095 which lie considerably above the correlation line in Fig. 3 show also very high values for the K/La ratio of 89 and 95, respectively, while sample 61016 has a K/La ratio of only 40. Hence, we have clear evidence for an enrichment of both K and Na in samples 60335 and 67095, which was caused by deposition of these elements and which must have been removed from other parts. Loss of Na and K is indeed evident for sample 61016.

As shown in Fig.4, F and Li are roughly correlated with each other. Both elements are mainly supplied by the KREEP component. Samples 60315, 65015 and 72395 which deviate most from the correlation line have obviously lost F by volatilization as indicated by the low Zn and Cl content of these samples.

Zn and Cl are also roughly correlated with each other in lunar highland breccias. However, this correlation improves considerably when plotting Cl/Li vs. Zn (Fig.5). Obviously, Cl is like Li mainly supplied by the KREEP component

and, hence, a constant Cl/Li ratio might be expected. The large variation of the Cl/Li ratio actually observed is the result of the redistribution of Cl which seems to be almost parallel to that of Zn. However, the correlation of the Cl/Li ratio with Zn can only be explained if we assume an originally constant Zn content of the samples in Fig. 5.

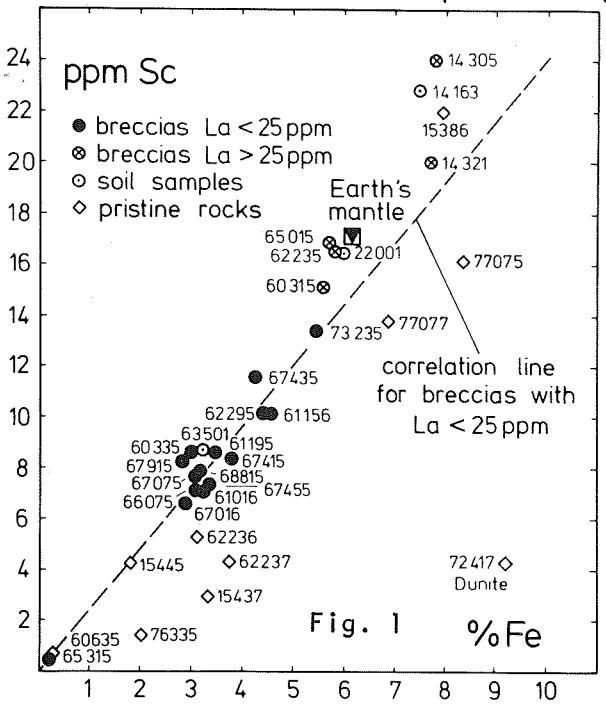

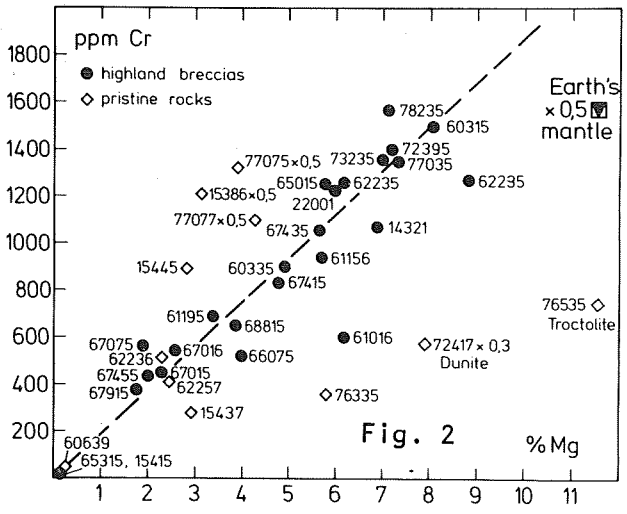

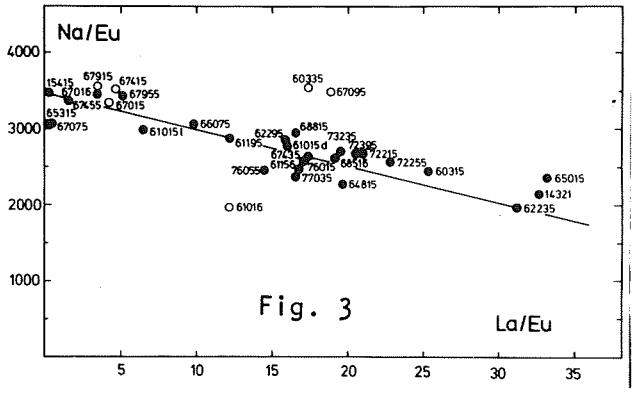

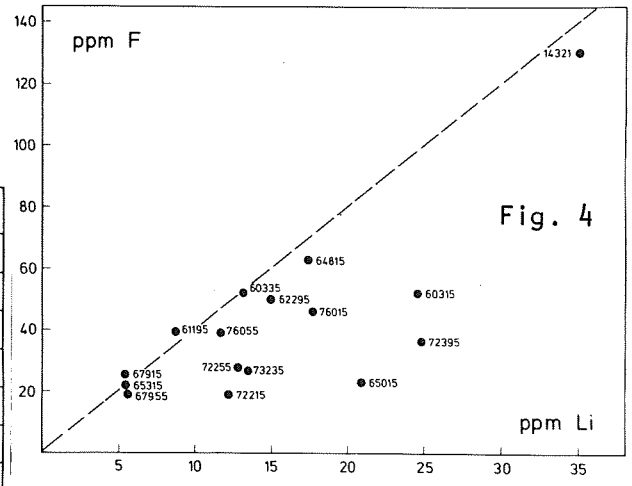

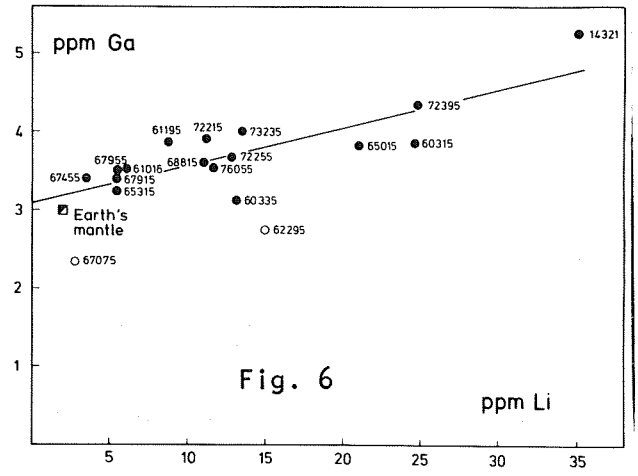

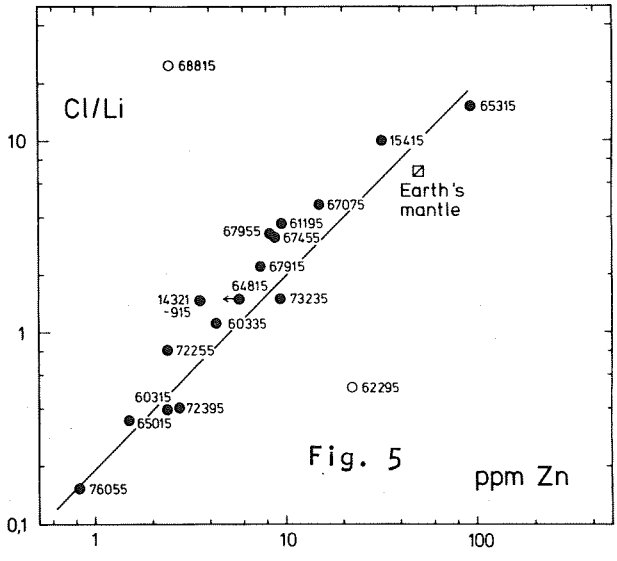

Data used in Figs. 1-6 from references (5-9) and from the Mainz laboratory.

MAJOR AND TRACE ELEMENT SYSTEMATICS

Wänke, H. et al.

Strikingly constant concentrations are also observed for Ga. Mare basalts have a mean Ga concentration of 3.88 ± 0.18 ppm, while for highland breccias a slight increase of Ga with the content of KREEP elements, e.g. with Li is found (Fig.6). For KREEP-free samples we extrapolate to a Ga value of 3.1ppm, nearly identical to the value of 3.0 ppm Ga obtained for the earth's mantle from studies of primitive ultramafic nodules.

Obviously, the general chemical similarity between the moon and the earth's mantle also includes moderately volatile elements like Ga. Elements of higher volatility are more depleted on the moon than on earth. Nevertheless, ratios among these more volatile elements are often similar on earth and moon (e.g. Na/K, Cl/Br, Cl/Zn). In addition, the Na/K and Cl/Br ratios are also close to the C1 values.

Another example for a chondritic element ratio of two volatile elements in lunar samples is the Pb/Br ratio. In Fig. 7 $Pb^{204}/U^{238}(\mu^{-1})$ is plotted against Br/U. A reference line corresponding to a Pb^{204}/Br weight ratio of about 52 is indicated. Most of the samples in Fig.7 have essentially the same Pb^{204}/Br ratio as carbonaceous chondrites.

Among the samples of Fig.7 having approximately chondritic Pb^{204}/Br ratios, there are samples of very different origin: a.) highland samples: soil samples 14163, 14259, 64501; highland rocks: KREEP basalt 15382, quartz-monzonite 15405 troctolite 76535, 4.2. b.y. old impactite 78155, aluminous basalt 14053 etc. b.) mare samples: basalts 75035, 15555, orange soil 74220, etc. In view of the rather uniform Pb^{204}/Br ratios in such diverse rock types there should be little doubt that the Pb^{204}/Br ratio of the bulk moon is within a factor of two chondritic.

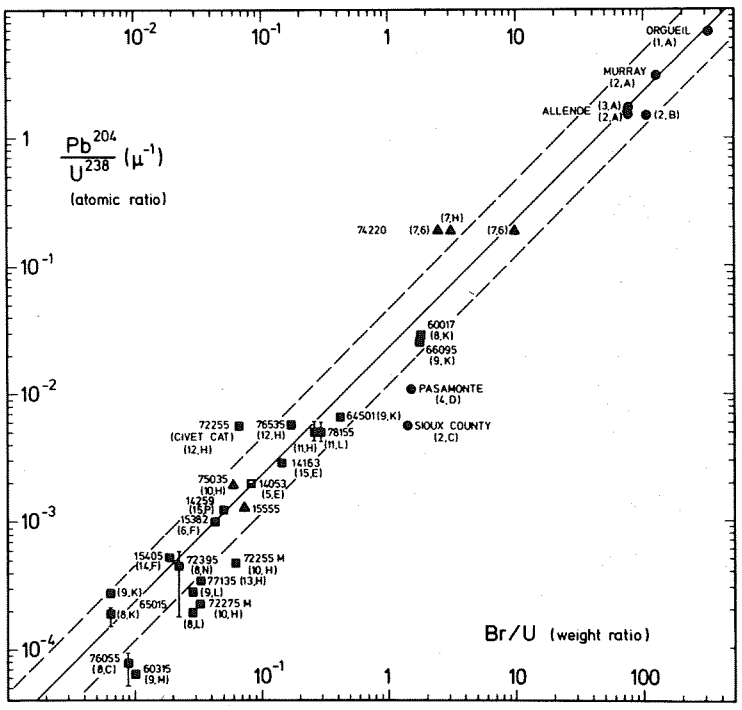

Fig.7: Sources for isotope data: 1) GCA 40,617. 2) Science 180,1279. 3) GCA 40, 635. 4) EPSL 37,1. 5)EPSL 14, 281. 6) Lunar Sci.VIII,750. 7) PLSC 5th,1480. 8) EPSL 22, 1. 9) PLSC 4th,1796. 10) PLSC 5th,1487. 11) PLSC 6th,1431. 12) PLSC 5th,1571. 13) EPSL 23, 445. 14) PLSC 7th,2107. 15) EPSL 13,457. Sources for Br data: A) unpubl.data,this lab. B) GCA 42,97. C) PLSC 9th,25. D) PLSC 8th,2191. E) PLSC 3rd, 1377. F) PLSC 7th,2403. G)PLSC 4th,1313. H) PLSC 5th,1703. K) PLSC 4th,1325. L) PLSC 7th,3479 M) PLSC 5th,1659. N) PLSC 5th, 1307. P) PLSC 3rd, 1989.

References: 1) Taylor S.R. and Bence A.E.(1975) PLSC 6th,1121. 2) Wänke H. et al.(1974) PLSC 5th,1307. 3) Wänke H. et al.(1977) PLSC 8th,2191. 4) Dreibus G. et al.(1977) PLSC 8th,211. 5) Laul J.C. and Schmitt R.A.(1975) PLSC 6th,1231. 6) Haskin L.A. et al.(1974) PLSC 5th,1213. 7) Winzer S.R.(1975) PLSC 6th,1219. 8) Laul J.C. and Schmitt R.A.(1973) PLSC 4th,1349. 9) Warren P.H. and Wasson J.T. (1978) PLSC 9th, 185.

AN INTRINSIC UNCERTAINTY IN DETERMINING THE CHEMICAL COMPOSITION OF THE EARLY LUNAR CRUST. J. L. Warner, NASA Johnson Space Center, Houston, TX 77058 and C. H. Simonds, Northrop Services, Inc., Houston, TX 77034

Attempts to decipher the petrogenetic history of the Moon require knowledge of the chemical composition of the upper part of the lunar crust in the time interval before the final bombardment. Two suites of samples are directly appropriate to this problem. Plutonic rocks (1) (coarse-grained members of Warren and Wasson's group of pristine rocks) presumably formed from cumulate processes between 4.55 and 4.4 Ga. Granulites (the feldspathic, granulitic impactites defined as a group by Warner et al. (2)) appear to have formed by thermal metamorphism of lithified impact debris in the time interval between 4.3 and 4.1 Ga (2,3). These rocks range from anorthosite to norite to rare dunite, but have a preferred composition near anorthositic troctolite and anorthositic norite. These samples are either observed to be or inferred to have been clasts in breccias. As such, it is instructive to consider the lithification of the host breccias in modifying the population of these ancient suites of lunar rocks.

Petrologic investigations of lunar and terrestrial impact breccias have demonstrated that the breccia lithification process progressivly digests clasts, and that clasts are digested in order of their melting temperature (e.g., 4). Thus glass-rich breccias that have been lithified by sintering or shock processes contain a broad range of clast compositions. In contrast, associated holocrystalline breccias with large fractions of impact-melt in their matrices contain a more restricted range of clast compositions characteristically refractory relative to the clast assemblage in the glass-bearing breccias. In the Station 6 boulder at Apollo 17 (4) the coarser-grained, impact-melt breccias with fewer clasts display a narrower range of refractory clast compositions than the adjacent, finer-grained, impact-melt breccias with more clasts. Similar relations are observed at terrestrial impact craters such as in the impact-melt breccia sheet at Manicouagan (5) where the remaining clasts are over 50% anorthosite although the target contains <5% anorthosite surrounded by gneisses.

Because most pre-final bombardment lunar samples were clasts in breccias, and because the breccia lithification process tends to bias clast populations toward more refractory assemblages, it is suggested that the observed suites of ancient lunar samples are a biased population. This means that although the observed clasts from the ancient lunar crust have a composition equivalent to anorthositic troctolite to anorthositic norite, the crustal composition before the final bombardment must have had less refractory constituents.

Because the suites of rocks that formed before the final bombardment do not yield a satisfactory early crustal composition, we look at the breccias that formed during the final bombardment to illuminate the problem. The clasts of these breccias are the anorthositic troctolites and anorthositic norites cited above. The matrix of these breccias are a distinctive basaltic component known as KREEP. KREEP is characteristically rich in lithophile trace elements with a distinctive LREE enriched abundance pattern (compared to chondritic meteorites). KREEP straddles the olivine-plagioclase cotectic, and is thus a low melting point component.

Breccia petrogenesis processes are moderately well understood as a result of the study of lunar and terrestrial breccias. Breccias form from a mechanical mixture of superheated melt and cold fragmental debris. Breccias now consist of a mixture of clasts and matrix. The matrix developed from melt and that fraction of the cold debris that had a low enough melting point so that it was melted and dissolved into the melt. The clasts developed from the cold

CHEMICAL COMPOSITION OF LUNAR CRUST

Warner, J.L.

debris less that fraction of cold debris that was dissolved into the melt. The fraction of the cold debris that acts as the low melting component is different for different volumes of melt and is a function of the proportion of melt in the volume considered, initial temperature of the target material, and composition of the target material.

The basaltic KREEP composition of the matrix of breccias that formed during the final bombardment is the complement of the enclosed clast's composition in that the matrix is the low melting component and is the very type component that is expected to be missing, or extracted, from the clasts. If breccia petrogenesis was the only consideration, the problem of determining the pre-final bombardment crustal composition would be relatively simple. The crustal composition would lie on a linear combination of the matrix and the clasts. Because impact debris is well mixed (4,6), any relatively large breccia sample with both clasts and matrix will yield the desired crustal composition. A breccia with a small amount of matrix would be essentially all clasts. A breccia with few clasts will have a matrix that represents the original melt plus cold debris. A bulk analysis of either of these extreme cases would yield the same crustal composition.

What if the pre-final bombardment lunar crust did not completely account for the provenance of the breccias that formed during the final bombardment? It is possible that the cataclysmic intensity of the final bombardment was an agent, direct or indirect, for the addition of a "new" type of material to the lunar surface. A "new" component might be: 1) from the impacting objects; or 2) due to endogenetic volcanism, perhaps triggered by the impacts; or 3) from a distinctive lithology excavated from depth by impacts.

If the "new" component is among the clasts, it could not be among the granulite clasts because they contain a clast-matrix structure and siderophile (meteorite) contamination indicating a prior history on the lunar surface. "New" material among the plutonic rock clasts could be accounted for by excavation of a plutonic lithology from depth by giant, basin-forming impacts.

If the "new" component is in the matrix, it is impossible to physically characterize: the "new" component would be a chemical additive in "solution" with an early crustal component. Such a chemical additive could have come from the excavation of KREEP material from depth; the KREEP perhaps originating in a pocket of material that formed from a late stage residual liquid generated during the fractional crystallization of the lunar crust. Such a chemical additive could also have originated as an endogenetic volcanic, perhaps formed during impact-triggered partial melting of the lower lunar crust. It is not clear that these cases can be distinguished: in a given system the chemical signatures of a late stage residual liquid and a first partial melt are similar.

The observed KREEP composition of breccia matrices could be accounted for if the matrices contain "new" material. This is because the KREEP composition approximates the composition that is expected for either a partial melt of the lower lunar crust or for a late stage residual liquid from the crystallization of the lunar crust. But the 4.4-4.2 Ga model ages for KREEP (7) dictate that at least some of the KREEP component material formed 100's of million of years before the final bombardment. The hypothesis that KREEP is exclusively a "new" component must be wrong.

The KREEP matrix composition of breccia matrices may also be accounted for utilizing our understanding of processes of breccia lithification. Both the superheated melt and cold fragmental debris that were mixed to form the breccia each had a bulk composition that approximated KREEP. During lithification, the low melting point fragments were resorbed into the melt, thus changing the melt's composition in a direction away from the remaining clasts

CHEMICAL COMPOSITION OF LUNAR CRUST

Warner, J.L.

(i.e., the melt becomes more KREEPy). The lack of KREEP material in the granulite clasts that formed before the final bombardment is due to a systematic biasing of the granulite compositions by breccia lithification processes.

There does not appear to be a scheme based on rock texture, mineral chemistry, or bulk chemistry that can adequately distinguish the various possibilities: (i) there is no "new" component present in the breccias and the breccias can yield an accurate composition for the early lunar crust, (ii) a "new" component is present among the plutonic rock clasts, (iii) a "new" component is present as a chemical additive to the matrix and the "new" component originated by endogenetic volcanism, and (iv) a "new" component is present as a chemical additive in the matrix and the "new" component originated by excavation of a lithology from depth. It is possible that there is an intrinsic uncertainity in accounting for the chemical composition of the lunar breccias, and hence in determining the chemical composition of the pre-final bombardment lunar crust?

References Cited

(1) Warner and Bickel (1978) Am. Mineralog., 63, 1010-1015.
Warren and Wasson (1977) Proc. Lunar Sci. Conf. 8th, 2215-2235.
_____(1978) Proc. Lunar Planet. Sci. Conf. 9th, 185-217.
_____(1979) Proc. Lunar Planet. Sci. Conf. 10th, in press.
(2) Warner et al. (1977) Proc. Lunar Sci. Conf. 8th, 2051-2066.
(3) Oberli et al. (1979) Lunar Planet. Sci. X, 940-942.
(4) Simonds et al. (1976) Am. Mineralog., 61, 569-577.
_____(1976) Proc. Lunar Sci. Conf. 7th, 2509-2528.
(5) _____ (1978) J. Geophys. Res., 83, 2773-2788.
(6) Kieffer and Simonds (1980) Rev. Geophys. Space Phys., in press.
(7) Nyquist et al. (1977) Phys. Chem. Earth, 10, 103-142.

PETROLOGY OF 60035, A POLYLITHOLOGIC ANT BRECCIA. R. D. Warner, G. J. Taylor, and K. Keil, Dept. of Geology and Institute of Meteoritics, Univ. of New Mexico, Albuquerque, NM 87131

Rock 60035 is a 1052 g sample that was collected in the LM/ALSEP area of the Apollo 16 landing site. It was originally set aside as a posterity rock and has only recently been made available for study. Consequently, no previous work has been done. Macroscopically, 60035 is a whitish rock that is partly glass-coated. The glass coating is dark gray to black and covers about half the surface area. In addition, numerous thin, dark glass veins are visible in non-coated portions of the sample. The white material is coherent and appears mostly to be fine-grained, although a few larger crystals (of plagioclase) up to $\sim$ 1 mm can be seen. Small black specks are distributed uniformly throughout the rock, and some bright white clasts are discernible, but otherwise the sample is nondescript.

We were allocated six polished thin sections for study by optical microscopy and electron microprobe. They sampled the following materials: 60035,5 - glass surface coating and adjacent portion of the whitish rock; 60035,17; 60035,19; and 60035,21 - widely separated portions of the whitish rock; 60035,4 and 60035,6 - a number of small chips which had broken off from 60035. Petrographic examination of the thin sections reveals that 60035 is a completely crystalline (except for the glass coating and intrusive glass veins), polylithologic breccia. Although some clasts can be identified, for the most part the distinction between clasts and matrix is obscure. For this reason, we emphasize the different lithologies that are present, even though we cannot in many instances decipher whether they should be categorized as "clast" or as "matrix".

A common lithology which often occurs as clasts is anorthositic troctolite or troctolitic anorthosite with $\sim$ 70-80% plagioclase. This lithology is characterized by a more or less granoblastic texture, with equant to subequant plagioclase ($\sim$ 0.05 - 0.2 mm across, some larger) and olivine (mostly 0.05 - 0.1 mm across) grains and, occasionally, minor poikiloblastic low-Ca pyroxene grains. Typically, a number of grains are shocked, especially the larger plagioclases, portions of which have been cataclasized or exhibit undulose extinction. Although this lithology frequently occurs as identifiable clasts, this is not always the case, so that in certain areas it grades imperceptibly into the surrounding rock.

A second lithology which is more abundant than the above, but less commonly occurs as identifiable clasts, is anorthositic norite/norite. This lithology constitutes the major portion of the breccia. In general, it is finer-grained, less feldspathic, and much more pyroxene-rich than the anorthositic troctolite/troctolite anorthosite lithology described above. Pyroxene (mostly low-Ca) has a spongy, poikiloblastic habit. Plagioclase occurs as small rounded grains enclosed by pyroxene, and as larger (several tenths of a mm long), equant to subequant crystals. Olivine is less abundant than pyroxene, and occurs mostly as small, equant to subequant grains. Some textural variation can be seen among different portions of the rock: e.g., the above lithology is slightly coarser-grained and somewhat more annealed in 60035,19 than in corresponding areas of 60035,17 and 60035,21. Clasts of anorthositic norite are occasionally visible. They tend to be noticeably more feldspathic than the surrounding noritic rock, and are characterized by subequant plagioclase and spongy, poikiloblastic pyroxene (mostly low-Ca) grains, and often contain minor amounts of olivine.

An interesting lithology which occurs in 60035,21 is granular troctolite. It is exposed over an $\sim$ 4 by 8 mm area at one edge of the thin section. Although presumably a clast, the contact between it and the

PETROLOGY OF 60035

Warner, R. D. et al.

adjacent rock is obscure. The texture of the troctolite is variable. One side of the clast consists of equigranular olivine (∿ 50%) and plagioclase (∿ 50%) grains 0.05 - 0.25 mm across. The middle portion of the clast is more plagioclase rich (≥ 60%), and contains some larger plagioclases, many of which are partly crushed and show undulose extinction, and an ∿ 0.8 mm subequant olivine. The other side contains more low-Ca pyroxene than olivine, and is finer-grained (e.g., low-Ca pyroxene grains are mostly < 0.05 mm across). The most notable feature of the troctolite is the more magnesian composition of its mafics compared to mafics elsewhere in the rock (see below).

We have identified several other lithologies in 60035. One of the chips broken off from the rock is a cataclastic anorthosite. It is nearly 100% plagioclast and consists of angular, shocked crystals up to ∿ 0.8 mm long surrounded by zones of very finely crushed material. Another broken-off piece is a recrystallized noritic anorthosite. Its texture approaches being granoblastic (e.g., some ∿ 120° triple junctions are present). Plagioclase crystals vary from < 0.05 to ∿ 0.7 mm in size; the larger grains are partly mosaicized. Minor interstitial mafics are present, mostly low-Ca pyroxene and some high-Ca pyroxene. Finally, several areas in the rock consist predominantly of fine-grained, lathy plagioclase, and thus appear to have crystallized from a plagioclase-rich melt. In addition to the lithologies described above, 60035 also contains identifiable mineral clasts. Most are shocked plagioclase crystals, some of which exceed 1 mm in size. Also present are a few, < 1 mm, isolated olivine mineral clasts.

Petrographic study of 60035,5 shows that the glass surface coating is highly vesicular and consists of subparallel bundles of feldspar crystallites separated by cryptocrystalline mesostasis. Locally, the texture is intersertal. The glass coating contains isolated mineral relics (mostly plagioclase). The transition between the glass and the underlying breccia occurs over a distance of < 0.5 mm. An average of three 100 μm diameter beam spots gave the following composition for the glass coating (in wt.%): SiO_2, 44.3; TiO_2, 0.29; Al_2O_3, 29.4; Cr_2O_3, 0.12; FeO, 5.1; MnO, 0.04; MgO, 5.7; CaO, 15.8; Na_2O, 0.25; K_2O, 0.06; and P_2O_5, 0.01. We have not as yet analyzed any of the glass veins which intrude 60035.

We have made a preliminary survey of mineral compositions in 60035. Plagioclase ranges from An_{91} to An_{98}. There appears to be little systematic difference in composition among the various lithologies, except that grains in the recrystallized noritic anorthosite chip tend to be the most calcic (An_{97-98}). Mafic mineral compositions are summarized in Fig. 1. For the most part, olivine ranges Fo_{76-82}, low-Ca pyroxene, $En_{75-82}Fs_{16-21}Wo_{3-6}$, and high-Ca pyroxene, $En_{46-52}Fs_{9-11}Wo_{37-45}$ (some of the variation in Wo may be analytical scatter due to small grain sizes). Some systematic differences emerge. These can be between subsamples: e.g., mafics in 60035,17 tend to be several mol % more Mg-rich than in 60035,19. Two lithologies have distinctly different mineral compositions. These are the noritic anorthosite chip (60035,4, B), which contains more Fe-rich mafics (low-Ca pyroxene ∿ $En_{52}Fs_{44}Wo_4$ and high-Ca pyroxene ∿ $En_{37}Fs_{20}Wo_{43}$), and the granular troctolite in 60035,21, which contains very Mg-rich mafics (olivine ∿ Fo_{88} and low-Ca pyroxene ∿ $En_{86}Fs_{11}Wo_3$). Metal compositions fall near the meteoritic range (1). Most grains are low in Ni (∿ 6 wt.%) and Co (∿ 0.8 wt.%), but in the granular troctolite the metal is of high-Ni (36-51 wt.%), low-Co (1.2 - 1.9 wt.%) composition.

Our preliminary petrologic study of 60035 leads us to conclude that the rock is a polylithologic ANT breccia and that the textures and mineral compositions in it are largely inherited from its ANT precursors. Clearly,

PETROLOGY OF 60035

Warner, R. D. et al.

the cataclastic anorthosite lithology, the large shocked plagioclase mineral clasts, and the plagioclase-rich melt areas attest to the fact that 60035 cannot have undergone prolonged annealing. Consequently, those lithologies such as anorthositic troctolite/troctolitic anorthosite and recrystallized noritic anorthosite, which have annealed textures, must have been annealed prior to their incorporation in 60035. The distinctive mafic mineral compositions shown by the granular troctolite in 60035,21 and the recrystallized noritic anorthosite (60035,4, B) imply that significant equilibration of mineral compositions has not occurred since consolidation of 60035. The lithologies we have identified all belong to the ANT-suite of rocks. None have preserved a pristine texture; however, the granular troctolite and recrystallized noritic anorthosite possibly have retained their original mineral compositions. The two most abundant lithologies - anorthositic troctolite/troctolitic anorthositic and anorthositie norite/-norite - probably are mixtures that have resulted from reworking of anorthosite and troctolite on the one hand and anorthosite and norite on the other. The anorthositic troctolite/troctolitic anorthosite lithology appears to be equivalent to feldspathic granulitic impactite (2).

The existence of two populations of metal compositions (high-Ni in granular troctolite lithology and low-Ni elsewhere in 60035) has important implications for the identification of meteorite groups in lunar samples (e.g., 3). If the two metal populations correspond to two distinct meteoritic components, it is possible that siderophile element abundances measured on a bulk sample of 60035 could yield a "false" composition that is an average of the two meteoritic components. (1) Goldstein, J. I. and Yakowitz, H. (1971) Proc. Lunar Sci. Conf. 2nd, p. 177-191. (2) Warner, J. L. et al. (1977) Proc. Lunar Sci. Conf. 8th, p. 2051-2066. (3) Ganapathy, R. et al. (1973) Proc. Lunar Sci. Conf. 4th, p. 1239-1261.

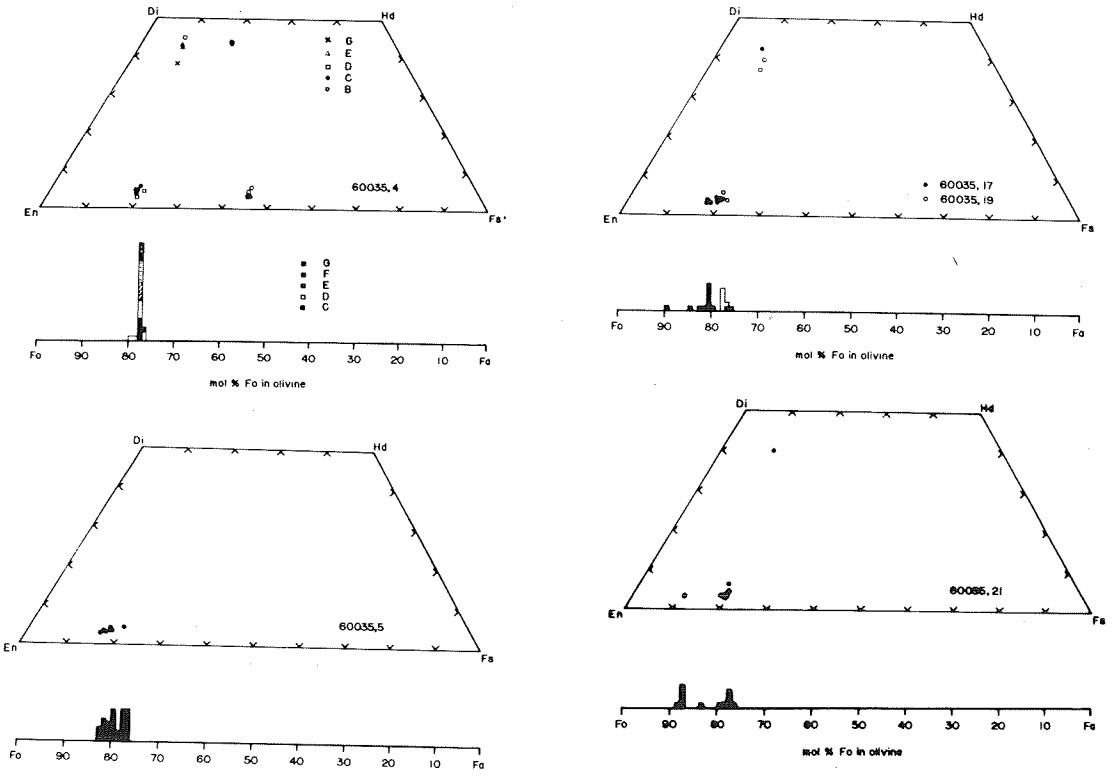

Fig.1. Pyroxene/olivine compositions.

CERTAIN PRISTINE NONMARE ROCKS FORMED AS CUMULATES FROM THE MAGMA OCEAN (BUT MANY OTHERS DID NOT). Paul H. Warren, Institute of Geophysics and Planetary Physics, University of California, Los Angeles, CA 90024, USA

The notion of a primordial moon-wide magma ocean appears to have gained general acceptance as the most likely explanation for the plagioclase enrichment in the nonmare crust. Curiously, almost no one has heretofore attempted to ascertain which (if any) pristine nonmare rocks, other than KREEPy ones, are not cumulates from the magma ocean (the "pristine" concept is discussed in [1] and [2]; since non-pristine rocks are, by definition, not endogenously igneous, they cannot be cumulates.

Several recent studies [3;4] recognize that anorthositic norite or "highlands basalt", the most abundant rock type among the non-pristine anorthosite-norite-troctolite (ANT) "suite", is virtually absent among pristine rocks [1; 3]. But some workers continue to "presume" that orthocumulate anorthositic norites formed the bulk of the primary crust, as plagioclase floated and entrapped noritic ocean-magma [5]; and even those who recognize the importance of pristine rocks make the unjustified assumption, either implicity [3], or explicitly [4], that all pristine nonmare rocks formed out of the magma ocean.

As was first noted by [6], on a plot of mean An in plagioclase vs. mean mg (molar Mg/(Mg+Fe) in mafic minerals, pristine rocks clearly divide into two distinct groups, "ferroan" anorthosites (FAs) and "Mg-rich plutonic" rocks (MGRPRs) (Fig. 1 is an updated version of the same diagram). The fact that the "trends" of the two groups have distinctly different slopes [6], and the persistence [1;2;7] of a wide gap between the most "Mg-rich" FA and the most "ferroan" MGRPR, indicate that the two groups are not co-genetic.

If the MGRPRs formed from the magma ocean, the process obviously seldom involved flotation [8]: Fig. 2, considered together with Fig. 1, summarizes buoyancy characteristics. On the other hand, the FAs are hardly likely to have sunk. It might be argued that the MGRPRs represent atypically mafic-rich "rhythmic" flotation cumulate layers, were it not for the fact of the gap between the groups on Fig. 1. The gap is also hard to reconcile with models in which the MGRPRs formed when cumulus mafics sank from the same magma that was forming the FAs by floating cumulus plagioclase [4;4]. In such a case, the existence of a wide gap would only be possible if the floated cumulates never incorporated any cumulus mafics, whilst the sunken cumulates formed equally devoid of cumulus plagioclase. It is hard to believe that crystal segregation processes could ever be that efficient. Moreover, we know that at least most of the mafics in the FAs are primary cumulus crystals. None of the most mafic-rich pristine FAs (15437, 62236 and 62237 [10]) have the high levels of incompatible element concentrations expected from high contents of "trapped liquid", even though some that are intermediate in mafic content (as pristine FAs go), such as the 67455 clasts with extremely Fe-rich "interstitial" pigeonite and olivine [11], do have high incompatible levels (Fig. 3). Another, perhaps more obvious, contradiction of the "trapped liquid" hypothesis is that no single type of liquid would engender the range of mafic phases found in pristine FAs [12] (calcic pyroxene in some, olivine in others, and so on).

The above evidence strongly indicates that the FAs formed as flotation cumulates, probably over the primordial magma ocean; that few, if any, of the MGRPRs formed as flotation cumulates; and that few, if any, of the MGRPRs

EXTRAOCEANIC PRISTINE NONMARE ROCKS

Paul H. Warren

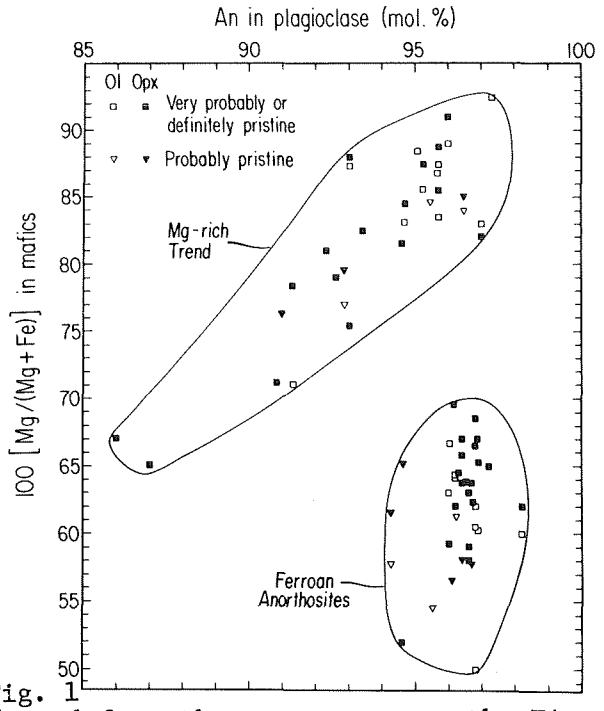

Fig. 1

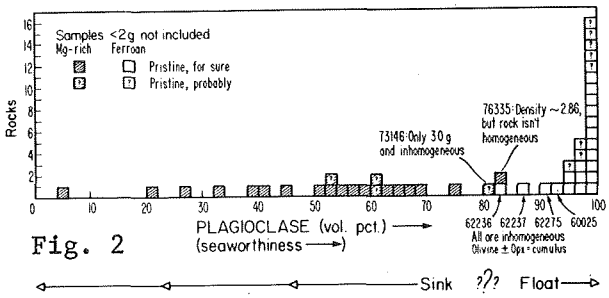

Fig. 2

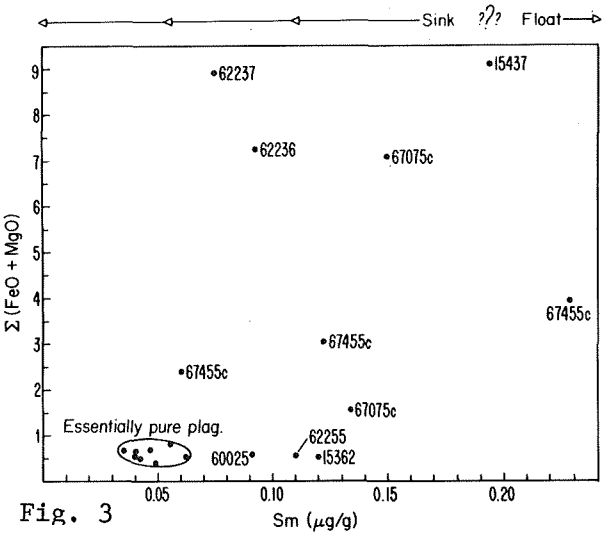

Fig. 3

formed from the same magma as the FAs. This view receives puissant support from Rb-Sr isotopic systematics. The (weighted) mean initial $^{87}Sr/^{86}Sr$ ratio of the five pristine FAs (15415, 60015, 60025, 61016c and 64423,13,1) analyzed (a total of 20 times) to date, after correction for interlaboratory bias [13], is 0.698925, with σ_μ (the 68% confidence error estimate) equal to 0.000005. The analogous values for the only four MGRPRs for which data exist (72255c, 72417, 76535 and 77215) are 0.699022 and 0.000010 [13; 14]. These data unambigously indicate that if both the FAs and the MGRPRs formed out of one magma, the FAs have to be older. In fact, even if they did not form from the same magma, for the FAs to be as young or younger than the MGRPRs, they would have to have been produced from magma which had always been in an extremely Rb-poor part of the moon; and yet, such a part of the moon would probably been similarly depleted in K, Th and U, which would make it unlikely to melt. The inescapable implication, that the MGRPRs formed later than the FAs, in turn confirms that the MGRPRs are not from the magma ocean, at least not from the magma ocean per se, because the fractional crystallization process could not possibly have produced the type of high-mg magmas that were parental to the MGRPRs, out of the type of low-mg magmas that were parental to the FAs.

The "rockberg" hypothesis [15;4] for the formation of the crust says that a compositional gradient may have developed at the top of the magma ocean, thus enabling a thick crust of feldspathic rock to form early in the evolution of the magma ocean. Since the theoretical modus operandi for crustal growth (repeated foundering of the crust, followed by rapid sinking of dense mafic crystals, leaving the magma locally rich in Ca and Al) seems viable only so long as the crust continues to founder, it seems logically inconsistent to suppose that a significant fraction of the pristine nonmare rocks were formed as parts of rockbergs. The main portion of the crust probably formed only after the magma ocean had crystallized to the point of plagioclase saturation [16]. By that point, the mg of the ocean had been substantially lowered. The conclusion that the only pristine nonmare rocks that appear to be magma ocean cumulates

Paul H. Warren

are all "ferroan" is consistent with the [16] model, and inconsistent with the rockberg hypothesis. The fact that FAs are preponderant among pristine rocks from Apollo 16, the only Apollo site remote from all basins whereas MGRPRs are preponderant among pristine nonmare rocks from Apollo 15 and Apollo 17, implies that the surficial part of the original crust was mainly FA, while in the deeper levels excavated by basin-forming events MGRPRs were abundant [1]. This provides further evidence that the MGRPRs are not from the earliest, "rockberg" crust; for if they were, they would be stratigraphically high, not low.

If they are not magma ocean cumulates, what then are the MGRPRs? We have established that they are (at least, for the most part) conventional sunken cumulates. Their trend on Fig. 1 is also conventional (i.e., it has a positive slope). The simplest explanation is that they formed in layered intrusions similar to those on the Earth. It isn't surprising, in this context, that these intrusions were intruded mainly below the earlier FA crust. Their parental magmas were denser than the FAs, just as the magma ocean had been. It would be surprising, though, if the parental magmas did not assimilate some plagioclase from the FAs, and some urKREEP (defined as the incompatible element rich residuum of the magma ocean, thought to have collected between the crust and the mantle [17]). It is interesting to note that the parental magmas of the MGRPRs are inferred to have had KREEP-like patterns of light to heavy REE enrichments, despite their otherwise primitive nature [4].

REFERENCES: (1) Warren P.H. and Wasson J.T. (1977) Proc. Lunar Sci. Conf. 8th, 2215-2235; (2) Warren P.H. and Wasson J.T. (1979) Proc. Lunar Sci. Conf. 10th, in press; (3) Minear J.W. and Fletcher C.R. (1978) Proc. Lunar Planet. Sci. Conf. 9th, 263-283; (4) Longhi J. and Boudreau A.E. (1979) Proc. Lunar Planet. Sci. Conf. 10th, in press; (5) Delano J.W. and Ringwood A.E. (1978) Proc. Lunar Planet. Sci. Conf. 9th, 111-159; (6) Warner J.L., Simonds C.H. and Phinney W.C. (1976) Lunar Science VII, 915-917; (7) Bickel C.E. and Warner J.L. (1978) Proc. Lunar Planet. Sci. Conf. 9th, 629-652; (8) Warren P.H., McEwing C.E., Afiatta-lab F. and Wasson J.T. (1978) Lunar Science IX, 1228-1230; (9) Wood J.A. (1975) Proc. Lunar Planet. Sci. Conf. 6th, 1087-1102; (10) Warren P.H. and Wasson (1978) Proc. Lunar Planet. Sci. Conf. 9th, 185-217; (11) Lindstrom M.M., Nava D.F., Londstrom D.J., Winzer S.R., Lum R.K.L., Schuhmann P.J., Schuhmann S. and Philpotts J.A. (1977) Proc. Lunar Planet. Sci. Conf. 8th, 2137-2151; (12) Norman M.D. and Ryder G. (1979) Proc. Lunar Planet Sci. Conf. 10th, in press; (13) Nyquist L.E. (1977) Phys. Chem. Earth 10, 103-142; (14) Compston W. and Gray C.M. (1974) In Interdisciplinary Studies of Samples from Boulder 1, Station 2, Apollo 17, Vol. 1 (J.A. Wood, ed.), Smithsonian Astrophysical Observatory, Cambridge, Mass.; (15) Herbert F., Drake M.J., Sonett C.P. and Wiskerchen (1977) Proc. Lunar Planet. Sci. Conf. 8th, 573-582; (16) Warren P.H. and Wasson J.T. (1979) Proc. Lunar Planet. Sci. Conf. 10th, in press; also in Papers Presented to the Conference on the Lunar Highlands Crust, this volume; (17) Warren P.H. and Wasson J.T. (1979) Rev. Geophys. Space Phys. 17, 73-88.

COMPARING FACTS ABOUT PRISTINE NONMARE ROCKS WITH THEORY ABOUT THE MAGMA OCEAN, TO CONSTRAIN THE BULK COMPOSITION OF THE MOON. Paul H. Warren and John T. Wasson, Institute of Geophysics and Planetary Physics, University of California, Los Angeles, CA 90024, USA

It is becoming increasingly clear that flotation of plagioclase over a global "ocean" of magma (1;2) is the most satisfactory mechanism to account for the extremely anorthositic nonmare crust. The details of the process remain controversial, but one point of general agreement is that the initial composition of the ocean was probably very close to the composition of the bulk moon.

Throughout the history of the magma ocean, and particularly during its earlier stages, crystallization must have taken place mainly along the bottom, because silicate liquidi are less steep in P-T coordinates than adiabats. The elevated pressures of the ocean's bottom probably caused the ocean to crystallize much more pyroxene (at the expense of olivine) than would be expected under 1 atm conditions (3). An important consequence of this is that plagioclase-olivine cumulates (troctolitic anorthosites) do not necessarily have to be products of an ocean with Ca/Si and Al/Si so high that no pyroxene crystallized until after plagioclase saturation occurred, as alleged by (4), (5), and (6), among others. In view of the downward revision of the lunar heat flow data (7), this removes the last major reason for believing the moon to be much richer in Ca, Al, U, Th, and other refractory elements than the silicate portions of ordinary chondrites.

Ordinary chondrites are, as their name implies, the most abundant type of planetary debris that hits the earth. There are several reasons for believing that the H-group ordinary chondrites and IAB chondrites both formed fairly close to 1 AU from the sun (8), which (prima facie) suggests that the bulk moon resembles these two chondrite types. The alternative that numerous researchers have extolled in the past, that the bulk moon is highly enriched in materials akin to the refractory-rich inclusions found in carbonaceous chondrites, is contradicted by the evidence from oxygen isotopes (9;3). To some degree the O-isotope data are consistent with a moon derived from CI carbonaceous chondrites, and Ringwood (10) has proposed this as the origin of the earth's mantle; but the composition he derived (by removing volatiles; sulfides; and siderophiles, including roughly half of the FeO, assigned to a model core) is quite similar to the silicate portion of an H chondrite, so we hardly need discriminate between his modified-CI model and our less complex ordinary chondrite (silicate portion) model. For the sake of brevity, we shall henceforth refer to these two types collectively as "chondritic" model compositions. Oxygen isotopic evidence is also not inconsistent with an enstatite-chondritic moon, but such a moon would have too little FeO to engender any even moderately ferroan materials (e.g., mare basalts), and too little Ca and Al to form the nonmare crust.

A magma ocean with an initial "chondritic" composition and a lunar pressure-depth gradient would probably crystallize in a quite predictable manner (3). In fact, the outcome of fractional crystallization in such a case is almost independent of the initial depth (D_i) involved, as far as the composition of the ocean at the point of first plagioclase crystallization is concerned (the D_i does affect the <u>path</u> to that outcome somewhat: the ratio of pyroxene to olivine in the pre-plagioclase cumulates might start out high and

COMPARING.....TO CONSTRAIN THE BULK COMPOSITION OF THE MOON

Paul H. Warren and John T. Wasson

end up only moderately high, or start out low and end up very high, depending on D_i; but the gross ratio of pyroxene to olivine in the total cumulates at the point where plagioclase begins crystallizing is nearly independent of D_i). Of course, this would not hold if, besides the stabilities, the compositions of crystallizing minerals were also functions of pressure. However, except for a slight effect on the Ca content of orthopyroxene, the olivine and orthopyroxene likely to crystallize from a "chondritic" ocean would be compositionally pressure independent.

The facility with which crystallization of "chondritic" magma oceans can be modeled up to the point of plagioclase saturation makes it possible to constrain the mg (mg=molar Mg/(Mg+Fe)) of the moon, provided we can identify among the pristine nonmare rocks those which formed from the ocean by flotation of plagioclase, and can estimate from their compositions the mg of the ocean at the time plagioclase first began to crystallize copiously. There can be little doubt that if any such petrogenetic process really took place, the rocks it produced are the ferroan anorthosites (see (11)). The mg values of the liquids out of which these rocks formed were apparently very low: estimates range from 0.3-0.4 for 60025 (12) to 0.14-0.34 for a set of 11 anorthosites (13). The best one can do is estimate these values, mainly because at least some of the Fe and Mg in some of the anorthosites must come from "trapped liquid", which is often difficult to detect, let alone quantify. It seems safe to say that the highest mg of any liquid which produced anorthosites was 0.4±1. Of course, those would be the first anorthosites; later, lower mg liquids were involved.

Even assuming a relatively Ca- and Al-rich initial composition for the ocean (e.g., GA''' (6)), it must have crystallized at least 50% of its mass as olivine and/or pyroxene (and/or minor spinel) before plagioclase saturation was reached. Because Mg/Fe is roughly 3.3-4.4 times greater in olivine and pyroxene than in liquid from which these minerals are crystallizing (14), the composition of the ocean at the point where the main part of the crust (i.e., the ferroan anorthosites) began to form must have been much different from its initial composition, not only in terms of higher Ca and Al concentrations, but also in terms of lower mg. Reasonably sophisticated, quantitative models of the crystallization of the magma ocean (3), which include pressure effects, probably could predict the "correct" mg value of the ocean at the time the anorthosites started to form to within 10 mole %, if the chosen initial composition for the ocean was "correct". This type of modeling predicts mg=0.18 for the ocean at the point of plagioclase formation if it started as the silicate portion of the H chondrite, but mg equals 0.67 if it started as the silicate portions of the IAB chondrites. It also predicts mg=0.43 using Ringwood's (10) "pyrolite", and mg=0.48 using his modified CI chondrite "model mantle", as starting compositions.

These results support Ringwood's theory that the moon was derived from the earth's mantle, but they are equally consistent with a model in which the moon consists of ordinary chondritic material, which lost siderophiles and volatiles during accretion of the moon from planetesimals in close prosimity to the earth (15). The ordinary chondritic hypothesis is consistent with the mg evidence assuming the planetesimals were either a mixture of H and IAB chondrites, or some equivalent type of "anomalous" intermediate chondritic material (the chondrites in terrestrial collections are probably only "a biased and incomplete selection of primitive solar system materials" (16). It is interesting to note that a hybrid intermediate between H and IAB chondrites could (with a slight amount of mass fractionation) also satisfy the oxygen isotope

constraint.

REFERENCES

(1) Wood, J.A., Kickey J.S., Marvin, U.B. and Powell, B.N. (1970), Proc. of the Apollo 11 Lunar Sci. Conf., p. 965-988.

(2) Smith, J.V., Anderson, A.T., Newton, R.C., Olsen, E.J., Wyllie, P.J., Crewe, A.V., Issacson, M.S., and Johnson, D. (1970), Proc. of the Apollo 11 Lunar Sci. Conf., p. 897-925.

(3) Warren, P.H., and Wasson, J.T., (1979a), Lunar Planet. Sci. X. p. 1304-1306; also Proc. Lunar Planet Sci. Conf. 10th, in press.

(4) Walker, D., Grove, T.L., Longhi, J., Stolper, E.M., and Hays, J.F. (1973) Earth Planet. Sci. Lett., 20, p. 325-336.

(5) Hodges, F.N., and Kushiro, I., (1974), Proc. Lunar Sci. Conf. 5th, P. 505-520.

(6) Longhi, J., (1978), Proc. Lunar Planet. Sci. Conf. 9th, p. 285-306.

(7) Langseth, M.G., Keihm, S.J., and Peters, K., (1976), Proc. Lunar Planet. Sci. Conf. 7th, p. 3143-3171.

(8) Wasson, J.T., (1977), In Comets Asteroids Meteorites: Interrelations, Evolution and Origin (A.H. Delsemme, ed.), Univ. Toledo, P. 551-559.

(9) Clayton, R.N., (1977), In Comets, Asteroids and Meteorites: Interrelations, Evolution and Origins (A.H. Delsemme, Ed.), The University of Toledo, p. 545-550.

(10) Ringwood, A.E., (1978), Composition and origin of the earth. Aust. Natl. Univ. Res. Sch. Ear. Sci. Publ., 1299, preprint.

(11) Warren, P.H., and Wasson, J.T., (1979b), In Papers Presented to the Conference on the Lunar Highlands Crust. This volume.

(12) Longhi, J., Walker, D., and Hays, J.F., (1976), Proc. Lunar Sci. Conf. 7th, p. 1281-1300.

(13) Hansen, E.C., Steele, I.M., and Smith, J.V., (1979), Proc. Lun. Planet. Sci. Conf. 10th, in press.

(14) Roeder, P.L., and Emslie, R.F., (1970), Contr. Mineral. Petrol., 29, p. 275-289.

(15) Wasson, J.T., and Warren, P.H., (1979), Lunar Planet. Sci. X, p. 1310-1312.

(16) Bild, R.W., and Wasson, J.T., (1977), Science, 197, p. 58-62.

SOLAR SYSTEM FORMATION AND HIGHLAND CRATERING. G. W. Wetherill, Department of Terrestrial Magnetism, Carnegie Institution of Washington, Washington, D.C. 20015

Until recently there has been little direct connection between the speculations of those concerned with solar system formation and the problems addressed by the working geologist. As a result of recent lunar, planetary, and meteoritic studies this is no longer the case. During the earliest history of the moon, and by plausible inference, the terrestrial planets as well, impact cratering was a major, and quite possibly the dominant geomorphological process. A number of suggestions have been made by various authors regarding the role this bombardment may have played in establishing the initial chemical, thermal, and tectonic boundary conditions for these planetary bodies. However, among other problems, the plausibility of these suggestions is limited by uncertainties regarding the immediately preceding events, viz. the processes by which these planets themselves were formed.

In some sense, the early bombardment history of the moon and planets must represent the "tail end of the accretion" of these planets. However, a statement as general as this does not adequately specify the magnitude, size or velocity distribution of the flux of impacting bodies, and it may be expected that various hypotheses of planetary formation, e.g. giant gaseous protoplanets (1, 2, 3) accumulation in a gaseous medium (4) or gas-free accumulation (5) will lead to differing predictions regarding these parameters. The role of residual planetesimals from the outermost solar system (6) is similarly obscure because of uncertainties regarding the formation of Uranus and Neptune. From the experimental and observational point of view, testing of these predictions will require a much more adequate understanding of such questions as the extent to which highland cratering represents a production or steady-state spectrum, the age, origin and uniqueness of characteristic highland rock types and the validity of alternative thermal and differentiation models for the early moon (e.g. complete melting, homogeneous magma ocean, heterogeneous melting). The cratering record to be associated with a particular variety of solar system formation, gas-free accumulation (5, 6, 7, 8), has been presented, without presuming the validity of this model of planetary formation. Subject to the assumption that the maximum size of the accumulating projectiles is limited by tidal disruption, this theory leads naturally to the general features of lunar cratering history, e.g. the combination of relatively long-lived ($\sim$150 m. y.) decay of early mare bombardment with abrupt termination of heavy bombardment at 3.9 b.y. This same approach leads to the possibility that at least some present-day sources of differentiated meteorites are residual terrestrial planetesimals implanted and stored in the inner asteroid belt (9). The observed anomalous size distribution of these asteroids (10) can be interpreted as a consequence of this mode of origin.

Whether or not all this really happened is of course not known. It is presented as an example of the strong coupling

SOLAR SYSTEM FORMATION AND HIGHLAND CRATERING

Wetherill, G. W.

between solar system formation, understanding of the lunar highlands, and the earliest history of the earth and terrestrial planets. Whether they like it or not, planetary cosmogonists and hard rock geologists are now bedfellows. (1) Kuiper, G. P. (1951) On the origin of the Solar System, Chapter 8 in Astrophysics, J. A. Hynek, ed., McGraw Hill, N.Y. (2) McCrea, W. H. (1960) The origin of the Solar System, Proc. Roy. Sci. London 256A, p. 245-266. (3) Cameron, A. G. W. (1978) Physics of the primitive solar accretion disk. The Moon and Planets 18, p. 5- . (4) Hayashi, C., Nakazawa, K., and Adachi, I. (1977) Long-term behavior of planetesimals and the formation of the planets, Publ. Astron. Soc. Japan 29, p. 163-196. (5) Safronov, V. S. (1969) Evolution of the protoplanetary cloud and formation of the Earth and Planets, Nauka, Moscow; translated for NASA and NSF by Israel Program for Scientific Translation NASA TT F-667, 1972. (6) Wetherill, G. W. (1975) Late heavy bombardment of the moon and terrestrial planets. Proc. Lunar Sci. Conf. 6th, p. 1539-1559. (7) Wetherill, G. W. (1976) The role of large bodies in the formation of the earth and moon. Proc. Lunar Sci. Conf 7th, p. 3245-3257. (8) Wetherill, G. W. (1977) Evolution of the earth's planetesimal swarm subsequent to the formation of the earth and moon, in Proc. Lunar Sci. Conf. 8th, p. 1-16. (9) Wetherill, G. W. and Williams, J. G. (1979) Origin of Differentiated Meteorites. In Origin and Distribution of the Elements, Second Symposium, L. H. Ahrens, ed., pp. 19-31. (10) Zellner, B. (1979) To be published in Asteroids, T. Gehrels, ed., Univ. of Arizona Press.

METEORITIC MATERIAL IN THE LUNAR HIGHLANDS: CLUES TO THE ACCRETION HISTORY OF THE MOON

Rainer Wolf and Edward Anders
Enrico Fermi Institute and Department of Chemistry
University of Chicago; Chicago, Illinois 60637

Highland breccias contain an ancient meteoritic component, judging from their enrichment in siderophiles (Ir, Re, Os, Ni, Pd, Au) relative to pristine highland rocks (Morgan *et al.*, 1972, 1974). From the proportions of siderophiles (primarily Ir/Au ratio), 8 discrete groups have been recognized (Gros *et al.*, 1976, Hertogen *et al.*, 1977). All are roughly "chondritic" in the sense that volatiles are slightly depleted relative to siderophiles (~0.1-0.5 x Cl), but only 2 of the 8 groups resemble present-day chondrites. Apparently they represent an extinct population of bodies that bombarded the Moon in the early stages of its history.

From the distribution of these groups over 7 landing sites (Janssens *et al.*, 1978), it appears that most are related to basins rather than craters, though at least one group (1H) is associated with a crater (Unnamed B at Apollo 16). Another group (7) compositionally resembles the bulk Moon (Ganapathy and Anders, 1974), and may represent mixed planetesimal debris from the final stages of the Moon's accretion.

A relative age scale of the meteoritic groups can be constructed from their textural relations (clasts vs. matrix) in breccias (Hertogen *et al.*, 1977). Surprisingly, the ages correlate with Ir/Au ratio, as expressed by group number, from 1LL (youngest) to 7 (oldest). This suggests that the most Moon-like, refractory-rich bodies fell first, and were superseded by progressively less Moon-like objects. This trend must obviously be checked by further measurements. If confirmed, it would imply a remarkable correlation between chemical composition and orbital parameters of small bodies in the early solar system.

References:

Ganapathy R. and Anders, E. (1974) Geochim. Cosmochim. Acta, Suppl. 5, p. 1181-1206.

Gros J., Takahashi H., Hertogen J., Morgan J.W., and Anders E. (1976) Geochim. Cosmochim. Acta, Suppl. 7, p. 2403-2425.

Hertogen J., Janssens M.-J., Takahashi H., Palme H., and Anders E. (1977) Geochim. Cosmochim. Acta, Suppl. 8, p. 17-45.

Janssens M.-J., Palme H., Hertogen J., Anderson A.T., and Anders E. (1978) Geochim. Cosmochim. Acta, Suppl. 10, p. 1537-1550.

Morgan J.W., Laul J.C., Krähenbühl, U., Ganapathy R., and Anders E. (1972) Geochim. Cosmochim. Acta, Suppl. 3, p. 1377-1395.

Morgan J.W., Ganapathy R., Higuchi H., Krähenbühl U., and Anders E. (1974) Geochim. Cosmochim. Acta, Suppl. 5, p. 1703-1736.

PRISTINE HIGHLAND ROCKS AND MARE BASALTS: COMPARISON OF SIDEROPHILE AND VOLATILE ELEMENTS

Rainer Wolf, Alicia Woodrow, and Edward Anders

Enrico Fermi Institute and Department of Chemistry

University of Chicago, Chicago, Illinois 60637

The nature of siderophile-free highland rocks has remained controversial. Some authors regard them as pristine remnants of the lunar crust that escaped meteoritic contamination during the late heavy bombardment (Morgan *et al.*, 1972; Gros *et al.*, 1976; Hertogen *et al.*, 1977; Warren and Wasson, 1977, 1978; Warren, 1979; Bickel and Warner, 1978; Herzberg, 1978, 1979). Ringwood and Wänke, however, question both their antiquity and pristineness, and regard them as late impact melts, whose siderophile element patterns are "not consistent with magmatic differentiation" (Delano and Ringwood, 1978, 1979; Wänke *et al.*, 1978, 1979). In the hope of clarifying their nature, we have compared them with the (indisputably igneous) low-Ti mare and terrestrial oceanic basalts, for the siderophile and volatile elements Ag, Au, Bi, Cd, Cs, Ge, In, Ir, Ni, Os, Pd, Rb, Re, Sb, Sn, Te, Tl, U, and Zn.

Though some pristine rocks have been altered by volatile transfer during metamorphism or fumarolic volcanism, most of them show reasonable abundance patterns, resembling those of lunar basalts or differing from them in plausible ways. Incompatibles (U, Rb, Cs) have similar median abundances but much wider ranges in pristine rocks (~10^2-10^3x vs ~5-20x), being lowest in anorthositic cumulates and highest in highly fractionated alkali-rich rocks. Volatile incompatibles (Tl, Br, In, Cd) show similar but more subdued trends. Most siderophiles (Ir, Re, Ni, Au, Ag, Ge), on the other hand, have very similar mean abundances and ranges in basalts and pristine rocks (20x-90x). Delano and Ringwood's (1978, 1979) argument, that these abundance ranges in pristine rocks are too "enormous" for magmatic fractionation, thus leads to the *reductio ad absurdum* that basalts, too, are non-igneous. This paradox is further dramatized by Sb, which shows a wider range in basalts (2000x) than in pristine rocks (140x).

Some moderately siderophile elements (Ge, Sb) behave differently on Moon and Earth; they have lower mean abundances and wider ranges in lunar basalts than in terrestrial basalts. This difference may reflect the early disappearance of the metal phase on the Earth, which forces these elements to be lithophile or chalcophile, whereas they have remained siderophile on the Moon.

PRISTINE HIGHLAND ROCKS AND MARE BASALTS

Wolf, R. *et al.*

Selenium shows a unique pattern: basalts have nearly constant abundances of 100-200 ppb, whereas pristine rocks are up to 3 orders of magnitude lower. The latter trend may reflect segregation of an FeS phase during initial differentiation of the Moon, and the former, full or partial saturation of basaltic lavas with FeS before eruption.

Non-mare or "high-Al" basalts, typified by 14053 or 60639, are distinctively enriched relative to mare basalts in U, Rb, Cs, Tl, Br, Bi, and especially In (≤10x) and Cd (10^1-10^3x). The source region of non-mare basalts apparently is strongly enriched in Cd, and these basalts may be the source of the excess Cd in lunar soils.

References:

Bickel C.E. and Warner J.L. (1978) *Proc. Lunar Sci. Conf. 9th,* p. 629-652.

Delano J.W. and Ringwood A.E. (1978) *Proc. Lunar Sci. Conf. 9th,* p. 111-159.

Delano J.W. and Ringwood A.E. (1979) *Lunar and Planetary Science X,* p. 289-291.

Gros J., Takahashi H., Hertogen J., and Anders E. (1976) *Proc. Lunar Sci. Conf. 7th,* p. 2403-2435.

Hertogen J., Janssens M.J., Takahashi H., Palme H., and Anders, E. (1977) *Proc. Lunar Sci. Conf. 8th,* p. 17-45.

Herzberg C.T. (1978) *Proc. Lunar Sci. Conf. 9th,* p. 319-336.

Herzberg C.T. (1979) *Lunar and Planetary Science X,* p. 537-539.

Morgan, J.W., Laul J.C., Krähenbühl U., Ganapathy R., and Anders E. (1972) *Proc. Lunar Sci. Conf. 3rd,* p. 1377-1395.

Wänke H., Dreibus G., and Palme H. (1978) *Proc. Lunar Sci. Conf. 9th,* p. 83-110.

Wänke H., Dreibus G., and Palme H. (1979) *Lunar and Planetary Science X,* p. 1280-1282.

Warren P.H. (1979) *Lunar and Planetary Science X,* p. 1301-1303.

Warren P.H. and Wasson J.T. (1977) *Proc. Lunar Sci. Conf. 8th,* p. 2215-2235.

Warren P.H. and Wasson J.T. (1978) *Proc. Lunar Sci. Conf 9th,* p. 185-217.

SAMPLE INDEX*

12013 166, 172
12033 172
14006 96
14053 132
14055 96
14063 96, 132
14066 96
14068 178
14072 132
14163 183
14276 178
14301 69
14305 183
14306 96, 160
14310 90, 111, 148, 178
14311 96
14312 96, 132
14313 47
14319 96
14320 96
14321 96, 132, 183
15010 108
15034 39
15102 119
15221 108
15271 108
15362 39, 111, 160
15364 39
15382 92
15386 47, 119, 178, 183
15405 47, 166
15415 39, 47, 111, 160, 183, 192
15434 178
15437 183, 192
15445 63, 92, 183
15455 119, 129
15689 39, 160
22001 183
60015 92, 192
60019 39
60025 39, 92, 111, 192, 195
60035 189
60215 92
60275 39
60315 18, 111, 129, 178, 183
60335 178, 183
60615 129
60618 111
60619 39, 160
60635 183
60639 183
60665 39, 160
61016 18, 129, 183, 192
61156 183
62235 18, 178, 183
62236 92, 183, 192
62237 92, 111, 183, 192
62255 47, 92, 111
62295 178, 183
63501 183
63549 178
64423 192
64455 178
64475 129
65015 18, 111, 138, 178
65055 178
65235 129
65315 111, 183, 183
65327 129
65515 47
66075 183
66095 18, 95, 114, 178
67015 18
67016 183
67075 39, 92, 111, 183
67415 111, 183
67435 92, 105
67455 117, 183
67529 160
67559 178
67635 39
67637 39, 160
67667 39, 129, 160
67746 39
67915 117, 166, 169, 183
68415 18, 53, 117, 129, 148, 178
68416 178
68815 183
69955 111
72255 39, 47, 129, 192
72275 56, 92, 129
72415 92, 105, 129
72417 47, 183, 192
72435 63, 111
73215 39, 87
73235 183
73255 129, 132
73263 30, 63

*Pagination refers to the first page of the paper in which a sample number is mentioned.

74220 81
76055 183
76215 111
76255 39
76335 183
76535 39, 47, 90, 92, 105, 160
76536 69
76635 192
77017 92, 129
77075 183
77077 39, 183
77115 39, 87
77135 111, 178
77215 87, 92, 192
77315 39
77538 166
78115 92
78135 111
78235 9, 39, 47, 90, 92, 105, 160, 183
78236 9
78238 90
79215 92

SUBJECT INDEX*

A

ANT 189
Accretion 148, 151
Ages 169
Ages of cumulate rocks 192
Albedo 50
Ancient 138
Anorthosite 39, 47, 66, 81, 92, 105, 111, 125, 195
Anorthosite, origin 151
Anorthositic gabbro 53
Antipodal effects 72
Apatite 90
Apollo 14 breccias 96
Apollo 16 soil 129
Apollo 17 Boulder 1, Station 2 132
Apollo 17 KREEPy basalt 56
Apollo 17, Station 6 boulder 132
Archean 66
Argon 39/40 138

B

Balmer crater 56, 157
Basalt 81, 119, 132
  highland rock relations 95
Basin 15, 53, 59, 72
Basin ejecta 53
Bombardment 198
Boundary layer 181
Breccia 96, 129, 148, 163, 189
  lithification 186
  texture 163
Bromine 95
  stepwise heating 95

C

Cataclastic rocks 163
Cayley Formation 1, 61, 172
Cayley plains 1
Center-of-mass offset 45
Central peaks 36
Chemistry 117
Chlorine 90
Chondrites 195
Chronology 9, 105, 138
Classification 117, 163
Clast population 96
Clasts 18, 114, 169, 186
Cones 61
Convection 128
Cooling rates 178
Cordierite cataclasite 63
Crater aging 175
Crater evolution 175
Cratering 198
Cratering process 99
Cratering rate 27
Craters 27
Crisium basin 53
Crust 92, 154
  chemistry 53
  composition 33, 186
  density 154
  models 3, 33
  origin 3
  thickness 157
Crustal thickness 154
Crystal-liquid differentiation 151
Crystalline matrix breccias 163
Cumulates 47, 105, 125, 151, 181
  extraoceanic 192

D

Dark halo 50
Density 33
Descartes 61
Differentiation 81
Diffusion 87
Domes 61

E

Earth 78
Ejecta blankets 172
Evolved magmas 166
Excavated cavity-depth 27
Experimental petrology 30, 87
Extinct isotopes 69

* Pagination refers to the first page of the paper in which a subject is cited.

F

Factor analysis 129
Feldspar 178
Ferroan anorthosites 6, 192, 195
Fission 69
  plagioclase 63, 66, 195
Fluorine 90
Fra Mauro 96
Fra Mauro basalt 18
Fractional crystallizations 166
Fractionation 125

G

Gamma ray 33, 81
Geochemical anomaly 56
Geology 145
Gramma-ray data 12
Granite 166, 172
Granulitic 189
Granulitic impactite 39
  earth 45
Gruithuisen 61

H

Halogens 90
Hansteen alpha 61
Heat flow 87
Heterogeneous accretion 172
High-magnesium component 30
Highland 36, 47, 119, 138
  basalt relationship 95
  basalt 18, 27
  breccias 96
  chemistry 33, 102, 129
  chronology 9
  melt rocks 178
  plains 1
  volcanism 56, 59, 61, 157
Homogeneous accretion 172

I

Igneous 119
Imaging 145
Imbrium 63
Imbrium event 18
Immiscibility 166
Impact basins 27, 141
Impact breccia 27
Impact craters 50, 59
Impact melt 18, 27, 50, 99, 148
Impact processes 27, 186
Impactite 92, 189
Infrared anomaly 175
Ion microprobe 111
Ion probe analyses 160
Iron 33
Iron core 128
Isostasy 33, 154
Isotopes 105

K

KREEP 18, 47, 56, 90, 92,
  108, 119, 132, 157, 186
KREEP basalt 157
KREEP volcanism 157
KREEPuth 172
KREEPy basalts 157

L

Langemak 56
Laser 138
Lateral heterogeneity 12
Layered intrusions 192
Layered lunar crust 63
Lead 244 69
Light plains 21
Lithosphere 154
  thickness 154
Lomonosov - Fleming basin 21
Low K Fra Mauro basalt 27
Low-K Fra Mauro basalt 53, 157
Luna 20 soil 129
Lunar bulk composition 183
Lunar craters 36
Lunar crust 102, 105, 125, 181
  asymmetry 45
  thickness 45
Lunar grid 36

Lunar highland rocks 163
Lunar magma ocean 63
asymmetry 45
Lunar origin 183
Lunar rock systematics 163
Lunar smooth plains 1

M

Magcons 72
Magma 81
density 66
mixing 105
ocean 66, 78, 95, 95, 105, 111, 148, 181, 192, 195
Magnesian dunites 6
Magnesian troctolites 6
Magnesium-rich plutonic rocks 39, 151, 192
Magnetic anomalies 72
Mairan 61
Major elements 47
Mare 132
Mare Imbrium 63
Mare Marginis 56, 157
Mare basalts 151
Mare volcanism 56
Mars 78
Mascon 154
Maturity 108
Megaregolith 15
Melt rocks 18
Melting 119
fragmental 87
Mercury (element) 95
stepwise heating 95
Mercury (planet) 78
Metasomatism 90
Mineral clasts 96
Mineralogy 178
Mixing 189
Mixing model 18, 53
Mixtures 129
Moon 78, 145
composition 195
sequential growth 151
Multi-ringed basins 141
Multispectral images 50, 145

N

Nearside 145
Nectaris basin 53
Nomenclature 163
Non-hydrostatic figure 128
Non-mare 119
Norites 9, 39, 47, 92

O

Olivine 39, 87, 178
Orbital XRF data 172
Orbital chemistry 1
Orbital data 47, 81
Orbital geochemistry 53
Orientale basin 53
Orthopyroxene 30, 63
Oxygen isotopes 195

P

Pattern recognition 117
Petrology 92, 132, 169
Plagioclase 39, 111
Plagioclase flotation 63, 66
trace elements 39, 160
Plains 61
Planetary crust 66, 141
Planetesimals 198
Plutonic rocks 6
Poikiloblastic rocks 18
Pole positions 128
Pre-mare volcanism 21
Primary matter 183
Pristine crustal rocks 6
Pristine rocks 96, 105, 119, 192, 195
Provenance 96, 186
Pyroxene 39, 178

Q

Q-mode 129
Quartz-monzodiorite 166

R

REE 47, 151
Radar anomaly 175
Red spots 59
Reflectance spectra 50
Refractory element 172, 195
Regolith 108
Remote sensing 33, 50, 81, 145
Rock fragments 96
Rockberg 192
Rusty Rock 18, 114

S

Samarium-Neodymium Chronology 9
Seismic modification 72
Serenitatis 63
Siderophiles 189
Silicate mineralogy 178
Skaergaard 66
Sodic-ferrogabbro 166, 169
Soil survey 172
Solar system origin 198
Spectra 145
Spinel cataclasite 30, 63
Stepwise Heating 95
Stillwater Complex 66, 125
Stratigraphy 15
Strontium 160
Suevite 27
Superheavy elements 128

T

Taruntuis 56
Tectonics 141, 154
Temperature estimate 30
Terrestrial planets 78
Thermal history 78, 87, 154
Thermal release patterns 95
Thermal structure 154
Thorium 47
Tides 45
Trace elements 39, 95, 160
Trapped liquid 47
Troctolite 39, 92, 105, 119
Troctolitic anorthosite 169
Tycho 50

V

Van de Graaff 56, 157
Venus 78
Volatile trace elements 95
Volatile/refractory element ratios 172
Volatiles 18, 114, 183
Volcanism 59, 132
  non-mare 61

W

Whole melting 128

X

X-ray 81
XRF 12

Z

Zoning 111

AUTHOR INDEX*

A

Adler I. 1
Anders E. 200, 201
Andre C. G. 1

B

Baker M. B. 63
Bansal B. 122
Basu A. 108
Bence A. E. 30, 102, 138
Binder A. B. 3, 6
Brande S. 102

C

Carlson R. W. 9
Clark P. E. 56
Conca J. 12
Cutts J. A. 175

D

De Hon R. A. 15
Drake M. J. 78
Dreibus G. 183

E

Ehrlich R. 129
Eichhorn G. 138
El-Baz F. 1, 21

F

Fico C. 129
Fryer K. H. 135
Fyfe W. S. 66

G

Garrison J. R. Jr. 18, 114
Geiss J. 169
Gifford A. W. 21
Goins N. R. 24
Grieve R. A. F. 27
Grove T. L. 30

H

Haines E. L. 33
Hale W. 36
Hansen E. C. 39, 151
Hartmann W. K. 42
Hartung J. B. 45
Haskin L. A. 47
Hawke B. R. 50, 53, 56, 99
Head J. W. 59, 61
Herzberg C. T. 63, 66
Hohenberg C. M. 69
Hood L. L. 72
Hörz F. 75, 135
Hostetler C. J. 78
Hubbard N. 81, 84
Hudson B. 69
Huebner J. S. 87

I

Irving A. J. 90

J

James O. 92
Jovanovic S. 95

K

Keil K. 166, 169, 189
King B.-S. 84
Knöll H.-D. 96, 163
Korotev R. L. 47

L

Lange M. A. 3, 99
Lindsley D. H. 30

*Pagination refers to the first page of the paper in which an author is cited.

Lindstrom M. M. 47
Livi K. 102
Longhi J. 105
Lugmair G. W. 9

M

MacLaskey D. 50
Marti K. 169
Maxwell T. A. 1
McCallum I. S. 125
McCord T. B. 50, 61
McKay D. S. 108
Mendenhall M. 143
Metzger A. E. 33
Meyer C. 111
Meyer R. W. 114
Moore C. B. 117

N

Norman M. D. 119
Nyquist L. 122

O

Ostertag R. 75

P

Palme H. 183
Papike J. J. 178
Parsons M. L. 117
Podosek F. A. 69
Pratt D. D. 117

R

Raedeke L. D. 125
Rainey D. A. 75
Reed G. W. Jr. 95
Rock B. 117
Roedder E. 169
Runcorn S. K. 128
Ryder G. 129, 132

S

Sanford R. F. 87
Schaal R. B. 135
Schaeffer O. A. 138
Schmitt R. A. 169
Schultz P. H. 141, 143
Seeger R. C. 145
Shih C.-Y. 122
Shorthill R. W. 175
Simonds C. H. 148, 186
Smith J. V. 39, 151, 160
Solomon S. C. 154
Spudis P. D. 53, 56, 132, 157
Steele I. M. 39, 160
Stöffler D. 96, 163

T

Taylor G. J. 166, 169, 189
Taylor L. A. 18, 114
Taylor S. R. 172
Thompson T. W. 175
Thornber C. R. 87

V

Vaniman D. T. 178

W

Walker D. 181
Wänke H. 183
Warner J. 186
Warner R. D. 166, 169, 189
Warren P. H. 192, 195
Wasson J. T. 195
Weiblen P. 169
Wetherill G. W. 198
Wiesmann H. 122
Wolf R. 200, 201
Wooden J. 122
Woodrow A. 201

Z

Zisk S. H. 175

NOTES